

**Structural and functional studies of Ly49B, a
key immune receptor in myeloid cells.**

**Katarzyna Maria Mickiewicz
Doctor of Philosophy (Integrated)**

**The Institute for Cell and Molecular Biosciences,
Newcastle University**

September 2012

Abstract

Murine Ly49 receptors are predominantly expressed on natural killer (NK) cells and play a key role in regulating immunological activity. The Ly49 family contains both inhibitory and activating receptors, which bind class I major histocompatibility complex (MHC I) or MHC-like molecules. Regulation of NK cell activity is the result of finely balanced signalling, which is delivered by the two receptor types upon ligand binding. Once activated, NK cells play an essential role in the elimination of cancerous and virus infected cells.

Ly49B differs from other members of the Ly49 family in that it is expressed on the surface of myeloid, rather than NK cells. It shares only 50 % sequence identity with other Ly49s and contains an additional 20 amino acids at its carboxyl-terminus. Furthermore, there are significant variations between Ly49Bs from different mouse strains. These inter- and intra-molecular variations suggest that different allelic forms could possess distinct structural and functional properties when compared with one another and with other members of the Ly49 family. This thesis seeks to provide an in-depth characterisation of the biochemical properties of Ly49B in comparison to other Ly49 receptors.

In this study a series of Ly49B mutants, created by site-directed mutagenesis, was used to identify residues critical for monoclonal anti-Ly49B antibody and ligand binding. Flow cytometric analysis of the mutants revealed that C57 Ly49B-specific residues, L166 and K167, are important for the integrity of the monoclonal 1A1 anti-Ly49B antibody epitope. The equivalent BALB/c Ly49B residues, W166 and N167, together with residue C251 were shown to play an essential role in MHC class I ligand binding.

Immunoprecipitation and Western blotting were used to demonstrate that Ly49B exists in multiple molecular forms in transfected and native cells, each of which most likely represents the receptor at different stages of glycosylation. Similar results have never before been presented for any Ly49 receptor. Finally, a method for refolding and purification of the extracellular portion of Ly49B was developed, following expression in *Escherichia coli*.

To my parents,
Krystyna and Jerzy Mickiewicz

Acknowledgements

I would like to acknowledge Professor Colin Brooks for being an amazing supervisor, for igniting my passion for immunology and for always being there as a mentor and a friend. I would like to thank Professor Richard Lewis for his continuous and enthusiastic guidance throughout this project.

With many thanks to Tomas Richardson, my boyfriend and treasure, for his proof-reading, feedback and endless patience. Thanks to Dr Timothy Cheek, who always had time for me and all of the other PhD students within the institute. Thanks also to Dr Jon Marles-Wright, Dr Arnaud Basle and the whole of the Lewis lab for their expertise and help in performing my protein refolding and purification experiments. A huge thank you to Frances Davison for showing me there are no obstacles in this world that we cannot overcome. And finally, thanks to my sister, Emilia Mickiewicz, for always believing in me.

Table of Contents

I.	Abstract	2
II.	Dedication	3
III.	Acknowledgements	4
IV.	Table of contest	5
V.	List of tables	10
VI.	List of figures	11
VII.	List of abbreviations	16
VIII.	Main thesis	19
1.	Introduction	19
1.1.	NK cell activation	20
1.1.1.	<i>The Major Histocompatibility Complex</i>	20
1.1.2.	<i>“The missing self” hypothesis</i>	22
1.2.	The Ly49 family	24
1.3.	Glycosylation of surface proteins	24
1.4.	Molecular characterisation of Ly49 receptors	27
1.5.	The Ly49 ligand binding	32
1.5.1.	<i>Ligand specificity</i>	32
1.5.2.	<i>The role of ligand glycosylation in Ly49-MHC class I interactions</i>	35
1.5.3.	<i>The role of Ly49 glycosylation in Ly49-MHC class I interactions</i>	37
1.6.	Structure of Ly49 receptors	38
1.6.1.	<i>Overview</i>	38
1.6.2.	<i>Crystal structures of Ly49s</i>	40
1.6.2.1.	<i>The CTLD fold</i>	40
1.6.2.2.	<i>Crystal structure of Ly49 NKD</i>	41
1.6.2.3.	<i>Crystal structure of Ly49 dimers</i>	42
1.6.2.4.	<i>Crystal structure of Ly49-MHC interface</i>	43
1.7.	Ly49-MHC class I <i>trans</i> and <i>cis</i> interactions	49
1.8.	Ly49 signalling	52

1.8.1. <i>Inhibitory pathway</i>	52
1.8.2. <i>Activating pathway</i>	54
1.9. Ly49B.....	54
1.9.1. <i>Sequence comparison of Ly49B with other Ly49s</i>	55
1.9.2. <i>Ly49B specificity and signalling</i>	56
1.10. Project aims	57
2. Materials and Methods.....	59
2.1. Bacterial strains and growth conditions	59
2.2. Cloning.....	60
2.2.1. <i>Cloning of the constructs for cell lines transformation</i>	60
2.2.2. <i>Cloning of Ly49B for refolding and purification</i>	61
2.3. DNA agarose gel electrophoresis.....	62
2.4. Mouse cells, tumour cell lines and transfection.....	62
2.5. Cell lysates preparation.....	64
2.6. Immunoprecipitation	64
2.7. Flow cytometry	65
2.8. Biotinylation.....	66
2.9. Sodium dodecyl phosphate gel electrophoresis	66
2.10. Western blotting	67
2.11. Protein expression.....	68
2.11.1. <i>Small scale protein expression</i>	68
2.11.2. <i>Large scale protein expression</i>	68
2.12. Protein refolding and purification.....	68
2.12.1. <i>Preparation of protein inclusion bodies</i>	68
2.12.2. <i>Protein refolding</i>	69
2.12.3. <i>Gel filtration chromatography</i>	70
2.12.4. <i>Immobilized metal ion affinity chromatography (IMAC)</i>	70
2.12.5. <i>Ion exchange chromatography</i>	70
2.12.6. <i>Dialysis</i>	70
2.13. Micro-scale nickel affinity pool-down assay.....	70
2.14. Microscopy	71

2.15. Circular dichroism (CD).....	71
3. Mutational binding analysis of Ly49 receptors.....	72
3.1. Introduction	72
3.2. Analysis of MHC class I tetramer binding to Ly49 receptors.....	74
3.3. Mapping of Ly49B residues responsible for selective binding of the 1A1 antibody	74
3.4. Mapping of Ly49B residues responsible for the selective binding of MHC class I ligands	81
3.4.1. <i>H-2K^b binding</i>	83
3.4.2. <i>H-2D^b binding</i>	85
3.4.3. <i>H-2D^d binding</i>	88
3.5. Establishing the role of the C-terminal 20 amino acids of Ly49B in ligand and antibody binding	90
3.5.1. <i>Antibody binding</i>	90
3.5.2. <i>H-2K^b binding</i>	91
3.5.3. <i>H-2D^b binding</i>	92
3.5.4. <i>H-2D^d binding</i>	93
3.6. Establishing the role of Ly49B glycosylation in ligand and antibody binding ..	94
3.6.1. Antibody binding	94
3.6.2. <i>H-2K^b staining</i>	96
3.6.3. <i>H-2D^b staining</i>	97
3.6.4. <i>H-2D^d binding</i>	99
3.7. Mapping of Ly49A residues responsible for binding of MHC class I ligands and anti-Ly49A antibodies	100
3.7.1. <i>Antibody binding</i>	100
3.7.2. <i>Ligand binding</i>	101
3.8. Establishing the influence of the HA-tag on Ly49 ligand binding.....	103
3.9. Analysis of residues influencing ligand and 1A1 binding by Ly49B	107
3.9.1. <i>Analysis of the nature of Ly49B residues predicted to be responsible for binding of 1A1 and MHC class I ligands</i>	107

3.9.2. <i>In silico</i> modelling of Ly49B residues proposed to be responsible for 1A1 antibody and ligand binding using published Ly49A dimer crystal structure and Ly49A-H-2Dd co-crystal structure	109
3.10. Summary.....	114
4. The molecular nature of Ly49B	115
4.1. Introduction	115
4.2. Ly49B exists in multiple molecular forms in cells transfected with Ly49B constructs	116
4.3. Multiple molecular weight forms of Ly49B represent differentially glycosylated Ly49B	122
4.4. Differentially glycosylated Ly49B forms exist in native cells expressing Ly49B	128
4.5. NK cell receptors tend to exist in multiple molecular forms in YB2/0 transfectant.....	133
4.5.1. <i>Assessment of Ly49B molecular forms</i>	133
4.5.2. <i>Assessment of Ly49A molecular forms</i>	133
4.5.3. <i>Assessment of Ly49G molecular forms</i>	134
4.5.4. <i>Assessment of Ly49Q molecular forms</i>	135
4.5.5. <i>Assessment of Clrg molecular forms</i>	135
4.5.6. <i>Assessment of Ly49E molecular forms</i>	135
4.6. Summary.....	137
5. Purification and refolding of Ly49B	138
5.1. Introduction	138
5.2. Construct design and cloning	139
5.3. Ly49B expression	141
5.4. Crude purification and solubilisation of Ly49B from inclusion bodies	144
5.5. Development of refolding strategy	145
5.6. Assessment of the refolded Ly49B.....	152
5.6.1. <i>Assessment of the refolded Ly49B using pull-down assay</i>	152
5.6.2. <i>Assessment of the refolded Ly49B using circular dichroism (CD)</i>	153

5.7. Summary.....	155
6. Discussion.....	156
6.1. Future work.....	166
7. References.....	168
8. Appendices.....	183
Appendix I) Alignment of all known C57 Ly49 receptor amino acid sequences, as well as that of BALB/c Ly49B.....	183
Appendix II) Characterisation of Ly49s and other NK cell receptors from murine strains by immunoprecipitation and Western blotting	185
Appendix III) Staining of Ly49B mutants	188
Appendix IV) Staining of Ly49A mutants.....	210

List of tables

<i>Table 1.1. Interactions between Ly49 and MHC-I molecules in the Ly49C-H-2K^b and Ly49A-H-2D^d complexes</i>	49
<i>Table 2.1. Bacterial strains used in this study for construct preparation and protein expression</i>	59
<i>Table 2.2. Primers used in this study</i>	61
<i>Table 2.3. Transfectants used in this study</i>	63
<i>Table 2.4. Reagents used for flow cytometry analysis</i>	65
<i>Table 2.5. Composition of SDS-PAGE gels</i>	66
<i>Table 2.6. Antibodies used for Western blot experiments</i>	67
<i>Table 2.7. Buffers used for refolding of Ly49B in this study</i>	69
<i>Table 3.1. Full names, abbreviations and amino acid codes of molecules used in Chapter 3</i> .76	
<i>Table 5.1. Ly49B constructs designed for this study</i>	139
<i>Table 5.2. Methods used to solubilise, refold and purify Ly49 receptors</i>	146

List of figures

<i>Figure 1.1. Genomic organisation of the major histocompatibility complex.....</i>	<i>20</i>
<i>Figure 1.2. Schematic structure of classical MHC molecules</i>	<i>21</i>
<i>Figure 1.3. A schematic diagram of NK cell activation.....</i>	<i>22</i>
<i>Figure 1.4. Examples of human and murine NK cell receptor families.....</i>	<i>23</i>
<i>Figure 1.5. Ly49 locus in the C57 mouse strain.....</i>	<i>24</i>
<i>Figure 1.6. N-glycosylation of eukaryotic proteins.....</i>	<i>26</i>
<i>Figure 1.7. Schematic structure of Ly49 and KIR receptors.....</i>	<i>39</i>
<i>Figure 1.8. Structures of Ly49A and Ly49I in comparison with other CTLD superfamily members.....</i>	<i>40</i>
<i>Figure 1.9. Variability in dimerisation mode of Ly49B receptors</i>	<i>42</i>
<i>Figure 1.10. Predicted glycosylation sites of Ly49G and Ly49I CRDs</i>	<i>43</i>
<i>Figure 1.11. Co-crystal structure of two Ly49A dimeric NKDs with H2-Dd MHC molecule .</i>	<i>44</i>
<i>Figure 1.12. Ly49C monomer in complex with H-2Kb</i>	<i>46</i>
<i>Figure 1.13. Ligand binding by Ly49C</i>	<i>46</i>
<i>Figure 1.14. Comparison of Ly49-MHC-I interfaces.....</i>	<i>47</i>
<i>Figure 1.15. Structural classification of Ly49 NK receptors</i>	<i>48</i>
<i>Figure 1.16. Hypothetical Model for trans and cis interactions of Ly49 Receptors with MHC-I Ligands</i>	<i>50</i>
<i>Figure 1.17. Current hypothetical Model for trans and cis interactions of Ly49 Receptors with MHC-I Ligands</i>	<i>51</i>
<i>Figure 1.18. Inhibitory signalling pathways in NK cells</i>	<i>53</i>
<i>Figure 3.1. Schematic representation of a flow cytometer.....</i>	<i>72</i>
<i>Figure 3.2. Alignment of BALB/c and C57 Ly49B sequences.....</i>	<i>73</i>
<i>Figure 3.3. Staining of various Ly49 transfectants with MHC class I tetramers.....</i>	<i>75</i>
<i>Figure 3.4. Schematic representation of chimeric C57/BALB/c Ly49B molecules.....</i>	<i>77</i>

Figure 3.5. Staining of Chimera 3 and 4 Ly49B mutants.....	77
Figure 3.6. Generation of mutant constructs by site directed mutagenesis	78
Figure 3.7. Schematic representation of chimera 3 and 4 Ly49B mutants	78
Figure 3.8. PstI digest of pMXs-IP vectors with Ly49B Chim4-V59L inserts	79
Figure 3.9. Staining of chimera 3 and chimera 4 Ly49B mutants	80
Figure 3.10. Schematic representation of Ly49B mutants	81
Figure 3.11. Staining of Ly49B mutants with 2G4 antibody.....	82
Figure 3.12. Staining of Ly49B mutants with H-2Kb.....	83
Figure 3.13. Staining of Ly49B mutants with H-2Db.....	86
Figure 3.14. Staining of Ly49B mutants with H-2Dd.....	89
Figure 3.15. Staining of Ly49B mutants lacking 20 C-terminal amino acids with 2G4 anti-Ly49B and anti-HA antibodies.....	91
Figure 3.16. Staining of Ly49B mutants lacking 20 C-terminal amino acids with H-2Kb.....	92
Figure 3.17. Staining of Ly49B mutants lacking 20 C-terminal amino acids with H-2Db.....	93
Figure 3.18. Staining of Ly49B mutants lacking 20 C-terminal amino acids with H-2Dd.....	93
Figure 3.19. Staining of Ly49B glycosylation mutants with 2G4 anti-Ly49B.....	95
Figure 3.20. Staining of Ly49B glycosylation mutants with 1A1 anti-Ly49B and anti-HA antibodies.....	96
Figure 3.21. Staining of Ly49B glycosylation mutants with H-2Kb.....	97
Figure 3.22. Staining of Ly49B glycosylation mutants with H-2Db	98
Figure 3.23. Staining of Ly49B glycosylation mutants with H-2Dd	99
Figure 3.24. Staining of Ly49A-HA, Ly49A-S167K-HA and Ly49A-W166L-HA transfectants with anti-HA, JR9, 1A and YE1-48 monoclonal antibodies.....	101
Figure 3.25. Staining of Ly49A-HA, Ly49A-S167K-HA and Ly49A-W166L-HA transfectants with H-2Kb, H-2Db and H-2Dd tetramers	102
Figure 3.26. Staining of HA-tagged and untagged Ly49B mutants with 2G4 anti-Ly49B	103
Figure 3.27. Staining of HA-tagged and untagged Ly49B mutants with H-2Kb	104
Figure 3.28. Staining of HA-tagged and untagged Ly49B mutants with H-2Db	105

Figure 3.29. Staining of HA-tagged and untagged Ly49B mutants with H-2Dd	106
Figure 3.30. Staining of HA-tagged and untagged Ly49A mutants with MHC class I tetramers and monoclonal anti-Ly49A antibodies.....	107
Figure 3.31. Crystal structure of the Ly49A homodimer	110
Figure 3.32. Crystal structures of Ly49A with the MHC class I ligand H-2Dd	111
Figure 3.33. In silico introduction of a W166L mutation to the Ly49A receptor	112
Figure 3.34. In silico introduction of an S167K mutation to the Ly49A receptor	113
Figure 3.35. In silico introduction of an S167N mutation to the Ly49A receptor	113
Figure 3.36. In silico introduction of a C251R mutation to the Ly49A receptor.....	113
Figure 4.1. N1027 anti-FLAG blot of NR and R lysates of RNK-Ly49B-FLAG, YB2-Ly49B-HA, RNK-Ly49H and YB2/0 cells	116
Figure 4.2. N1028 anti-HA blot of NR and R lysates of YB2-Ly49B-HA, RNK-Ly49B-FLAG, RNK-Ly49H and YB2/0 cells.....	117
Figure 4.3. N1184 2G4 anti-Ly49B blot of NR and R lysates of YB2-Ly49B, YB2-Ly49B-HA, RNK-Ly49H and YB2/0 cells.....	118
Figure 4.4. N1176 biotin 2G4 anti-Ly49B and N869 biotin 1A1 anti-Ly49B blot of R and NR YB2-C57 Ly49B-HA cell lysates	119
Figure 4.5. N1028 anti-HA, N1176 biotin 2G4 anti-Ly49B, N869 biotin 1A1 anti-Ly49B, N1229 biotin rabbit anti-HA and N1222 biotin 16.43 anti-HA blot of R and NR YB2-C57 Ly49B-HA lysates.....	120
Figure 4.6. N1176 biotin 2G4 anti-Ly49B blot of NR and R C57 Ly49B-HA immunoprecipitated from YB2-C57 Ly49B-HA lysates using sepharose protein G beads coated with a range of antibodies.....	121
Figure 4.7. N1176 biotin 2G4 anti-Ly49B blot of NR and R Ly49B glycosylation mutants ..	123
Figure 4.8. Western blot of biotinylated NR and R C57 Ly49B-HA immunoprecipitated from YB2-C57 Ly49B-HA lysates using protein G beads coated with 2G4 anti-Ly49B	124
Figure 4.9. N1176 biotin 2G4 anti-Ly49B blot of NR and R C57 Ly49B-HA treated with PNGase F and Endo H enzymes	126
Figure 4.10. N1176 biotin 2G4 anti-Ly49B blot of NR and R BALB/c Ly49B single glycosylation mutants.....	127

Figure 4.11. Staining of C57 spleen and bone marrow (BM) macrophages with 2G4 anti-Ly49B antibody	129
Figure 4.12. N1176 biotin 2G4 anti-Ly49B blot of NR and R cell lysates prepared from YB2/0, YB2-C57 Ly49B-HA transfectants and C57 spleen and bone marrow cells cultured with MCSF followed by either INF- α or LPS	130
Figure 4.13. Staining of C57 spleen macrophages with 2G4 anti-Ly49B antibody (A) and LNK cells with a variety of monoclonal anti-Ly49 antibodies (B)	131
Figure 4.14. N1176 biotin 2G4 anti-Ly49B and N869 biotin 1A1 anti-Ly49B blots of NR cell lysates prepared from YB2/0, YB2-C57 Ly49B-HA transfectants, LNK cells and C57 spleen cells cultured with MCSF followed by INF- α or LPS	132
Figure 4.15. N1229 biotin anti-HA blot of NR and R YB2-C57 Ly49B-HA, YB2-Ly49A-HA, YB2-Ly49E-HA, YB2-Ly49G-HA, YB2-Ly49Q-HA and YB2-Clrg-HA cell lysates	134
Figure 4.16. Western blot of biotinylated NR C57 Ly49B-HA and Ly49E-HA immunoprecipitated from YB2-C57 Ly49B-HA lysates or YB2-Ly49E-HA lysates respectively, using protein G beads coated with anti-HA antibody.....	136
Figure 5.1. Verification of PCR amplification of C57 constructs by agarose gel electrophoresis.....	140
Figure 5.2. Restriction patterns of Pvu II/Sal I - digested pET28b plasmids with and without the NKDFx C57 insert	141
Figure 5.3. Phase contrast image of induced and non-induced BL21 Tuner culture transfected with a plasmid encoding Ly49B	143
Figure 5.4. Ly49B expression test in BL21 Tuner and Origami 2 E.coli stains with varying amounts of IPTG.....	144
Figure 5.5. Expression of Ly49B EC C57 in E. coli BL21 Tuner strain.....	144
Figure 5.6. Preparation of Ly49B inclusion bodies	145
Figure 5.7. Refolding and purification of Ly49B using rapid dilution and gel filtration	147
Figure 5.8. Size exclusion chromatographic purification of refolded Ly49B EC C57	148
Figure 5.9. Refolding and purification of Ly49B by dialysis, affinity chromatography and gel filtration chromatography.....	149
Figure 5.10. 10 % SDS analysis of Ly49B ECFX C57 purified by affinity chromatography	149
Figure 5.11. Refolding of Ly49B by dialysis, affinity chromatography and gel filtration chromatography.....	150

Figure 5.12. Gel filtration of Ly49B ECFX C57151

Figure 5.13. 15 % SDS-PAGE analysis of Ly49B ECFX C57 purified by gel filtration.....151

Figure 5.14. Ly49B binding assay.....153

Figure 5.15. Typical CD spectra for an alpha helix, a beta sheet and a random coil structure .
.....154

Figure 5.16. Circular dichroism spectra of unfolded and re-folded Ly49B EC C57 at 1
mg/ml.....154

List of abbreviations

APC – antigen presenting cell

APS – ammonium persulfate

β 2m – β 2 microglobulin

CD – cluster of differentiation, when used together with a number eg. CD8, CD16

CD – circular dichroism, when used on its own

CRD – carbohydrate recognition domain

CTLD – C-type lectin-like domain

EC – extracellular

E.coli – *Escherichia coli*

Endo-H – endoglycosidase H

ER – endoplasmic reticulum

FRET – fluorescence resonance energy transfer

GlcNAc – N-Acetylglucosamine

H-2 – histocompatibility 2

HA tag –hemagglutinin tag

His tag – polyhistidine tag

HLA – human leukocyte antigen

IB – inclusion bodies

IL – interleukin

INF – interferon

IP – immunoprecipitation

IPTG – Isopropyl β -D-1-thiogalactopyranoside

ITAM – Immunoreceptor Tyrosine-based Activation Motif

ITIM – Immunoreceptor Tyrosine Based Inhibition Motifs

KIR – killer-cell immunoglobulin-like receptor

LPS – lipopolysaccharide

mAb – monoclonal antibody

MBP-A – mannose-binding protein A

MCMV – murine cytomegalovirus

MCSF – macrophage colony stimulating factor

M ϕ – macrophage

MHC I – major histocompatibility complex class I

MHC II – major histocompatibility complex class II

NK – natural killer

NKC – natural killer complex

NKD – natural killer domain

NKRP – natural killer receptor protein

NMR – nuclear magnetic resonance

SDS-PAGE – sodium dodecyl sulphate polyacrylamide gel electrophoresis

SH2 domains – Src Homology 2 domains

SPR – surface plasmon resonance

TCR – T cell receptor

TEMED – Tetramethylethylenediamine

TNF – tumour necrosis factor

TM – transmembrane

WB – Western blot

WT – wild type

2D SDS-PAGE – two-dimensional sodium dodecyl sulphate polyacrylamide gel electrophoresis

2ME – β -mercaptoethanol, 2-mercaptoethanol

Chapter 1. Introduction

An organism's ability to maintain an internal homeostasis and protect itself from external factors are fundamental requirements for survival. The smarter those strategies are, the broader the organism's potential niche and the more competitive it becomes. In higher Eukaryotes the immune system plays a crucial role in protecting against pathogens and homeostatic deviations such as cancer.

The immune system broadly comprises innate and adaptive components (Janeway 2001). Innate responses are immediate, first line defences maintained by the complement system together with several white blood cell types including macrophages, natural killer (NK) cells, eosinophils, neutrophils and basophils. Adaptive responses, on the other hand, develop several days post-infection; they are specific for a given pathogen, confer long-lasting protective immunity for the host and involve T cells and antibody-producing B cells (Janeway 2001).

Historically, the adaptive part of the immune system has been considered a more attractive mechanism for explaining how the body fights infection. As such, the majority of immunological research has tended to lend its focus to that field. The range of currently available vaccines and the use of monoclonal antibodies in cancer therapy are just two examples of how this research has been applied in practice. However, more recently immunologists have realised that the adaptive part of the immune system works in tandem with the innate system and that the former cannot be fully appreciated without understanding the latter.

Natural killer (NK) cells are an integral part of the innate immune system. They constitute 5-10 % of the circulating lymphocytes in mammalian blood and are characterised in humans by expression of the CD56 marker and by the NK1.1 marker in murine species (Janeway 2001; Zimmer 2010). The majority of human and murine NK cells also express CD16, which is additionally found on macrophages and neutrophils (Cassatella *et al.* 1989). NK cells produce a number of signalling molecules of the immune system, known as cytokines, including interferon gamma (IFN- γ) and tumour necrosis factor (TNF) (Zimmer 2010). However, NK cells are best known for their cytotoxic activity against tumours and virus-infected cells, which is accomplished by the release of granzymes and perforins (Zimmer 2010).

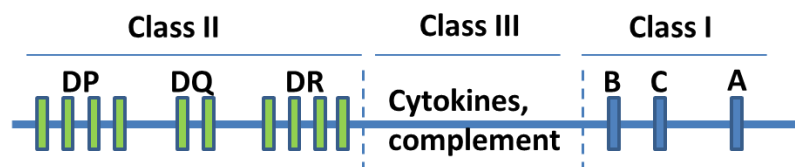
1.1. NK cell activation

1.1.1. The Major Histocompatibility Complex

The major histocompatibility complex (MHC) is a region of highly polymorphic genes located on chromosome 17 in mice and chromosome 6 in humans (**Figure 1.1**) (Trowsdale 1993; Stroynowski 1990). For historical reasons, human MHC molecules are referred to as HLA (human leucocyte antigen) molecules, while mouse MHC molecules are referred to as H-2 (histocompatibility 2) molecules. There are at least 128 functional genes encoded in the human MHC locus and approximately 20 % of them have functions in immunity (Janeway 2001).

There are two major classes of MHC genes: MHC class I and MHC class II. The remaining genes are sometimes referred to as MHC class III and include genes that encode proteins with known immunological functions (for example complement components and cytokines) and others with no known immune function (Trowsdale 1993; Stroynowski 1990; Janeway 2001).

A) Human (HLA)



B) Mouse (H-2)

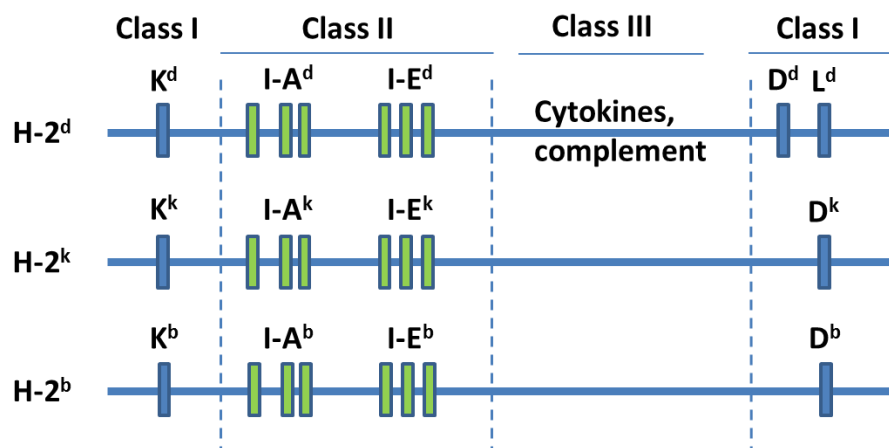


Figure 1.1. Genomic organisation of the major histocompatibility complex. A) Simplified diagram of the human MHC complex. B) Simplified diagram of the mouse MHC complex. Letters in superscript indicate different haplotypes of inbred strains of mice. Blue=classical class I genes, Green=classical class II genes.

Class I and class II genes are divided into classical and non-classical. The classical genes encode MHC class I and II molecules (**Figure 1.2**) and the non-classical, MHC class I and II-like molecules, which are structurally similar to the classical MHC molecules, as well as proteins involved in processing of MHC class I and II molecules. All genes that encode the various chains of class I and class II MHC molecules exist as multiple copies within the MHC, with the exception of the $\beta 2$ microglobulin chain of MHC class I, which is encoded on a different chromosome. Each cell expressing MHC genes displays several different MHC molecules. (Trowsdale 1993; Stroynowski 1990; Janeway 2001).

MHC class I and class II molecules are able to bind short peptides and present them to CD8 positive and CD4 positive T cells, respectively (Vyas *et al.* 2008). MHC molecules interact with T cells via T cell receptors (TCR) and CD4/CD8 molecules. The peptides in the binding grooves of MHC molecules are usually endogenous, in which case they are referred to as “self” peptides. Presentation of “self” peptides to T cells keeps them in an inactive state. However, during infection by pathogens MHC molecules bind peptides of foreign origin and present them to T cells, resulting in their activation. MHC class I molecules are able to present peptides from intracellular pathogens and, for this reason, are constitutively expressed on all nucleated cells in the body. MHC class II molecules present peptides that originate from extracellular pathogens and are expressed on a restricted number of cells called antigen presenting cells (APCs). APCs include B cells, dendritic cells and macrophages. The aforementioned diversity of MHC molecules that are expressed on a single cell allows presentation of a greater number of peptides, thereby increasing the chances of recognising infective agents (Vyas *et al.* 2008).

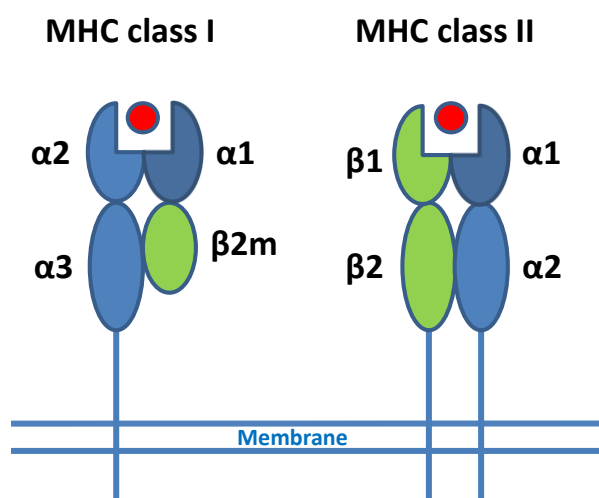


Figure 1.2. Schematic structure of classical MHC molecules. The MHC class I molecule is made up of a heavy α chain (~43 kDa) non-covalently linked to a smaller peptide (~11 kDa) called the $\beta 2$ microglobulin ($\beta 2m$). The α chain forms three globular α domains ($\alpha 1$, $\alpha 2$ and $\alpha 3$) stabilised by disulphide bonds. A hydrophobic section of the molecule anchors MHC class I in the cell membrane. The $\alpha 1$ and $\alpha 2$ domains form a peptide binding groove. The MHC class II molecule is made up of an α chain of ~34 kDa and a β chain of ~28 kDa, both of which anchor the protein in the membrane. The α and β chains form two globular domains. $\alpha 1$ and $\beta 1$ form a peptide binding groove similar to that found in the MHC class I molecule. α = α chain, β = β chain, $\beta 2m$ = $\beta 2$ - microglobulin, 1-3= globular domains, red circle = peptide in peptide binding groove.

1.1.2. “The missing self” hypothesis

It is not known for certain how NK cells recognise diseased cells but the key advance in our current understanding was made by Klas Kärre who proposed the “missing self” hypothesis (Kärre 1981) in the early 1980s. Tumours and virus-infected cells are sometimes characterised by the low level expression of MHC class I molecules, which makes them difficult to recognise by T cells (Browning 1999). Kärre proposed that NK cells, just like T cells, recognise class I MHC molecules. However, rather than being activated by the presence of exogenous peptide in the MHC groove, NK cells instead react when MHC levels are abnormally low (Kärre 1981). This revolutionary theory was confirmed several years later by Wayne Yokoyama, who showed that IL-2 activated mouse NK cells, which express Ly49A do not lyse cells expressing H-2^d or H-2^k MHC class I molecules, which are effectively lysed by Ly49A deficient NK cells. The protection from lysis by Ly49A expressing cells did not apply to cells expressing H-2D^b molecules. Transfection of susceptible cells with H-2D^d, but not H-2K^d or H-2L^d, made them resistant to lysis by Ly49A positive NK cells. The resistance of H-2D^d-transfected cells could be abolished by monoclonal anti-Ly49A or anti- H-2D^d antibodies (Karlhofer *et al.* 1992). These experiments have shown that Ly49 receptors expressed on the surface of NK cells can specifically recognise particular alleles of MHC class I molecules on target cells and deliver an inhibitory signal upon ligand binding. In the absence of “self” MHC ligand, NK cells therefore become activated. The “missing-self” hypothesis provides an elegant explanation as to why NK cells are non-reactive against the body’s own, healthy cells but noxious towards diseased cells.

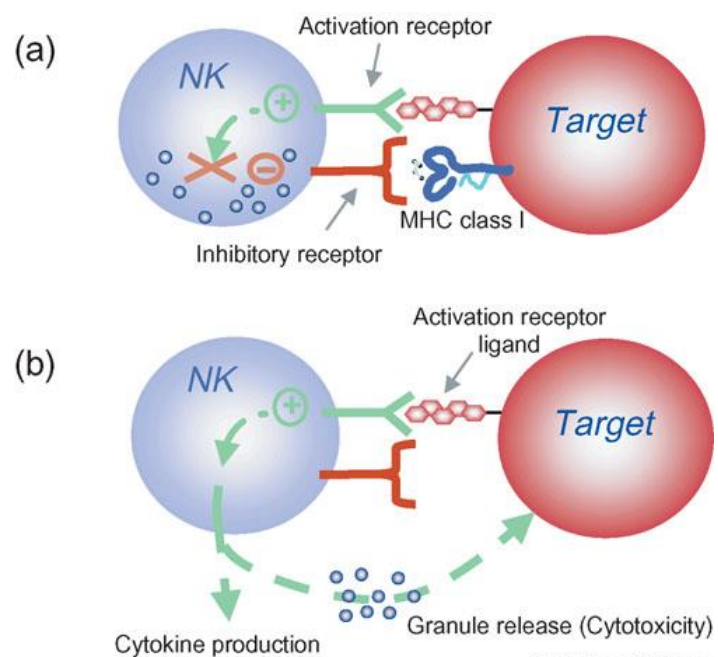


Figure 1.3. A schematic diagram of NK cell activation. a) The NK cell adopts an anergic state when balanced signals are delivered from inhibitory and activatory receptors. b) NK cell activation occurs when the inhibitory signal is missing. Figure taken from French and Yokoyama 2006.

1.2. The Ly49 family

The genes that encode mouse Ly49 receptors are clustered at the telomeric end of chromosome 6 within the NK gene complex (NKC), along with several other types of NK receptors including CLR, NKRP1 and CD94/NKG2 receptors (Yokoyama and Plougastle 2003; Zimmer 2010). The only known human Ly49 homologue, Ly49L, is encoded on chromosome 12 and was found to be a pseudogene (Westgaard *et al.* 1998). To date 23 members of the Ly49 family have been identified (each indicated by a unique character, A to W), as well as at least 15 allelic variants. Different strains of mice contain unique sets of Ly49s (Yokoyama and Plougastle 2003); the C57 strain, for example, contains 11 functional Ly49 genes and 4 pseudogenes (**Figure 1.5**), whereas the BALB/c strain contains only 8 Ly49 genes, two of which are pseudogenes (Anderson *et al.* 2001; Dimasi *et al.* 2002).

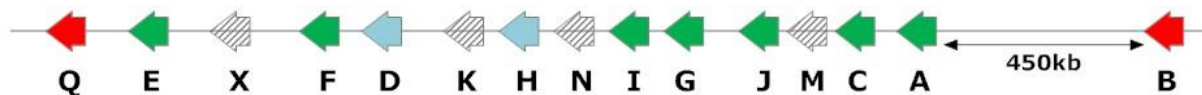


Figure 1.5. The Ly49 locus of the C57 mouse strain. Genes encoding inhibitory Ly49s that are expressed on NK cells are indicated in green. Activating Ly49s are indicated in blue. Arrows representing non-functional pseudogenes are hatched. Ly49s expressed on myeloid cells are indicated in red. Ly49B is physically separated from the rest of the Ly49 genes by a region of roughly 450 kb. (adapted from master's thesis of Katarzyna Mickiewicz, 2009)

The majority of Ly49s (but not all) are expressed in an unusual stochastic and mono-allelic manner (Held and Kunz 1998; Gays *et al.* 2011). Typically, a single mouse NK cell will express only 2-3 Ly49 receptors of the available pool and each of them from only one of the parental alleles. Different NK cells within a population express different sets of Ly49s. This mode of expression enables the generation of a diverse NK cell repertoire, which is able to recognise a variety of MHC class I alleles.

1.3. Glycosylation of surface proteins

Both Ly49s and their ligands are heavily glycosylated. Glycosylation is a form of an enzyme dependent, co-translational or post-translational modification of proteins, lipids and other organic molecules, which relies on attachment of carbohydrates to a specific site of the modified molecules (Taylor *et al.* 2006). It occurs in ER, Golgi apparatus, cytoplasm and

nucleus of eukaryotic cells. Glycosylation is also a common event in archaea but very rarely occurs in bacteria (Taylor *et al.* 2006). Glycan modifications are important for correct folding of many eukaryotic proteins, they confer stability of some secreted proteins and also play a role in cell to cell adhesion (Taylor *et al.* 2006).

There are five types of glycosylation:

- N-glycosylation, which involves attachment of glycans to a nitrogen of asparagine or arginine side chains.
- O-glycosylation, where glycans are attached to hydroxy oxygen of serine, threonine, tyrosine, hydroxylysine, or hydroxyproline side chains, or to oxygens of lipids such as ceramide. The process occurs specifically in Golgi apparatus.
- Phospho-Serine glycosylation, where glycans are attached to serine through a phosphate
- C-mannosylation, involving attachment of a sugar to a carbon of a tryptophan side chain
- Glypiation (GPI anchors), which is the addition of a GPI anchor that links proteins to lipids through glycan linkages.

The majority of secreted and surface-associated eukaryotic proteins, including Ly49s, undergo N-glycosylation. As these proteins travel from the ER to the cell surface glycans are attached at critical asparagine residues, which are then cleaved and modified (Taylor *et al.* 2006; Moremen *et al.* 2012). The subsequent stages in the N-glycosylation pathway are illustrated in **Figure 1.6** (Moremen *et al.* 2012). Glycosyltransferases in the cytosol initially facilitate the assembly of a glycan from monosaccharides. The monosaccharides are attached stepwise onto a so-called “lipid anchor”, which is situated within the endoplasmic reticulum (ER) membrane. The assembled glycan is referred to as a lipid-linked oligosaccharide (LLO). The LLO is then flipped onto the luminal side of the ER where it can be further modified and serve as a donor for glycosylation. Eukaryotic LLOs contain a conserved core comprising $\text{Glc}_3\text{Man}_9\text{GlcNAc}_2$, where Glc is glucose, Man is mannose and GlcNAc is N-acetylglucosamine. Ribosomes inside the cytoplasm assemble with a protein called SEC61 translocon within the ER membrane. mRNAs that encode Asn-X-Ser/Thr acceptor sequons (AKA glycosylation motifs) are translated into proteins, which enter the ER via the SEC61. Upon protein entry into the ER, LLO-associated glycans are transferred *en bloc* to critical

asparagine residues with the acceptor sequons by oligosaccharyltransferase (OST). The resulting glycoprotein is partially folded and undergoes further glycan modifications, beginning with the removal of two glucose residues (glycan trimming) by α -glucosidase I (GIsI) and the α -glucosidase II α - β heterodimer (GIsII α / β), which also facilitates protein folding.

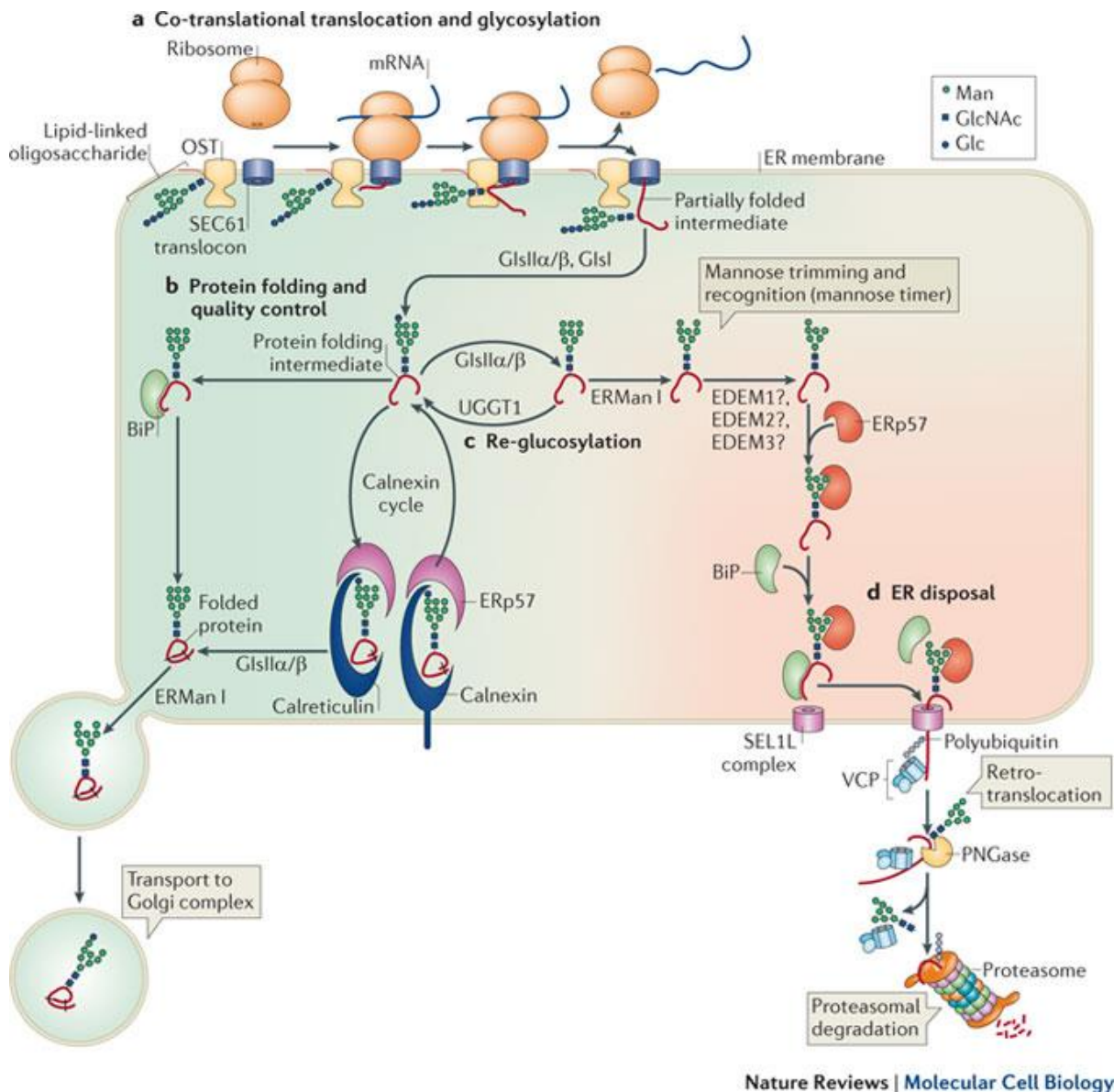


Figure 1.6. N-glycosylation of eukaryotic proteins. a) co-translocation and glycosylation b) protein folding and quality control. c) re-glycosylation of misfolded proteins d) ER disposal of terminally misfolded proteins Figure taken from Moremen et al. 2012.

Proteins with terminal glucose modifications are targets for the two lectins; calnexin (CNX) and its membrane bound homologue, calreticulin (CRT). CNX and CRT retain glycoproteins until they are properly folded and help prevent their aggregation. Dissociation

from CNX/CRT results from the removal of the remaining glucose residue by GlcII α/β . In the event of improper folding, glucose can be re-added by UDP-glucose glycoprotein glucosyltransferase 1 (UGGT1) and the glycoprotein re-introduced into the CNX/CRT cycle, which continues until the protein is correctly folded. The CNX/CRT cycle is assisted by ERp57 and Bip chaperones. During this process glycoproteins can be targeted by ER mannosidase I (ERManI), which removes one of the mannose residues. Terminally misfolded glycoproteins are subjected to further glycan trimming in the presence of ER degradation-enhancing α -mannosidase-like proteins (EDEMs), disentangled from aggregates and reduced using Bip and ERp57 proteins, before finally being translocated into the cytoplasm. Here, the denatured glycoproteins are ubiquitinated, processed by valosin containing protein (VSP) and completely de-glycosylated by PNGase before being targeted for degradation in the proteasome.

Correctly folded glycoproteins leaving the CNX/CRT cycle are usually associated with Man₉GlcNAc₂ or Man₈GlcNAc₂ structures and are targets for the ER-Golgi intermediate compartment marker, ERGIC53, which acts as a broad specificity receptor for all large-mannose chains. Vesicular integral protein 36 (VIP36), VIP36-like protein (VIPL) and mannan-binding protein also facilitate transport of glycoproteins to the Golgi. In the Golgi glycoproteins undergo further mannose trimming, by the Man₅GlcNAc₂ by the *cis*-Golgi α -mannosidases; IA, IB and/or IC. Glycoproteins, that resist trimming to Man₅GlcNAc₂ can be retrieved by VIP36 and subjected to new rounds of trimming. Structures Man₉GlcNAc₂ to Man₅GlcNAc₂ are referred to as high-mannose forms. Proteins possessing these kinds of modifications are rarely released from *cis*-Golgi and do not normally reach the cell surface. High-mannose modifications therefore can act as a reliable marker for immature proteins. The majority of glycoproteins undergo further modification in *medial*-Golgi, where two further mannose residues are removed, while three glyNac and one fructose residues are added. Finally, in *trans*-Golgi, three galactose residues followed by three N-acetylneuraminic acid residues are added and the protein with this complex oligosaccharide modification can be targeted for the membrane or secretion.

1.4. Molecular characterisation of Ly49 receptors

The first attempts to characterise Ly49s began during the early 1980s. At the time very little was known about this family of receptors and several immunoprecipitation (IP)

experiments were carried out to determine the specificity of newly developed monoclonal antibodies, which were generated against previously unidentified surface molecules. Studies would eventually go on to demonstrate that the molecules were in fact Ly49 receptors.

Chan *et al.* developed YE1/48 and YE1/32 monoclonal antibodies that recognised a protein, which was expressed on the surface of EL-4 and MBL-2 T cell lymphomas and, to a lesser extent, normal splenocytes and thymocytes (Takei 1983; Chan and Takei 1986; Chan and Takei 1988). The cells were surface radiolabelled with ^{125}I isotope and lysed. Lysates were subjected to immunoprecipitation with YE1/48 and YE1/32 monoclonal antibodies. The eluted proteins were then analysed by SDS-PAGE with and without the reducing agent, 2-mercaptoethanol (2ME), and visualised using autoradiography. Immunoprecipitated material migrated on SDS-PAGE as a 45-50 kDa dispersed band under reducing conditions and as an 85-100 kDa band under non-reducing conditions, suggesting that the molecule of interest was a disulphide-linked dimer. Since the monomer migrated at roughly half the size of the dimer, it was proposed that the molecule of interest was a homodimer. An additional high molecular weight band appeared in some of the reduced and non-reduced samples, suggesting that the immunoprecipitated antigen may be capable of multimerisation.

The dispersed nature of the bands was thought to be due to glycosylation of the protein. The protein was therefore treated with a range of concentrations of endoglycosidase F, which removes all N-linked glycans that are attached to polypeptides at asparagine residues. On analysis by SDS-PAGE, the reduced IP material migrated at a molecular weight of 42 kDa (no glycosidase), 38 kDa (12.5 U/ml glycosidase for 3 h) and 32 kDa (50 U/ml glycosidase for 22 h), which suggested that the monomer had at least 3 N-glycosylation sites. The 38 kDa and 32 kDa bands persisted, after prolonged exposure to the enzyme, suggesting that the dimeric molecule may in fact be a heterodimer made of two subunits of 38 and 32 kDa in size. Alternatively, the protein core of the subunits could have been the same but one of the subunits could possess a carbohydrate modification, which was resistant to enzymatic treatment. Interestingly, all of the samples contained some residual non-reduced material, suggesting that the dimeric protein was robust and resistant to reduction. A high molecular weight band, of a similar size to that previously described, was also present in all of the samples.

When the YE1/48 antigen was purified from EL-4 cells and separated by diagonal SDS-PAGE, two very similar subunits were detected; one more acidic than the other (Chan and Takei 1988). Tryptic peptide profiles of the two subunits were different but much more similar than, for example, profiles of T cell receptor subunits. These results provided further evidence that the core peptides of the two antigen subunits might in fact be the same, but that they might undergo different posttranslational modifications.

Around the same time, Nagasawa and colleagues immunised BALB/c mice with EL-4 cells and developed a monoclonal antibody, termed 1A, which reacted with two T lymphoma cells of C57 origin (EL-4 and CGVBL). However, the 1A antibody did not react with normal C57 splenocytes, thymocytes, C57 T cell clones or other T and B lymphomas, as revealed by complement-mediated cytotoxicity or indirect immunofluorescent staining (Nagasawa *et al.* 1987). The antibody was used to immunoprecipitate an as-yet unknown molecule, which migrated on SDS-PAGE gels as a dispersed band of ~43 kDa under reducing conditions and a band of ~85 kDa under non-reducing conditions. Interestingly, small amounts of the antigen were also immunoprecipitated from normal splenocytes and thymocytes. The authors concluded that the antigen may not have been accessible by the antibody on the surface of the cells, thus explaining why it was not detected by FACS analysis. However, following lysis the relevant epitopes became available.

When the antigen was subjected to 2D SDS-PAGE and peptide mapping, similar results were obtained as for the antigen identified by Chan *et al.*, except the more acidic subunit could not be surface labelled by ^{125}I . Chan *et al.* also described difficulties encountered in surface labelling of the acidic subunit, although they did eventually succeed.

Further investigation revealed that all three of the aforementioned antibodies (YE1/48, YE1/32 and 1A) bind the same dimeric protein but that they might recognise different epitopes. Eventually cDNA of the YE1/48 antigen was obtained and sequenced, revealing that the protein of interest contained 262 amino acids and had a predicted molecular weight of 30.5 kDa (Chan and Takei 1989; Yokoyama *et al.* 1989). 44 amino acids were predicted to comprise the cytoplasmic domain, 22 amino acids the transmembrane region and 196 amino acids the extracellular domain. The protein had characteristics of a type II transmembrane protein, with an intracellular N-terminus and a C-terminus exposed to the surface. Three putative N-glycosylation sites were identified in the sequence. For

consistency in the immunological nomenclature the YE1/48 antigen was named Ly49. Southern blot analysis using Ly49 cDNA probes revealed a multiple band pattern, suggesting cross-hybridisation with other related proteins (Chan and Takei 1989; Yokoyama *et al.* 1989). Ly49 appeared to be a prototypic member of a newly identified family of receptors and was therefore named Ly49A. Similar results to those described by Chan *et al.* and Nagasawa *et al.* regarding the molecular nature of Ly49A were obtained for IL-2-activated NK cells (Mason *et al.* 1996; Ortaldo *et al.* 1999), M14T cells (Roland and Cazenave 1992) as well as in COS transfectants (Yokoyama *et al.* 1989), and C1498 transfectants (Scarpellino *et al.* 2007). Several studies also confirmed the results for EL-4 cells (Roland and Cazenave 1992; Yokoyama *et al.* 1989; Chang *et al.* 1996).

In 1988 Mason *et al.* used immunoprecipitation to confirm that an antibody they had developed (4D11) recognises a unique antigen on mouse spleen and liver NK cells. The antigen ran on SDS-PAGE gel in the range of 85-89 kDa under non-reducing and reducing conditions. (Mason *et al.* 1988). They failed to comment on a band of ~40 kDa in size, which most likely represented a monomer and was present even in the non-reduced samples. This finding was potentially highly significant, suggesting that the identified antigen may exist in NK cells as a monomer. They called the antigen LGL-1, but it has since been renamed Ly49G2. Subsequent studies, in which higher amounts of reducing agent were used revealed, that Ly49G2 was a disulphide linked dimer, which was notoriously difficult to reduce most likely due to the presence of multiple internal disulphide bridges (Mason *et al.* 1995; Mason *et al.* 1994; Chang *et al.* 1999).

Another group from the University of Texas generated the SW5E6 antibody, which bound ~50 % of mouse NK cells. The antigen recognised by SW5E6 migrated by SDS-PAGE as a band of ~54 kDa under reducing conditions and as a ~110 kDa band under non-reducing conditions (Sentman *et al.* 1989). The antigen was later identified as Ly49C (Mason *et al.* 1996; Ortaldo *et al.* 1999; Scarpellino *et al.* 2007). Similar experiments, revealing the dimeric nature of Ly49s have since been performed on Ly49H, Ly49Q, Ly49P and Ly49I (Smith *et al.* 2000; Toyama-Sorimachi *et al.* 2004; Ortaldo *et al.* 1999; Scarpellino *et al.* 2007). The identified molecular sizes of the monomers and dimers as well as methods used for the characterisation of those and others NK cell receptors are summarised in **Appendix II**.

When in 1996 Ly49D was characterised, a sequential immunoprecipitation was performed with 1A, 4D11 and SW5E6 antibodies before probing with a putative 12A8 anti-Ly49D antibody to confirm its specificity (Mason *et al.* 1996). IP material from the subsequent stages was analysed by SDS-PAGE under reducing and non-reducing conditions and revealed a pattern characteristic for previously observed glycosylated Ly49 monomers and dimers. However, when the individual monomers and dimers were compared with each other on the same gel, they ran at slightly different sizes, indicating that 12A8 specifically recognises Ly49D and not any of the previously characterised Ly49s.

Ly49A and Ly49C are co-expressed on the surface of approximately 5 % of C57 NK cells and show very close homology in their amino acid sequences (Brennan *et al.* 1995). In order to determine whether or not they are able to form heterodimers, COS cells were co-transfected with Ly49A and Ly49C, lysed and subjected to sequential IP with anti-Ly49A in the first round and anti-Ly49C in the second round and vice versa. If Ly49A and C had been able to form heterodimers, the fraction precipitated by the first antibody should have been re-precipitated by the second. SDS-PAGE analysis revealed that this was not the case, suggesting that Ly49A and Ly49C monomers are not able to dimerise on the surface of COS transfectants and most likely exist exclusively as homodimers on the surface of cells, in which they are natively expressed (Brennan *et al.* 1995). The experiment did not exclude the possibility that the two subunits may be differentially modified.

Examples of other murine NK cell receptors that have been examined by Western blotting and immunoprecipitation include CD94 (Perez-Villar *et al.* 1996; Lazetic *et al.* 1996), rat Ly49i2 (Naper *et al.* 1998; Naper, *et al.* 2002a), NKR-P1C (Kveberg *et al.* 2006a) and KLRH1 (Naper *et al.* 2002b) and the results are summarised in **Appendix II**. More information regarding the molecular nature of Ly49 receptors has since been elucidated through the use of crystallographic studies, details of which are described in **Section 1.6**.

1.5. The Ly49 ligand binding

1.5.1. Ligand specificity

The primary function of Ly49 receptors concerns regulation of NK cell activation, which is achieved through binding of Ly49 ligands. MHC class I molecules act as ligands for inhibitory Ly49s. As described in **Section 1.1.2**, functional studies have revealed that the specificity of each Ly49 receptor is restricted to a particular individual or set of MHC class I molecules. Ly49A has been shown to inhibit lysis of target cells expressing H-2D^d and H-2D^k MHC class I molecules (Karlhofer *et al.* 1992). Antibodies directed against Ly49A or its ligand are able to block the inhibition. Similar experiments have shown that Ly49G2 associates with H-2D^d (Mason *et al.* 1995).

The specificity of Ly49 receptors has also been studied *in vivo*. Ly49G2-expressing NK cells have been shown to reject bone marrow allografts expressing H-2^b but not H-2^d, confirming H-2^d specificity of Ly49G2 (Raziuddin *et al.* 1996). Bone marrow graft rejection experiments also confirmed that H-2K^b acts as a ligand for Ly49C and the closely-related Ly49I (Yu *et al.* 1996).

Cell-cell adhesion assays have been used to show the direct association of Ly49A with H-2D^d (Daniels *et al.* 1994; Takei *et al.* 1997). COS-7 cells transfected with Ly49C were shown to associate with cells expressing H-2^b, H-2^d, H-2^k and H-2^s, while cells transfected with Ly49I were shown not to associate with any of the tested MHC expressing cells, which is in contrary to graft rejection experiments (Brennan *et al.* 1996a; Brennan *et al.* 1996b).

Another direct association assay that has been used to demonstrate Ly49 interactions involved coating plates with isolated, soluble MHC class I molecules. EL-4 lymphoma cells expressing Ly49A have been shown to bind to plastic microtiter plates coated with H-2D^d, H-2D^k, and H-2K^b, but not H-2K^d, H-2K^k, or H2-D^b and the binding was inhibited by A1 anti-Ly49A antibody (Kane 1994). A more robust assay has since been developed to assess direct Ly49-ligand interactions, in which α chains of mouse MHC class I molecules are expressed in *E.coli*, then refolded in the presence of human β 2m and assembled into soluble tetramers

that are conjugated to fluorophores (Hanke *et al.* 1999). The tetramers were incubated with cells expressing Ly49 receptors and binding assessed using flow cytometry.

Seven different Ly49 receptors (A, B, C, E, F, G2 and I) were tested with a variety of tetramers (H-2K^b, H-2D^b, H-2K^d, H-2D^d, H-2L^d, H-2D^k) (Hanke *et al.* 1999). Ly49A was shown to specifically bind H-2D^d and H-2D^k tetramers and Ly49G2 bound weakly to H-2D^d, which confirmed previous findings. Ly49C associated with all of the tested tetramers apart from H-2L^d, which was consistent with most of the cell adhesion assays; although H-2D^b was previously shown not to associate. The authors concluded that binding of tetramers would be much stronger than a single MHC class I molecule, thus explaining why an association between H-2D^b and Ly49C was not previously detected. Ly49B and Ly49F showed very little reactivity with any of the tested tetramers. Ly49I was shown to associate with H-2K^d and H-2D^d; this was in contrast with data obtained in the cell adhesion assays, which indicated that H-2K^b is a specific Ly49I ligand. The discrepancy was thought to be due to the specificity of Ly49I for a specific peptide bound to the MHC class I molecule. Five different peptides bound to H-2K^b molecules were tested with only two of them enabling binding by Ly49I. Ly49C was also tested in parallel for peptide specificity and was shown to bind H-2K^b regardless of which of the five peptides it associated with. Ly49A tested in similar studies also showed no selectivity for different peptides (Correa and Raulet 1995; Orihuela *et al.* 1996).

Co-crystal structures of Ly49A and Ly49C with their ligands (described in detail in **Section 1.6.2**) show that the binding site between Ly49s and their ligands involves residues in all three α -chain domains of MHC class I and β 2m. Tetramer binding assay was repeated using MHC molecules that were refolded with mouse, rather than human, β 2m (Scarpellino *et al.* 2007). Unexpectedly, Ly49A was found to react, not just with H-2D^k and H-2D^d, but also with H-2K^d and very weakly with H-2K^b and H-2D^b. Ly49C reacted with all of the tested tetramers which is consistent with the Hanke *et al.* tetramer binding experiment. Interestingly Ly49B was also found to react with all of the tested tetramers, which is in stark contrast to what was found in the previous study. However, it was since hypothesised that the lack of interaction of Ly49B with tetramers in the Hanke *et al.* study was due to the presence of HA-tag (Scarpellino *et al.* 2007). A weak interaction was observed between Ly49G2 and H-2D^d and between Ly49I and both H-2K^b and H-2K^d. Ly49Q was shown to bind H-2K^b as a primary ligand; an interaction was also observed with H-2D^d, albeit only

roughly half as strong. Ly49D, E, F and H showed very little reactivity with all of the tested ligands.

The significance of species-specific residues of $\beta 2m$ was investigated in another study, which showed that replacing murine $\beta 2m$ with human $\beta 2m$ in H-2D^b, H-2K^b and H-2D^d tetramers resulted in a loss of binding by Ly49A and Ly49C (Michaelsson *et al.* 2001). Sequence analyses, combined with *in silico* analyses of available crystal structures, revealed that lysine at position 3, threonines at positions 4 and 28 and glutamine at position 29 could be directly involved in the interactions between Ly49A and H-2D^d (Michaelsson *et al.* 2001). An alternative explanation was that replacement with the human $\beta 2m$ affects folding of α chain, thereby indirectly influencing binding by Ly49 receptors. Another study, which utilised site-directed mutagenesis, revealed that residues glutamine 29 and lysine 58 of $\beta 2m$ are critical for Ly49A binding (Wang *et al.* 2002a).

Prior to solving co-crystal structures of Ly49A and Ly49C with their ligands, several studies indicated that Ly49A interacts with the $\alpha 2$ domain of H-2D^d, with further possible contributions from the $\alpha 1$ domain. Chimeric MHC class I molecules, in which the $\alpha 1$, $\alpha 2$ and $\alpha 3$ domains of H-2D^d were replaced by the corresponding domains of H-2D^b, were transfected into YB2/0 cells. Transfectants were then tested for association with RNK cells expressing Ly49A. Only transfectants expressing chimeric molecules with the $\alpha 2$ domain of H-2D^d origin were able to associate with Ly49A-expressing cells, suggesting that the $\alpha 2$ domain alone is responsible for the allelic specificity of Ly49A (Sundback *et al.* 1998). Another study has shown that incubation of H-2D^d-expressing cells with antibody directed against $\alpha 1/\alpha 2$, but not $\alpha 3$, had an inhibitory effect on binding Ly49A-expressing CHO cells (Daniels *et al.* 1994). The role of the $\alpha 1$ motif and N-terminal residues of $\alpha 2$ in Ly49A binding was further confirmed by another study where ten recombinant H-2D^d/H-2K^d molecules were tested for binding to Ly49A (Matsumoto *et al.* 1998)

Murine Ly49 NK cell receptors belong to the C-type lectin superfamily, which is characterised by a carbohydrate recognition domain (CRD) and the ability to bind sugars in the presence of calcium. Despite this, Ly49s were shown to bind their MHC class I ligands in a calcium-independent manner. To address the question of whether or not Ly49s can bind carbohydrates, such as other C-type lectins, a variety of readily available potential ligands were tested. Sulfated glycans, including fucoidan and dextran sulfate, were shown to inhibit

Ly49A- and Ly49C-mediated adhesion (Brennan *et al.* 1995; Daniels *et al.* 1994). Fucoidan was able to block binding of anti-Ly49A and anti-Ly49C monoclonal antibodies to cells transfected with Ly49A and Ly49C (Brennan *et al.* 1995; Lian *et al.* 1998). These findings demonstrate that Ly49A and Ly49C may possess a functional carbohydrate-binding domain. However, the tested polysaccharides are not natural, endogenous Ly49 ligands and the significance of these data is unclear. It is possible that Ly49s possess other, as-yet unidentified, exogenous ligands, which could, for example, originate from pathogens and become important during infection.

1.5.2. The role of ligand glycosylation in Ly49-MHC class I interactions

Both Ly49s and their MHC class I ligands are heavily glycosylated. Several studies have been carried out in order to assess whether or not glycosylation of MHC class I molecules is important for their interactions with Ly49 receptors. Treatment of H-2D^d-transfected cells with the glycosylation inhibitor, tunicamycin, has been shown to reduce Ly49A-mediated NK cell inhibition (Daniels *et al.* 1994). Treatment of cells expressing Ly49C ligands with fucosidase had a similar effect on inhibitory Ly49C function (Brennan *et al.* 1995). These results suggest that the level of ligand glycosylation might contribute to binding affinity between Ly49 and MHC class I molecules.

The exact nature of MHC glycans is unknown. However, the ability of Ly49s to bind sulphated polysaccharides and no others, together with the binding assays previously outlined, indicate that MHC class I sugars may be sulphated. This prediction has been confirmed by Chang *et al.*, who showed that the SO₄ 2- label on H-2D^d is removed by N-glycosidase F but resistant to endoglycosidase H, suggesting that the glycans are indeed sulfated and that the sulfate groups are located on mature, N-linked oligosaccharides (Chang and Kane 1998). H-2D^d-Ly49A interactions were diminished by treatment of target cells with a sulfation inhibitor (sodium chlorate), suggesting that sulfate modifications can influence Ly49-MHC binding.

The position of most N-glycans can be predicted since they are usually attached to asparagine residues that occur in the tripeptide sequence, Asn-X-Ser or Asn-X-Thr, where X may be any amino acid except proline (Taylor *et al.* 2006). Mouse MHC class I molecules possess two conserved N-glycosylation sites at positions 86 and 176 located in the $\alpha 1$ and $\alpha 2$ domains, respectively (Chang and Kane 1998). Two independent groups have created H-2D^d

glycosylation mutants to assess the role of glycan modifications in the binding of Ly49A (Matsumoto *et al.* 1998; Lian *et al.* 1998). Interestingly, one of the studies reported that both N86 and N176 mutants were recognised by Ly49A, suggesting that glycosylation is not essential for MHC binding (Matsumoto *et al.* 1998). The second study, on the other hand, indicated that glycosylation at N176, but not N86, is important for binding (Lian *et al.* 1998). Both groups created their mutants by site directed mutagenesis. However, the first group achieved it by replacing asparagine residues with glutamine, when the second one replaced serine 88 and threonine 178 with glycine. Both methods appeared to be sufficient to remove glycans, as demonstrated by altered migration patterns in SDS-PAGE analyses, following immunoprecipitation, when compared with wild type MHC molecules.

Correct folding of the mutants was confirmed by FACS analysis and staining with monoclonal antibodies. The expression levels of mutants on transfected cells were found to be comparable to wild type H-2D^d. However, one cannot discount the possibility that the mutageneses introduced discrete changes to the structure of H-2D^d. Such changes might not have been detected using the methods described, but could still have influenced ligand binding. It seems likely, that the replacement of asparagine with glutamine, which differs by just one methylene group, would have a smaller effect on the overall protein structure than replacement of threonine with the smallest amino acid, glycine. Despite the inconclusive nature of these results, it would appear that glycosylation of MHC class I molecules is not essential for interactions with Ly49 receptors, however, it may affect the strength and, perhaps, duration of binding.

The most recent study on activatory Ly49H receptor appears to confirm the above conclusions (Guseva *et al.* 2010). Ly49H recognizes a non-classical MHC class I molecule: murine cytomegalovirus (MCMV) m157 protein. M157 has four N-glycosylation sites and is natively expressed in multiple, differentially glycosylated forms. Single and combinatorial asparagine to glutamine mutants were used to establish that glycosylation enhances expression of m157 and binding to Ly49H. Interestingly, glycosylation was also shown to be important for the physical transfer of m157 to Ly49H-expressing cells, in a process known as trogocytosis.

1.5.3. *The role of Ly49 glycosylation in Ly49-MHC class I interactions*

The first evidence that Ly49 receptors themselves are glycosylated comes from experiments performed in the late 1980s using newly identified monoclonal antibodies against Ly49A was tested and have been described in **Section 1.4** (Chan and Takei 1986; Chan and Takei 1988; Nagasawa *et al.* 1987). **Appendix I** shows an alignment of all C57 Ly49s, together with BALB/c Ly49B, with predicted N-glycosylation motifs highlighted. Most of Ly49s contain two N-glycosylation motifs in the stalk region at residues corresponding to Ly49A 86-88 and 103-105, where the first residue of the motif is asparagine and the last, serine. Curiously, Ly49B lacks the first of these conserved sites, while Ly49Q lacks the second. Several other partially- or non-conserved N-glycosylation motifs can be identified in other Ly49 receptors within the stalk regions and CRDs. Although glycosylation motifs may be predicted *in silico*, the predicted sites do not always correspond to the situation *in vivo*. For example, if the glycosylation motif is buried well inside the folded protein, it is not plausible for a sugar side chain to be attached there.

Apart from the conserved among Ly49s glycosylation motifs at positions equivalent to residues 86-88 and 103-105 in Ly49A, Ly49D activating and Ly49G2 inhibitory receptors contain an additional glycosylation site at residues NTT (221-223). Ly49D also contains a second, additional glycosylation motif (NSS) at residues 169-171. All three of these receptors share the same ligand (H-2D^d), but Ly49D and Ly49G2 bind with lower affinity than Ly49A. Mason *et al.* created a series of glycosylation mutants of Ly49D, Ly49G2 and Ly49A (Mason *et al.* 2003). In order to disrupt the Ly49D NTT (221-223) glycosylation motif, asparagine 221 was replaced with alanine, arginine or glutamine. Another mutant was also created, in which tyrosine 223 was replaced with arginine. A library, rather than a single mutant, was created to ensure that the glycosylation site was successfully perturbed and to assess the role of individual amino acids in binding of Ly49 ligands. In order to disrupt the NTT motif in Ly49G2, two mutants were created with asparagine 221 replaced by glutamine and tyrosine 223 with arginine. The non-glycosylated NTR (221-223) motif in Ly49A was replaced with both NST and NRT sequences to introduce a sugar-binding site. Additional constructs were made for the remaining Ly49D glycosylation sites with asparagines, 86, 103 and 169, replaced with alanine.

Of the four Ly49D glycosylation sites, only the most N-terminal site (86-89) appeared to be unglycosylated, as observed by SDS-PAGE gel analysis. All of the mutants, apart from N86, migrated more rapidly than the wild type protein. The Ly49A mutant protein had a higher molecular weight than the WT suggesting, that the mutant was successfully glycosylated. The mutants were used in MHC tetramer binding assays, which have shown that the presence of sugar at the NTT (221-223) site interferes with H-2D^d ligand binding to Ly49D, Ly49G2 and Ly49A mutant. The effect was apparent for all Ly49D glycosylation mutants, but the most conserved mutant (N221A) did bind with smaller affinity than N221R, and the least conserved mutant T223R did bind with the highest affinity. Moreover, Ly49D N221R and T223R mutants did bind to H-2D^b tetramers with higher affinity, suggesting that the arginine 223 in Ly49A sequence could be important for binding class I molecules other than H-2D^d. The mutants were also used to assess the role of NTT 221-223 glycosylation in Ly49D function. Disruption of the motif reduced Ly49D-mediated activation in the presence of H-2D^d targets. Taken together, the above results suggest that the carbohydrate modifications, although not essential, can influence the strength of Ly49-ligand interactions.

1.6. Structure of Ly49 receptors

1.6.1. Overview

Sequence analysis revealed that Ly49s are type II transmembrane homodimers, i.e. with their C-termini exposed to the extracellular space (**Figure 1.7A**) (Dimasi 2005). Each monomer has got a molecular weight of ~30 kDa and is composed of a globular NK domain (NKD) of approximately 120 amino acids, a stalk region of ~70 amino acids, a transmembrane domain (TM) of ~20 amino acids and an intracellular signalling domain of ~45 amino acids (**Figure 1.7A**). The Ly49 NKD adopts a C-type lectin-like domain (CTLD) fold and its stalk is composed of three consecutive alpha helices. Monomeric Ly49s dimerise through disulphide bonds that form between the two stalk regions (**Figure 1.7A**). Signalling domains of inhibitory Ly49s contain Immunoreceptor Tyrosine Based Inhibition Motifs (ITIMs), which recruit phosphatases that contain Src Homology 2 (SH2) domains. The activating Ly49 transmembrane domain contain a positively charged arginine residue, which mediates signalling through interactions with a negatively charged aspartic acid residue contained within the DAP12 protein (**Figure 1.7A**) (McVicar *et al.* 1998; Anderson *et al.* 2001).

The structure of the extracellular portion of Ly49s is markedly different to that of human KIR receptors, which are composed of 2 or 3 immunoglobulin-like domains (**Figure 1.7B**) (Radaev and Sun 2003). Moreover, KIRs are expressed as type I monomers, i.e. with their C-termini located intracellularly, rather than type II dimers. However, the transmembrane and signalling domains are similar in both cases (**Figure 1.7**). It is a remarkable example of convergent evolution where two molecules with markedly different structures are capable of fulfilling the same role.

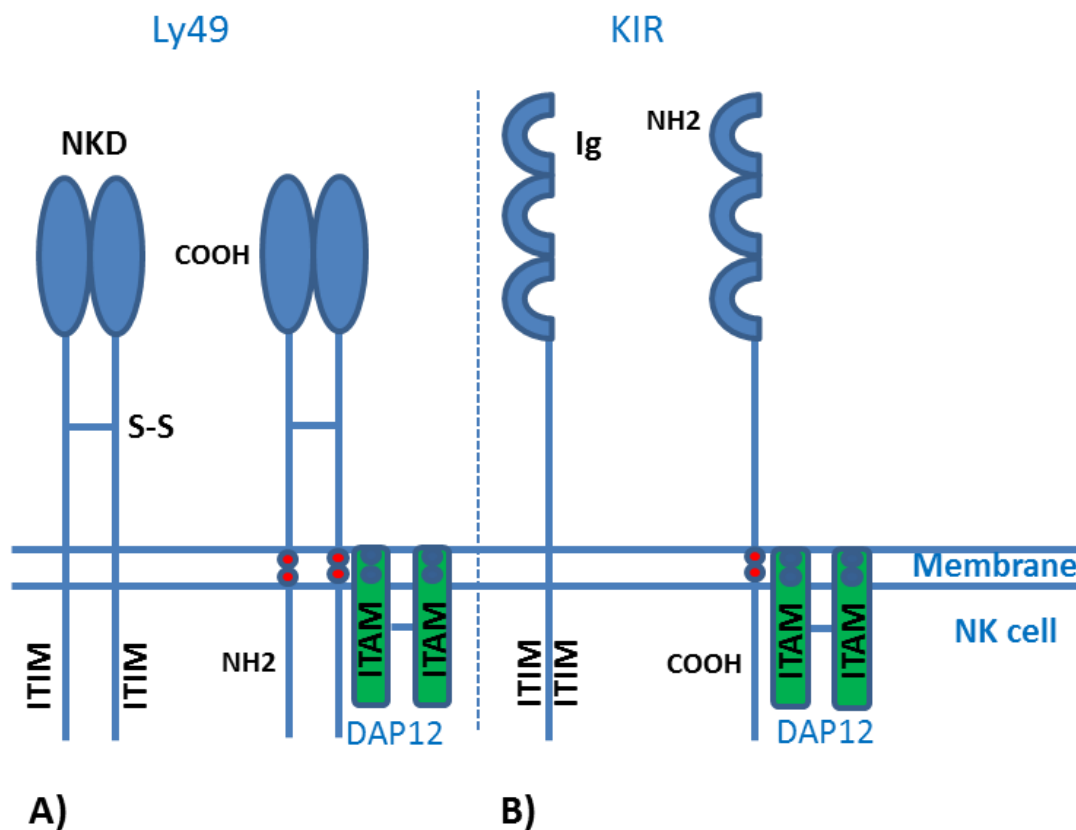


Figure 1.7. Schematic structure of Ly49 and KIR receptors. **A)** The left hand panel shows an inhibitory receptor. The right hand panel shows an activatory receptor. Ly49 monomers are composed of a globular NK cell domain (NKD), a stalk region, a transmembrane domain and an intracellular domain. Two monomers are linked by disulphide bonds. Within their intracellular domains inhibitory receptors contain ITIM motifs, which facilitate inhibitory signalling upon ligand binding. Within their transmembrane regions activatory receptors contain positively charged arginine residues (red), which interact with negatively charged aspartic acid residues (blue) in the DAP12 protein. DAP 12 contains an activatory ITAM motif, which facilitates downstream activatory signalling events. **B)** KIR receptors. The left hand panel shows an inhibitory receptor and the right hand panel an activatory receptor. KIR receptors exist as monomers with 2 or 3 immunoglobulin-like domains (Ig). The monomer also contains a stalk region, transmembrane domain and intracellular domain. The intracellular portions of the inhibitory and activatory KIRs are analogous to those of Ly49 receptors, but KIR monomers contain two ITIMs, rather than one. COOH – C' terminus, NH2- N' terminus, ITIM - Immunoreceptor Tyrosine Based Inhibition Motif, ITAM - Immunoreceptor Tyrosine Based Activation Motif.

1.6.2. Crystal structures of Ly49s

To date the structures of Ly49A, C, G, I and L have all been solved by X-ray crystallography: (Tormo *et al.* 1999; Dimasi *et al.* 2002; Dam *et al.* 2003; Deng *et al.* 2008; Back *et al.* 2009). All of them include the NKD region but only the Ly49L structure contains the flexible stalk region. None of the structures contain transmembrane or intracellular domains, in part due to the inherent difficulty in expressing and purifying full length eukaryotic transmembrane proteins. Ly49A and Ly49C were co-crystallised with their MHC class I ligands, alleles H-2D^d and H-2K^b, respectively (Tormo *et al.* 1999; Dam *et al.* 2003).

1.6.2.1. The CTLD fold

The Ly49 NKD folds according to the C-type lectin-like domain (CTLD) model adopted by the CTLD superfamily of proteins, which includes mannose-binding protein (MBP-A) as a prototypical member (**Figure 1.8**) (Zelensky and Gready 2005; Weis *et al.* 1998). Many CTLD proteins are calcium-dependent (C-type), carbohydrate-binding lectins, that mediate important biological events in animals such as cell-cell adhesion and serum glycoprotein turnover.

Structural and functional data has revealed a high degree of diversity within the CTLD family in terms of ligand binding, oligomerisation mode and overall structure (Weis *et al.* 1998). Unlike true C-type lectins, C-type lectin-like molecules often bind ligands other than carbohydrates in a Ca²⁺-independent manner; the Ly49 family is one such example.

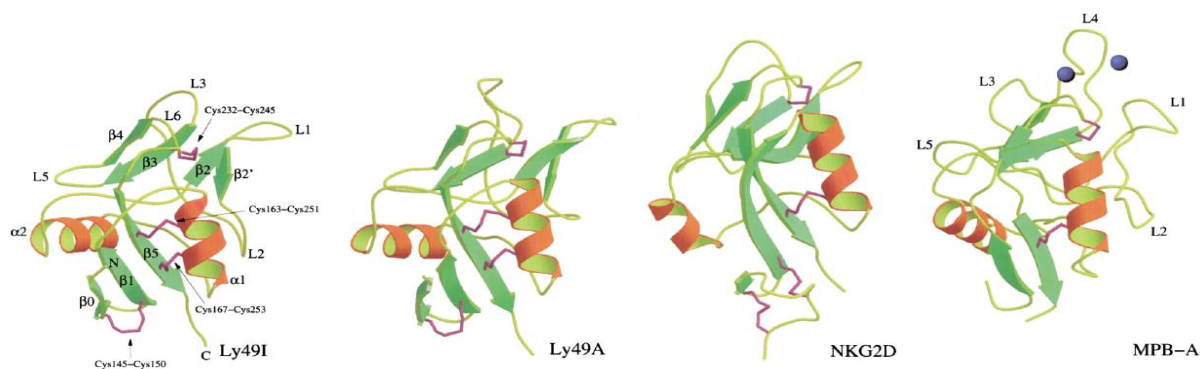


Figure 1.8. Structures of Ly49A and Ly49I in comparison with other CTLD superfamily members. Ly49I displays a C-type lectin-like fold, in common with Ly49A (PDB entry code 1Q03), NKG2D (1HQ8) and MBP-A (1YTT). Secondary structure elements of Ly49I are labelled consistently with the numbering for MBP-A, and are coloured as follows: α =helices, red and yellow; β =strands, green; loop regions, gold. The N- and C-termini are also indicated. Disulphide bonds are highlighted in violet. Calcium ions bound to MBP-A are drawn as blue spheres. Figure taken from Dimasi *et al.* 2002.

The core CTLD fold is highly conserved and includes two α -helices ($\alpha 1$ and $\alpha 2$) and two antiparallel β -sheets formed by β -strands; ($\beta 0$, $\beta 1$ and $\beta 5$) and ($\beta 2$, $\beta 2'$, $\beta 3$ and $\beta 4$) respectively (Weis *et al.* 1998; Radaev and Sun 2003). The CTLD fold is characterised by the presence of a double-loop structure known as a ‘loop-in-a-loop’, which is stabilised by two highly conserved disulphide bridges located at the bases of the loops. One of the loops, referred to as the long loop is involved in calcium-dependent carbohydrate binding or interaction with other ligands. CTLDs that do not contain the long loop are referred to as “compact”. Examples of compact CTLDs include Link/PTR domain and bacterial CTLDs (Zelensky and Gready 2005). Most of the diversity amongst CTLDs originates from the aforementioned double loop structure and other, non-conserved loops that might be present.

1.6.2.2. Crystal structure of Ly49 NKD

The core structure of all Ly49 NKDs determined so far is the same as that of other CTLDs (Zelensky and Gready 2005; Weis *et al.* 1998). The Ly49 NKD α -helices and β -sheets are held together by four intrachain disulphide bonds: two of which are conserved amongst all animal C-type lectins (residues corresponding to Cys167-Cys253 and Cys232-Cys245 in Ly49A, **Figure 1.8**); another is specific to the so-called long form of C-type lectins (residues corresponding to Cys145-Cys150 in Ly49A, **Figure 1.8**); while the last one is found only in Ly49s (residues corresponding to Cys163-Cys251 in Ly49A, **Figure 1.8**). There are five loops connecting the core of Ly49 NKDs. The main difference between individual Ly49s comes from loop 3, which links the $\beta 2'$ and $\beta 3$ strands through residues corresponding to residues 222-235 of Ly49A (**Figure 1.8**) (Dimasi *et al.* 2002). The Ly49 NKD fold was found similar to that of the NKD of the human NK receptor NKG2D (**Figure 1.8**). Both receptors lack the Ca^{2+} binding site conserved amongst other members of the family.

Ca^{2+} binding influences ligand specificity and stability of the other members of the C-type lectin superfamily. The conformation of the Ly49 NKD described here is stable in the absence of Ca^{2+} . Such dramatic changes also affect ligand specificity. Despite the fact that Ly49s belong to a lectin-like family, they do not bind carbohydrates as lectins do.

1.6.2.3. Crystal structure of Ly49 dimers

Ly49s are thought to dimerise through the formation of disulphide bonds in the stalk region (**Figure 1.7**). Crystal structures of Ly49 NKDs revealed that they are capable of forming homodimers, which are stabilised by hydrogen bonds, in the absence of the stalk region. Ly49 dimers can exist in two distinct conformations, termed “open” and “closed” (**Figure 1.9**) (Dimasi *et al.* 2002; Dam *et al.* 2006). The Ly49A dimer was analysed by NMR and shown to be capable of adopting both conformations (Dam *et al.* 2006). Ly49C and Ly49G (Dimasi *et al.* 2002; Dam *et al.* 2003) were crystallised in the open conformation, Ly49A and Ly49I (Tormo *et al.* 1999; Deng *et al.* 2008) in the closed conformation and Ly49L in both conformations (Back *et al.* 2009).

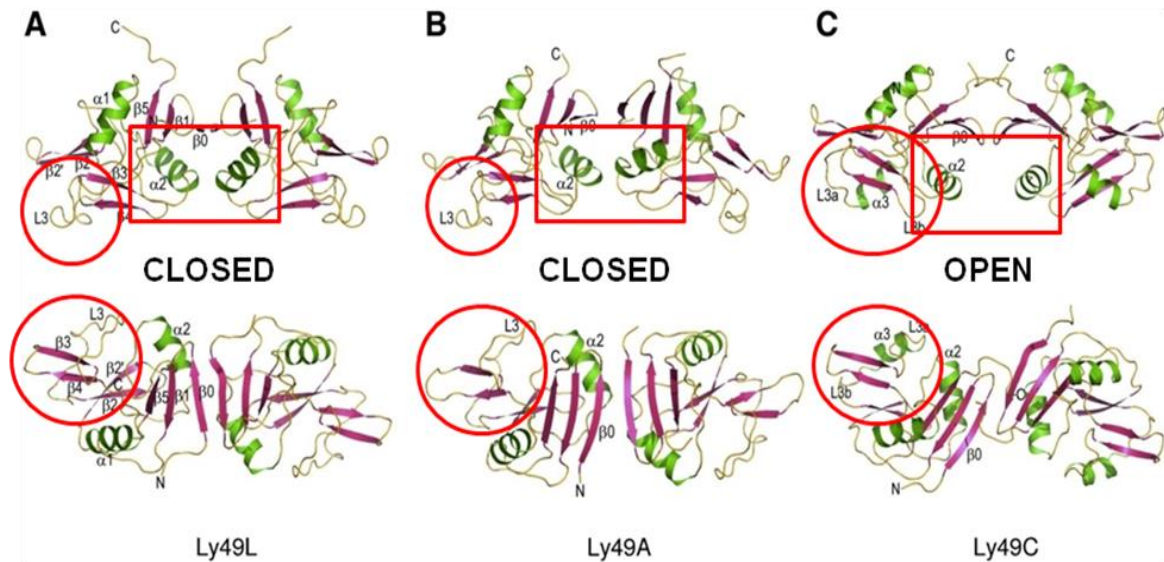


Figure 1.9. Variability in dimerisation mode of Ly49B receptors. Side views are shown in the top panel and top views in the bottom. All of the structures lack stalk regions; α helices are indicated in green, β strands in pink and loops in yellow. Loop 3 is marked with a red circle and the dimer interface is marked with a red square. Figure taken from Back *et al.* 2009.

In the closed conformation the NKD $\alpha 2$ helices are juxtaposed across the dimer interface, the $\beta 0$ strands of the two monomers interact with each other to form an extended antiparallel β -sheet, which is held together by main chain-main chain hydrogen bonds (**Figure 1.9 A and B**). In the open conformation the $\alpha 2$ helices are not in contact with one another and the register between the two $\beta 0$ strands is shifted by four residues when compared to the closed conformation (**Figure 1.9 C**). The two conformations most likely reflect two distinct modes of ligand binding, each of which is described in more detail in **Section 1.5 (Figures 1.17 and 1.18)**.

As explained in **Section 1.5.3** glycosylation may play an important role in Ly49 structure and function. Unfortunately, Ly49A NKDs destined for crystallisation were expressed in *E.coli*, which is unable to carry out posttranslational modifications including glycosylation. However, it is possible to estimate using the available crystal structures, which of the predicted glycosylation sites are likely to be on the surface of the protein, and therefore have a glycan attached. None of the Ly49 structures were solved with the full length stalk region so it is only possible to analyse the predicted glycosylation sites within the CRDs. **Figure 1.10** shows Ly49G and Ly49I dimers with their glycosylation sites highlighted in red (NTT [221-223] for Ly49G and NKT [160-162] for Ly49I). Considering the position of these motifs, on the surface of the CRDs, it seems likely that they may undergo glycosylation.

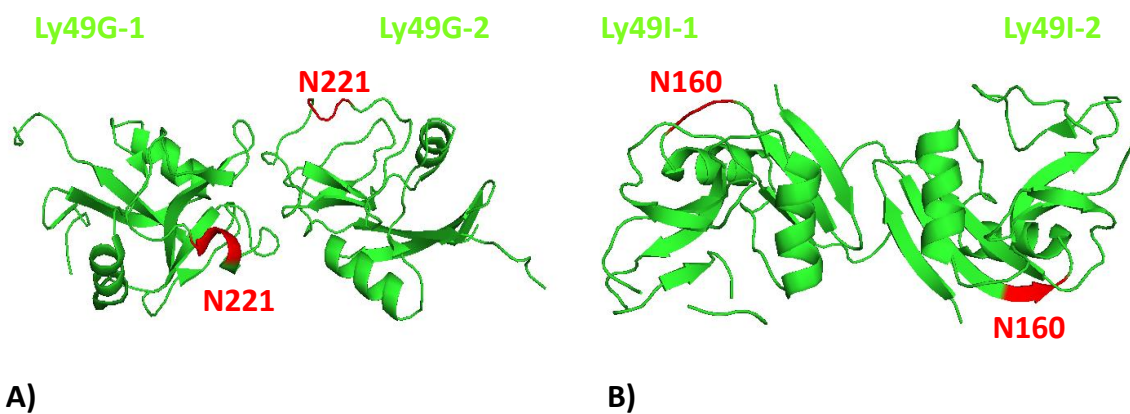


Figure 1.10. Predicted glycosylation sites of Ly49G and Ly49I CRDs. The glycosylation motifs of each monomer are marked in red. Of the two monomers, one contains a flexible loop at its glycosylation motif, while the other contains a beta sheet. The inconsistency of the electron density map at these sites is due to the flexibility of CRDs, however, the highlighted regions represent the same residues within the two monomers. A) Ly49G dimer with NTT (221-223) glycosylation motif (PDB accession- 3CAD) B) Ly49I dimer with NKT (160-162) glycosylation motif (PDB accession- 1JA3).

1.6.2.4. The crystal structure of Ly49-MHC interface

The first co-crystal structure to be determined was that of Ly49A bound to its H2-D^d ligand (Tormo *et al.* 1999). The structure was solved via molecular replacement at 2.3 Å resolution. The structure suggested that the Ly49A NKD dimer might interact with H-2D^d molecule at two separate interfaces, referred to as site 1 and site 2 (**Figure 1.11**). The surface adjacent to the MHC class I peptide-binding groove was shown to interact with a single molecule of Ly49A at the less extensive site 1, which corresponds to the carbohydrate

binding site of other C- type lectins. The Ly49A NKD interface engaged two of the loops and the β 4-strand located at the top part of the molecule. The H-2D^d molecule interacts with a region, which is highly polymorphic among MHC class I molecules, incorporating the N terminus of the α 1 helix and the C terminus of the α 2 helix; located just above the N176 residue. The interface was dominated with strong electrostatic interactions between the receptor and ligand atoms. Interacting surfaces were precisely matched as indicated by the 0.78 degree of complementarity, where a shape complementarity of 1 represents a perfect interface.

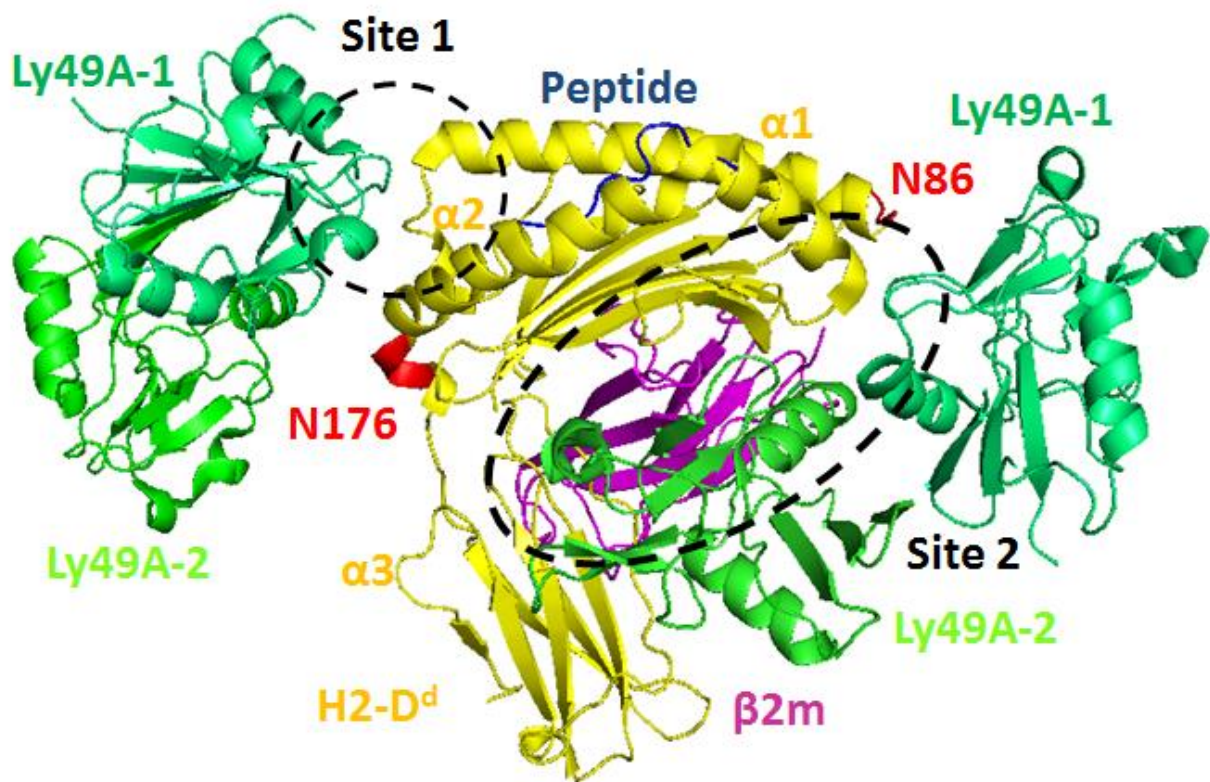


Figure 1.11. Co-crystal structure of two Ly49A dimeric NKDs bound to a H2-D^d MHC molecule. Two Ly49A monomers are highlighted in different shades of green. The H2-D^d MHC α chain is shown in yellow. β 2m is shown in magenta. The peptide in the MHC peptide binding groove is shown in blue. Asparagine residues of two conserved glycosylation sites of H2-D^d are shown in red. Site 1 and site 2 are circled with black dashed lines (PDB accession- 1QO3).

At the less accessible site 2, the α 2 and α 3 heavy chains of H-2D^d and β 2m form a cavity, into which the Ly49A NKD is intercalated. This area, with a surface of 3,342 Å², was shown to be located underneath the peptide binding surface of the MHC-I molecule and

extended to the CD8-binding site. The interface at site 2 was not as precisely matched as site 1, exhibiting a 0.54 degree of complementarity. Here, as with site 1, the putative carbohydrate-binding site was identified near the MHC class I conserved glycosylation site at position N86 of the $\alpha 1$ helix. 21 hydrogen bonds were identified between the partners of the complex, facilitating interactions at site 2. Importantly, the peptide antigen embedded in the MHC-binding groove was not involved in interactions at any of these sites, suggesting that, although Ly49 receptors are specific for particular MHC alleles, they are not restricted by the antigen presented by those molecules. Moreover the authors showed that site 1 and site 2 on H-2D^d are topologically distinct from the T cell receptor (TCR) binding site, indicating that both Ly49A and a TCR could be bound to one MHC molecule at the same time. Such an arrangement could potentially have implications in the regulation of NK T cells, which express both Ly49A and TCR receptors on their surface.

As explained in **Section 1.5.2** H-2D^d MHC class I molecule contains two glycosylation sites with critical asparagine residues at positions 86 and 176 shown in red in **Figure 1.11**. Binding of Ly49A to H-2D^d MHC-I in physiological conditions was shown by one study to be much stronger and more precise in the presence of glycan at position N176 of H-2D^d, but not in the presence of glycan at position N86 (Hanke *et al.* 1999).

The fact that Ly49A NKD and H-2D^d expressed in the absence of putative carbohydrates were able to dimerise confirms the studies which have shown that Ly49A and H-2D^d interactions are not dependent on receptor and ligand glycosylation (Tormo *et al.* 1999) but do not exclude possibility that glycosylation can affect the strength of binding. To establish the extent of the glycosylation effect, the MHC molecule would have to be expressed in the system able to support the process, for example insects or mammalian cells.

Two sugar residues, an N-Acetylglucosamine (GlcNAc) and a fructose, were modelled onto an MHC-I putative glycosylation site (N176), shown in red in **Figure 1.11** (Tormo *et al.* 1999). Both fructose and GlcNAc (to lesser extent) fitted into an open cavity formed between H-2D^d and the Ly49A NKD. Moreover, the flat hydrophobic surface of Ly49A around this region was large enough to accommodate other modified residues, which could also influence the affinity of binding. Ly49A seems to have evolved from a carbohydrate-binding receptor to a protein-binding receptor, whose ligand interaction could potentially be fine-tuned by the presence of sugar residues.

Figure 1.12 shows a Ly49C monomer bound to a H-2K^b molecule (Dam *et al.* 2003). Ly49C engages the surface of H-2K^b just below the MHC peptide-binding groove and comes into contact with β -2 microglobulin. Ly49C contains a glycosylation motif at residues NKT (160-162), which is conserved in Ly49I, as well as in Ly49H and Ly49J. The motif lies on the surface of the CRD in very close proximity to the MHC-Ly49C interface. The motif is therefore likely to have a glycan attached, which could influence Ly49-ligand interactions.

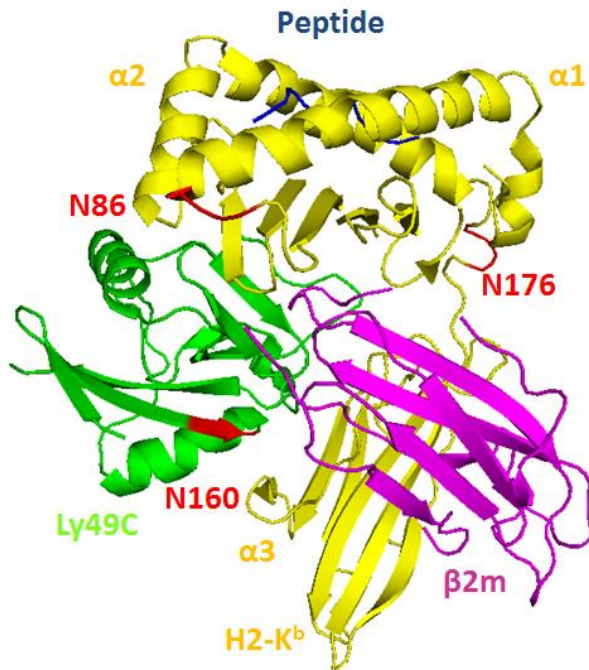


Figure 1.12. Ly49C monomer in complex with H-2K^b. Ly49C monomer is shown in green and the Ly49C glycosylation motif at residues NKT (160-162) in red. α chain of MHC class I molecule is highlighted in yellow, β 2-microglobulin is shown in pink and the peptide in the binding groove is light blue. Asparagine residues of two conserved glycosylation sites of H2-K^b are shown in red (PDB accession - 3C8K).

The discovery of sites 1 and 2 in the Ly49A NKD-H-2D^d co-crystal raised the question of whether or not both of these spatially separated interaction sites are functional. Several groups have addressed this question using site-directed mutants of Ly49A and the H-2D^d (Chung *et al.* 1999; Chung *et al.* 2000; Matsumoto *et al.* 2001b). Surprisingly, all of these studies identified site 2 as the primary site mediating interactions between Ly49A and H-2D^d. Site 1 on the other hand turned out to be a crystallographic artefact.

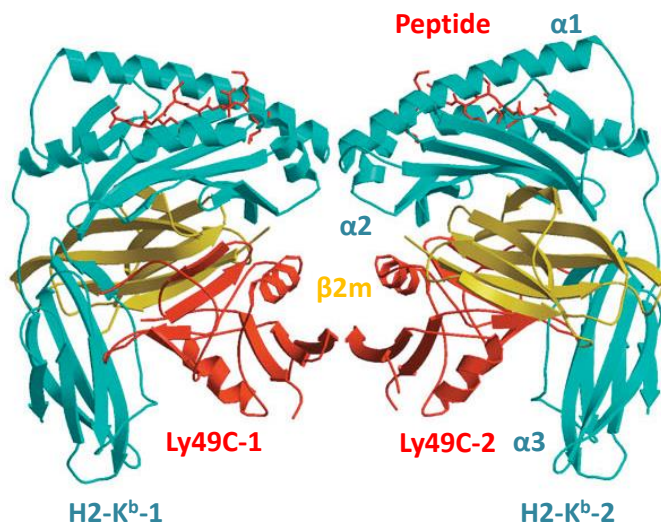


Figure 1.13. Ligand binding by Ly49C. The Ly49C dimer engages two MHC class I molecules through the same region, equivalent to site 2 in the Ly49A dimer. The region is highlighted in red. Two H-2K^b molecules are shown in blue. β 2m is shown in yellow (Dam *et al.* 2003).

The co-crystal structure of Ly49C and H-2K^b revealed that two H-2K^b molecules are able to interact with the Ly49C dimer simultaneously, engaging with each of the monomers through a site analogous to site 2 in the Ly49A NKD-H-2D^d co-crystal, suggesting that site 2 may be the primary interface utilised by all Ly49 receptors for MHC class I binding (**Figure 1.13**) (Dam *et al.* 2003). Notably, even though the Ly49C-H-2K^b interaction site occupied the region analogous to site 2 (i.e. just beneath the peptide binding groove), the interacting residues at the two interfaces were different (**Figure 1.14**) (Deng *et al.* 2008). Crystal structures of both Ly49A-H-2D^d and Ly49C-H-2K^b complexes have been refined since they were first published and **Figure 1.14** incorporates these changes. **Table 1.1** lists all of the residues that have been found to be involved in forming receptor-ligand interactions in the refined structures (Deng *et al.* 2008). Since the H-2K^b and H-2D^d contact residues at both interfaces are similar, differences are largely attributable to the individual Ly49 receptors. The main difference originates from loop 3, which includes residues 211-231 in Ly49C and contains an α -helix. Ly49A loop 3 does not contain this α -helix and spans the region between residues 222 and 235. Additional crystallographic, NMR and SPR analyses have shown significant variability in Ly49 regions engaged in MHC binding, particularly loop 3 (Natarajan *et al.* 1999; Michaelsson *et al.* 2000; Sawicki *et al.* 2001; Dam *et al.* 2003), providing further evidence for the role of this region in determining specificity.

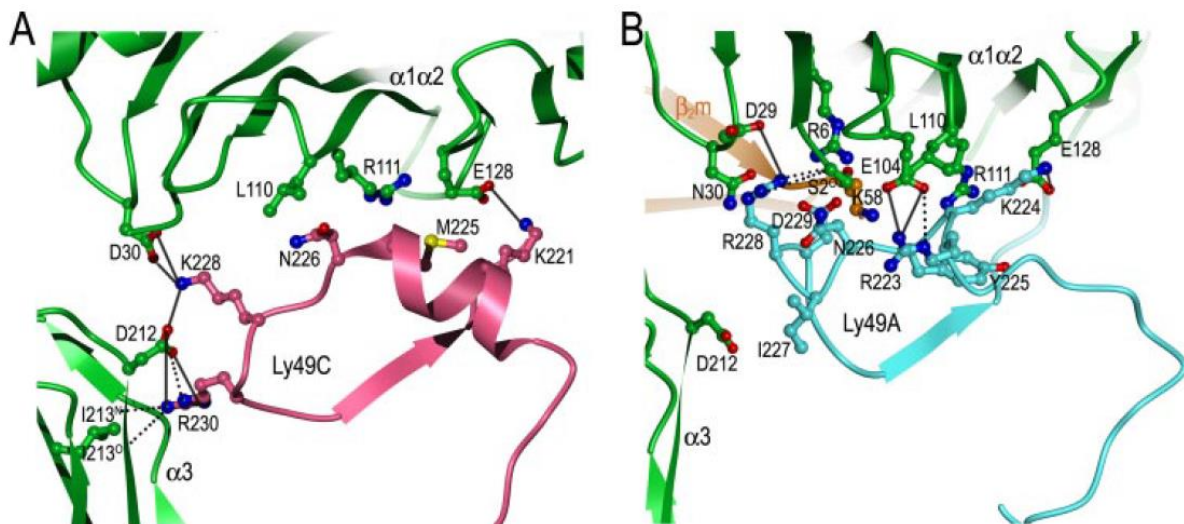


Figure 1.14. Comparison of Ly49-MHC-I interfaces. A) Ly49C-H-2K^b interface, highlighting interactions made by residues 211–231 of Ly49C. B) Ly49A-H-2D^d complex, showing interactions made by the corresponding region of Ly49A. The side chains of interacting residues are drawn in ball-and-stick representation, with carbon atoms in rose (Ly49C), cyan (Ly49A), green (H-2K^b or H-2D^d), or orange (β 2m). Oxygen atoms are shown in red, nitrogen atoms in blue, and sulfur atoms in yellow. Salt bridges and hydrogen bonds are represented by solid and dotted lines, respectively. Figure taken from Deng *et al.* 2008.

Based on successful structural analyses and sequence comparisons, the Ly49 receptors have been divided into four groups (I-IV), each of which has the potential to bind MHC class I molecules in a distinct manner (**Figure 1.15**) (Sawicki *et al.* 2001).

Group I Ly49s recognize both MHC class I H-2D and H-2K alleles; the archetypal member of this group being Ly49C. Group II is epitomised by Ly49A; it is defined by the ability of its members to recognise only H-2D alleles and by the presence of a continuous loop 3 (Wang *et al.* 2002a). Based on sequence variation in loop 6, groups I and II were further divided into subgroups Ia, Ib, IIa and IIb, each of which recognizes different variants of the H-2D and H-2K alleles. Groups III and IV are represented by only one member each, Ly49Q and Ly49B, respectively. The manners in which groups III and IV bind their ligands remain to be established.

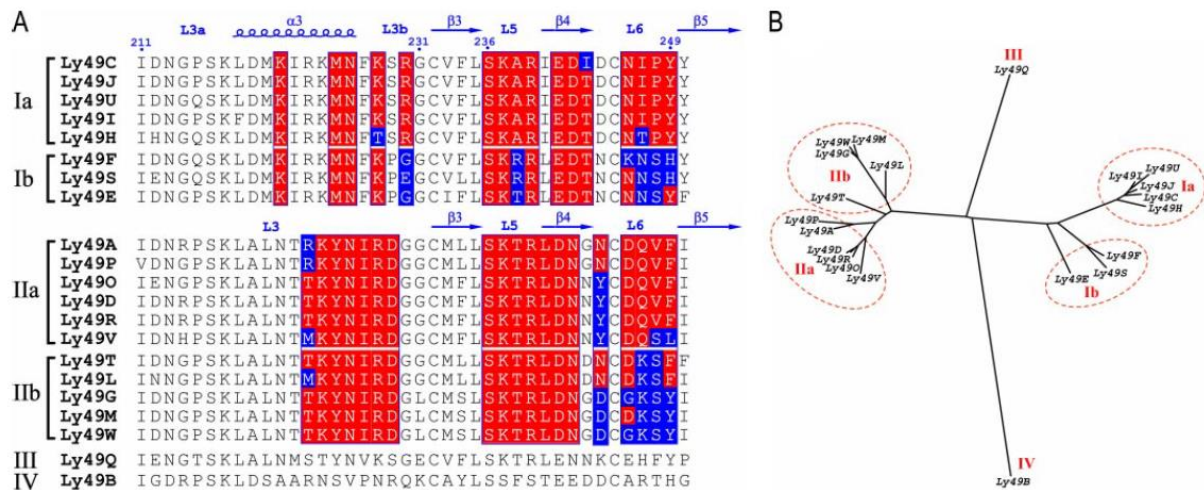


Figure 1.15. Structural classification of Ly49 NK receptors. A) Structure-based sequence alignment of the MHC-binding regions of Ly49 NKDs. Residues highlighted in red indicate putative MHC-contacting residues that are strictly or mostly conserved in group I or II. Blue residues indicate variability. B) Dendrogram of Ly49 NK receptors. Figure taken from Deng *et al.* 2008.

Table 1.1. Interactions between Ly49 and MHC-I molecules in the Ly49C-H-2Kb and Ly49A-H-2Dd complexes. Residues of H-2Kb or H-2Dd forming hydrogen bonds or salt bridges (bold letters) with Ly49C or Ly49A are in red. The number of hydrogen bonds or salt bridges formed between two residues is shown in parentheses if more than one. Residues of H-2Kb or H-2Dd forming van der Waals contacts with Ly49s are in black. Hydrogen bonds and salt bridges were calculated using cut off distances of 3.4 Å and 4.0 Å, respectively. The cut off distance for van der Waals contacts was 4.0 Å. Residues from the L3/α3 region of Ly49C and Ly49A are shown in blue. Residues from the L6 loop are shown in green. Numbering of residues in Ly49C are respective to equivalent residues in Ly49A rather than exact residues in Ly49C Figure taken from Deng et al. 2008.

Ly49 C	H-2K ^b			Ly49 A	H-2D ^d			
	α1α2	α3	β ₂ M		α1α2	α3	β ₂ M	
				R ¹⁵⁷			T ⁴ (2) Q ²⁹	K ³ T ⁴ Q ²⁹
S ¹⁶¹			I ²²⁵					
P ¹⁹²		C ¹²¹		Q ¹⁶⁵ S ¹⁹²		E ²²⁷	E ²²⁷	I ¹
N ¹⁹⁴				D ¹⁹³ S ¹⁹⁴				I ¹ K ³ D ⁵⁹
K ²⁰³		E²²³(2)	T ²¹⁶ E ²²³ Y ²⁶²	N ²⁰³			T ²¹⁴	
K ²⁰⁴		E²²³	E ²²³					
K ²²¹	E¹²⁸	E ¹²⁸						
				R ²²³ K ²²⁴	E¹⁰⁴(2) E¹²⁸	E ¹⁰⁴ L ¹¹⁰ L ¹¹⁰ R ¹¹¹ E ¹²⁸		
M ²²⁵		R ¹¹¹ E ¹²⁸		Y ²²⁵		R ¹¹¹		
N ²²⁶		L ¹¹⁰		N ²²⁶ I ²²⁷	S²	S ²		
							D ²¹²	
K ²²⁸	D³⁰(2)		D²¹²(2)	R ²²⁸ D ²²⁹	S²(2) D²⁹ R⁶(3)	S ² D ²⁹ N ³⁰ R ⁶ N ³⁰		K ⁵⁸ K ⁵⁸
R ²³⁰			D²¹² D²¹² I²¹³					
S ²³⁶	D¹²²	D ¹²²		S ²³⁶	D¹²²	D ¹²²		
K ²³⁷	D¹²²	D ¹²²		K ²³⁷	A¹³⁶	D ¹²² T ¹³⁴ A ¹³⁶		
A ²³⁸	D¹²²	D ¹²² V ¹²⁵ T ¹³⁴		T ²³⁸	D¹²²(2)	D ¹²² Y ¹²³ A ¹²⁵ T ¹³⁴ A ¹³⁵ A ¹³⁶		
R ²³⁹	Q¹¹⁵ D¹²²	I⁹⁸ Q¹¹⁵ D ¹²²		K ⁵⁸ (2) W ⁶⁰	K ⁵⁸ D ⁵⁹ W ⁶⁰	R ²³⁹ L ²⁴⁰	D¹²²(2) D¹²²(2)	D ¹²² A ¹²⁵ Q ¹¹⁵
E ²⁴¹	R¹¹¹(2)	R ¹¹¹ Q ¹¹⁵		K ⁵⁸	K ⁵⁸	D ²⁴¹	R¹¹¹(2)	R ¹¹¹
D ²⁴²				K ⁵⁸	K ⁵⁸	N ²⁴²		K ⁵⁸ (2) K ⁵⁸
I ²⁴³					K ⁵⁸			
						N ²⁴⁴		
N ²⁴⁶			L²³⁰	L ²³⁰ V ²³¹ E ²³²			K²⁴³	Q ²³² L ²³⁰ K ²⁴³
I ²⁴⁷						Q ²⁹	E²³²	E ²³²
P ²⁴⁸				Q ²⁹	Q²⁴⁷ V²⁴⁸			Q ²⁹ Q ⁶
Y ²⁴⁹				D ⁵⁹	D ⁵⁹	F ²⁴⁹		Q ²⁹ D ⁵⁹

1.7. Ly49-MHC class I *trans* and *cis* interactions

The discovery that Ly49A could potentially recognise its ligand through two different sites led to the hypothesis that Ly49s may utilise those spatially distinct sites to bind MHC class I molecules on the surface of other cells or in the plane of the same cell forming *trans* or *cis* interactions respectively (Doucey et al. 2004). It was shown that Ly49A-mediated inhibition of NK cells was much less efficient in the case of NK cells co-expressing Ly49A

and H-2D^d than in NK cells expressing only the Ly49A receptor. Both cell types were cultured in the same environments, expressed similar levels of Ly49A and were equally well activated. These results therefore indicated that H-2D^d expressed on NK cells determines the capacity of Ly49A to inhibit NK cell function. Confocal microscopy images have shown that Ly49A and H-2D^d expressed on the same NK cell co-localised on the cell surface. Ly49A and H-2D^d readily co-immunoprecipitated from lysates derived from Ly49A and H-2D^d-expressing cells, showing that those two molecules interact directly (Doucey *et al.* 2004).

To determine, whether Ly49A and H-2D^d interact in *cis* through site 1 or site 2, β 2m-deficient/Ly49A positive cells were first transfected with H-2D^d and human or mouse β 2m (Doucey *et al.* 2004). Soluble H-2D^k MHC class I tetramers, which can also act as Ly49A ligands, were shown to bind ~25 % weaker to cells co-transfected with mouse β 2m and H-2D^d than to non-transfected counterparts. However, H-2D^k tetramer staining was virtually 100% efficient in cells co-transfected with *human* β 2m and H-2D^d, indicating that *cis*-interactions may be dependent on species-specific residues in β 2m. Since interactions at site 2, but not site 1 are partially dependent on β 2m, it was concluded that *cis* interactions are mediated through site 2. Surprisingly, *trans*-interactions were also shown to be dependent on mouse β 2m, indicating that *trans*-interactions may also be mediated through site 2. This provided further evidence that site 1 is non-functional (Doucey *et al.* 2004). **Figure 1.16** shows the proposed model of *cis* and *trans* interactions. In *trans* the Ly49 molecule is in an extended conformation but in *cis* Ly49 is back-folded on its stalk to facilitate interactions through the same site as is utilised in *trans*. Further studies have shown that several other Ly49 receptors are capable of association with their ligands in *cis* (Scarpellino *et al.* 2007).

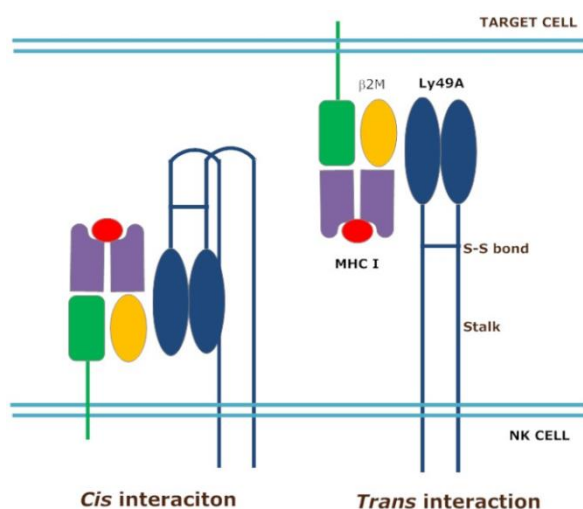


Figure 1.16. Hypothetical Model for *trans* and *cis* interactions of Ly49 Receptors with MHC-I Ligands. Ly49s interact with MHC class I molecules utilising the same binding site both in *trans* and in *cis*. In *trans* the Ly49 stalk is extended. In *cis* the Ly49 globular domain is back-folded on the stalk. Ly49 is shown in blue, the α 1/ α 2 domain of the MHC class I molecule is shown in purple, the α 3 domain of MHC class I is shown in green, the β 2m is shown in yellow and the peptide in the MHC peptide binding groove is shown in red.

It was proposed that the open and closed conformations of Ly49 receptors identified in several crystal structures (**Figure 1.9**) might mediate MHC class I recognition in *trans* and *cis* (Back *et al.* 2009; Ito *et al.* 2009). The recently solved structure of Ly49L, which demonstrated the flexible stalk region for the first time, led to a model in which the bivalently-engaged Ly49 NKD is folded back on the stalk when in *trans*, thereby forcing it into an open conformation. In the *cis* interaction, with only one MHC molecule bound, the stalk is extended and the NKD adopts a closed conformation (**Figure 1.17**) (Back *et al.* 2009; Ito *et al.* 2009).

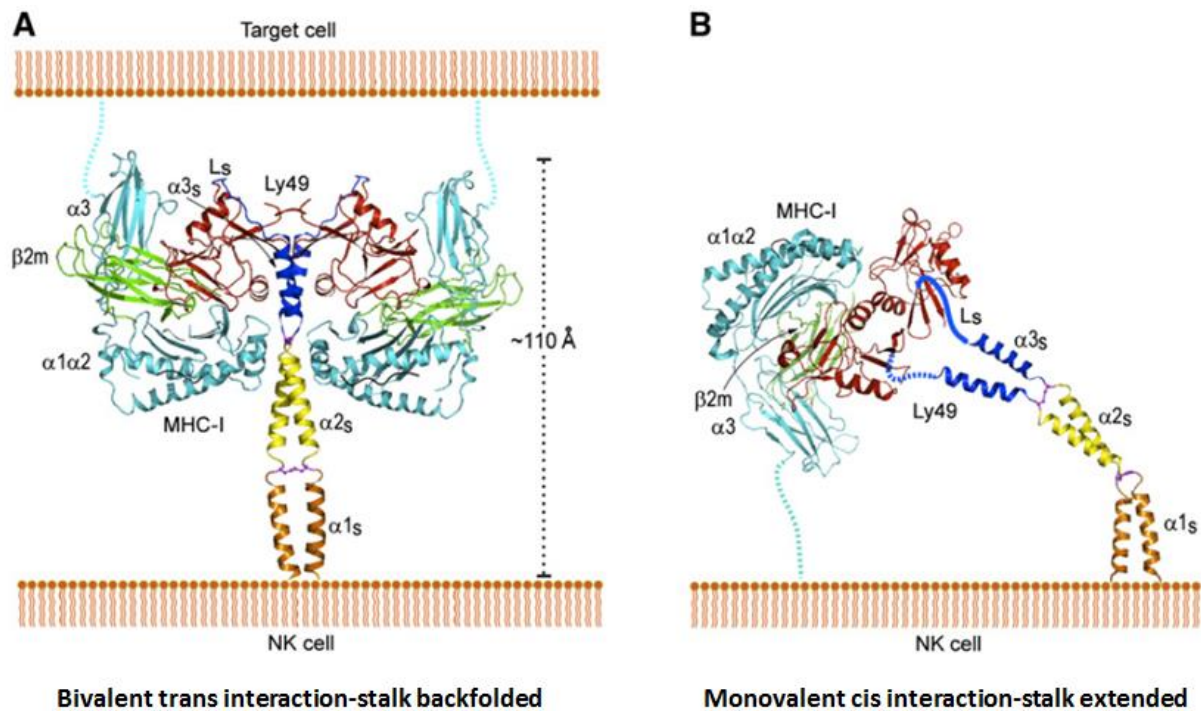


Figure 1.17. Current hypothetical Model for *trans* and *cis* interactions of Ly49 Receptors with MHC-I Ligands Current hypothetical Model for *trans* and *cis* interactions of Ly49 Receptors with MHC-I Ligands (A) *Trans* interaction of a Ly49 receptor with two MHC-I molecules, based on the structures of Ly49L-EC and the Ly49C-H-2Kb complex (PDB accession code 3C8K). The $\alpha 1$, $\alpha 2$, and $\alpha 3$ domains of the MHC-I heavy chain are shown in cyan. $\beta 2m$ is shown in green. The Ly49 NKD is shown in red. The $\alpha 3S$ helix of the Ly49 stalk and the LS loop connecting $\alpha 3S$ to the NKD are shown in blue. The disulphide bond linking the $\alpha 3S$ helices is shown in magenta. The predicted $\alpha 1S$ and $\alpha 2S$ helices of the stalk are drawn arbitrarily in orange and yellow, respectively, with the putative disulphide bond in magenta. The Ly49 homodimer on the NK cell binds two MHC-I molecules on the target cell. In order to bind in *trans*, the stalks must adopt a backfolded conformation, as the N-termini of the Ly49 monomers point away from the NK cell membrane (Ly49s are type II transmembrane proteins). (B) *Cis* interaction of Ly49 with MHC-I. The LS loops connecting the $\alpha 3S$ helices to the NKDs are drawn arbitrarily. The Ly49 homodimer binds one MHC-I molecule on the NK cell itself. In this case, the stalks must assume an extended conformation, as the N termini of the Ly49 monomers point towards the NK cell Figure taken from Back *et al.* 2009.

This model was further scrutinised using a series of Ly49A mutants with varying stalk length and measuring the distance between the ligand-binding domain and the cell membrane using fluorescence resonance energy transfer (FRET). Co-expression of the MHC-I ligand reduced FRET in the case of Ly49A mutants with shorter stalks, indicating that *cis* interactions are associated with conformational change in Ly49A (Back *et al.* 2011). The significance of *cis* interactions is uncertain, but it has been proposed that they may prevent inappropriate NK cell activation (Doucey *et al.* 2004; Back *et al.* 2007).

1.8. Ly49 signalling

1.8.1. Inhibitory pathway

As previously stated, Ly49s, just like human KIRs, can be categorised according to their activating or inhibitory nature (Anderson *et al.* 2001; McVicar and Burshtyn 2001). Each inhibitory Ly49 monomer possesses a single ITIM in its intracellular domain (Long *et al.* 1997), whereas inhibitory KIRs, on the other hand, which always exist as monomers, possess two ITIMs. It is therefore possible that dimerisation of Ly49s is required for efficient signalling (Anderson *et al.* 2001).

Figure 1.18 summarises the pathway involved in the inhibitory signalling of NK cell receptors. Upon ligand binding, ITIMs become tyrosine phosphorylated, most likely by members of the Src and Syk/ZAP-70 tyrosine kinase families (Burshtyn *et al.* 1996; Hoglund and Brodin 2010). Levels of ITIM phosphorylation have been shown to be much higher when inhibitory receptors are co-cross-linked to activating receptors, suggesting that ITIMs are phosphorylated as a result of the inhibitory receptor being brought into close proximity with the activation pathway that is to be inhibited (Blery *et al.* 1997; Mason *et al.* 1997). Once phosphorylated, ITIMs become recruitment points for Src homology 2 (SH-2) domain-containing SHP-1 or SHP-2 protein tyrosine phosphatases. SHIP-1 phosphatase, which is thought to play a role in negative intracellular signalling through its degradation of phosphatidylinositol 3,4,5-triphosphate, was recently shown to constitutively associate with some ITIM containing Ly49 receptors (Wang *et al.* 2002b; Wahle *et al.* 2006). Recruitment of SHP-1, SHP-2 or SHIP-1 is believed to lead to dephosphorylation of substrates critical to the cellular activation pathway such as the guanine nucleotide exchange factor VAV1, which results in repression of activating signal propagation (Olcese *et al.* 1996; Hoglund and Brodin 2010). Phosphorylation and dephosphorylation of VAV1 is thought to act as a central

integration point of inhibitory and activating pathways of NK cell receptors (**Figure 1.18-1**) (Mesecke *et al.* 2011). An alternative inhibition pathway is proposed to involve tyrosine-protein kinase ABL1-mediated phosphorylation of the adaptor protein, CRK, which disrupts an activation complex composed of E3-ubiquitin ligase Casitas B-lineage lymphoma (CBL or c-Cbl), CRK and the guanine exchange factor, C3G (**Figure 1.18-2**) (Peterson and Long 2008). However, this mechanism awaits further confirmation by other groups. Finally, CBL is thought to exert an inhibitory effect on phosphorylated VAV1, which must be overcome for the activating signal to proceed (**Figure 1.18-3**) (Bryceson *et al.* 2006; Kim *et al.* 2010). This mechanism is thought to be involved in modulating the threshold for the activating signal and is unlikely to be directly linked to the ligation of the inhibitory receptors.

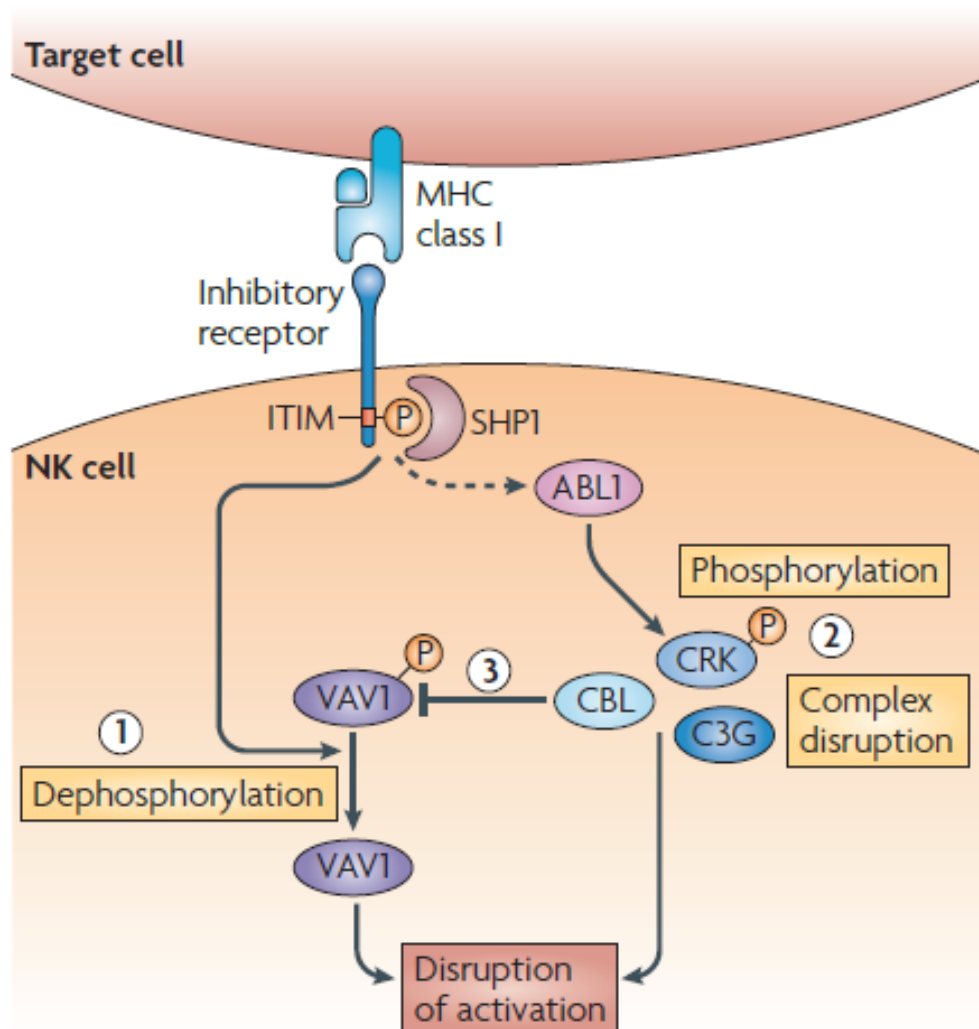


Figure 1.18) Inhibitory signalling pathways in NK cells. 1. Inhibition via dephosphorylation of VAV1, 2. Inhibition via disruption of CRK-CBL-C3G activation complex, 3. Inhibition of phosphorylated VAV1 by CBL. Taken from Hoglund and Brodin (2010).

1.8.2. Activating pathway

Activating Ly49s and KIRs lack intracellular ITIMs and instead possess a positively charged arginine residue in their transmembrane regions (McVicar and Burshtyn 2001, Lanier 2003). The type I transmembrane homodimer DAP12 associates with activating Ly49s via a negatively charged aspartic acid. DAP12 contains an Immunoreceptor Tyrosine-based Activation Motif (ITAM) in its signal transduction chain and coupling of activating Ly49s and KIRs to DAP12 leads to recruitment and phosphorylation of the tyrosine kinases including Syk and ZAP70. Downstream events include the phosphorylation of phospholipase C, C-Cbl, SLP-76, 3BP2, which in turn activate protein VAV1 and its homologue VAV2. Tyrosine phosphorylation of VAV1 and VAV2 leads to activation of mitogen activated protein kinase (MAPK) cascade and cellular responses in the form of degranulation and the production of cytokines (McVicar *et al.* 1998, Lanier 2003).

It is worth noting that one of the Ly49s, Ly49E, contains both an ITIM in its intracellular domain and a positively-charged arginine in its transmembrane region. However, it has been shown to act as an inhibitory receptor upon binding the unusual ligand, urokinase plasminogen (Van Den Broeck *et al.* 2008).

1.9. Ly49B

The majority of Ly49 receptors are expressed predominantly on NK cells, however, expression has also been observed in T cells and NK T cells (Yokoyama and Plougastel 2003). Surprisingly, the Ly49s encoded at the two extremes of the NK locus, Ly49B and Ly49Q, have been shown to be expressed on non-overlapping populations of myeloid cells (Toyama-Sorimachi *et al.* 2004; Gays *et al.* 2006). Multiple populations of Gr-1- and CD11b-positive myeloid cells, with morphologies characteristic of granulocytes and macrophages, were found to express Ly49B. CD11c-, B220-, CD4- and CD8-positive plasmacytoid dendritic cells, on the other hand, were found to express Ly49Q. These findings indicate that Ly49B and Q receptors most likely play distinct roles from other Ly49s; as such, their characterisation is of particular interest.

Ly49B has been found on myeloid cells in both lymphoid and non-lymphoid tissues, including spleen, bone marrow, lymph nodes, thymus and lung. However, Ly49B has been shown to be particularly abundant on macrophages of the gut. Furthermore, expression of

Ly49B is up-regulated in the presence of the inflammatory cytokines, IFN- γ , IFN- α and lipopolysaccharide (LPS) from bacterial cell walls (Gays *et al.* 2006). These results suggest that Ly49B is likely to play an important role in homeostasis of the gastrointestinal tract through regulation of immune responses to pathogens. Interestingly, Ly49B transcripts are present in both NK cells and T cells (particularly CD8-positive cells), which suggests that Ly49B expression on the surface of these cells may be induced in specific circumstances (Gays *et al.* 2006). Low expression levels of Ly49B were detected in immature NK cell lines cultured in the presence of IL-2 and mature NK cells incubated with IL-12 and IL-18 (Gays *et al.* 2006). Like interferons, IL-2, IL-12 and IL-18 are also inflammatory cytokines and their effect on Ly49B expression in NK cells provides further indication that Ly49B may play an important role in the prevention of pathogenesis.

1.9.1. Sequence comparison of Ly49B with other Ly49s

Appendix I shows an alignment of all known C57 Ly49 receptor sequences, as well as that of BALB/c Ly49B. Most Ly49 receptors share 60-90 % amino acid identity, while Ly49B displays only ~50 % homology with other family members. Moreover, the C-terminus of Ly49B contains an additional 20 amino acids, which are not present in any of the other Ly49s. Significant sequence variability is also observed in Ly49Bs from different mouse strains; in particular C57 and 129, which differ by 12 amino acids compared to the BALB/c and CBA strains (residues highlighted in purple in **Appendix I**). Eleven of these variable residues reside in the carbohydrate recognition domain (CRD); the other is located in the transmembrane (TM) domain. Perhaps, the most notable difference amongst these is the substitution of cysteine 251, which is conserved in nearly all other C-type lectins, for arginine in the C57 and 129 strains (Zelensky and Gready 2005). This switch would prevent the formation of a conserved disulphide bond found in all crystal structures of CTLDs solved to date. The only known CTLD sequences that do not contain this conserved cysteine, are those of CLR family receptors and their human orthologue, LLT1 (Boles *et al.* 1999; Plougastel *et al.* 2001). A monoclonal antibody, named 1A1, was previously generated in our laboratory and has been shown to specifically recognize the C57 form of Ly49B, not the BALB/c form (Gays *et al.* 2006).

Apart from cysteine 251 in BALB/c Ly49B and conserved cysteines throughout the sequence, both Ly49B forms contain four non-conserved cysteines: two of which lie in the

stalk region and two in the CDR (residues highlighted in dark green in **Appendix I**). The extracellular domain of both Ly49Bs lacks the highly conserved WAW motif (bold residues in **Appendix I**) and has radically different amino acid sequence from residues 230 to 240. Both forms of Ly49B contain four glycosylation motifs with critical asparagine residues at positions 94, 105, 114 and 177 (highlighted in red in **Appendix I**). The N105 glycosylation motif in Ly49B is shifted by 4 residues in relation to a conserved glycosylation motif in other Ly49s. Notably, this conserved motif contains cysteine in other Ly49s, which does not occur in Ly49B. The Ly49B glycosylation motif with N114 is also present in Ly49C (**Appendix I**). The remaining motifs are specific for Ly49Bs. All of these variations are likely to influence the tertiary structure of Ly49B, which is predicted to differ significantly from those of other Ly49s.

1.9.2. Ly49B specificity and signalling

Ligand binding analyses using soluble MHC class I tetramers were somehow controversial. As outlined in **Section 1.5.1** study by Hanke *et al.* have shown that Ly49B did not bind to any of the tested MHC class I tetramers and studies by Scarpellino *et al.* have shown that Ly49B did bind to whole range of tested MHC class I molecules. The discrepancy was thought to be due to the presence of HA-tag in the first study, which could have interfered with MHC tetramer binding. However, as yet, the controversy was not unambiguously solved in direct comparison of tetramer staining of HA-tagged and untagged Ly49B.

Interestingly, as illustrated by the alignment shown in **Appendix I**, residues equivalent to four out of 12 variable Ly49B residues (167, 209, 236 and 242) were shown to come into contact in with the ligand in Ly49C-H-2K^b and Ly49A-H-2D^d co-crystal structures (Deng 2008). However, due to the various differences described in **Section 1.9.1.**, it is highly likely that the residues responsible for Ly49B ligand binding are different to those of other Ly49s.

Analysis of the Ly49B sequence has shown that it contains an ITIM-like sequence (VTYTTTL-underlined in the **Appendix I**) in the cytoplasmic domain, which is preceded and followed by five amino acids conserved among the inhibitory Ly49s (Zimmer 2010). It is therefore predicted that Ly49B is likely to deliver an inhibitory signal upon ligand binding. Immunoprecipitation of Ly49B transfected into RNK cells in the presence or absence of

irreversible protein-tyrosine phosphatase inhibitor have shown that Ly49B recruits SHIP-1 phosphatase in the absence of the inhibitor and SHP-1 and SHP-2 phosphatases, when the inhibitor is present (Gays *et al.* 2006). It has been speculated that Ly49B recognises endogenous ligand and constitutively associates with SHIP-1, resulting in delivery of an inhibitory signal, which prevents spontaneous myeloid cells activation and controls their expansion. However, in a pathological situation Ly49B is up-regulated and develops new interactions with SHP-1 and SHP-2. In that respect Ly49B is likely to act as a receptor that dampens activation of myeloid cells in a healthy physiological situation and stimulates them in the presence of pathogens (Gays *et al.* 2006). Further investigation is needed to unambiguously establish the nature of Ly49B signalling.

1.10. Project aims

This thesis seeks to provide an in-depth characterisation of the biochemical properties of Ly49B in comparison to other Ly49 receptors. Chapter 3 describes the flow cytometric analysis of cells transfected with mutant variants of Ly49B. The primary objective of this analysis was to solve the controversy regarding the ligand specificity of Ly49B, as well as to identify residues that are responsible for binding of MHC class I molecules and the 1A1 monoclonal anti-Ly49B antibody. The roles of glycosylation and the extended C-terminal region were also assessed in the context of ligand and antibody binding.

Traditionally, one of the principal techniques used in the biochemical characterisation of Ly49s involves immunoprecipitation of surface-labelled receptors, followed by Western blotting. In doing so, the signal generated from the label is used to visualise the receptor by Western blotting. Throughout chapter 4, as well as employing this method, a different approach has been used, in which monoclonal antibodies specific to either the receptor or its tag were used to perform the blots. This approach enabled visualisation of both the intra- and extracellular populations of receptors, thus providing a unique insight into the biology of Ly49B and other Ly49 receptors.

The main objective of Chapter 5 was the refolding and purification of the extracellular portion of Ly49B. Development of a strategy that involved small- and large-scale expression of the extracellular portion of both the C57 and BALB/c forms of Ly49B in *E. coli* is described in detail, as well as the numerous, subsequent attempts at protein refolding and

purification. An antibody binding assay and circular dichroism were used to assess the integrity of the reconstituted receptor and to establish that it was correctly refolded.

Chapter 2. Materials and Methods

2.1. Bacterial strains and growth conditions

All strains of bacteria used in this study are listed in **Table 2.1**. Transformation of chemically-competent bacteria was performed by standard heat shock treatment. Transformants were selected on LB agar plates containing appropriate antibiotics (kanamycin at a final concentration of 50 µg/ml and/or chloramphenicol at 34 µg/ml; tetracycline at 12.5 µg/ml; streptomycin at 50 µg/ml) and grown at 37 °C for 16 hours. Monoclonal cultures were then set up and grown in Luria-Bertani broth (LB) under selective conditions for 16 hours at 37 °C, 200 rpm before being used in plasmid DNA extractions or to inoculate full-scale grow-ups for protein expression.

Table 2.1. Bacterial strains used in this study for construct preparation and protein expression.

Strain	Characteristics	Source
<i>E. coli</i> XL1B	Standard cloning strain	Stratagene
<i>E. coli</i> BL21 (DE3)	<i>E. coli</i> BL21 derivative expression strain with DE3, a λ prophage encoding T7 RNA polymerase and lacking <i>lon</i> and <i>omp</i> genes encoding T7 proteases. Encodes tRNAs recognizing rare codons.	Novagen
<i>E. coli</i> BL21 (DE3) CodonPlus type RIL	<i>E. coli</i> BL21 DE3 derivative expression strain encoding tRNAs recognizing rare codons.	Novagen
<i>E. coli</i> BL21 (DE3) Tuner	<i>E. coli</i> BL21 DE3 derivative <i>lac</i> permease (<i>lacY</i>) deletion mutant. The mutation allows uniform entry of IPTG into all cells in the population, which produces a concentration-dependent, homogenous level of induction carrying	Novagen
<i>E. coli</i> BL21 (DE3) Origami 2	<i>E. coli</i> BL21 DE3 derivative <i>lac</i> permease (<i>lacY</i>) and <i>trxB/gor</i> deletion mutant. The thioredoxin reductase (<i>trxB</i>) and glutathione reductase (<i>gor</i>) mutations greatly enhance disulphide bond formation in the cytoplasm. The <i>trxB</i> and <i>gor</i> mutations are selectable on streptomycin and tetracycline, respectively.	Novagen
<i>E. coli</i> Stbl2 (DE3)	Cloning strain for unstable sequences	Invitrogen

2.2. Cloning

2.2.1. Cloning of the constructs for cell lines transformation

Table 2.2 contains a list of the primers used for cloning in this study. For insert amplification a mix containing Velocity polymerase (Bioline) at a final concentration of 20 U/ml, dNTPs (NEB) at 0.02 mM, primers at 0.4 μ M in 1xGC buffer (Finzymes) was used with the following cycling conditions: initial melting stage (98 °C for 1 min), followed by 30 cycles of amplification (98 °C for 30 sec, 55 °C for 30 sec, 72 °C for 1.5 min), followed by a final extension stage (72 °C for 5 min).

PCR products were purified using MinElute PCR purification kit (QIAGEN), and the amplified inserts were digested for 1 h at 37 °C with NotI, BamHI and DpnI restriction enzymes (NEB) at final concentration of 100 U/ml. The digested inserts were subjected to agarose gel electrophoresis, purified using MinElute Gel Extraction Kit (QIAGEN) and ligated into pMXs-IP shuttle vector using T4 DNA ligase (Promega) at a final concentration of 0.5 U/ μ l. Cloned plasmids were transfected into *E. coli* Stbl2, grown up under selective conditions using Chloramphenicol and purified by miniprep according to the laboratory protocol. Positive clones were identified by performing analytical restriction digests using PstI restriction endonucleases (Promega) and by full sequencing of the cloned regions (by DBS Genomics, Durham).

For site directed mutagenesis (SDM), overlapping primers were designed for each of the constructs (listed in **Table 2.2**) and used at a final concentration of 1 μ M in a mix with Velocity polymerase (Bioline) at a final concentration of 20 U/ml, dNTPs (NEB) at 0.2 mM, a pMXs-IP plasmid containing desired template insert at a final concentration 2 μ g/ml in 1xGC buffer (Finzymes) with the following cycling conditions: initial melting stage (98 °C for 1 min), followed by 25 cycles of amplification (98 °C for 30 sec, 55 °C for 30 sec, 72 °C for 8 min), followed by a final extension stage (72 °C for 16 min). The SDM products were digested for 3 h at 37 °C with DpnI at a final concentration 0.3 U/ μ l, verified by agarose gel electrophoresis and used for transfection into *E.coli* Stbl2 as described for plasmids with the cloned inserts. Positive clones were identified by performing analytical restriction digests using PstI restriction endonuclease (NEB) and by full sequencing of the cloned regions (by DBS Genomics, Durham).

Table 2.2. Primers used in this study.

No.	Name	Sequence 5' to 3'
KP1	Ly49B-EC-f1	AAGACATATGCACATTTTCCGGGATGGACAA
KP2	Ly49B-ECFx-f1	AAGACATATGATCGAGGGAAGGCACATTTTCCGGGATGGACAA
KP3	Ly49B-NKD-f1	AAGACATATGTCACAGAACAAAGGCAAGCAAGT
KP4	Ly49B-NKDFx-f1	AAGACATATGATCGAGGGAAGGTACAGAACAAAGGCAAGCAAGT
KP5	Ly49B-r2	AAGAGGATCCTCATTAACTTTTCATCTTCATCCCT
KP6	pET-Seq-f1	CACGATGCGTCCGGCGTAGA
KP7	pET-Seq-r1	GCTAGTTATTGCTCAGCGG
KP8	L59V-f	CTTCTGCTGGTAACTGTGGCAGTGTGGTGATACACATTTTC
KP9	L59V-r	CACAGTTACCAGCAGAAGGAAACAGAGGATTCC
KP10	W166L-f	GATAAAAAATTGAATGGATGTAACAGATCTGCCAGGATTAC
KP11	W166L-r	GATCTGTTTACATCCATTCAATTTTTATCATCCATGATGAAATAATAAC
KP12	N167K-f	GATAAAAAATGGAAAGGATGTAACAGATCTGCCAGGATTAC
KP13	N167K-r	GTTTACATCCTTTCCATTTTTTATCATCCATGATGAAATAATAAC
KP14	V59L-f	CTTCTGCTGCTAACTGTGGCAGTGTGGTGATACACATTTTC
KP15	V59L-r	CACAGTTAGCAGCAGAAGGAAACAGAGGATTCC
KP16	Ly49ABGHQ-Bam-f	CGTTAGGATCCGCCACCATGAGTGAGCAGGAGGTCCT
KP17	Ly49E-Bam-f	CGTTAGGATCCGCCACCATGAGTGAACCAGAGGTCCT
KP18	Ly49AHA-Not-r	CGTTAGCGGCCGCTCAGGCGTAGTCGGGCACGTCGTAGGGGTAATGAGGGAATTTATCCAGTCT
KP19	Ly49GHA-Not-r	CGTTAGCGGCCGCTCAGGCGTAGTCGGGCACGTCGTAGGGGTAATGAGGGAATTTATCCAGTCT
KP20	Ly49EHA-Not-r	CGTTAGCGGCCGCTCAGGCGTAGTCGGGCACGTCGTAGGGGTAACCAGGGAATGATCCAGTT
KP21	Ly49QHA-Not-r	CGTTAGCGGCCGCTCAGGCGTAGTCGGGCACGTCGTAGGGGTAACGTGTTGTTGGGGAGCGAATCA
KP22	3W166L-f	GATAAAAAATTGAATGGATGTAACAGATCTGCCAGGCTTAC
KP23	3N167K-f	GATAAAAAATGGAAAGGATGTAACAGATCTGCCAGGCTTAC
KP24	Ly49B-His-HA-r	CGTTAGCGGCCGCTCAGGCGTAGTCGGGCACGTCGTAGGGGTAGTGAGGGAATTTATTCAATCTC
KP25	Ly49B-BK-f	CGTTAGGATCCGCCACCATGAGTGAGCAGGAGGTCCT
KP26	Ly49B-His-r	CGTTAGCGGCCGCTCAGTGAGGGAATTTATTCAATCTC
KP27	N105Q-f	GTAAAGACAGAAGTCTTCAGAGTGAAGG
KP28	N105Q-r	GAAGACTTCTGTCTTAACATTTCTCCATTAAG
KP29	N114Q-f	GGCCCTCCAGGATAGCCTGCACCTACCTCAACAG
KP30	N114Q-r	GGCTATCCTGGAGGGCCTTACACTCTGAAG
KP31	N177Q-f	GGATTACCAGTTAACTCTTTTGAAGACAAATG
KP32	N177Q-r	GTAAACTGGTAATCCTGGCAGATCTGTTTAC
KP33	R251C-f	GAGGATGACTGTGCTAGAAAATCATGGTTGTATTTGTGAAAAGAG
KP34	R251C-r	CTAGCACAGTCATCCTCTTCTGTAGAAAATGAATTTAGATATGCACAC
KP35	AW166L-f	GAAAACATTGAGTGGATGTAACAGACCTGCCAGAGTTCCAG
KP36	AW166L-r	GGTCTGTTTACATCCACTCAATGTTTTCTGTCCATGACGAAATAATAACATTTTCATACC
KP37	AS167K-f	GAAAACATGGAAAGGATGTAACAGACCTGCCAGAGTTCCAG
KP38	AS167K-r	GGTCTGTTTACATCCTTTCCATGTTTTCTGTCCATGACGAAATAATAACATTTTCATACC
KP39	N167S-f	GATAAAAAATGGAGTGGATGTAACAGATCTGCCAGGATTAC
KP40	N167S-r	GTTTACATCCACTCCATTTTTTATCATCCATGATGAAATAATAAC
KP41	N94Q-f	GTCATGAAACAGGACAGCTCCTTAATGGAAGAAATGTTAAGAAATAAGTCTTCAGAG
KP42	N94Q-r	GGAGCTGTCTGTTTCATGACCTGGTACTCTTGACGGAGG
KP43	2N105Q-f	GTAAAGACAGAAGTCTTCAGAGTGAAGGCCCTCAATGATAGCCTGC
KP44	2N105Q-r	GAAGACTTCTGTCTTAACATTTCTCCATTAAGGAGCTGTC

2.2.2. Cloning of Ly49B for refolding and purification

ORFs encoding the full-length extracellular domains (EC) and natural killer domains (NKD) of C57 and BALB/c Ly49B were amplified from full length genomic Ly49B sequence from plasmids generated previously in the lab (lab stocks D1756 and D1697 for C57 and BALB/c respectively) using KOD polymerase (Novagen) with the primers listed in

Table 2.2. PCR was carried out in 1x KOD1 reaction buffer, 2 mM MgCl₂, 0.2 mM each dNTP and 0.4 μM each primers with the following cycling conditions: initial melting stage (95 °C for 1 min), followed by 25 cycles of amplification (95 °C for 30 sec, 58 °C for 30 sec, 72 °C for 15 sec), followed by a final extension stage (72 °C for 2 min). Amplicons containing the 5' Factor Xa cleavage site, introduced by PCR amplification, were cloned into the pET28b expression vector (Novagen) downstream of the polyhistidine (His) tag. Those without the factor Xa site were cloned into pET24a (Novagen) using NdeI and BamHI restriction sites in all cases. PCR products were purified using MinElute PCR purification kit (QIAGEN), digested with NdeI and BamHI restriction enzymes (NEB), purified using MinElute Gel Extraction Kit (QIAGEN) and ligated into pET24a and pET28b vectors using T4 DNA ligase (Promega). Cloned plasmids were transfected into *E. coli* XL1B, grown up under selective conditions and purified using a QIAprep Spin Miniprep kit (Qiagen) according to the manufacturer's protocol. Positive clones were identified by performing analytical restriction digests using PvuII and SalI restriction endonucleases (Promega) and by full sequencing of the cloned regions (by DBS Genomics, Durham).

2.3. DNA agarose gel electrophoresis

Agarose gels were prepared using 0.7 – 1 % agarose (w/v) in TBE buffer (40 mM Tris (pH 8.3); 40 mM boric acid, 1 mM EDTA) and supplemented with 1 μg/ml ethidium bromide. Gels were run at 70 V for 1 hour in 1xTBE running buffer (Lonza) and run along 100 bp DNA ladder or 1 kb DNA ladder (New England BioLabs).

2.4. Mouse cells, tumour cell lines and transfection

The cell transfectants generated in this study and previously in the lab are listed in the **Table 2.3.** For transfection, YB2/0 or RNK/0 cells were concentrated to 1x10⁶/ ml and 0.5 ml aliquots were mixed with 40 μl of plasmid DNA at 100 μg/ml and electroporated at 960 μF and 300 V. The cells were cultured in 24 well plates in D10F medium (Dulbecco's Modified Eagle Medium (DMEM + 10 % FBS) for 16 h and then transferred to flasks with 5 ml of D5F medium (DMEM + 5 % FBS) with 0.5 μg/ml puromycin. After 16 h puromycin concentration was increased to 1.5 μg/ml. The cells were cultured in the flasks for approximately 2 weeks until the puromycin selected transfectants formed dense population and the remaining cells died. The cells were then transferred into 24 well plates and maintained in DF5 1.5 μg/ml puromycin. Expression levels of the transfected proteins were assessed by FACS analysis.

Table 2.3. Transfectants used in this study. * = transfectants generated previously in the lab, 20= Ly49B mutants lacking last 20aa. The amino acid code indicates variable residues between C57 and BALB/c Ly49B. C57 specific residues are shown in black and BALB/c residues are shown in red.

Transfected construct	Name abbreviation	Amino acid code	Cell type	Selective marker
C57 Ly49B *	C57	VLKAAEPVENRN	YB2/0	G418
BALB/c Ly49B *	BALB	LWNSKLDQSCT	YB2/0	Puromycin
C57 Ly49B HA	C57-HA	VLKAAEPVENRN-HA	YB2/0	Puromycin
BALB/c Ly49B HA*	BALB-HA	LWNSKLDQSCT-HA	YB2/0	G418
C57 Ly49B FLAG *	C57-FLAG	VLKAAEPVENRN-FLAG	RNK/0	G418
CLRg HA*	Clrg	-	YB2/0	Puromycin
Ly49Q HA*	Q	-	YB2/0	G418
Ly49A HA	A	-	YB2/0	Puromycin
Ly49E HA*	E	-	YB2/0	Puromycin
Ly49G HA	G	-	YB2/0	Puromycin
C57 Ly49B-V59L	C57-V59L	LLKAAEPVENRN	YB2/0	Puromycin
BALB/c Ly49B-N167K	BALB-N167K	LWKDSKLDQSCT	YB2/0	Puromycin
BALB/c Ly49B-N167S	BALB-N167S	LWSDSKLDQSCT	YB2/0	Puromycin
Chimera 1*	-	LWNSKLDENRN	YB2/0	Puromycin
Chimera 2*	-	VLKAAEPVQSCT	YB2/0	Puromycin
Chimera 2-V59L	2.1	LLKAAEPVQSCT	YB2/0	Puromycin
Chimera 2-L166W	2.3	VWKAAEPVQSCT	YB2/0	Puromycin
Chimera 2-K167N	2.4	VLNAAEPVQSCT	YB2/0	Puromycin
Chimera 3*	-	LWNAAEPVENRN	YB2/0	Puromycin
Chimera 3-L59V	3.1	VWNAAEPVENRN	YB2/0	Puromycin
Chimera 3-W166L	3.2	LLNAAEPVENRN	YB2/0	Puromycin
Chimera 3-N167K	3.3	LWKAAEPVENRN	YB2/0	Puromycin
Chimera 3-L59V-W166L	3.4	VLNAAEPVENRN	YB2/0	Puromycin
Chimera 3-L59V-N167K	3.5	VWKAAEPVENRN	YB2/0	Puromycin
Chimera 4*	-	VLKDSKLDQSCT	YB2/0	Puromycin
Chimera 4-V59L	4.1	LLKDSKLDQSCT	YB2/0	Puromycin
Chimera 4-L166W	4.2	VWKDSKLDQSCT	YB2/0	Puromycin
Chimera 4-K167N	4.3	VLNDSKLDQSCT	YB2/0	Puromycin
Chimera 4-V59L-L166W	4.4	LWKDSKLDQSCT	YB2/0	Puromycin
Chimera 4-V59L-K167N	4.5	LLNDSKLDQSCT	YB2/0	Puromycin
Chimera 5*	-	VLKDSKLDENRN	YB2/0	Puromycin
Chimera 6*	-	LWNAAEPVQSCT	YB2/0	Puromycin
Chimera 6-L59V	6.1	VWNAAEPVQSCT	YB2/0	Puromycin
Chimera 7	-	LWNAAEPVENCN	YB2/0	Puromycin
Chimera 7-L59V	7.1	VWNAAEPVENCN	YB2/0	Puromycin
Chimera 7-L59V-W166L	7.2	VLNAAEPVENCN	YB2/0	Puromycin
Chimera 7-L59V-N167K	7.3	VWKAAEPVENCN	YB2/0	Puromycin
Chimera 7-HA*	-	LWNAAEPVENCN-HA	YB2/0	Puromycin
Chimera 7-L59V-HA	7.1-HA	VWNAAEPVENCN-HA	YB2/0	Puromycin
Chimera 7-L59V-W166L-HA	7.2-HA	VLNAAEPVENCN-HA	YB2/0	Puromycin
Chimera 7-L59V-N167K-HA	7.3-HA	VWKAAEPVENCN-HA	YB2/0	Puromycin
Ly49B BALB/c N94Q	BALB-A	-	YB2/0	Puromycin
Ly49B BALB/c N105Q	BALB-B	-	YB2/0	Puromycin
Ly49B BALB/c N114Q	BALB-C	-	YB2/0	Puromycin
Ly49B BALB/c N177Q	BALB-D	-	YB2/0	Puromycin
Ly49B BALB/c N105Q-N114Q	BALB-BC	-	YB2/0	Puromycin
Ly49B BALB/c N94Q-N105Q-N114Q-N177Q-HA	BALB-ABCD-HA	-	YB2/0	Puromycin
Ly49B C57 N94Q-N105Q-N114Q-N177Q	C57-ABCD	-	YB2/0	Puromycin
Ly49B C57 N94Q-N105Q-N114Q-N177Q-HA	C57-ABCD-HA	-	YB2/0	Puromycin
BALB/c Ly49B-20-H	BALB-20-H	-	YB2/0	Puromycin
BALB/c Ly49B-20-H-HA	BALB-20-H-HA	-	YB2/0	Puromycin

Six week old female C57 mice were used to obtain spleen and bone marrow cells. All procedures were approved by the UK licensing authorities. C57 spleen (S) cells were obtained by smashing the spleens with forceps and the bone marrow (BM) cells were eluted from femurs and tibias following removal of the bone heads using narrow gauge needles. 5×10^6 cells of each kind were cultured in DMEM (Invitrogen) made up in highly purified water and supplemented with $2\times$ nonessential amino acids, 5×10^{-5} M 2-ME, 10 % FBS (Sigma-Aldrich) and 10 % heat inactivated horse serum in 90 mm bacteriological grade Petri dishes with 5 % macrophage colony stimulating factor (MCSF) for 10 days. The non-adherent and adherent cells were then harvested together using Ca^{2+} and Mg^{2+} free PBS with 0.5 mM EDTA, divided into 18 x 1 ml aliquots containing 1×10^6 cells, six of which were cultured in low adherence 24 well plates for 2 days with 10^4 U/ml IFN- α , another six with 2 mg/ml LPS and the remaining six with nothing. Non-adherent and adherent cells were harvested as outlined above. LNK cells were cultured in 24 well plates in DMEM + 10 % FBS with 100 U/ml IL-2.

2.5. Cell lysate preparation

Cells were centrifuged for 1 min at 16,000 g and washed once in ice cold PBS. The supernatant was aspirated apart from 25 μl , which was used to create homogenous cell slurry. The slurry was lysed using 100 μl or 250 μl of lysis buffer (1 % Triton X-100, 150 mM NaCl, 50 mM Tris HCl pH 8.0) per 1×10^6 of cells and the lysis was allowed to proceed over the period of 30min at 4 °C. Insoluble material was removed by centrifugation at 16,000 g for 1 min and the supernatant was transferred into a fresh microfuge tube and mixed with 100 μl or 250 μl 2xSDS-PAGE loading buffer (+/- 2ME) to give final dilution of 5000 or 2000 cells/ μl . The samples were stored at -20 °C.

2.6. Immunoprecipitation

Cell lysates were diluted 5x in ice cold 1xPBS and 250 μl aliquots containing 4000 cells/ μl were incubated for 5h on a rotating mixer at 4 °C with 10 μl of Sepharose beads pre-coated with an appropriate antibody. The beads were washed 3x in lysis buffer diluted 1/5 in 1xPBS by centrifugation at 3,500 g at 4 °C. The beads were then resuspended in 250 μl of 2xSDS-PAGE loading buffer and boiled for 5 min, followed by centrifugation at 3,500 g. The supernatant was divided into two aliquots, one of which was mixed with equal amount of lysis buffer diluted 1/5 in 1x PBS and the second one with 1/5 lysis buffer solution + 5 %

2ME, giving final concentration of the samples at 2000 cells/ μ l. The samples were stored at -20 °C.

2.7. Flow cytometry

2×10^5 aliquots of transfected and control cells were suspended in 25 μ l of H2FA medium and incubated for 20 min at room temperature with 25 μ l of an antibody or a MHC class I tetramer at a desired concentration (**Table 2.4**). The cells were then washed twice with H2FA medium and stained for further 20 min with the secondary antibody if required, washed once with H2FA and resuspended in 0.5 ml of H2FA medium for flow cytometric analysis. The second incubation step was omitted in case of reagents conjugated directly to fluorophores. FACSscan machine (BD Biosciences) was used to collect staining results and data were analyzed using FCS Express V2 software (DeNovo Software).

Table 2.4. Reagents used for flow cytometry analysis.

Reagent number	Reagent name	Concentration (mg/ml)	Final dilution used for staining	Source
N1244	PE H-2K ^b (SINFEKL) MHC class I tetramers	1.2	1/300	NIH Tetramer Facility
N1245	PE H-2D ^b (KAVYNFATM) MHC class I tetramers	1.2	1/300	NIH Tetramer Facility
N1246	PE H-2D ^d (RGPGRAFVTI) MHC class I tetramers	1.2	1/300	NIH Tetramer Facility
N1239	PE mouse anti-Ly49F IgGi	1		Becton-Dickinson
N837	2G4 rat anti-L49B IgG2c	1	1/30	Produced in the lab
N838	1A1 rat anti-L49B (C57) IgGi	1	1/30	Produced in the lab
N924	AF647 streptavidin	2	1/1000	Invitrogen
N538	JR9 rat anti-Ly49A IgG	1	1/1000	Jacques Roland
N509	1A rat anti-Ly49A IgG	1	1/200	James Allison
N358	YE1/48 rat anti-Ly49A IgG	1	1/40	Fumio Takei
N415	2.4G2 rat anti-CD16/32 IgG2b		1/100	Jay Unkless
N382	Biotin rat anti mouse-F4/80 IgG	0.5	1/500	BioLegend
N1059	AF647 MR3 IgG2c isotype control		1/500	Geoff Butcher
N1058	AF647 2G4 rat anti-Ly49B IgG2c		1/500	Produced in the lab
N1176	Biotin 2G4 rat anti-Ly49B IgG2c		1/1000	Produced in the lab
N883	PE streptavidin	0.5	1/1000	Pharmingen
N156	4D11 rat anti-Ly49G IgG2a	20	1/10,000	Llewellyn Mason
N865	CM4 rat anti-Ly49E/F IgG2a		1/10	Produced in the lab
N1217	AF647 chicken anti-rat IgG	2	1/10,000	Invitrogen
N1222	Biotin 16.43 rat anti-HA IgG2a	1	1/1000	Produced in the lab

C57 spleen and bone marrow cells were harvested and incubated for 10 min with a saturating concentration of N415 2.4G2 anti-CD16/32 at a final dilution of 1/100 to block FcR, followed by 20 min incubation with N382 Biotin F4/80 at a final dilution of 1/500. The cultures were divided into four samples, which were stained for 20 min with the following: A) medium, B) medium, C) N1059 AF647 MR3 IgG2c isotype control at final 1/500 dilution, D) N1058 AF647 2G4 anti-Ly49B at final 1/500 dilution. The samples were then washed 2 times with H2FA and samples B-D were additionally stained for 20 min with N883 PE streptavidin at a final dilution of 1/1000. In parallel with this, staining of two samples of YB2-C57 Ly49B-HA cells was performed with medium and N1058 AF647 2G4 anti-Ly49B at a final dilution of 1/500.

2.8. Biotinylation of cell surface proteins

Cells were washed 3x with ice cold 1xPBS (pH 8.0) and the concentration was adjusted to 25×10^6 /ml. The cell slurry was incubated for 30min at room temperature with 10 mM EZ-Link Sulfo-NHS-LC-Biotin reagent followed by three washes with 1xPBS +100 mM glycine (pH 2.4).

2.9. Sodium dodecyl sulphate polyacrylamide gel electrophoresis (SDS-PAGE)

SDS polyacrylamide gels were prepared using the reagents specified in a **Table 2.5** as previously described by Laemmli (Laemmli 1970). The gels were run at a constant voltage of 200 V in 1x SDS-running buffer (25 mM Tris-HCl [pH 8.3], 192 mM Glycine, 0.1 % [w/v] SDS) for 1 h 30 min against biotinylated protein marker (NEB).

Table 2.5. Composition of SDS-PAGE gels. The amounts are sufficient for two 0.75 mm gels.

Reagent	Volume
15 % Resolving gel	
30 % Bis-acrylamide	5 ml
H2O	2.35 ml
0.5 M Tris ph 8.8	2.5 ml
10 % SDS	100 µl
10 % APS	100 µl
TEMED	5 µl
5 % Stacking gel	
30 % Bis-acrylamide	410 µl
H2O	1.8 ml
0.5 M Tris ph 8.8	315 µl
10 % SDS	50 µl
10 % APS	50 µl
TEMED	5 µl

2.10. Western blotting

SDS-PAGE gels were washed for 30 min on a rocking platform in 1x transfer buffer (25 mM Tris-HCl (pH 8.3), 192 mM Glycine, 10 % methanol) and the resolved proteins were transferred into nitrocellulose membrane (Whatman) at 200 V in 1x transfer buffer using Biorad Western blot wet apparatus. The transfer was carried out on ice over the period of 1 h 30min. Alternatively, the proteins were transferred for 17 min at 1.3 A and 25 V using the Trans-Blot Turbo system (BioRad). The membranes were blotted for 30 min in 1xPBS/0.1 % Tween/ 5 % low fat powder Milk (Marvel) on a rocker at room temperature and then incubated overnight in the blocking solution with a primary antibody at 4 °C with rocking. The membranes were washed on a rocking platform in 1xPBS/0.1 % Tween solution for 1 h. After washing the membranes were incubated on a rocking platform at a room temperature for 1 h with a secondary antibody in 1xPBS/0.1 % Tween or 1xPBS/0.1 % Tween/ 5 % low fat powder milk (Marvel). The second round of washing was carried out as described above for the period of 2 h. The proteins of interest were visualised using ECL reagent (Pierce or Thermo) and GE Healthcare hyperfilm with varied exposure times, depending on the intensity of bands. The primary and secondary antibodies are specified in **Table 2.6**. The exact procedure for each experiment is outlined under the relevant figures.

Table 2.6. Antibodies used for Western blot experiments. NEB- New England Biolabs, SC- Santa Cruz Biotechnology, IS-Immune Systems Ltd, ICL-Immunology Consultants Laboratory.

Reagent number	Reagent name	Concentration (µg/ml)	Source
N880	1A1 rat anti-Ly49B (C57) IgGi	100 ug/ml	Produced in the lab
N869	Biotin 1A1 rat anti-Ly49B (C57) IgGi	100 ug/ml	Produced in the lab
N1027	Rabbit anti-FLAG IgG	10 ug/ml	ICL
N1028	Rabbit anti-HA IgG	10 ug/ml	ICL
N1089	MR3 rat IgG2c	100 ug/ml	ICL
N1193	Biotynylated marker	-	NEB
N1194	Goat anti-biotin IgG HRPO	-	NEB
N1196	Goat anti-mouse IgG HRPO	20 ug/ml	ICL
N1197	Bovine anti-rabbit IgG HRPO	400 ug/ml	SCB
N1176	Bitotyn 2G4 rat anti-Ly49B IgG2c	20 ug/ml	Produced in the lab
N1243	Goat anti-biotin IgG HRPO	-	NEB
N1184	2G4-anti-The Ly49B (THE C57 and The BALB/c)	100 ug/ml	Produced in the lab
N1222	Biotynylated 16.43 rat anti-HA	100 ug/ml	IS
N1229	Biotynylated rabbit anti-HA	100 ug/ml	IS

2.11. Protein expression

2.11.1. Small-scale expression

E. coli BL21 (DE3), BL21 (DE3) CodonPlus (RIL), BL21 (DE3) Tuner and BL21 (DE3) Origami 2 cells were transfected with the cloned plasmids previously described. 10 ml aliquots of LB broth containing appropriate antibiotic(s) were inoculated with 500 µl of 16 hour old culture for each condition and grown at 37 °C, 200 rpm until the OD₆₀₀ reached 0.6. 1 ml samples were then removed and centrifuged at 16,000 g for 1 min at room temperature. The pellet was resuspended in 50 µl of SDS-PAGE loading buffer and stored at -20 °C. The remaining cultures were induced with IPTG at concentrations of 1 mM, 0.5 mM, 0.25 mM and 0.1 mM and incubated at 37 °C, 30 °C or 16 °C, 200 rpm for 16 hours. 1 ml samples of culture were harvested, as previously described, every hour post-induction for 6 hours and then finally another at 16 hours. In order to assess expression levels of the recombinant proteins under each condition, samples were examined by SDS-PAGE.

2.11.2. Large-scale expression

After optimising expression conditions, preparative-scale grow-ups were performed using 2 x 1 l of LB broth containing appropriate antibiotic inoculated with 2 x 50 ml of 16 hour old transfected bacterial culture. Cultures were grown at 37 °C, 200 rpm until the OD₆₀₀ reached 0.6, at which point 1 ml samples were removed and harvested as previously described. The cultures were induced with 1 mM IPTG and grown for either 3 hours at 30 °C or 16 hours at 16 °C, 200 rpm. 1 ml samples were taken (as previously described) just prior to harvesting in order to test expression levels. Cells from the 2 l culture were washed in 1XPBS and centrifuged at 60372 g for 20 min at 4 °C. The cell pellets were stored at -80 °C. Before attempting to purify protein, expression of the recombinant protein was verified by comparing uninduced and induced samples by SDS-PAGE.

2.12. Protein refolding and purification

2.12.1. Preparation of protein inclusion bodies

Bacterial pellets from large scale grow-ups were resuspended in cold 1xPBS and then disrupted by sonication at 4 °C, (50%, level 5, 30 pulses) using an HD2070 Banlelin SONOPLUS sonicator, and centrifuged at 20,000 g, 4 °C for 30 min. The pellet containing the inclusion bodies was washed with ice-cold Triton X-100 wash buffer (50 mM Tris pH 8.0, 100 mM NaCl, 0.5 % Triton X-100), re-suspended using a homogeniser and then centrifuged

at 25,000 g, 4 °C for 30 min. This step was repeated until the supernatant became clear, at which point a final wash was performed using ice-cold, detergent-free, wash buffer. The inclusion bodies were solubilised in denaturing buffer (6 M guanidine hydrochloride, 50 mM Tris pH 8.0, 100 mM NaCl, with or without 10 mM EDTA) at 4°C overnight on a rotating mixer.

2.12.2. Protein refolding

2 ml or 10 ml of solubilised, denatured protein (20 mg/ml) were incubated with 10 mM DTT for one hour at room temperature to reduce any cysteine residues present. The reduced protein solution was then either added drop-wise to or dialysed against 500 ml of refolding buffer at 4 °C (**Table 2.7**), stirring at high speed to prevent aggregation; stirring was continued overnight or for 48 hours at 4 °C. Solutions were centrifuged at 60372 g, 4 °C, for thirty minutes to remove large aggregates of protein and then in the case of the protein refolded by rapid dilution, concentrated to 10 ml, using a 50 ml Centricon or Vivacel 250 ml concentrator (Vivascience), with a 10 kDa molecular weight cut off insert.

Table 2.7. Buffers used for refolding of Ly49B in this study.

Buffer #	Buffer composition
1	200 mM Tris HCl (pH 8.0); 1 M L-arginine; 10 mM EDTA; 0.5 mM oxidised glutathione; 5 mM reduced glutathione;
2	200 mM Tris HCl (pH 8.0); 0.4 M L-arginine; 10 mM EDTA; 0.5 mM oxidised glutathione; 5 mM reduced glutathione;
3	200 mM Tris HCl (pH 8.0); 0.2 M L-arginine; 0.5 mM oxidised glutathione; 5 mM reduced glutathione;
4	200 mM Tris HCl (pH 8.0); 0.4 M L-arginine; 0.5 mM oxidised glutathione; 5 mM reduced glutathione;
5	200 mM Tris HCl (pH 8.0); 0.4 M L-arginine; 0.5 mM oxidised glutathione; 5 mM reduced glutathione; 0.4 M NaCl; 2 M guanidine hydrochloride;
6	200 mM Tris HCl (pH 8.0); 0.4 M L-arginine; 0.5 mM oxidised glutathione; 5 mM reduced glutathione; 0.4 M NaCl; 2 M guanidine hydrochloride;
7	50 mM Tris HCl (pH 8.0); 0.5 M L-arginine; 9.6 mM NaCl; 1 mM EDTA, 0.4 M Sucrose; 0.5 mM oxidised glutathione; 5 mM reduced glutathione;

2.12.3. Gel filtration chromatography

Samples were concentrated to 2 ml volumes and their protein concentrations determined at 280 nm using the Beer-Lambert equation. The protein was purified using an ÄKTA/FPLC chromatographic system and a Superdex-75 10/300 or HiLoad Superdex 75 prep grade gel filtration column (GE Healthcare). The gel filtration buffer contained 200 mM NaCl and 50 mM Tris (pH8.0) and the run was performed at 0.5 ml/min. Peak fractions were analysed by SDS-PAGE.

2.12.4. Immobilized metal ion affinity chromatography (IMAC)

Recombinant protein possessing a polyhistidine tag was purified using a nickel charged 5 ml HiTrapTM Chelating HP Column (GE Healthcare Life Sciences) attached to an ÄKTA chromatographic system (GE Healthcare, formerly Amersham Biosciences). The crude protein solution was applied to the pre-equilibrated column at 1 ml/min and eluted at over a linear 30 ml gradient of 0-500 mM imidazole in 25 mM Tris-HCl (pH 8.0), 500 mM NaCl at 1 ml/min. 3 ml fractions were collected and the protein content of each fraction assessed by SDS-PAGE.

2.12.5. Ion exchange chromatography

Protein was purified using a 25 ml Sepharose Q column (GE Healthcare Life Sciences) attached to an ÄKTA chromatographic system (GE Healthcare). The protein solution was applied to the pre-equilibrated column at 1 ml/min and eluted at over a linear 200 ml gradient of 0-1 M NaCl in 25 mM Tris-HCl (pH 8.0). 3ml fractions were collected and the protein content of each fraction assessed by SDS-PAGE.

2.12.6. Dialysis

Tubing for dialysis was prepared as described by Maniatis (Maniatis T 1989). Dialysis was carried out for 16 h, 24 h or 48 h at 4 °C. The protein was dialysed to 500 ml of refolding buffers (listed in **Section 2.12.2**), 1 l of gel filtration buffer (200 mM NaCl and 50 mM Tris (pH8.0) with or without 1 mM EDTA) or 1 l of His-trap loading buffer (25 mM Tris, 50 mM Imidazole, 500 mM NaCl).

2.13. Micro-scale nickel affinity pull-down assay

Ni-NTA agarose beads resin (Qiagen) was prepared as described in product literature and equilibrated with binding buffer (50 mM Tris-HCl [pH 8.0]; 200 mM NaCl; 10 mM imidazole). Approximately equimolar concentrations of Ly49B protein and 2G4 anti-Ly49B

antibody (lab stock) were mixed with the beads and incubated on a rotator at room temperature for 1 hour. The controls (with the antibody and the protein on their own) were treated the same. Non-specifically bound protein was removed by performing three washes using binding buffer and the remaining protein eluted with elution buffer (50 mM Tris-HCl [pH 8.0]; 200 mM NaCl; 200 mM imidazole). All fractions were analysed by SDS-PAGE.

2.14. Microscopy

Phase contrast images of inclusion bodies were captured using an Andor iXonEM+ 885 EMCCD camera coupled to a Nikon Ti-E microscope using a 100x/NA 1.4 oil immersion objective. Images were acquired with NIS-ELEMENTS software (Nikon) and processed using ImageJ.

2.15. Circular dichroism (CD)

To analyse the protein by the CD, the 1 mg/ml sample was placed in 0.2 mm quartz cuvette (Hellma Analytics UK). CD spectra were acquired by a Jasco-810 CD spectrometer (Jasco UK). The machine was calibrated with camphorsulfonic acid and the parameters were set as described by Chaffey *et al.* 2008.

Chapter 3. Mutational binding analysis of Ly49 receptors

3.1. Introduction

In this chapter the binding specificity of Ly49B for MHC class I molecules is examined. C57 and BALB/c forms of Ly49B, as well as several other Ly49 receptors, were expressed in YB2/0 cells and tested for binding of soluble MHC class I tetramers conjugated to fluorophores. Binding was assessed by flow cytometry, in which cells expressing Ly49 receptors were incubated prior to the assay with tetramers and washed. The cells were then hydro-dynamically focused, one at the time, through a flow cell and subjected to a beam of light (**Figure 3.1**). Cells that associated with tetramers generated a positive signal because the conjugated fluorophores were excited to a higher energy state and emitted light on their return to the lower energy state. The differing wavelengths of emitted light were then converted into electrical signals and processed by the flow cytometer machinery (Ibrahim and Van den Engh 2007, Rieseberg *et al.* 2001). The intensity of fluorescence was recorded and plotted against cell count in the form of histograms.

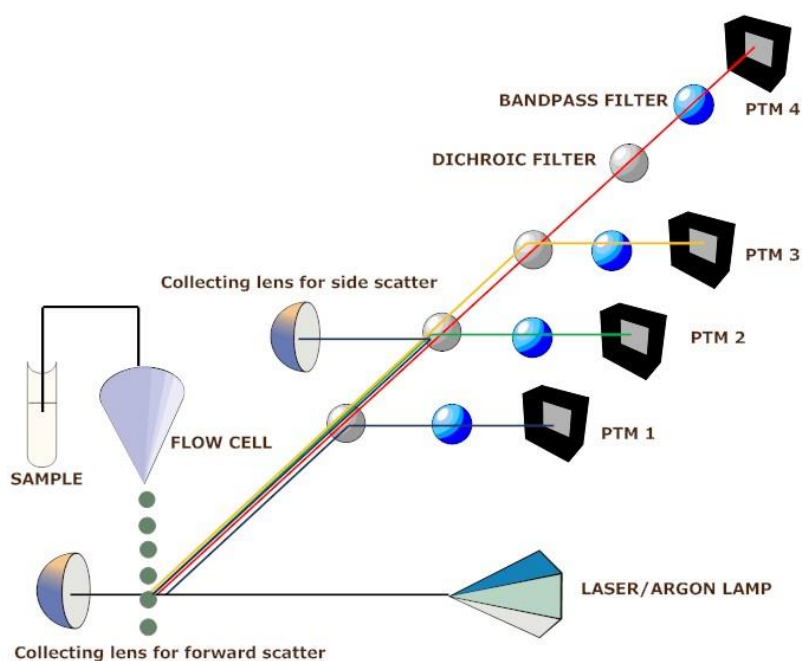


Figure 3.1. Schematic representation of a flow cytometer. A sample of cells flows through the beam of light. Upon encountering each cell, light is scattered and a relative proportion of the scattered light is detected by a forward or side scatter lens. The different emission spectra of attached fluorophores are detected by different photomultipliers (PTMs).

BALB/c and C57 Ly49B isoforms differ in sequence by 12 amino acids (**Figure 3.2**). A primary objective of this chapter was to formally establish which variable residues in Ly49B are responsible for selective binding of the monoclonal 1A1 antibody and, more importantly, binding of Ly49B's putative MHC class I ligands. A series of Ly49B mutants was created by site-directed mutagenesis, transfected into the YB2/0 cell line and examined by flow cytometry. The roles of Ly49B glycosylation and its additional 20 C-terminal amino acids were also evaluated in terms of both ligand and antibody binding. The importance of Ly49A amino acids, whose equivalent residues in Ly49B were identified as critical for ligand binding, were also assessed. Finally, the effect of adding a C-terminal hemagglutinin (HA) tag to Ly49 receptors was considered, again, in the context of ligand binding.

C57	1	MSEQEVTYTTLRFHKSSGLQNPVRPEETQRPDRVGHRECSVPWKFIVIVLGLCFLLLVT	60
BALB/c	1	MSEQEVTYTTLRFHKSSGLQNPVRPEETQRPDRVGHRECSVPWKFIVIVLGLCFLLLIT	60
C57	61	VAVLVIHIFRDGQEKHEQEKTLLNNLRQEQVMKNDSSLMEEMLRNKSSECKALNDSLHYL	120
BALB/c	61	VAVLVIHIFRDGQEKHEQEKTLLNNLRQEQVMKNDSSLMEEMLRNKSSECKALNDSLHYL	120
C57	121	NREQNRCLRKTKIVLDCSQNKGKQVEGYWFCCGMKCYFIMDDKKLRGCKQICQAYNLTL	180
BALB/c	121	NREQNRCLRKTKIVLDCSQNKGKQVEGYWFCCGMKCYFIMDDKKWNGCKQICQDYNLTL	180
C57	181	LKTNDEDELKFLKSQIQRNTYWIALTHHESKEESQIGDRPSKPVSAARNSVPNREKCAAY	240
BALB/c	181	LKTNDEDELKFLKSQIQRNTYWISLTHHESKEESQIGDRPSKLD SAARNSVPNRQKCAAY	240
C57	241	LNSFSTEEDDRARNHGCICEKRLNKFPIPGSCAKGRTQSALQRDEDES	288
BALB/c	241	LSSFSTEEDDCARTHGCICEKRLNKFPIPGSCAKGRTQSALQRDEDES	288

Figure 3.2. Alignment of BALB/c and C57 Ly49B sequences. Green = intracellular region, Yellow = transmembrane region, White = stalk region, Blue = NK domain, Purple – variable residues between BALB/c and C57 Ly49B sequences.

3.2. Analysis of MHC class I tetramer binding to Ly49 receptors

In order to establish which MHC class I molecules associate with Ly49 receptors, a series of YB2 transfectants, each expressing one of C57 Ly49B-HA, BALB/c Ly49B-HA, C57 Ly49A-HA, Ly49E-HA, Ly49F, Ly49G-HA and Ly49Q-HA was incubated with PE-conjugated H-2K^b, H-2D^b and H-2D^d MHC class I tetramers. The cells were subsequently washed and analysed by flow cytometry for the intensity of fluorescent signal. **Figure 3.3** shows the results of this staining. Most interestingly, the C57 Ly49B-HA transfectants did not associate with any of the tested tetramers, whereas the BALB/c Ly49B-HA transfectants associated with all of the tested tetramers, of which the H-2D^d ligand bound most strongly. This data indicates that C57 and BALB/c Ly49B may have very different structure and that at least in the case of BALB/c Ly49B the presence of C-terminal HA-tag does not interfere with ligand binding. The Ly49A-HA transfectants stained strongly with the H-2D^d tetramers and exhibited a negligible association with both H-2D^b and H-2K^b. The Ly49E-HA, Ly49F and Ly49G-HA transfectants did not exhibit a significant association with any of the tested tetramers. The L49Q-HA transfectants stained very weakly with the H-2K^b tetramer but not with any of the others.

3.3. Mapping of Ly49B residues responsible for selective binding of the 1A1 antibody

The BALB/c Ly49B and the C57 Ly49B isoforms differ by 12 amino acids (**Appendix I**). Two monoclonal anti-Ly49B antibodies were generated previously, referred to as 1A1 and 2G4 (Gays *et al.* 2006). It was found that 1A1 recognises the C57 form, while 2G4 recognises both the C57 and BALB/c isoforms of Ly49B (Gays *et al.* 2006). The finding that C57 and BALB/c Ly49B isoforms also differ in ligand binding pattern (**Section 3.2**) suggests that the two proteins may fold in a dissimilar manner and that the variation in Ly49B recognition by 1A1 antibody may result from the aforementioned differences. It was hypothesised that the same variable Ly49B residues (or residues in a close proximity) may be responsible for selective mode of 1A1 and MHC tetramers binding. Identification of Ly49B residues responsible for 1A1 binding could narrow down the search for residues responsible for ligand binding and was therefore a primary objective of this study.

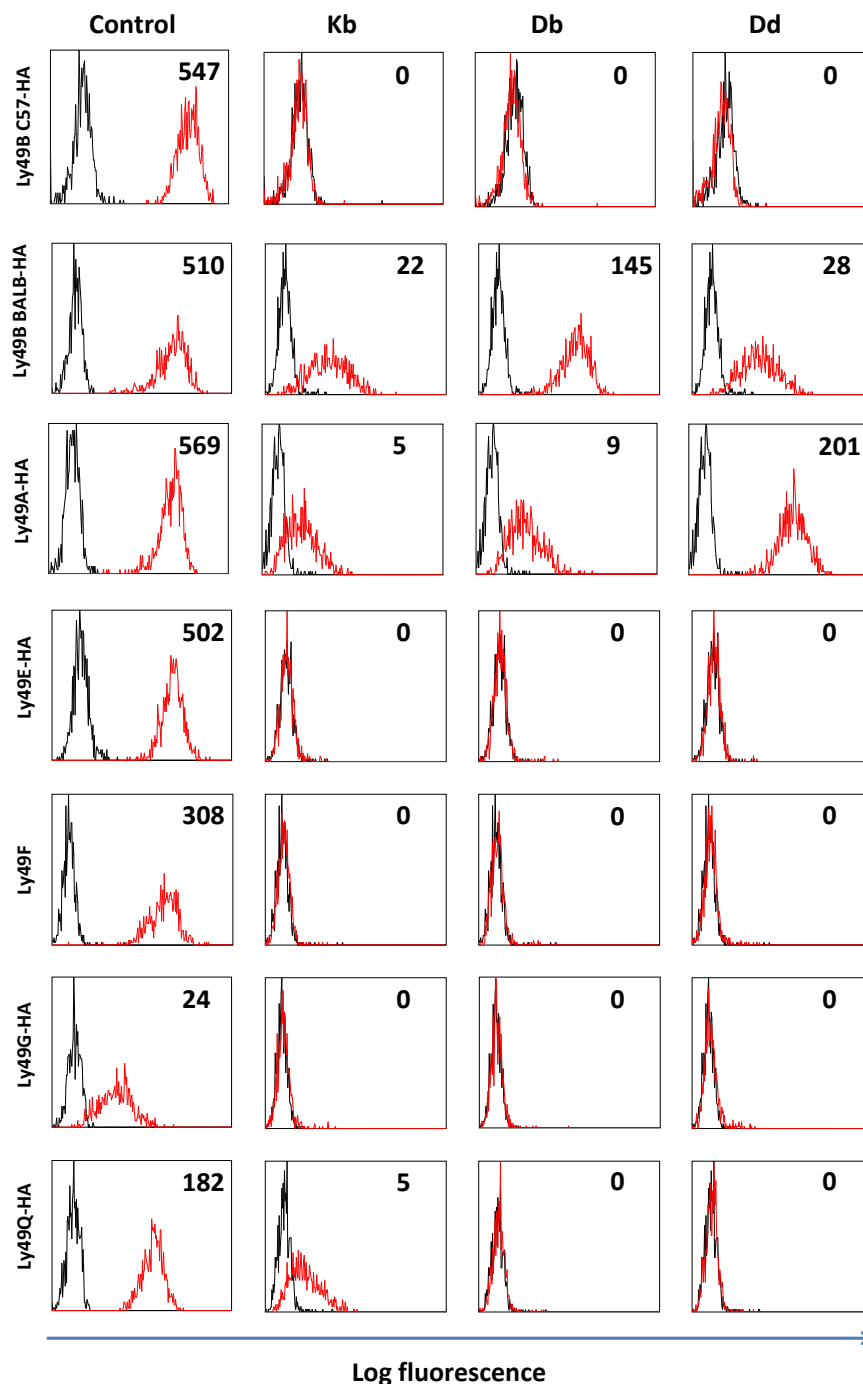


Figure 3.3. Staining of various Ly49 transfectants with MHC class I tetramers. YB2 cells transfected with pMXs-IP plasmids encoding C57 Ly49B-HA, BALB/c Ly49B-HA, Ly49A-HA, Ly49E-HA, Ly49F, Ly49G-HA and Ly49Q-HA constructs were stained with PE-conjugated H-2K^b, H-2D^b and H-2D^d tetramers and control antibodies. The cells expressing HA-tagged constructs were stained with N1222 Biotin 16.43 rat anti-HA IgG2a anti-HA antibody control followed by N924 AF647 streptavidin and the cells expressing untagged Ly49F with N1239 PE-conjugated mouse anti-Ly49F IgG1 antibody. The intensity of staining was expressed in log fluorescence values and marked on the X axis. Black peaks on the histograms represent cells stained with medium and the red peaks represent the cells stained with the tetramers or antibodies. The number in the top right corner of each histogram represents log fluorescent value generated by the stained cells minus the background generated by the unstained cells.

Table 3.1. Full names, abbreviations and amino acid codes of molecules used in Chapter 3. * = transfectants generated previously in the lab.

Full construct name	Name abbreviation	Amino acid code
C57 Ly49B *	C57	VLKAAEPVENRN
BALB/c Ly49B *	BALB	LWNSKLDQSCT
C57 Ly49B HA	C57-HA	VLKAAEPVENRN-HA
BALB/c Ly49B HA*	BALB-HA	LWNSKLDQSCT-HA
C57 Ly49B-V59L	C57-V59L	LLKAAEPVENRN
BALB/c Ly49B-N167K	BALB-N167K	LWKDSKLDQSCT
BALB/c Ly49B-N167S	BALB-N167S	LWSDSKLDQSCT
Chimera 1*	-	LWNSKLDENRN
Chimera 2*	-	VLKAAEPVQSCT
Chimera 2-V59L	2.1	LLKAAEPVQSCT
Chimera 2-L166W	2.3	VWKAAEPVQSCT
Chimera 2-K167N	2.4	VLNAAEPVQSCT
Chimera 3*	-	LWNAAEPVENRN
Chimera 3-L59V	3.1	VWNAAEPVENRN
Chimera 3-W166L	3.2	LLNAAEPVENRN
Chimera 3-N167K	3.3	LWKAAEPVENRN
Chimera 3-L59V-W166L	3.4	VLNAAEPVENRN
Chimera 3-L59V-N167K	3.5	VWKAAEPVENRN
Chimera 4*	-	VLKDSKLDQSCT
Chimera 4-V59L	4.1	LLKDSKLDQSCT
Chimera 4-L166W	4.2	VWKDSKLDQSCT
Chimera 4-K167N	4.3	VLNDSKLDQSCT
Chimera 4-V59L-L166W	4.4	LWKDSKLDQSCT
Chimera 4-V59L-K167N	4.5	LLNDSKLDQSCT
Chimera 5*	-	VLKDSKLDENRN
Chimera 6*	-	LWNAAEPVQSCT
Chimera 6-L59V	6.1	VWNAAEPVQSCT
Chimera 7*	-	LWNAAEPVENCN
Chimera 7-L59V	7.1	VWNAAEPVENCN
Chimera 7-L59V-W166L	7.2	VLNAAEPVENCN
Chimera 7-L59V-N167K	7.3	VWKAAEPVENCN
Chimera 7-HA*	-	LWNAAEPVENCN-HA
Chimera 7-L59V-HA	7.1-HA	VWNAAEPVENCN-HA
Chimera 7-L59V-W166L-HA	7.2-HA	VLNAAEPVENCN-HA
Chimera 7-L59V-N167K-HA	7.3-HA	VWKAAEPVENCN-HA
Ly49B BALB/c N94Q	BALB-A	-
Ly49B BALB/c N105Q	BALB-B	-
Ly49B BALB/c N114Q	BALB-C	-
Ly49B BALB/c N177Q	BALB-D	-
Ly49B BALB/c N105Q-N114Q	BALB-BC	-
Ly49B BALB/c N94Q-N105Q-N114Q-N177Q-HA	BALB-ABCD-HA	-
Ly49B C57 N94Q-N105Q-N114Q-N177Q	C57-ABCD	-
Ly49B C57 N94Q-N105Q-N114Q-N177Q-HA	C57-ABCD-HA	-
BALB/c Ly49B-20-H	BALB-20-H	-
BALB/c Ly49B-20-H-HA	BALB-20-H-HA	-

Naturally occurring enzyme restriction sites in the Ly49B sequences allowed generation of a series of chimeric C57/BALB/c Ly49B YB2 transfectants with random combination of 12 variable amino acids, previously in the lab (**Figure 3.4**). **Table 3.1** contains full names of the chimeric molecules and other mutants generated in this study together with the names abbreviations and sequence of variable Ly49B amino acids where applicable.

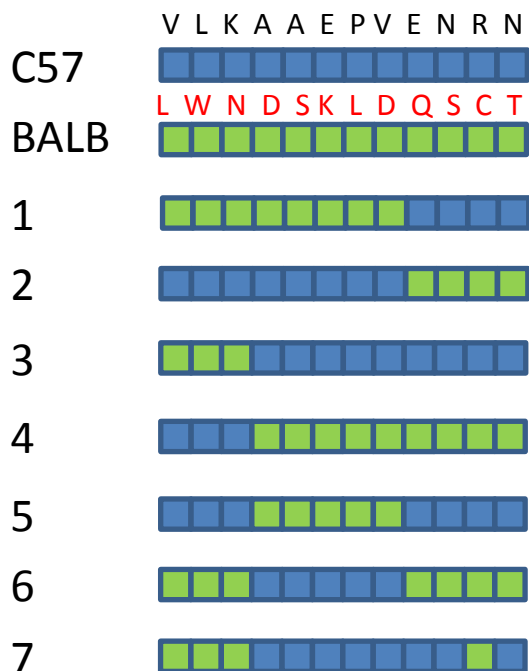


Figure 3.4. Schematic representation of chimeric C57/BALB/c Ly49B molecules. The twelve small squares represent the twelve variable residues between C57 and BALB/c Ly49B. The blue squares represent C57 residues. Green squares represent BALB/c residues. C57 Ly49B is labelled as C57. BALB/c Ly49B is labelled as BALB. Chimeras 1-7 are labelled 1-7.

To determine which of the 12 amino acids are responsible for 1A1 binding the chimeric transfectants were stained with 1A1 and 2G4 antibodies followed by secondary antibodies conjugated to fluorophores, washed and analysed by flow cytometry. It was found that chimera 3, which contains BALB/c residues at positions 59, 166 and 167 and the C57 residues at the remaining variable positions, did not stain with 1A1, whereas chimera 4, which has got an opposite combination of residues (C57 residues at positions 59, 166 and 167, and BALB/c residues at the remaining variable positions) did stain with 1A1 (**Figure 3.5**).

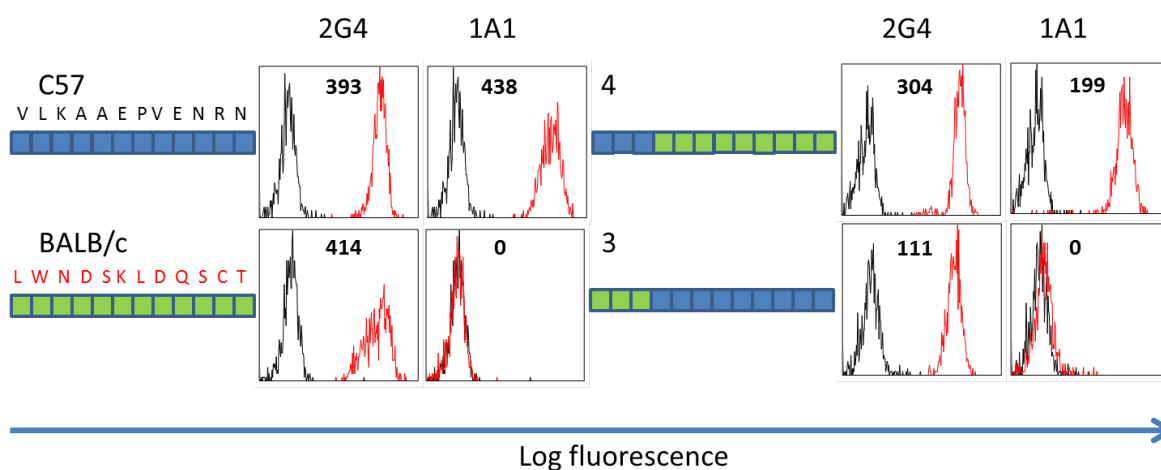


Figure 3.5. Staining of Chimera 3 and 4 Ly49B mutants. YB2 cells transfected with the specified constructs were stained with N837 2G4 rat anti-L49B IgG2c or N838 1A1 rat anti-L49B (C57) IgGi monoclonal rat anti-L49B antibodies and then with a secondary N1217 AF647 conjugated chicken anti-rat antibody. The intensity of staining was expressed in log fluorescence values and marked on the X axis. Black peaks on the histograms represent cells stained with medium and the red peaks represent the cells stained with the antibodies. C57- C57 Ly49B, BALB- BALB/c Ly49B, 3- chimera 3, 4- chimera 4. Colour coding of the schematic representation of the constructs- the same as in Figure 3.3.

These results suggested that one or more of variable amino acids at positions 59, 166 and 167 are responsible for the selective mode of 1A1 binding. To assess which of the three residues are critical, a series of mutations was introduced by site directed mutagenesis (**Figure 3.6**) into both the chimera 3 and chimera 4 molecules, as illustrated schematically in **Figure 3.7**. A Ly49B C57-V59L mutant was also created to unambiguously determine the impact of the BALB/c 59 residue on the C57 Ly49B and its schematic representation was included in **Figure 3.7**.

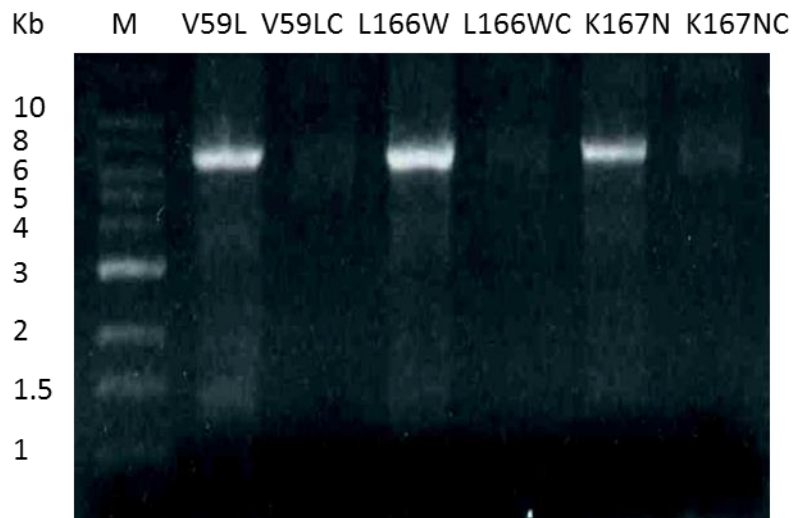


Figure 3.6. Generation of mutant constructs by site directed mutagenesis. The above panel is a representative example. The remaining constructs were generated in a similar way. Chim4-V59L (59), Chim4-L166W (166) and Chim4-K167N (167) were amplified by PCR using pMX-s-IP vector with Chimera 4 insert as a template, overlapping primers and Velocity polymerase (Bioline). In the same time controls were run without the enzyme. PCR products were then digested by DpnI to remove the template and separated by agarose gel electrophoresis. The expected product was to be 6766bp in size. The control lines show that there was no non-specific amplification and all of the template was digested with DpnI.

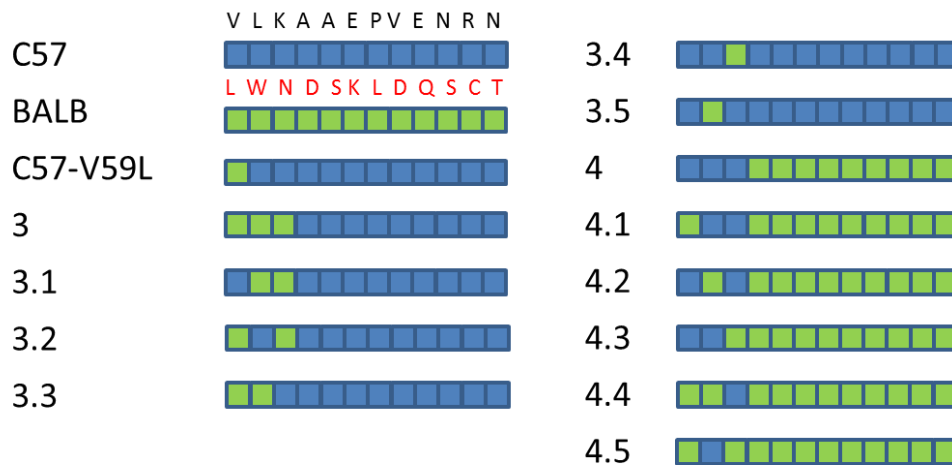


Figure 3.7. Schematic representation of chimera 3 and 4 mutants. C57- C57 Ly49B, BALB- BALB/c Ly49B, 3- chimera 3, 4- chimera 4. Colour coding- the same as in Figure 3.3.

Plasmids containing the desired sequences were confirmed by performing diagnostic restriction digests (**Figure 3.8**), followed by full sequencing. Vectors containing the desired sequences were amplified and transfected into YB2 cell lines by electroporation. **Figure 3.9** shows 1A1 and 2G4 flow cytometric staining of the mutants.

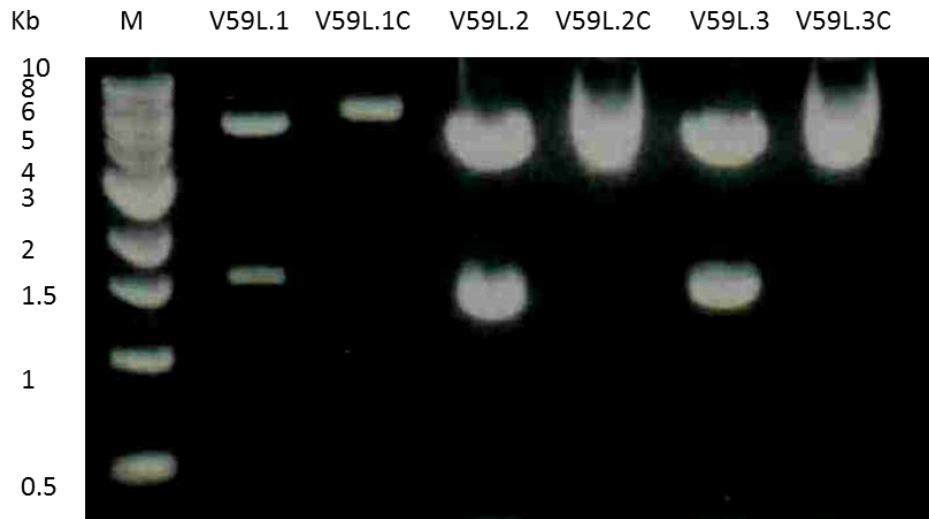


Figure 3.8. *PstI* digest of pMXs-IP vectors with Ly49B Chim4-V59L inserts. The above panel is a representative example. All of the remaining constructs were verified by digest in the same way. Minipreps from 3 colonies transformed with pMXs-IP-Ly49B Chim4-V59L (59.1, 59.2 and 59.3) were digested with *PstI* and the resulting bands were separated by agarose gel-electrophoresis. The plasmids with inserts were expected to give bands 4989bp, 1601 and 176bp in size. The smallest band is not visible on the gel. Control lines (C) contain plasmids which were not digested by *PstI*.

Mutation V59L did not prevent 1A1 binding of either C57-V59L or mutant 4.1. Moreover, switching the BALB/c residue at position 59 to its C57 equivalent, as in mutant 3.1, was insufficient to restore 1A1 binding. Based on these results, residue 59 was formally excluded as playing a key role in the selective mode of 1A1 binding.

Mutation L166W was sufficient to prevent 1A1 binding to 4.2 and 4.4 mutants. The same result was obtained for mutation K167N as in mutants 4.3 and 4.5. These results suggest that in isolation the C57 residues at positions 166 and 167 are unable to confer binding of 1A1 to the BALB/c molecule; both are needed for the integrity of the 1A1 epitope in the BALB/c background.

Mutation W166L from the BALB/c form to C57 resulted in the restoration of 1A1 binding in mutants 3.2 and 3.4. However, the analogous mutation of residue 167 as in mutants 3.3 and 3.5 did not have the same effect, implying that L166 alone is necessary and sufficient for binding of the 1A1 antibody to C57 Ly49B.

In summary, residue 59 does not appear to be important for a selective binding of 1A1 anti-Ly49B antibody. The C57 L166 and K167 residues are necessary to impose 1A1 binding on BALB/c Ly49B molecule. The C57 L166 is necessary to maintain 1A1 epitope by C57 Ly49B.

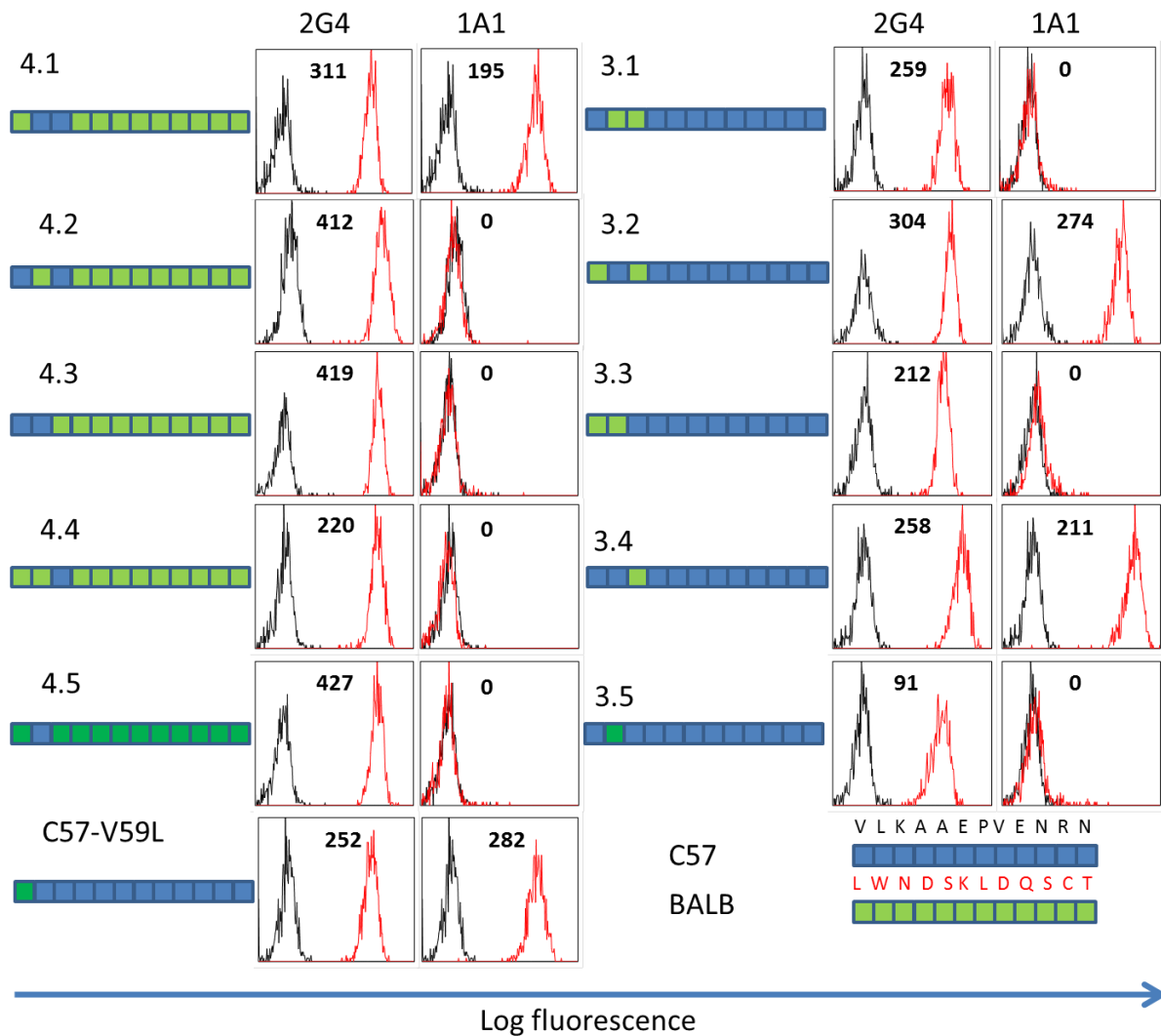


Figure 3.9. Staining of chimera 3 and chimera 4 Ly49B mutants. YB2 cells transfected with the specified constructs were stained with N837 2G4 rat anti-L49B IgG2c or N838 1A1 rat anti-L49B (C57) IgG1 monoclonal rat anti-L49B antibodies and then with a secondary N1217 AF647 conjugated chicken anti-rat antibody. The intensity of staining was expressed in log fluorescence values and marked on the X axis. Black peaks on the histograms represent cells stained with medium and the red peaks represent the cells stained with the antibodies. C57- C57 Ly49B, 3- chimera 3, 4- chimera 4. Colour coding of the schematic representation of the constructs- the same as in Figure 3.3.

3.4. Mapping of Ly49B residues responsible for the selective binding of MHC class I ligands

The experiment outlined in **Section 3.2** have shown that the BALB/c Ly49B form interacts with at least three MHC class I molecules; H-2K^b, H-2D^b and H-2D^d, whereas the C57 Ly49B form does not bind any of the tested tetramers. In order to establish which residues are critical for binding of MHC class I ligands, a series of Ly49B mutants was created by site directed mutagenesis, using the previously generated chimeric constructs as templates. The transfectants used for determining which residues are critical for 1A1 staining were also included. Additionally, a BALB/c Ly49B mutant was created with S167 due to the strong level of conservation of this residue among several other Ly49s. All of the tested mutants are schematically shown in **Figure 3.10** and their full names, corresponding abbreviations and amino acid code with the sequence of variable Ly49B residues can be found in **Table 3.1**. The YB2 cells transfected with the mutants, the C57 Ly49B, the BALB/c Ly49B and the previously generated chimeric molecules were stained with three MHC class I tetramers (H-2K^b, H-2D^b and H-2D^d), as well as the 2G4 antibody as a control.

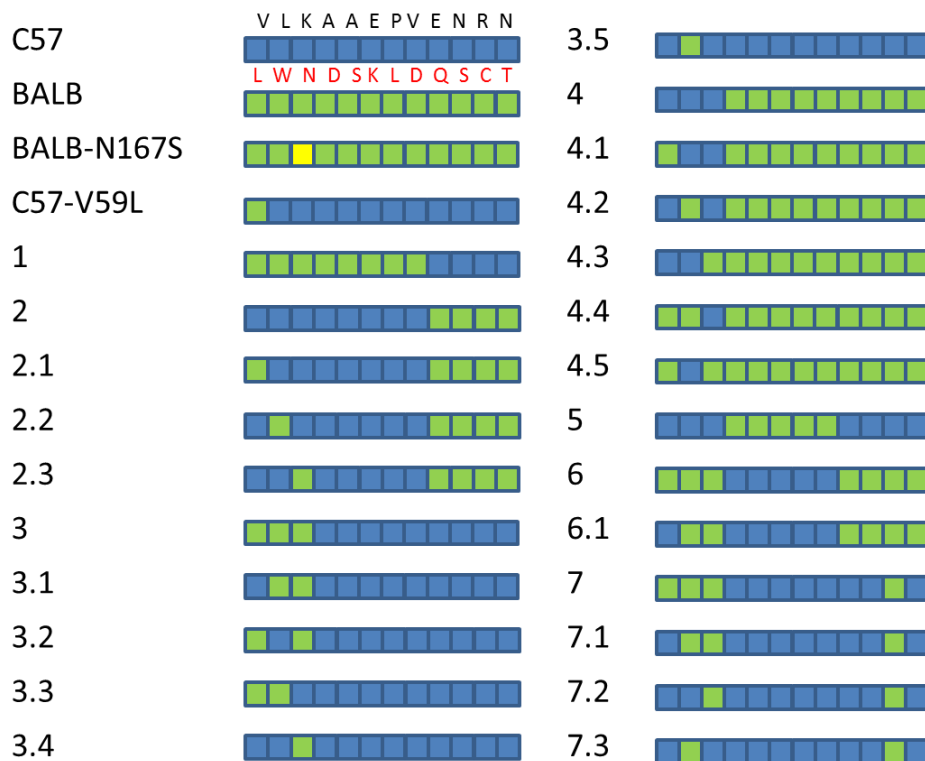


Figure 3.10. Schematic representation of Ly49B mutants. C57- C57 Ly49B, BALB- BALB/c Ly49B numbers 1-7 – chimeras 1-7. Colour coding- the same as in Figure 3.3, apart from the yellow square in mutant BALB-N167S, which represents serine at position 167 conserved among other Ly49s apart from Ly49B.

Two types of figures were generated for staining of each of the tetramers. The first contains bar charts with average net median fluorescence values for each mutant and demonstrates how strongly the tetramers bound. An additional figure was also prepared showing control data for 2G4 binding (**Figure 3.11**). The second type of figures contains bar charts showing the strength of tetramer binding, expressed as a percentage, in comparison to staining with 2G4. This second set of data accounts for variations in expression levels for each mutant. All of the raw staining data are compiled in **Appendix III**.

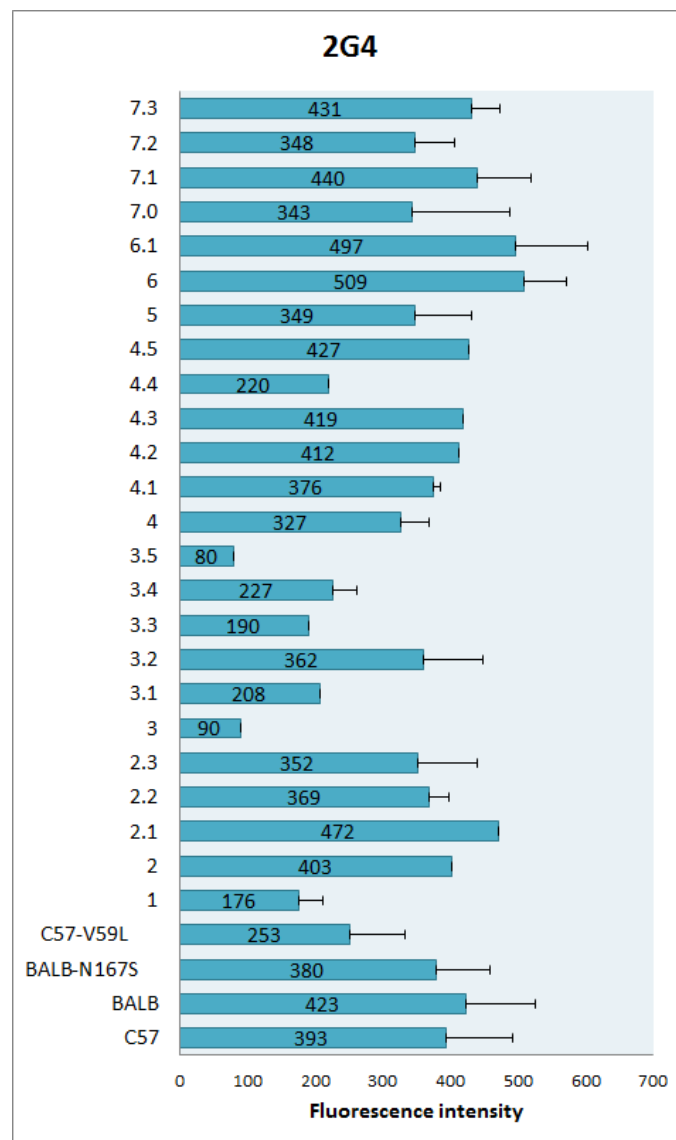


Figure 3.11. Staining of Ly49B mutants with 2G4 antibody. YB2 cells transfected with the specified constructs were stained with biotinylated 2G4 monoclonal rat anti-L49B antibody and then with AF647 conjugated streptavidin. The staining was repeated at least 3 times for each of the transfectants and the numbers in the centre of the blue bars represent average net median fluorescence values. Error bars (SD) are shown in black. C57- C57 Ly49B, BALB- BALB/c Ly49B numbers 1-7 – chimeras 1-7.

3.4.1. H-2K^b binding

Figure 3.12 shows the flow cytometric staining of mutants described in the **Section 3.4** using the H-2K^b tetramer. The results of staining of the C57, BALB/c and Ly49B transfectants agree well with previous findings, showing that C57 form does not bind the tetramer but the BALB/c form does. The roles of the remaining variable residues assessed individually and in combination with one another, are described below.

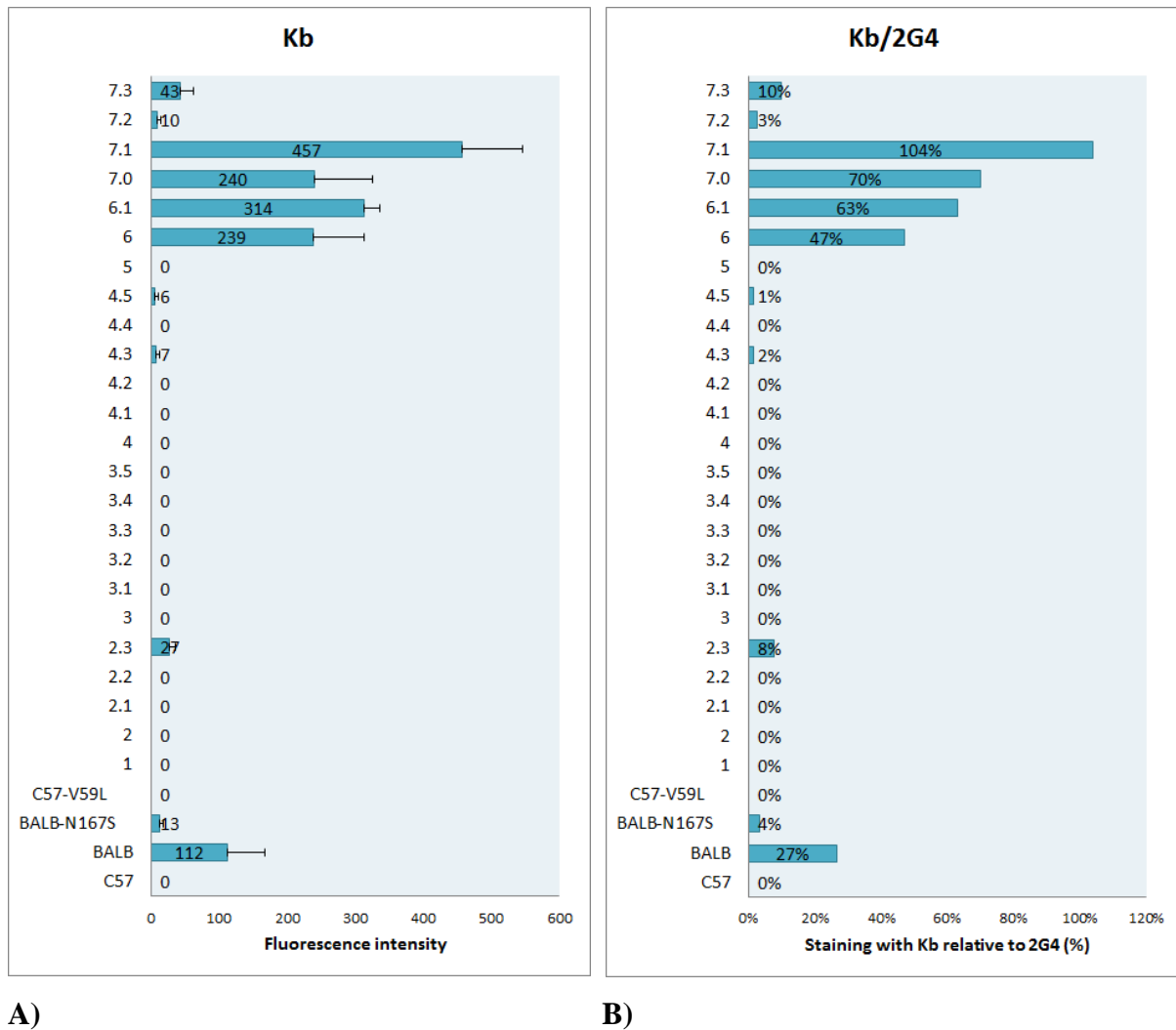


Figure 3.12. Staining of Ly49B mutants with H-2K^b. YB2 cells transfected with the specified constructs were stained with PE-conjugated H-2K^b tetramers. **A)** The staining was repeated at least 3 times for each of the positive transfectants and at least 2 times for the negative transfectants. The numbers in the centre of the blue bars represent average net median fluorescence values. Error bars (SD) are shown in black. **B)** The intensity of staining was expressed as a percentage of staining with H-2K^b tetramer (Figure 17 A) relative to staining with 2G4 (Figure 16). Kb - H-2K^b MHC class I tetramers, C57- C57 Ly49B, BALB- BALB/c Ly49B numbers 1-7 – chimeras 1-7.

Mutation V59L in the Ly49B C57, chimera 2 and chimera 4 backgrounds was not sufficient to confer H-2K^b binding to those molecules. Similarly, the reciprocal mutation in

chimera 3 had no effect, suggesting that, as with 1A1, residue 59 is not critical for H-2K^b ligand binding. Surprisingly, L59V mutation in chimeras 6 and 7 resulted in increased binding of the tetramer in comparison to 2G4 by 16 % and 34 % respectively. From these results, it would appear that although residue 59 is not directly involved in forming interactions with the H-2K^b tetramer, it is capable of exerting an influence on the strength of the association with the ligand. Furthermore, it is the C57 residue that promotes the more favourable binding of the two residues.

Mutation L166W in chimera 2, 4 and mutant 4.1 backgrounds did not result in the restoration of H-2K^b binding. Similarly, none of the chimera 3 mutants with the BALB/c residue, W166, bound the H-2K^b tetramer. Interestingly, mutant 7.3, which only contains BALB/c residues at variable positions 166 and 251, exhibited some, albeit very weak, binding (10 %). These results were surprising since several of the mutants that did not bind had greater amino acid sequence similarity to wild type BALB/c Ly49B than the mutant 7.3: mutant 2.3 contains BALB/c residues, not only at positions 166 and 251, but also at the three remaining C-terminal variable positions; mutant 4.2 is identical to BALB/c with the exception of residues 59 and 167; and mutant 4.4 is entirely BALB/c apart from residue 167. The introduction of BALB/c W166 in the C57 background is not sufficient to produce H-2K^b binding. Binding can be partially restored when the BALB/c residue is introduced at position 251 and the remaining variable residues from the C57 background.

Mutation K167N in the chimera 2, 4 and mutant 4.1 backgrounds led to an induction of H-2K^b binding relative to 2G4 at a very low level (8 %, 2 % and 1 % respectively). None of the chimera 3 mutants with N167 associated with H-2K^b. Mutant 7.2, which contains BALB/c amino acids at positions 167 and 251, exhibited binding at 3 % of the level of 2G4 staining. These results indicate that introduction of the BALB/c residue at position 167 restores binding of the H-2K^b ligand to a small extent only if the BALB/c residue is also present at position 251.

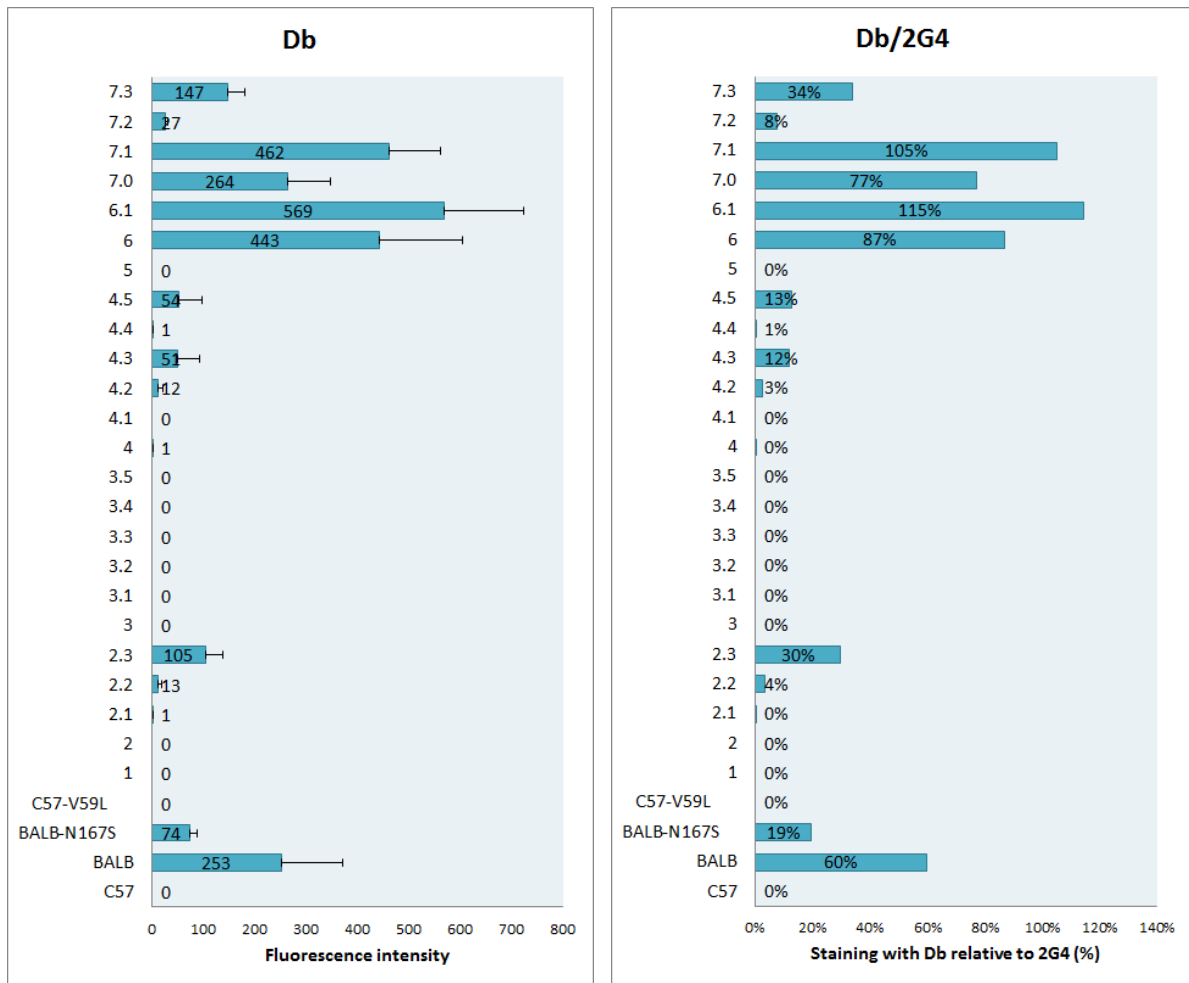
H-2K^b association was retained in the BALB-N167S mutant. However, it was reduced about 9 times in comparison to the WT. From this observation it seems that the presence of N167 in Ly49B is more favourable for H-2K^b binding than the conserved S167. Moreover, it might be concluded that S167 in other Ly49s would not prevent them from H-2K^b binding.

The strongest binding was observed with mutant 7.1, followed by chimera 7, then mutant 6.1 and finally chimera 6; all of these mutants contain BALB/c residues at positions 166, 167 and 251. Interestingly, the association was 20 % to 77 % stronger in comparison to 2G4 than with the WT Ly49B BALB/c. Chimera 7 associated 23 % more strongly in comparison to 2G4 than chimera 6. The main difference between these two variants is that chimera 6 contains three more variable residues of BALB/c origin than chimera 7. As with mutant 7.3, which exhibited greater H-2K^b binding than mutants that contained more BALB/c amino acids at variable positions (other than 166, 167 and 251), the same subtle difference also seems to produce a stronger association for chimera 7. Furthermore, as previously mentioned, the presence of V59 (as found in C57) in mutants 6.1 and 7.1 produced stronger binding than in chimeras 6 and 7.

In conclusion residue 59 does not directly influence H-2K^b binding. However, adoption of the C57 residue at this position does increase binding strength via residues which are directly involved, as compared to adoption of the BALB/c residue. The most favourable combination of residues for H-2K^b binding is BALB/c amino acids at positions 166, 167 and 251 (W, N, C respectively) in the C57 background. BALB/c residues at position 251 and either 166 or 167 are essential to impose marginal H-2K^b binding on C57 Ly49B. Introduction of further BALB/c residues into the C57 background leads to loss of integrity of the H-2K^b binding motif by the mutants with BALB/c residues at positions 166 and 251, but not those with BALB/c residues at positions 167 and 251.

3.4.2. H-2D^b binding

Figure 3.13 shows the results of flow cytometric staining with the H-2D^b tetramer. Staining of the C57 and BALB/c transfectants was consistent with previous findings, as discussed in the introduction.



A)

B)

Figure 3.13. Staining of Ly49B mutants with H-2D^b. YB2 cells transfected with the specified constructs were stained with PE-conjugated H-2D^b tetramers. **A)** The staining was repeated at least 3 times for each of the positive transfectants and at least 2 times for the negative transfectants. The numbers in the centre of the blue bars represent average net median fluorescence values. Error bars (SD) are shown in black. **B)** The intensity of staining was expressed as a percentage of staining with H-2D^b tetramer (Figure 18 A) relative to staining with 2G4 (Figure 16). Dd - H-2D^b MHC class I tetramers, C57- C57 Ly49B, BALB- BALB/c Ly49B numbers 1-7 – chimeras 1-7.

As with flow cytometric staining using the H-2K^b tetramer, residue 59 did not appear to have a direct effect on H-2D^b binding but did influence the strength of binding mediated by other crucial residues. Mutants 6.1 and 7.1 interacted with H-2D^b 28 % more strongly relative to 2G4 than chimera 6 and 7 respectively, suggesting that the C57 residue at position 59 promotes more favourable binding by the mutants than with the equivalent BALB/c residue present.

All of the mutants that contained BALB/c residues at positions 166 and 251, or 167 and 251, did support binding of H-2D^b regardless of which of the other variable residues were

present. However, the first combination of residues did promote much weaker binding in comparison to 2G4 in mutants 2.2 (4 %), 4.2 (3 %), and 4.4 (1 %), than the second combination, which was present in chimera 2.3 (30 %), 4.3 (12 %) and 4.5 (13 %). On the other hand, mutant 7.3, which contains BALB/c residues at positions 167 and 251 stained 26 % stronger in comparison to 2G4 than mutant 7.3, which contains BALB/c residues at positions 166 and 251 and stained at 8 % level in comparison to 2G4. These results suggest that BALB/c residues at positions 166 and 251 support stronger H-2D^b binding in the C57 background, but when further BALB/c residues are introduced residues 167 and 251 appear to mediate stronger H-2D^b binding.

Mutant BALB-N167S exhibited 41 % reduced binding relative to 2G4 compared to the wild type BALB/c Ly49B receptor. This result is analogous to that which was obtained with the H-2K^b tetramer. However, the H-2D^b tetramer associated 18 % more strongly in comparison to 2G4. The WT BALB/c Ly49B also bound the H-2D^b tetramer more strongly than the H-2K^b. These results suggest that N167 in Ly49B promotes stronger ligand binding than the S167, which is highly conserved amongst other Ly49s, would. Introduction of S167 did not change the relative relationship between binding strength of the H-2D^b and H-2K^b tetramers, with H-2D^b consistently acting as the stronger binding ligand.

As with binding of the H-2K^b tetramer, mutants containing BALB/c residues at positions 166, 167 and 251 associated with H-2D^b most strongly. The strength of binding was comparable between chimeras 6 and 7 (87 % and 77 %) and mutants 6.1 and 7.1 (115 % and 105 %), suggesting that when BALB/c residues are present at positions 166, 167 and 251, the C57 or BALB/c identity of residues at the remaining variable positions of chimeras 6 and 7 does not significantly influence ligand binding. Analogous to the results obtained for the H-2K^b tetramer, binding of H-2D^b to chimeras 7 and 6, as well as mutants 7.1 and 6.1 was 16 % to 44 % stronger relative to 2G4 than the one exerted by the WT. However, the increase in strength of binding was not as profound as in the case of H-2K^b binding.

In summary, the pattern of H-2D^b binding is similar to that of H-2K^b binding. Residue 59 does not have a direct effect on H-2D^b binding but ligand binding is promoted with the C57 residue present at this position via its influence on other residues. The most favourable combination is BALB/c residues at positions 166, 167 and 251 (W, N, C respectively) in the C57 background. The results presented here seem to indicate that BALB/c residues at either position 166 or 167, combined with the BALB/c residue at

position 251, are likely to support H-2D^b binding regardless of the background strain of the molecule. This is in contrast with binding of the H-2K^b tetramer, which is retained by all of the mutants with BALB/c residues at positions 167 and 251, but lost by several mutants with BALB/c residues at positions 166 and 251.

3.4.3. H-2D^d binding

Figure 3.14 shows the results of flow cytometric staining using the H-2D^d tetramer. Control staining of transfectants expressing the C57 and BALB/c was in close agreement with previous findings.

Residue 59 had no direct effect on H-2D^d binding but as with the results for the H-2K^b and H-2D^b tetramers, introduction of the C57 residue at this position did promote H-2D^d binding in certain backgrounds. Mutant 6.1, for example, interacted 22 % more strongly in comparison to 2G4 than chimera 6. Similarly, mutant 7.1 interacted 16 % more strongly relative to 2G4 than chimera 7.

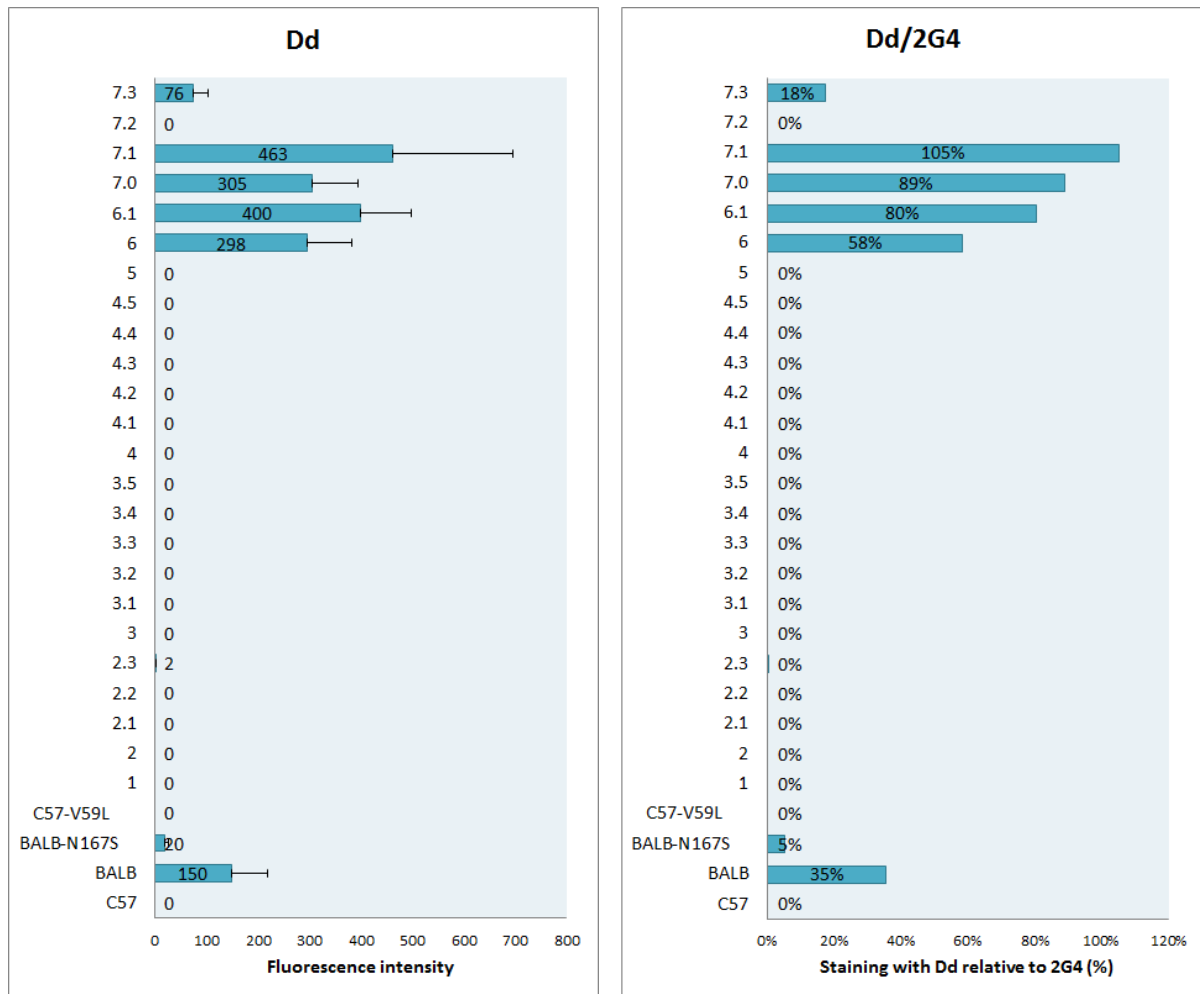
Mutant 7.3, which contains BALB/c residues at positions 166 and 251 in the C57 background, was able to support H-2D^d binding at 18 % of the level of 2G4 binding. Introduction of additional BALB/c residues at positions other than 167 resulted in further loss of binding. These results suggest that the BALB/c residue at position 166 is able to promote binding of the H-2D^d tetramer if the BALB/c residue is present at position 251 and if all of the remaining variable residues are of C57 origin.

None of the mutants that contain the BALB/c residue at position 167 with C57 residues at positions 166 and 251 exhibited significant binding to the H-2D^d tetramer. These results suggest that, in isolation, residue 167 does not influence H-2D^d binding.

As was the case for the H-2K^b and H-2D^b tetramers, mutant BALB-N167S exhibited reduced H-2D^d binding compared to the WT BALB/c Ly49B. This result indicates that the presence of the highly conserved S167 in BALB/c Ly49B does not abolish the H-2D^d interaction, but does reduce its strength.

H-2D^d binding results for mutants with BALB/c residues at positions 166, 167 and 251 are very similar to those obtained for the H-2K^b tetramer. All of the mutants associated 23 % to 70 % more strongly relative to 2G4 than the wild type BALB/c Ly49B. Mutant 7.1 bound most strongly, followed by chimera 7, mutant 6.1 and finally chimera 6. It seems that,

as with the H-2K^b tetramer, C57 residues at positions other than 166, 167 and 251 serve to promote interactions with the H-2D^d tetramer.



A)

B)

Figure 3.14. Staining of Ly49B mutants with H-2D^d. YB2 cells transfected with the specified constructs were stained with PE-conjugated H-2D^d tetramers. **A)** The staining was repeated at least 3 times for each of the positive transfectants and at least 2 times for the negative transfectants. The numbers in the centre of the blue bars represent average net median fluorescence values. Error bars (SD) are shown in black. **B)** The intensity of staining was expressed as a percentage of staining with H-2D^d tetramer (Figure 19 A) relative to staining with 2G4 (Figure 16). Dd - H-2D^d MHC class I tetramers, C57- C57 Ly49B, BALB- BALB/c Ly49B numbers 1-7 – chimeras 1-7.

From these results it seems that binding of the H-2D^d tetramer generally requires Ly49B to possess three BALB/c amino acids at positions 166, 167 and 251 (W, N, C respectively). The only exception being mutant chimera 7.3, which contains BALB/c residues at positions 166 and 251 in the C57 background and does still associate with the H-2D^d tetramer; albeit much less strongly. This is in contrast to binding of the H-2K^b and H-2D^b tetramers, which can be rescued by several other combinations of amino acids.

3.5. Establishing the role of the C-terminal 20 amino acids of Ly49B in ligand and antibody binding

Ly49B contains 20 additional amino acids at its C-terminus compared to other Ly49s. In order to assess their role in ligand and antibody binding, two mutant transfectants were created. One transfectant expressed the BALB/c Ly49B without the 20 C-terminal amino acids and with the terminal residue at the truncated end substituted from isoleucine to histidine. The second construct was identical to this molecule but additionally contained a C-terminal HA-tag. This second construct was created to assess mutant expression levels using an anti-HA antibody in case 2G4 and/or ligand binding was abolished due to the truncated C-terminus. The mutants were stained, along with HA-tagged and untagged Ly49B BALB/c transfectants, with the H-2K^b, H-2D^b and H-2D^d MHC class I tetramers. The 2G4 anti-Ly49B antibody and anti-HA antibody were also tested. Results are presented in two types of figures; one with average net fluorescence median values for each molecule and the second showing staining of the tetramers, expressed as a percentage, in comparison to staining with the anti-HA antibody. All raw staining data are compiled in **Appendix III**.

3.5.1. Antibody binding

Figure 3.15 A shows staining of the mutants with the 2G4 antibody. The control transfectants stained at a similar level to one another, but staining of the mutants was completely abolished. These results may indicate that there was no surface expression of the mutants, or that the protein did not fold correctly in the absence of C-terminal amino acids and the 2G4 epitope became inaccessible or destroyed. For example, the epitope could have been masked by incorrectly folded parts of the protein. Alternatively, if the 2G4 epitope was discontinuous, altered conformation of the protein could affect the correct epitope folding.

In order to assess surface mutant expression levels, anti-HA staining was performed. As shown in **Figure 3.15 B**, untagged constructs did not stain but the HA-tagged control and mutant were both positive. Mutant staining was decreased by ~50 % compared to the control, suggesting that either expression levels were lower or that the C-terminus was less accessible in the mutated protein. Unfortunately, expression levels of the untagged mutant protein could not be directly assessed; nevertheless, the mutant transfectant was still used for staining with the MHC class I tetramers.

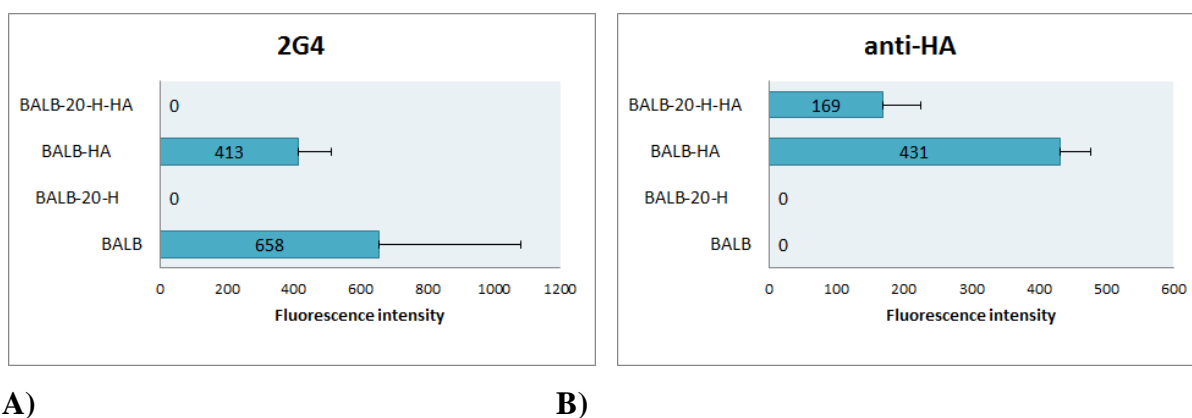


Figure 3.15. Staining of Ly49B mutants lacking 20 C-terminal amino acids with 2G4 anti-Ly49B and anti-HA antibodies. YB2 cells transfected with the specified constructs were stained with **A)** biotinylated 2G4 monoclonal rat anti-Ly49B antibody and then with AF647 conjugated streptavidin or with **B)** biotinylated anti-HA antibody and then AF647 conjugated streptavidin. The staining was repeated at least 3 times for each of the positive transfectants and at least 2 times for the negative transfectants. The numbers in the centre of the blue bars represent average net median fluorescence values. Error bars (SD) are shown in black. BALB- BALB/c Ly49B, BALB-20-HA- BALB/c Ly49B lacking C-terminal 20 amino acids and where the last amino acid was replaced with histidine, HA-hemagglutinin tag.

3.5.2. H-2K^b binding

Figure 3.16 A shows the results of staining with H-2K^b tetramer expressed in average net median fluorescence values. The wild type Ly49B did stain the strongest and Ly49B 20-H-HA, Ly49B-HA, and Ly49B 20-H stained at a similar level. The results cannot be directly compared since the expression levels of the untagged Ly49B 20-H are unknown. However, since the expression levels of the controls were shown to be similar (**Figure 3.16 A**) it was possible to directly compare the results for Ly49B and Ly49B-HA looking at average net median fluorescence values. Interestingly, H-2K^b did bind nearly eight times weaker to the HA-tagged construct. Since the HA-tag was on the C-terminus it is reasonable to conclude that the C-terminus is important for H-2K^b binding and the tag did interfere with it.

Figure 3.16 B takes into account the expression levels of the tagged constructs assessed with anti-HA antibody and shows that the removal of C-terminal 20 amino acids resulted in a modest 4 % increase in H-2K^b binding, which suggests that the C-terminal amino acids do not significantly affect H-2K^b binding.

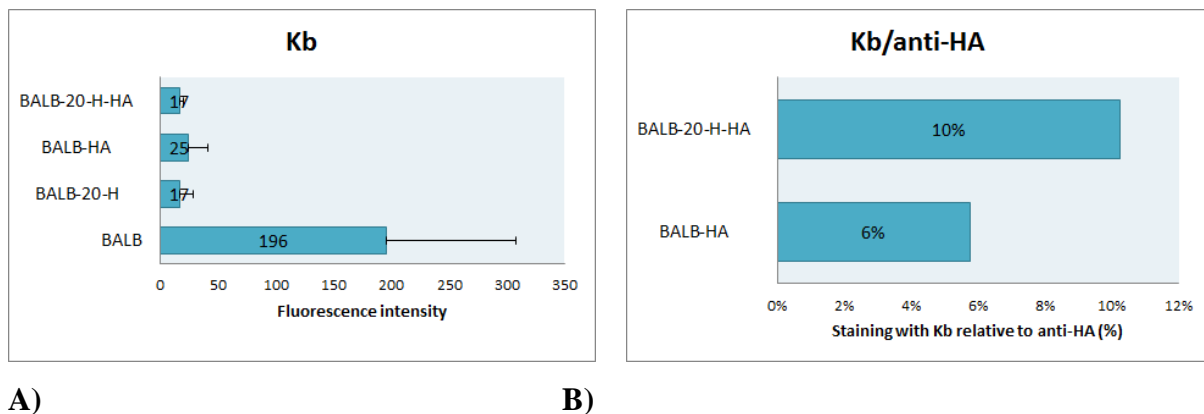


Figure 3.16. Staining of Ly49B mutants lacking 20 C-terminal amino acids with H-2K^b. YB2 cells transfected with the specified constructs were stained with PE-conjugated H-2K^b tetramers. **A)** The staining was repeated at least 3 times for each of the transfectants and the numbers in the centre of the blue bars represent average net median fluorescence values. Error bars (SD) are shown in black. **B)** The intensity of staining was expressed as a percentage of staining with H-2K^b tetramer (Figure 21 A) relative to staining with anti-HA (Figure 20 B). Kb - H-2K^b MHC class I tetramers, BALB- BALB/c Ly49B, BALB-20-HA- BALB/c Ly49B lacking C-terminal 20 amino acids and where the last amino acid was replaced with histidine, HA- hemagglutinin tag.

3.5.3. H-2D^b binding

Figure 3.17 A shows the results of H-2D^b binding expressed in net average median fluorescent values. Ly49B BALB did stain the most strongly, then Ly49B BALB-HA followed by Ly49B 20-H and Ly49B 20-H-HA, which stained at a similar level. Again the results cannot be directly compared, because of the uncertain expression levels of the mutant without HA-tag. Like in the case of H-2K^b, H-2D^b binding was reduced for HA-tagged Ly49B in comparison to the untagged construct. However, the effect was not as prominent (about three times reduction in comparison to eight times), suggesting that the C-terminus is not as important for H-2D^b binding as it is for H-2K^b.

Figure 3.17 B shows that HA-tagged Ly49B did stain at a similar level to its counterpart lacking the 20 C-terminal amino acids. It seems that this region does not significantly influence H-2D^b binding.

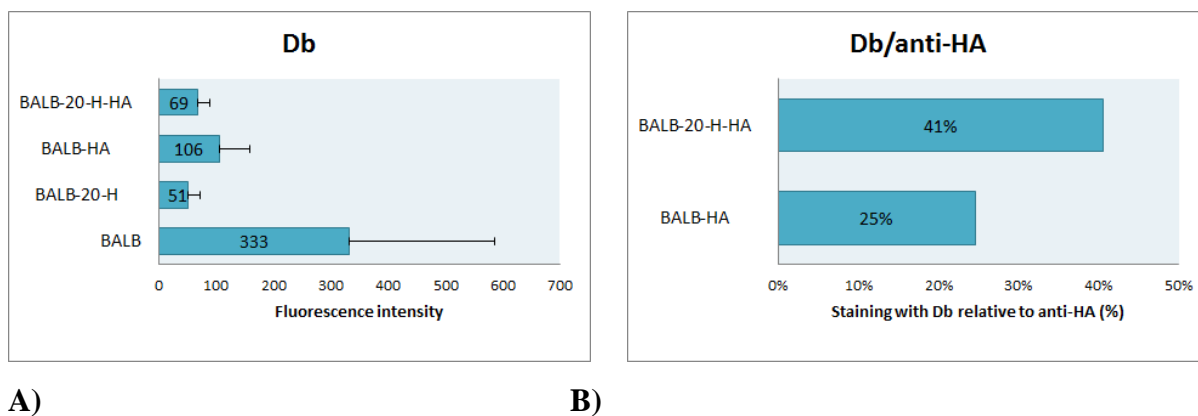


Figure 3.17. Staining of Ly49B mutants lacking 20 C-terminal amino acids with H-2D^b. YB2 cells transfected with the specified constructs were stained with PE-conjugated H-2D^b tetramers. **A)** The staining was repeated at least 3 times for each of the transfectants and the numbers in the centre of the blue bars represent average net median fluorescence values. Error bars (SD) are shown in black. **B)** The intensity of staining was expressed as a percentage of staining with H-2D^b tetramer (Figure 22 A) relative to staining with anti-HA (Figure 20 B). Db - H-2D^b MHC class I tetramers, BALB- BALB/c Ly49B, BALB-20-HA- BALB/c Ly49B lacking C-terminal 20 amino acids and where the last amino acid was replaced with histidine, HA- hemagglutinin tag.

3.5.4. H-2D^d binding

The results of H-2D^d binding are very similar to the results obtained for H-2K^b tetramer. **Figure 3.18 A** shows that the presence of HA-tag on the full length Ly49B construct did reduce H-2D^d binding in comparison to the untagged version by approximately eight times.

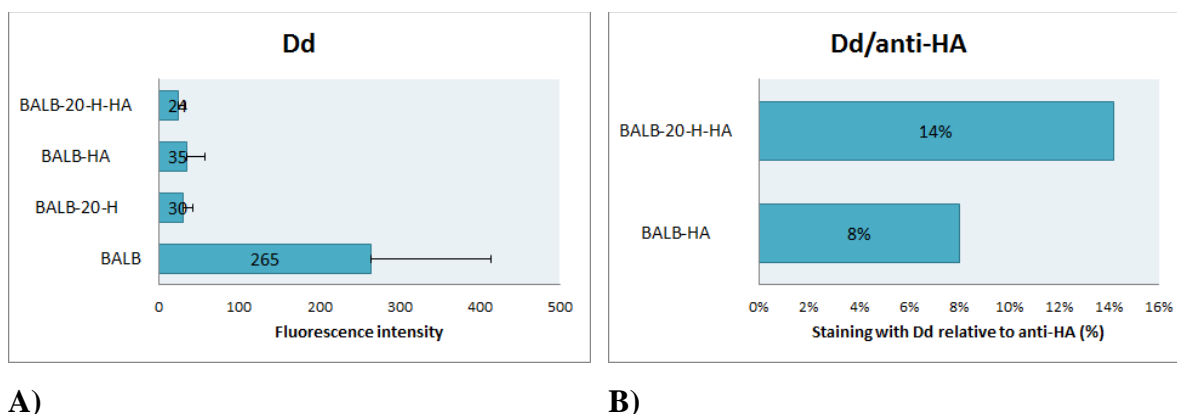


Figure 3.18. Staining of Ly49B mutants lacking 20 C-terminal amino acids with H-2D^d. YB2 cells transfected with the specified constructs were stained with PE-conjugated H-2D^d tetramers. **A)** The staining was repeated at least 3 times for each of the transfectants and the numbers in the centre of the blue bars represent average net median fluorescence values. Error bars (SD) are shown in black. **B)** The intensity of staining was expressed as a percentage of staining with H-2D^d tetramer (Figure 23 A) relative to staining with anti-HA (Figure 20 B). Dd - H-2D^d MHC class I tetramers, BALB- BALB/c Ly49B, BALB-20-HA- BALB/c Ly49B lacking C-terminal 20 amino acids and where the last amino acid was replaced with histidine, HA- hemagglutinin tag.

Association of H-2D^d with the Ly49B 20-H-HA was about 6 % stronger than with the HA-tagged full length construct (**Figure 3.18 B**). Analogous to the H-2K^b, binding of H-2D^d seem to be unaffected by the presence of the 20 or absence of C-terminal amino acids.

3.6. Establishing the role of Ly49B glycosylation in ligand and antibody binding

Both Ly49B forms contain four N-glycosylation motifs containing crucial asparagine residues at positions 94, 105, 114 and 177 (**Appendix I**). In order to assess their role in ligand and antibody binding, a library of Ly49B mutants was created (**Table 3.1**), in which the glycosylation motifs were disrupted by exchanging the asparagine residues for glutamine. The library included: four single Ly49B BALB/c mutants, targeting each of the four aforementioned residues; one double mutant, in which residues 105 and 114 were mutated; a HA-tagged Ly49B BALB/c mutant (BALB-ABCD-HA) with all four residues exchanged; and HA-tagged and untagged versions of Ly49B C57 with all four residues mutated. The mutants were expressed in YB2 cells and stained using three MHC class I tetramers (H-2K^b, H-2D^b and H-2D^d) and the 2G4 anti-Ly49B antibody. Cells expressing the relevant constructs were also stained with 1A1 anti-Ly49B and anti-HA antibodies. Raw staining data are compiled in **Appendix III**.

3.6.1. Antibody binding

In order to assess expression levels of the mutant receptors, 2G4 flow cytometric staining was performed. As shown on **Figure 3.19**, Ly49B BALB/c N114Q expressed at a similar level to wild type Ly49B BALB/c. Transfectants expressing the three remaining single glycosylation site mutants stained slightly weaker, indicating that expression levels were reduced in these strains. The double Ly49B BALB/c N105Q-N114Q mutant stained at 50 % of the level of WT Ly49B BALB/c. The BALB-ABCD-HA mutant stained about 8 times weaker than the HA-tagged WT Ly49B BALB/c. The greatest reduction in binding was observed for the two C57 mutants, both of which stained at roughly 2 % of the level of the WT proteins.

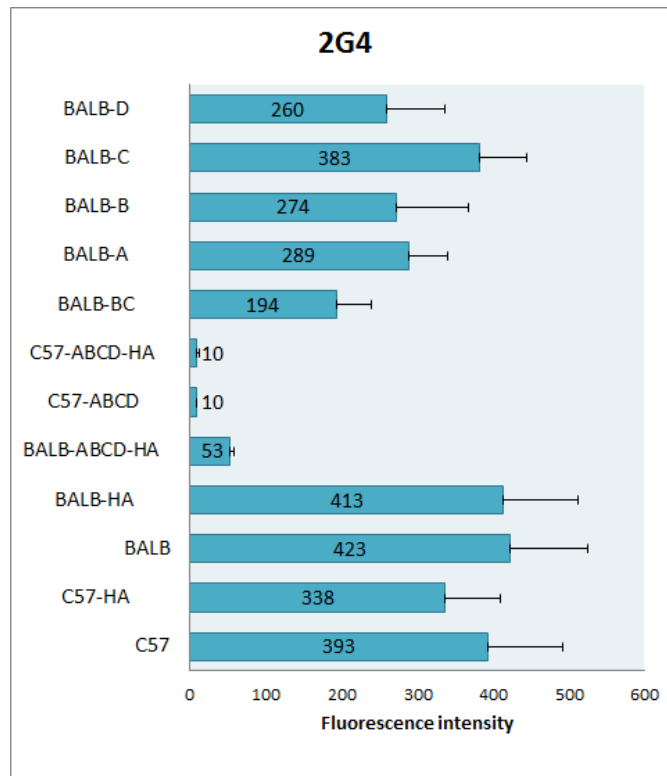


Figure 3.19. Staining of Ly49B glycosylation mutants with 2G4 anti-Ly49B. YB2 cells transfected with the specified constructs were stained with biotinylated 2G4 monoclonal rat anti-Ly49B antibody and then with AF647 conjugated streptavidin. The staining was repeated at least 3 times for each of the transfectants and the numbers in the centre of the blue bars represent average net median fluorescence values. Error bars (SD) are shown in black. The full names of the constructs are specified in Table 3.1.

To assess whether the observed reduction in staining was due to reduced expression levels or compromised binding by the 2G4 antibody, additional stainings were performed with 1A1 and anti-HA antibodies. 1A1 staining of the untagged C57 mutant transfectants was again roughly 2 % of the level of cells expressing the untagged wild type receptor, while the HA-tagged C57 mutant stained at roughly 1.5 % of the level of the equivalent wild type transfectants (**Figure 3.20 A**). The results of anti-HA staining of the HA-tagged Ly49B BALB/c and the BALB-ABCD-HA mutant were similar as for 2G4 staining, indicating a 10-fold decrease with the mutant transfectant compared to the wild type (**Figure 3.20 B**).



A)

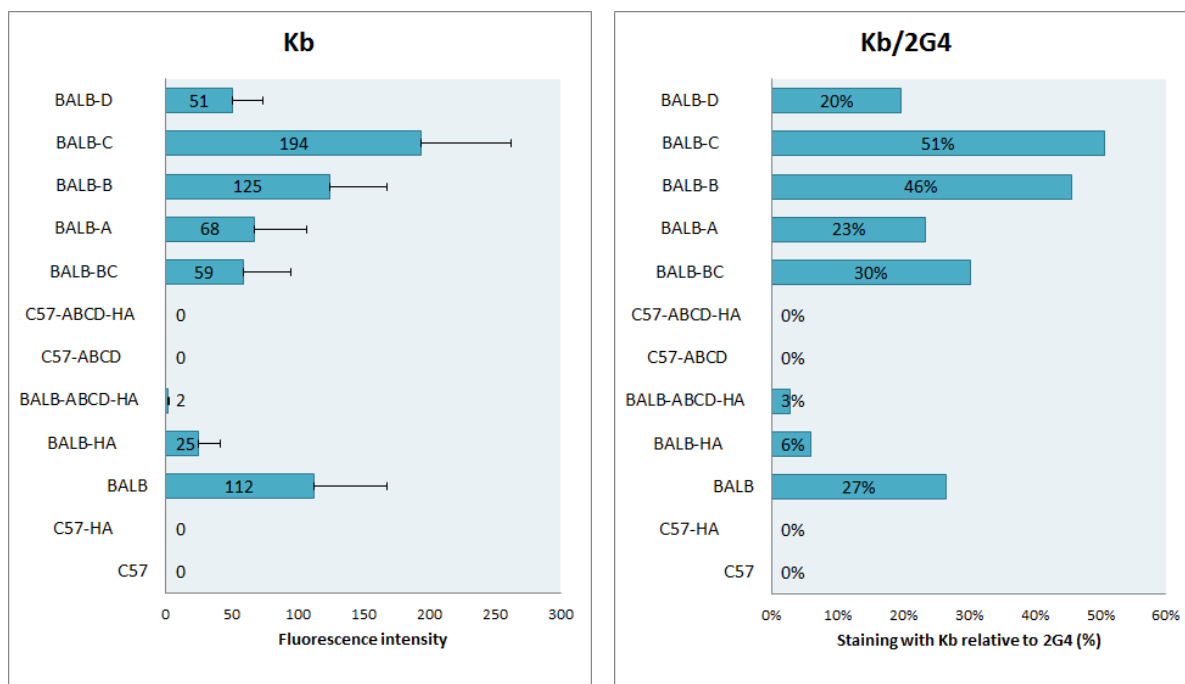
B)

Figure 3.20. Staining of Ly49B glycosylation mutants with 1A1 anti-Ly49B and anti-HA antibodies. YB2 cells transfected with the specified constructs were stained with A) 1A1 monoclonal rat anti-Ly49B antibody and then with a secondary AF647 conjugated chicken anti-rat antibody, or with B) biotinylated anti-HA antibody and then AF647 conjugated streptavidin. The staining was repeated at least 3 times for each of the transfectants and the numbers in the centre of the blue bars represent average net median fluorescence values. Error bars (SD) are shown in black. The full names of the constructs are specified in Table 3.1.

In general, staining with all three antibodies was much weaker for the multiple glycosylation mutants. It seems highly unlikely that binding of all three antibodies was equally affected by the removal of glycans, so the reduction in the levels of staining most likely reflects a reduction in expression levels of the mutant receptors. It seems that an absence of glycosylation results in impaired surface expression levels of Ly49B.

3.6.2. H-2K^b staining

Figure 3.21 shows the results of flow cytometric staining using the H-2K^b tetramer. None of the C57 WT or mutant transfectants stained positively, which is consistent with the finding that C57 Ly49B does not associate with H-2K^b. Interestingly, H-2K^b binding by the Ly49B BALB/c N105Q and Ly49B BALB/c N114Q single mutants was 19 % and 24 % stronger, respectively, than WT Ly49B BALB/c, relative to 2G4 staining. However, staining of the double mutant Ly49B BALB/c N105Q-N114Q was only 3 % stronger than WT Ly49B BALB/c, relative to 2G4 staining. These results suggest that glycosylation of arginine at Ly49B BALB/c positions 105 and 114 may limit H-2K^b binding.



A)

B)

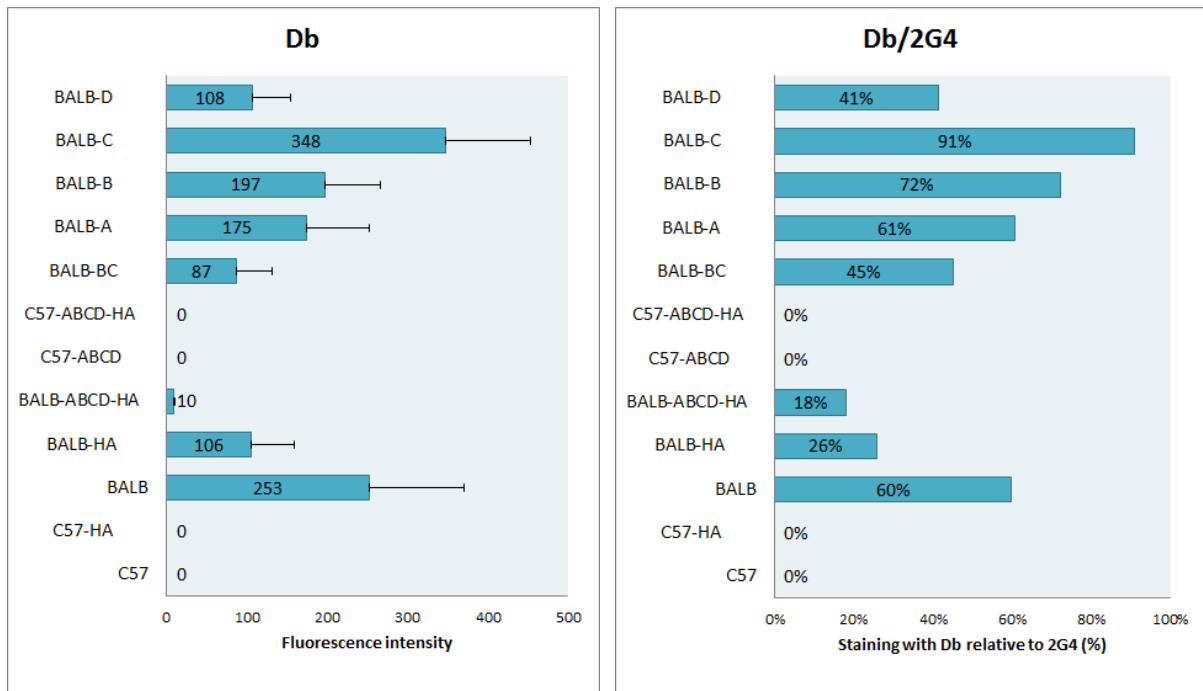
Figure 3.21. Staining of Ly49B glycosylation mutants with H-2K^b. YB2 cells transfected with the specified constructs were stained with PE-conjugated H-2K^b tetramers. **A)** The staining was repeated at least 3 times for each of the positive transfectants and at least 2 times for the negative transfectants. The numbers in the centre of the blue bars represent average net median fluorescence values. Error bars (SD) are shown in black. **B)** The intensity of staining was expressed as a percentage of staining with H-2K^b tetramer (Figure 26 A) relative to staining with 2G4 (Figure 24). The full names of the constructs are specified in Table 3.1. Kb – H-2K^b MHC class I tetramers.

The Ly49B BALB/c N94Q and Ly49B BALB/c N177Q single mutants stained at a comparable level to WT Ly49B BALB/c, suggesting that on their own glycans attached at positions 94 and 177 do not influence H-2K^b binding. The HA-tagged BALB/c mutant with all glycosylation sites removed stained at 50 % of the level of the WT Ly49B BALB-HA, indicating that glycosylation of all four sites may disrupt assembly of the H-2K^b binding motif.

3.6.3. H-2D^b staining

As shown on **Figure 3.22**, the wild type and mutant C57 transfectants did not exhibit H-2D^b binding. The Ly49B BALB/c N105Q and Ly49B BALB/c N114Q single mutant transfectants stained 12% and 31% more strongly, respectively, than wild type Ly49B BALB/c, relative to 2G4. Interestingly, the double Ly49B BALB/c N105Q-N114Q mutant stained 20 % weaker than wild type Ly49B BALB/c, in comparison to 2G4. This suggests that glycosylation of residues 105 and 114 may partially prevent H-2D^b from binding to WT

Ly49B BALB/c but that glycans at these positions may simultaneously be important for promoting correct folding of the protein and thus the integrity of the H-2D^b binding motif.



A)

B)

Figure 3.22. Staining of Ly49B glycosylation mutants with H-2D^b. YB2 cells transfected with the specified constructs were stained with PE-conjugated H-2K^b tetramers. **A)** The staining was repeated at least 3 times for each of the positive transfectants and at least 2 times for each of the negative transfectants. The numbers in the centre of the blue bars represent average net median fluorescence values. Error bars (SD) are shown in black. **B)** The intensity of staining was expressed as a percentage of staining with H-2D^b tetramer (Figure 27 A) relative to staining with 2G4 (Figure 24). The full names of the constructs are specified in Table 3.1. Dd - H-2D^b MHC class I tetramers.

Using the H-2D^b tetramer, the Ly49B BALB/c N94Q mutant stained with the same intensity as WT Ly49B-BALB/c, which implies that glycosylation of residue 94 does not have a direct effect on H-2D^b binding. Staining of the Ly49B BALB/c N177Q mutant was 19 % weaker than WT BALB/c, in comparison to 2G4, suggesting that the glycan, which attaches to residue 177, may promote slightly stronger binding of the H-2D^b ligand. The BALB-ABCD-HA mutant bound H-2D^b only marginally weaker than BALB-HA, which suggests that perhaps the positive effect on the binding exerted by the glycan attached at position 177 is equalised by the negative effect exerted by the glycans at positions 105 and 114.

3.6.4. H-2D^d binding

Figure 3.23 shows the compiled results of flow cytometric staining with the H-2D^d tetramer. As with the other two tetramers, no H-2D^d binding was detected for any of the C57 transfectants. Single mutations of N105Q and N114Q enhanced H-2D^d binding by approximately 20 % in comparison to the wild type Ly49B BALB/c while the double mutant with both of these residues mutated stained slightly weaker than the wild type BALB/c Ly49B transfectant. From these results one can infer that glycans at positions 105 and 114 may directly restrict H-2D^d binding, but simultaneously promote optimal folding of Ly49B and indirectly affect the conformation of the H-2D^d binding motif.

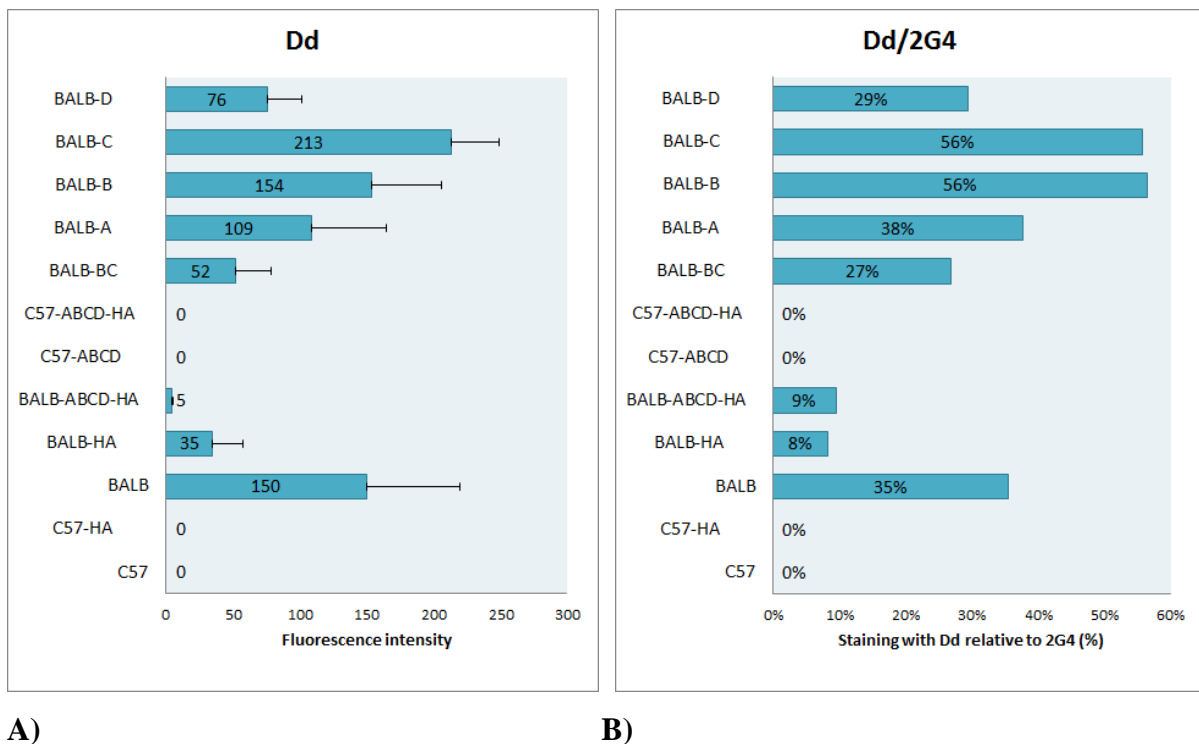


Figure 3.23. Staining of Ly49B glycosylation mutants with H-2D^d. YB2 cells transfected with the specified constructs were stained with PE-conjugated H-2D^d tetramers. **A)** The staining was repeated at least 3 times for each of the positive transfectants and at least 2 times for the negative transfectants. The numbers in the centre of the blue bars represent average net median fluorescence values. Error bars (SD) are shown in black. **B)** The intensity of staining was expressed as a percentage of staining with H-2D^d tetramer (Figure 28 A) relative to staining with 2G4 (Figure 24). The full names of the constructs are specified in Table 3.1. Dd –H-2D^d MHC class I tetramers.

As with the H-2K^b tetramer, H-2D^d binding was not directly affected by Ly49B glycosylation at positions 105 and 177, as shown in the results of staining using the Ly49B BALB/c N94Q and Ly49B BALB/c N177Q mutants, both of which associated with the H-2D^d tetramer to the same extent as the wild type Ly49B BALB/c receptor. Comparable results were also obtained for the BALB-ABCD-HA mutant, which stained with the same

intensity as the BALB-HA transfectant. Based on these findings, it can be concluded that glycosylation is not crucial for association of Ly49B BALB/c with the H-2D^d tetramer.

3.7. Mapping of Ly49A residues responsible for binding of MHC class I ligands and anti-Ly49A antibodies

The staining of chimeric Ly49B mutants pointed strongly to residues 166 and/or 167 playing a crucial role in binding of the monoclonal 1A1 antibody and MHC class I ligands. In the BALB/c form Ly49B residues 166 and 167 are tryptophan and asparagine, respectively. The tryptophan 166 is conserved amongst all other Ly49s with the exception of Ly49B C57, which contains leucine at the corresponding position (**Appendix I**). The asparagine residue of BALB/c located at position 167 is replaced by lysine in C57 Ly49B, by arginine in Ly49Q and serine in all other Ly49s (**Appendix I**).

In order to check whether introduction of the Ly49B C57 residues at positions corresponding to Ly49B 166 and 167 residues in Ly49A would affect binding of monoclonal antibodies and ligands, two HA-tagged mutants were created; Ly49A-W166L-HA and Ly49A-S167K-HA. Since the corresponding Ly49A residues to Ly49B residues 166 and 167 are at positions 160 and 161 respectively, ultimately, the first construct contained W to L mutation in Ly49A sequence at position 160 and the second one mutation S to K at position 161. The HA-tag was introduced to accurately determine expression levels of the mutant receptors. YB2 cells were transfected with the single residue mutants (and Ly49A-HA as a control), then stained with three monoclonal anti-Ly49A antibodies (JR9, A1 and YE1/48) and MHC class I tetramers (H-2K^b, H-2D^b and H-2D^d). The raw staining data are compiled in **Appendix IV**.

3.7.1. Antibody binding

Staining of mutant transfectants with the anti-HA antibody revealed that expression levels were similar for the control Ly49A-HA and Ly49A-S167K-HA transfectants, but about eight times lower for the Ly49A-W166L-HA transfectant (**Figure 3.24 A**). Staining using all three monoclonal anti-Ly49A antibodies revealed that binding of the Ly49A-W166L-HA mutant was completely abolished (**Figures 3.24 A, B and C**), suggesting that W166 is essential for maintaining the integrity of all three antibody epitopes and, most likely, for maintaining the tertiary structure of Ly49A.

All three monoclonal antibodies bound the Ly49A-S167K-HA mutant at a similar level to Ly49A-HA. These results indicate that the presence of lysine, rather than serine, at position 167 does not influence staining using monoclonal antibodies for Ly49A.

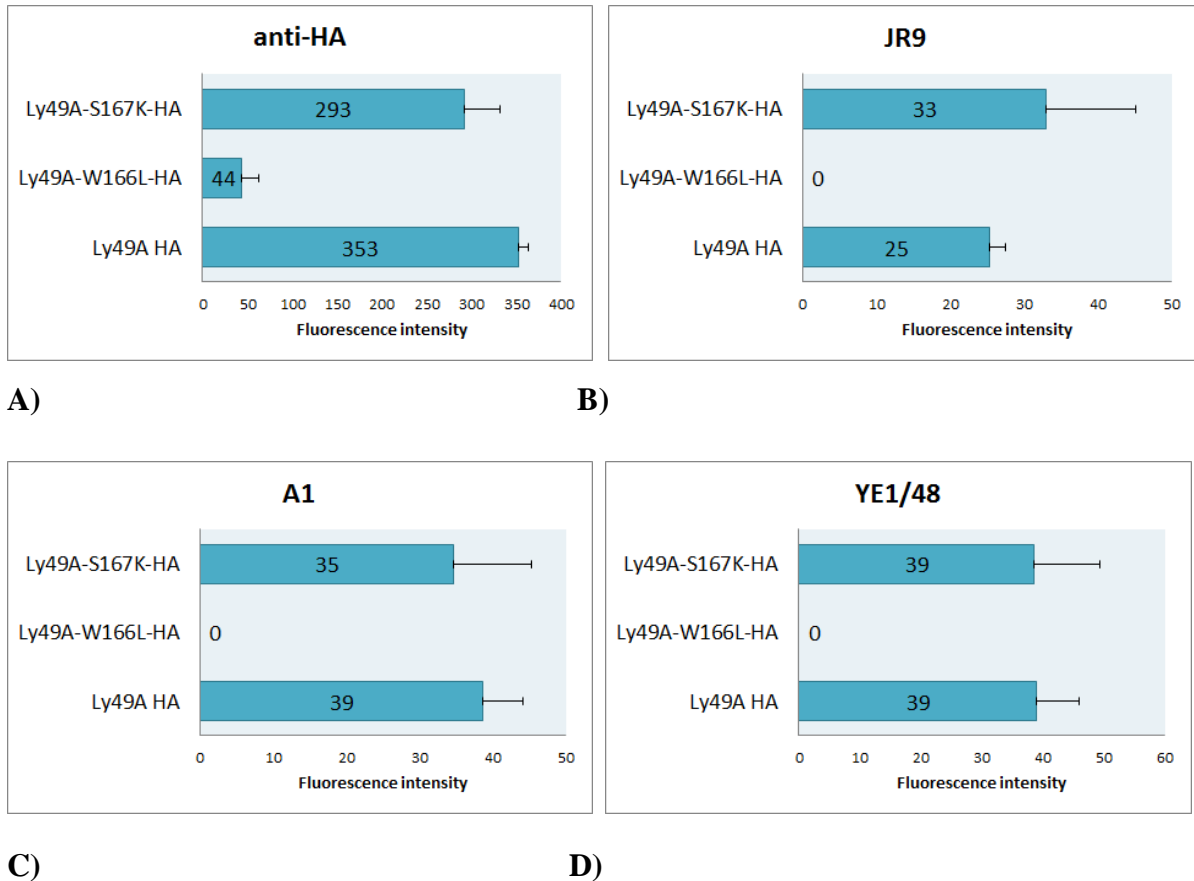


Figure 3.24. Staining of Ly49A-HA, Ly49A-S167K-HA and Ly49A-W166L-HA transfectants with anti-HA, JR9, IA and YE1-48 monoclonal antibodies. YB2 cells transfected with the specified constructs were stained with A) biotinylated anti-HA antibody and then AF647 conjugated streptavidin, or with B) JR9 anti-Ly49A antibody and then AF647 conjugated chicken anti-rat antibody, or with C) IA anti-Ly49A antibody and then AF647 conjugated chicken anti-rat antibody, or with D) YE1/48 anti-Ly49A antibody and then AF647 conjugated chicken anti-rat antibody. The staining was repeated at least 3 times for each of the positive transfectants and at least 2 times for the negative transfectants. The numbers in the centre of the blue bars represent average net median fluorescence values. Error bars (SD) are shown in black. HA- hemagglutinin tag.

3.7.2. Ligand binding

Figure 3.25 demonstrates that switching residue 166 from tryptophan, which is highly conserved amongst Ly49s, to leucine, as occurs in Ly49B C57, resulted in a complete loss of ligand binding. From these results one can conclude that tryptophan 166 is essential for ligand binding by Ly49A.

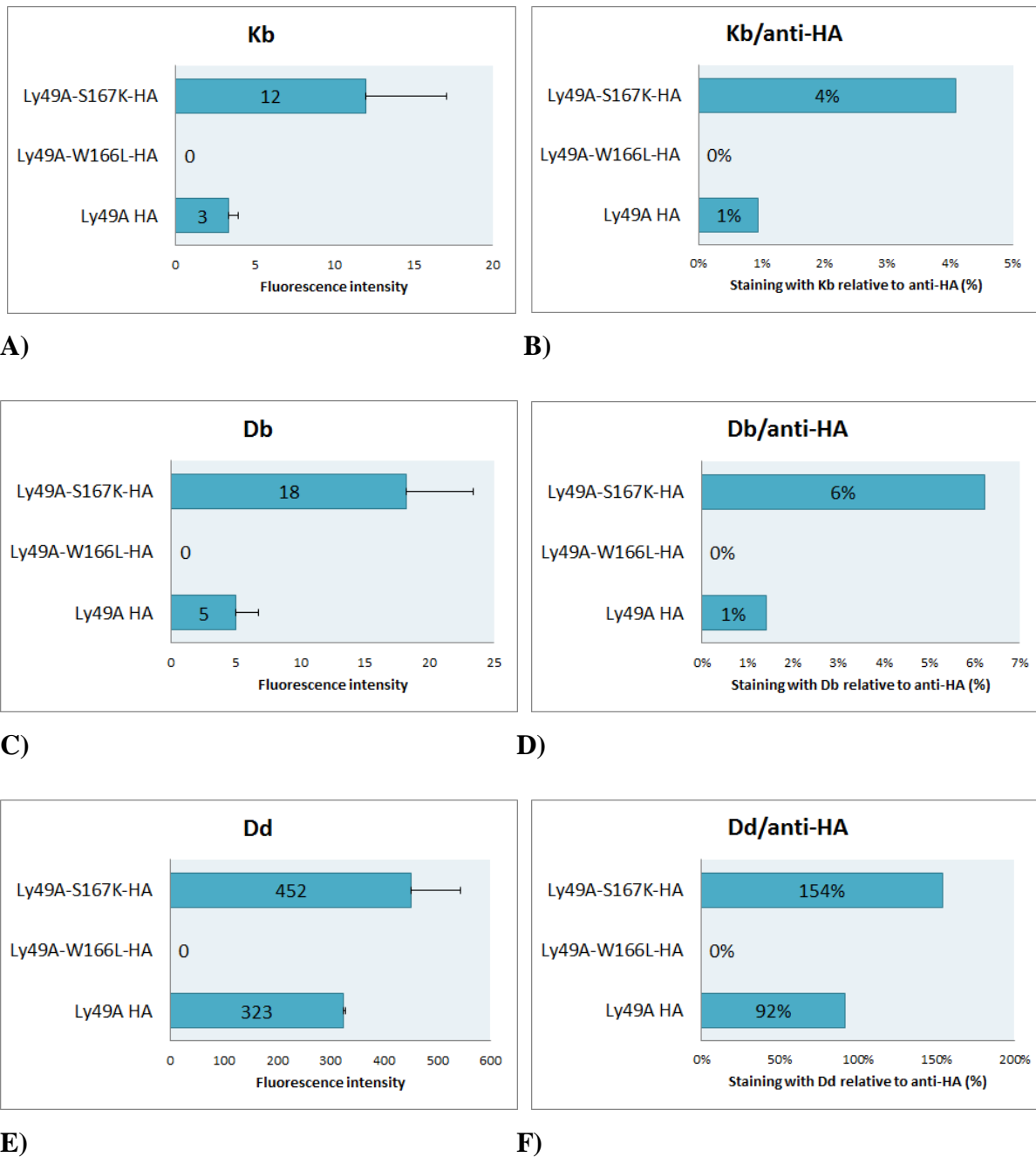


Figure 3.25. Staining of Ly49A-HA, Ly49A-S167K-HA and Ly49A-W166L-HA transfectants with H-2K^b, H-2D^b and H-2D^d tetramers. YB2 cells transfected with the specified constructs were stained with PE-conjugated H-2K^b (A and B), H-2D^b (C and D) and H-2D^d (E and F) tetramers. A, C and E) The staining was repeated at least 3 times for each of the positive transfectants and at least 2 times for the negative transfectants. The numbers in the centre of the blue bars represent average net median fluorescence values. Error bars (SD) are shown in black. B, D and F) The intensity of staining was expressed as a percentage of staining with the specified tetramer relative to staining with anti-HA (Figure 29 A). HA- hemagglutinin tag. Kb - H-2K^b MHC class I tetramers, Db – H-2D^b MHC class I tetramers, Dd - H-2D^d MHC class I tetramers

Surprisingly, the Ly49A-S167K-HA mutant showed a roughly four-fold increase in binding of the H-2K^b and H-2D^b ligands, compared to the Ly49A-HA receptor (Figures 3.25 B, D), and an increase of roughly 40 % with the H-2D^d ligand (Figure 3.25 F). These results

indicate that lysine at position 167 promotes ligand binding in Ly49A, despite the fact that it exerts an inhibitory effect in Ly49B BALB/c and completely abolishes binding in Ly49B C57.

3.8. Establishing the influence of the HA-tag on Ly49 ligand binding

During assessment of the role of the 20 additional C-terminal amino acids of BALB/c Ly49B (Section 3.5), control cells transfected with the HA-tagged wild type Ly49B BALB/c construct consistently stained more weakly with the H-2K^b, H-2D^b and H-2D^d tetramers than the equivalent untagged construct, even though expression levels, as assessed using the monoclonal 2G4 antibody, were very similar in the tagged and untagged transfectants. Moreover, it was hypothesised by Scarpellino *et al.* (2007) that the presence of C-terminal HA-tag, may have abolish the ability of Ly49B to bind its ligands.

In order to assess whether the presence of the HA-tag can affect the way recombinant Ly49B proteins fold and, ultimately, the strength of ligand binding, a series of chimera 7 mutants was expressed with and without the HA-tag and stained using all three tetramers. The results of these analyses were combined with results obtained in Section 3.5 (Figure 3.26).

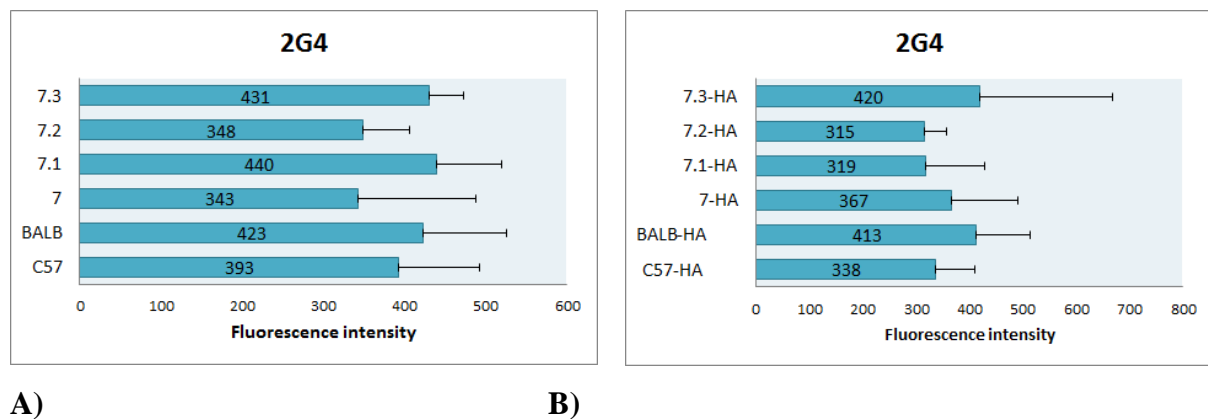


Figure 3.26. Staining of HA-tagged and untagged Ly49B mutants with 2G4 anti-Ly49B. YB2 cells transfected with the specified constructs were stained with biotinylated 2G4 monoclonal rat anti-Ly49B antibody and then with AF647 conjugated streptavidin. The staining was repeated at least 3 times for each of the transfectants and the numbers in the centre of the blue bars represent average net median fluorescence values. Error bars (SD) are shown in black. C57- C57 Ly49B, BALB- BALB/c Ly49B 7 – chimera 7, HA- hemagglutinin tag. A) untagged construct B) HA-tagged constructs.

2G4 staining levels were comparable between the HA-tagged and untagged mutants, indicating that expression levels of both sets of constructs were roughly the same. H-2K^b

staining was roughly 4.5 times stronger for the untagged wild type BALB/c Ly49B transfectant than for the equivalent tagged control (**Figure 3.27 C and D**). The results of H-2K^b staining for all of the other pairs of constructs indicated that HA-tagged and untagged chimeras stained at very similar levels to one another (**Figure 3.27 C and D**).

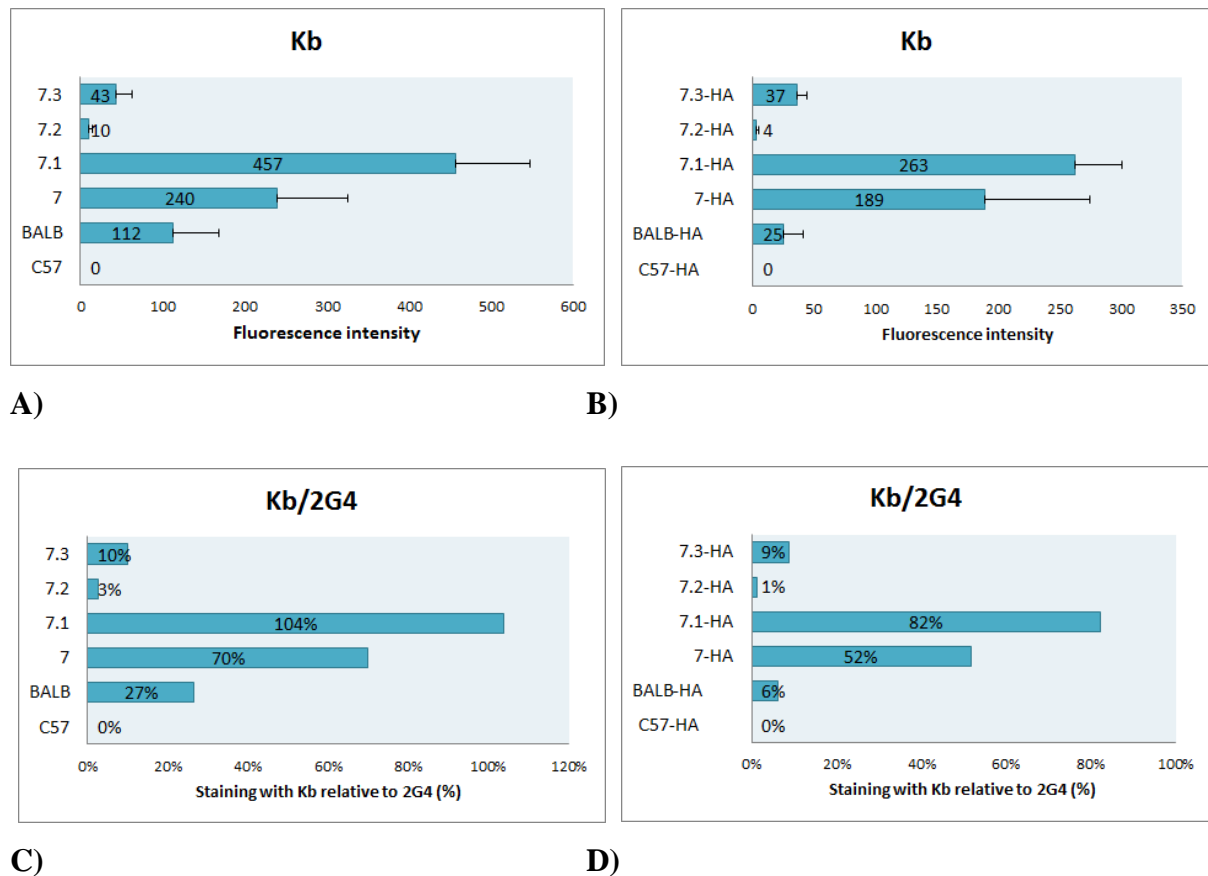


Figure 3.27. Staining of HA-tagged and untagged Ly49B mutants with H-2K^b. YB2 cells transfected with the specified constructs were stained with PE-conjugated H-2K^b tetramers. **A and B**) The staining was repeated at least 3 times for each of the positive transfectants and at least 2 times for each of the negative transfectants. The numbers in the centre of the blue bars represent average net median fluorescence values. Error bars (SD) are shown in black. **C and D**) The intensity of staining was expressed as a percentage of staining with H-2K^b tetramer (Figure 32 A or B) relative to staining with 2G4 (Figure 31 A and B). C57- C57 Ly49B, BALB-BALB/c Ly49B 7 – chimera 7, HA- hemagglutinin tag. Kb – H-2K^b MHC class I tetramers, **A and C**) untagged construct **B and D**) HA-tagged constructs

Results using the H-2D^b tetramer were very similar to those found using the H-2K^b tetramer. Staining was approximately 2 times stronger for the untagged wild type BALB/c Ly49B (**Figure 3.28 C and D**). The remaining pairs of constructs stained with a similar intensity to one another (**Figure 3.28 C and D**).

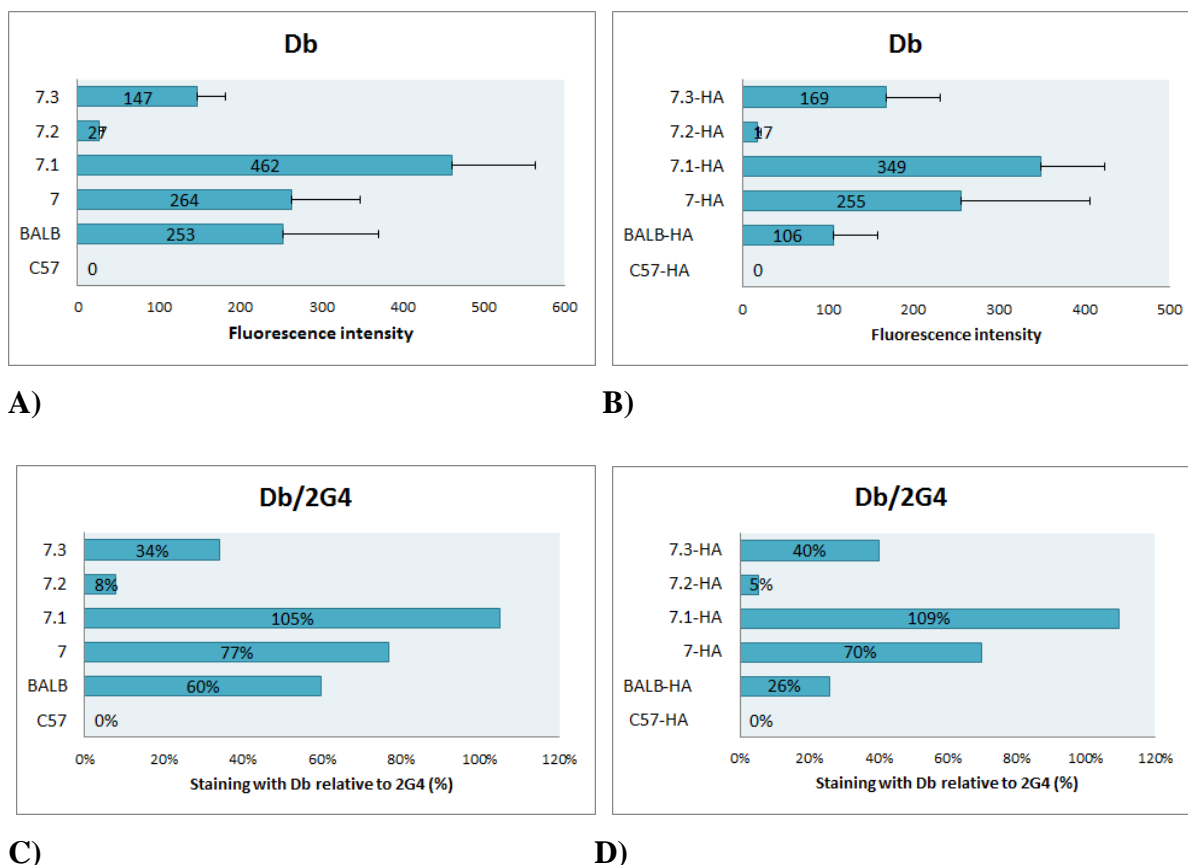
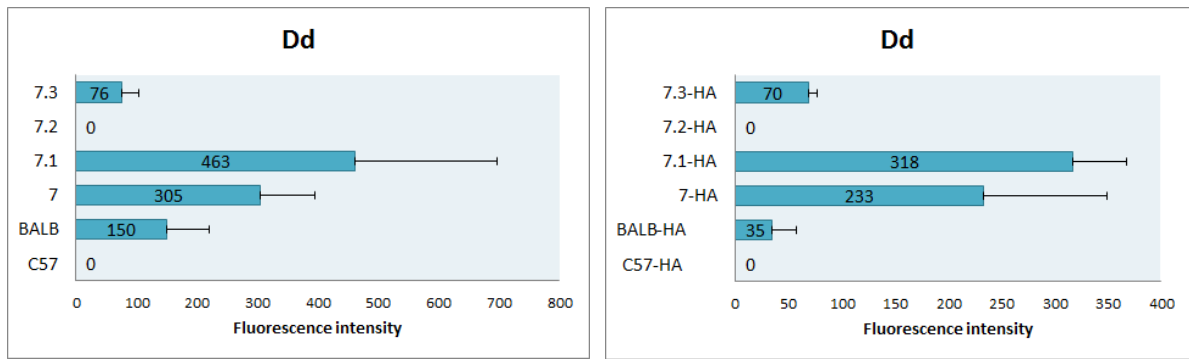


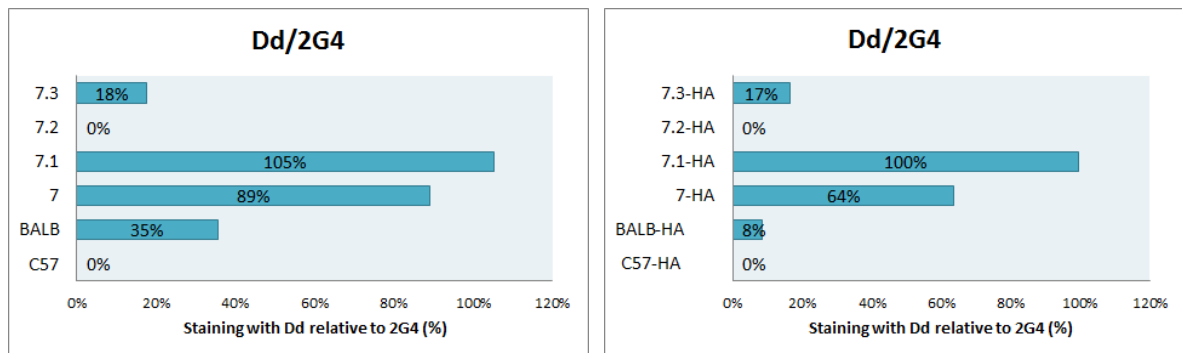
Figure 3.28. Staining of HA-tagged and untagged Ly49B mutants with H-2D^b. YB2 cells transfected with the specified constructs were stained with PE-conjugated H-2D^b tetramers. **A and B)** The staining was repeated at least 3 times for each of the positive transfectants and at least 2 times for each of the negative transfectants. The numbers in the centre of the blue bars represent average net median fluorescence values. Error bars (SD) are shown in black. **C and D)** The intensity of staining was expressed as a percentage of staining with H-2D^b tetramer (Figure 33 A or B) relative to staining with 2G4 (Figure 31 A and B). C57- C57 Ly49B, BALB-BALB/c Ly49B 7 – chimera 7, HA- hemagglutinin tag. Db – H-2D^b MHC class I tetramers. **A and C)** untagged construct **B and D)** HA-tagged constructs

The results of staining using the H-2D^d tetramer indicated that the untagged wild type BALB/c Ly49B receptor associated approximately 4 times more strongly than the tagged version (**Figure 3.29 C and D**). All other tagged versus untagged pairs stained with similar intensities to one another (**Figure 3.29 C and D**).



A)

B)

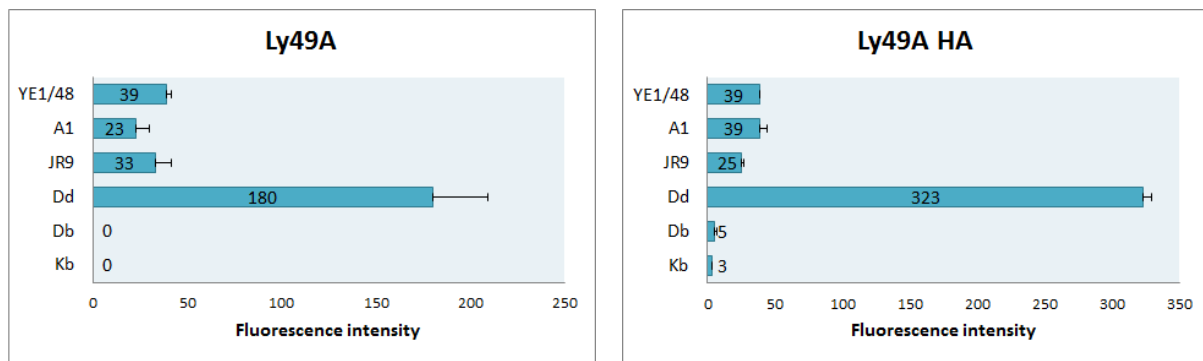


C)

D)

Figure 3.29. Staining of HA-tagged and untagged Ly49B mutants with H-2D^d. YB2 cells transfected with the specified constructs were stained with PE-conjugated H-2D^d tetramers. **A and B)** The staining was repeated at least 3 times for each of the positive transfectants and at least 2 times for each of the negative transfectants. The numbers in the centre of the blue bars represent average net median fluorescence values. Error bars (SD) are shown in black. **C and D)** The intensity of staining was expressed as a percentage of staining with H-2D^d tetramer (Figure 34 A or B) relative to staining with 2G4 (Figure 31 A and B). C57- C57 Ly49B, BALB-BALB/c Ly49B 7 – chimera 7, HA- hemagglutinin tag. Dd – H-2D^d MHC class I tetramers. **A and C)** untagged construct **B and D)** HA-tagged constructs

In order to further assess the influence of the HA-tag on ligand binding, staining of tagged and untagged Ly49A transfectants was performed using the H-2K^b, H-2D^b and H-2D^d tetramers and three monoclonal anti-Ly49A antibodies (**Figure 3.30**). Expression levels were comparable between HA-tagged and untagged Ly49A, as assessed by staining with all three monoclonal antibodies. Interestingly, the untagged Ly49A transfectant exhibited no staining with the H-2K^b and H-2D^b tetramers, and only a marginal association was detected with the tagged version. Staining using the H-2D^d tetramer indicated higher levels of association but the tagged Ly49A stained nearly twice as strongly as the untagged version.



A)

B)

Figure 3.30. Staining of HA-tagged and untagged Ly49A mutants with MHC class I tetramers and monoclonal anti-Ly49A antibodies. YB2 cells transfected with A) Ly49A or B) Ly49A-HA were stained with JR9, A1 and YE1/48 anti- Ly49A antibodies and then AF647 conjugated chicken anti-rat antibodies or with PE-conjugated H-2K^b, H-2D^b and H-2D^d tetramers. The staining was repeated at least 3 times for each of the positive transfectants and at least 2 times for the negative transfectants. The numbers in the centre of the blue bars represent average net median fluorescence values. Error bars (SD) are shown in black. HA- hemagglutinin tag. Kb - H-2K^b MHC class I tetramers , Db - H-2D^b MHC class I tetramers Dd – H-2D^d MHC class I tetramers

In summary, it seems that the presence of a C-terminal HA-tag can marginally influence the strength of ligand binding by Ly49 receptors. Interestingly, the tag had an inhibitory effect on Ly49B ligand binding, as opposed to the stimulatory effect observed with Ly49A. Most importantly, C-terminal HA-tag does not seem to have ability to completely abolish Ly49 ligand binding.

3.9. Analysis of residues influencing ligand and 1A1 binding by Ly49B

3.9.1. Analysis of the nature of Ly49B residues predicted to be responsible for binding of 1A1 and MHC class I ligands

Variable residues 166 and 167 were shown here to influence 1A1 anti-Ly49B binding and together with residue 251 also ligand binding. The first candidate amino acid: residue 166 lies within the C-type lectin receptor domain (CRD). In C57 residue 166 is leucine, whereas in BALB/c it is tryptophan and the BALB/c amino acid is conserved amongst other Ly49s; C57 L166 is very much the exception (**Appendix I**). Both tryptophan and leucine are hydrophobic and non-polar by nature (Berg and Stryer 2002). Leucine is an aliphatic amino acid and contains only carbon and hydrogen atoms in its side chain. Tryptophan on the other hand is indolic, comprising an additional nitrogen atom that forms part of a bicyclic aromatic group. Since this nitrogen atom can donate a hydrogen bond, tryptophan is often found on the surface of folded proteins in spite of its hydrophobic nature (Berg and Stryer 2002).

Switching tryptophan to leucine could potentially produce dramatic structural changes to the region in its immediate proximity, thereby enabling binding by the 1A1 antibody or disabling binding of the MHC ligands.

The second potential residue to be identified was 167, which is lysine in the C57 isoform and asparagine in the BALB/c form. All of the other Ly49s contain serine at this position, except for Ly49Q, which contains arginine (**Appendix I**). Lysine is a polar amino acid with a side chain made up of three hydrophobic methylene groups and a positively charged amino group at the end (Berg and Stryer 2002). It is often found buried inside folded proteins with only the amino group exposed to the solvent. Asparagine is also a polar amino acid; it is uncharged and is regularly found both on the inside and on the surface of proteins. Asparagine often provides a site for carbohydrate attachment, however, in the case of C57 Ly49B, N167 is not anticipated to be glycosylated since its neighbouring residues differ from the canonical N-glycosylation motif (i.e. NX[S/T], where N is asparagine, X is any amino acid except proline, S is serine and T is threonine (Berg and Stryer 2002). Substitution of N167 in BALB/c with the lysine residue of C57 could result in structural changes that would allow binding of 1A1 or abolish association with MHC class I ligands.

Perhaps the most dramatic variation amongst the three identified residues appears to occur at position 251. In C57 Ly49B the residue is arginine, whereas in the BALB/c isoform and all other Ly49s it is cysteine. In extracellular proteins cysteine is often involved in the formation of disulphide (S-S) bonds, in which pairs of cysteine residues are oxidised to form a covalent bond (Berg and Stryer 2002). Intracellular environments are largely reducing so proteins containing disulphide bridges are much rarer. Cysteine residues in a given disulphide bond may be separated by a considerable number of amino acids, with the formation of the bridge bringing together distant parts of the protein. Pairs of cysteine residues are therefore extremely important in determining the tertiary structure and stability of extracellular proteins. Cysteines that are not involved in S-S bonds often occur within active and binding sites. The intrinsic sulfhydryl side chain of cysteine is ideally suited for coordination of metals, for example in binding of zinc by zinc finger motifs (Berg and Stryer 2002). Cysteine also often acts as a nucleophile, i.e. as the reactive centre of an enzyme. In cysteine proteases, such as caspases or papains, cysteine acts as a key catalytic residue (Grzonka *et al.* 2001).

Substitution of cysteine to any other amino acid is therefore likely to cause significant changes in protein structure and/or function. However, the exchange in C57 Ly49B to arginine may be particularly significant due to its larger size and polarity. Arginine is considered somewhat amphipathic, because the end of its side chain is positively charged, while the rest of the side chain is hydrophobic (Berg and Stryer 2002). As such, the arginine backbone and the proximal part of its side chain are sometimes buried internally with the charged end exposed. However, most of the time arginines are found on the surface of proteins.

Further evidence for the significance of cysteine substitution to arginine at position 251 in C57 Ly49B stems from the fact that arginine residues form salt bridges with negatively charged amino acids. Salt bridges are classified as non-covalent interactions that rely on a combination of hydrogen bonds and electrostatic interactions (Berg and Stryer 2002). They play an important role in stabilizing entropically unfavourable protein conformations. The ability of arginine to form multiple hydrogen bonds means that it is also often found in protein active centres, for example in src 2 homology (SH2) domains (Yeo 2006). In light of the considerable differences between cysteine and arginine, it is unsurprising that substitution of cysteine at position 251 resulted in the loss of MHC class I ligand binding in Ly49B C57. Interestingly the results presented here did not reveal any effect on 1A1 binding.

3.9.2. In silico modelling of Ly49B residues proposed to be responsible for 1A1 antibody and ligand binding using published Ly49A dimer crystal structure and Ly49A-H-2D^d co-crystal structure

Crystallographic studies provide telling information concerning interacting residues of receptors and their ligands. Unfortunately, at present no crystal structure exists for Ly49B. However, assuming that Ly49B folds in a similar manner to other Ly49s, information can be inferred from available crystal structures of other Ly49s. **Figure 3.31** shows the dimeric crystal structure of the carbohydrate binding domains of the best characterised Ly49 receptor, Ly49A (Tormo *et al.* 1999). Residues corresponding to Ly49B residues 166, 167 and 251 have been highlighted in red, light blue and pink respectively.

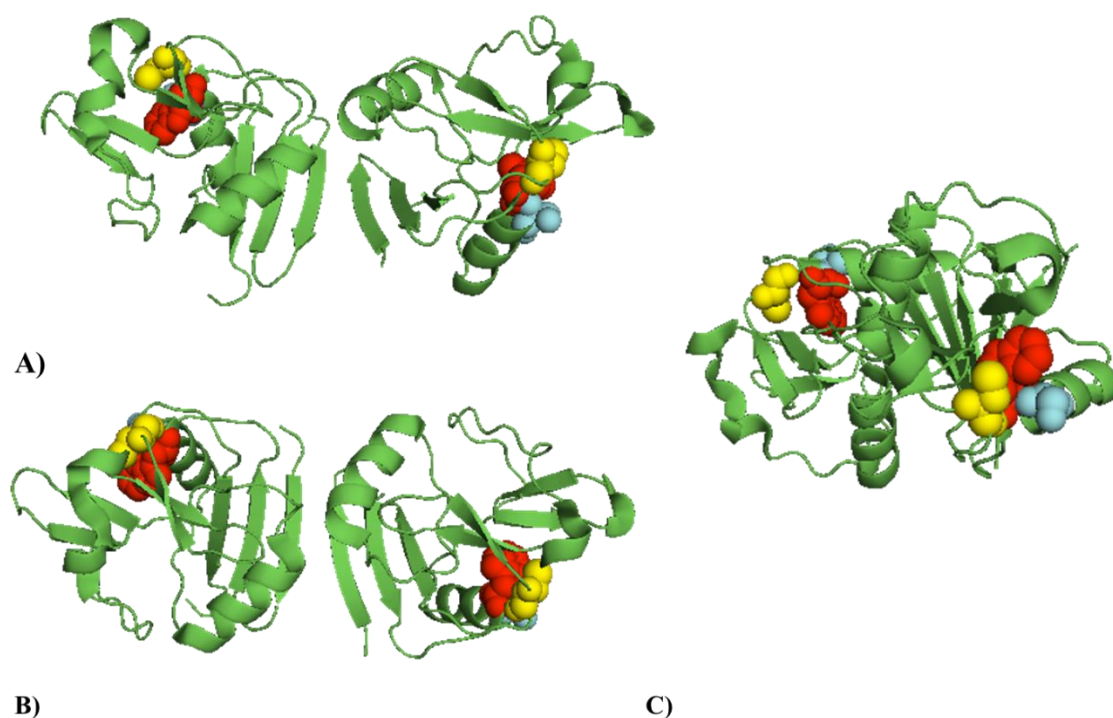


Figure 3.31. Crystal structure of the Ly49A homodimer. Green – Ly49A homodimer. Red – residue equivalent to Ly49B residue 166, light blue – residue equivalent to Ly49B residue 167. Yellow- residue equivalent to Ly49B residue 251. A) Front view. B) Top view. C) Side view. (PDB accession- 1QO3).

With reference to **Figure 3.31**, the first notable observation is that although in the linearised molecule residue 245 (equivalent to Ly49B residue 251) is situated 84 and 85 residues away from residues 160 and 161 (Ly49B residues 166 and 167), respectively, the residues are brought into close proximity to one another due to the manner in which Ly49A folds. It is therefore likely that together the three residues are capable of forming a functional ligand-binding motif. Moreover, the residues are located on the surface of the Ly49A dimer, which makes them easily accessible to both the ligands and monoclonal antibodies.

Figure 3.32 shows a co-crystal structure of Ly49A in complex with the MHC class I molecule H-2D^d (Tormo *et al.* 1999). The residues predicted to form hydrogen bonds and salt bridges between Ly49A and its ligand are highlighted in blue in the alignment in **Appendix I**. None of the Ly49A residues corresponding to residues 166, 167 and 251 in Ly49B were identified as being in direct contact between Ly49A and its ligand. However, Ly49A residues 160 and 161 (equivalent to Ly49B residues 166 and 167) form part of the $\alpha 1$ alpha helix (**Appendix I**), which comes into contact with the $\alpha 3$ helix of its putative MHC class I ligand. Ly49A residue 245 is one of five amino acids forming a loop between beta sheets 4 and 5 (**Appendix I**) and is the only one of these five predicted not to be in direct

contact with the ligand. The remaining four are thought to form interactions with residues in the $\alpha 3$ helix and $\beta 2$ microglobulin of H-2D^d. Since Ly49B residues 166, 167 and 251 are predicted to be in close proximity to residues that do appear to come into direct contact with the ligand, it is possible that their alteration may significantly influence the structure of adjacent regions and, consequently, the ability of the receptor to bind its ligand.

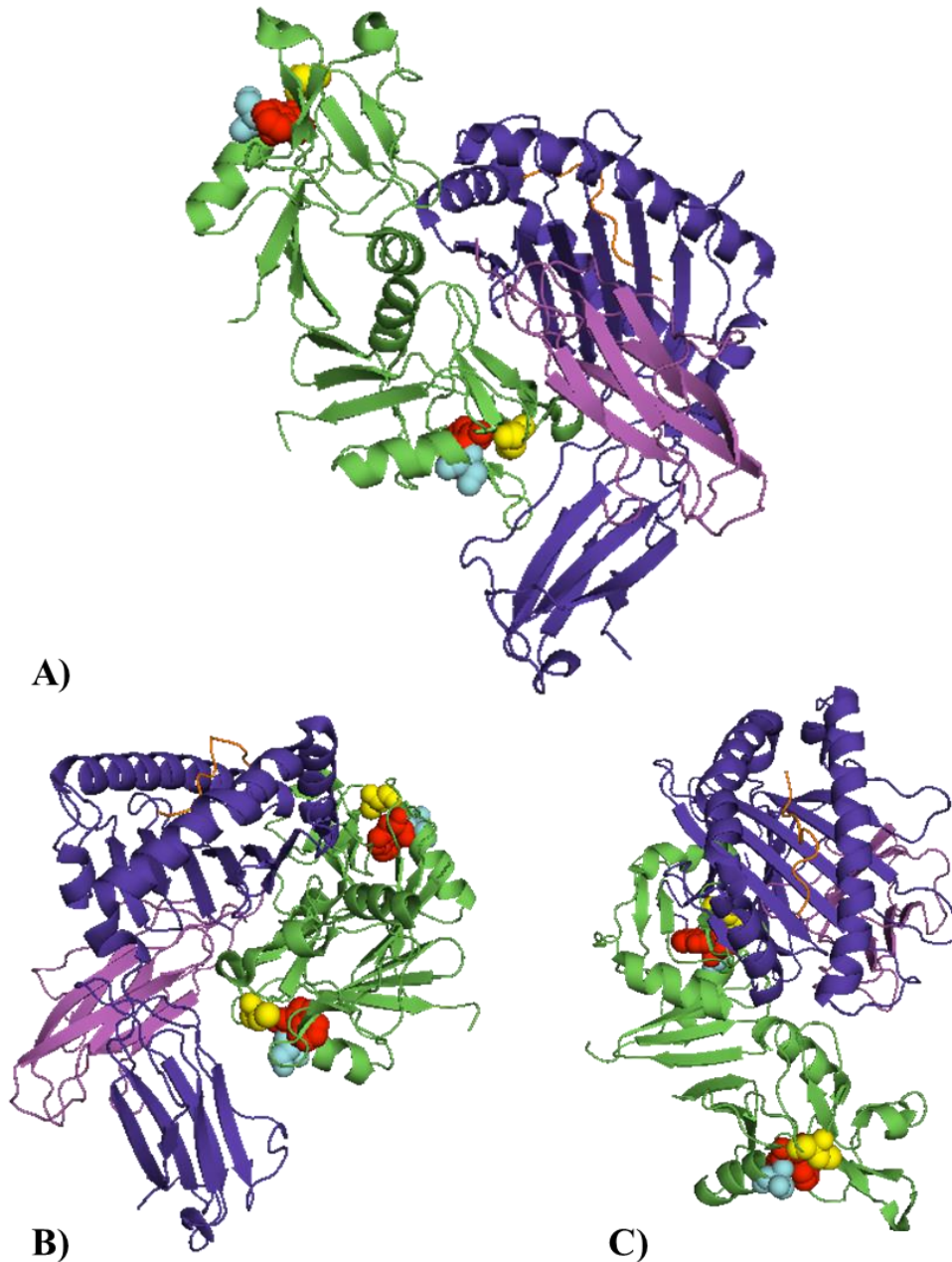


Figure 3.32. Crystal structures of Ly49A with the MHC class I ligand H-2D^d. Green – Ly49A. Blue – MHC class I H-2D^d α chain. Purple – MHC class I H-2D^d $\beta 2$ microglobulin. Orange – peptide in MHC class I binding groove. Red – residue equivalent to Ly49B residue 166, light blue – residue equivalent to Ly49B residue 167. Yellow- residue equivalent to Ly49B residue 251. A), B) and C) – Ly49A-MHC class I H-2D^d complex shown from different angles. (PDB accession- 1QO3).

In order to visualise the effects of the differing side chains of residues 166, 167 and 251 in C57 and BALB/c isoforms of Ly49B, appropriate mutations were introduced to the Ly49A amino acid sequence and simulated using PyMOL. In **Figure 3.33** the tryptophan residue at position 166, which is present in Ly49A (position 160) and BALB/c Ly49B, has been replaced with leucine, as occurs in C57 Ly49B. **Figures 3.34** and **3.35** show substitution of serine 161 in Ly49A with lysine and asparagine, as occur in C57 and BALB/c Ly49B (at position 167), respectively. **Figure 3.36** shows the result of substituting cysteine 245, which is present in Ly49A and BALB/c Ly49B (at position 251) with arginine, as occurs in C57 Ly49B.

Due to the technical limitations of PyMOL, *in silico* point mutations do not produce steric changes, which could occur in the surrounding region. However, from the generated images it is clear that the C57 and BALB/c Ly49B-specific residues at positions 166, 167 and 251 have significant structural differences from one another and from the corresponding Ly49A residues. Considering also the differing biochemical properties of these residues described in **Section 3.9.1**, it seems likely that the selected mutations could have a profound effect on ligand and antibody binding.

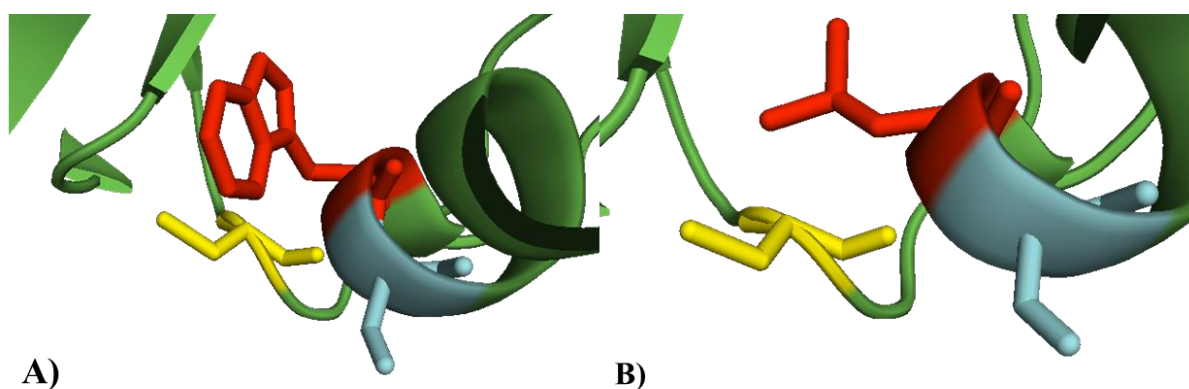


Figure 3.33. *In silico* introduction of a W166L mutation to the Ly49A receptor. **A)** Ly49A with wild type residues at positions equivalent to Ly49B 166 (tryptophan), 167 (serine) and 251 (cysteine). **B)** Ly49A with tryptophan 166 substituted with the equivalent C57 Ly49B residue, leucine. Colour coding as in Figure 3.31. (PDB accession- 1QO3).

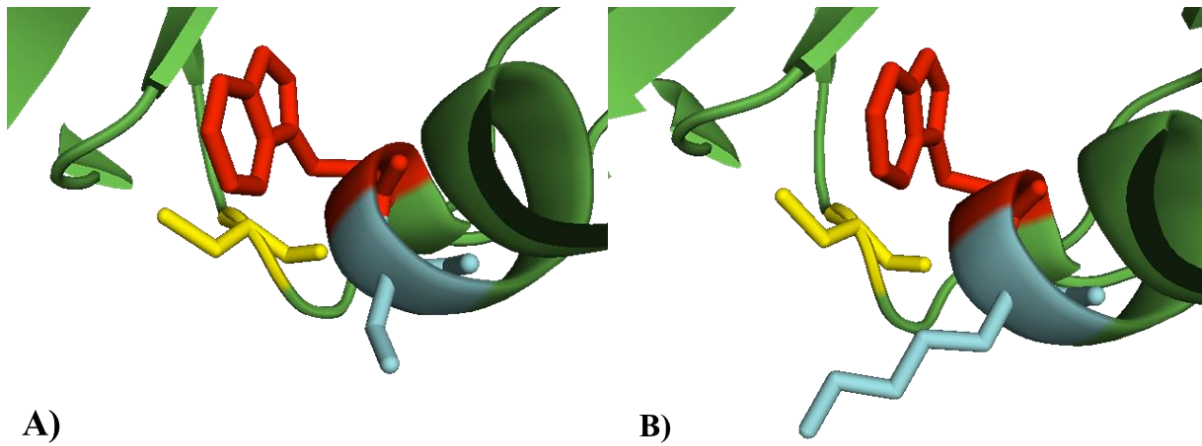


Figure 3.34. *In silico* introduction of an S167K mutation to the Ly49A receptor. **A)** Ly49A with wild type residues at positions equivalent to Ly49B 166 (tryptophan), 167 (serine) and 251 (cysteine). **B)** Ly49A with serine 167 substituted with the equivalent C57 Ly49B residue, lysine. Colour coding as in Figure 3.31

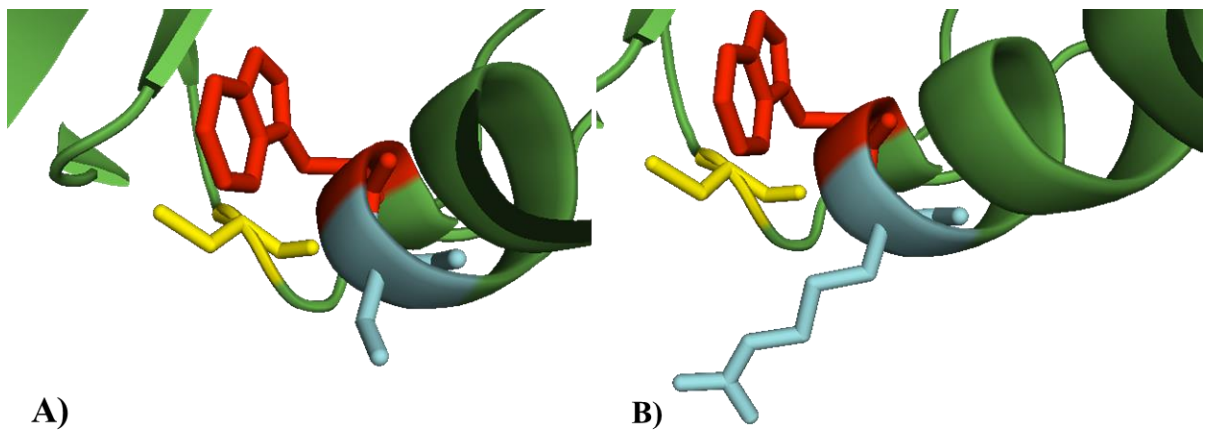


Figure 3.35. *In silico* introduction of an S167N mutation to the Ly49A receptor. **A)** Ly49A with wild type residues at positions equivalent to Ly49B 166 (tryptophan), 167 (serine) and 251 (cysteine). **B)** Ly49A with residue 167 substituted with the equivalent BALB/c Ly49B residue, asparagine. Colour coding as in Figure 3.31.

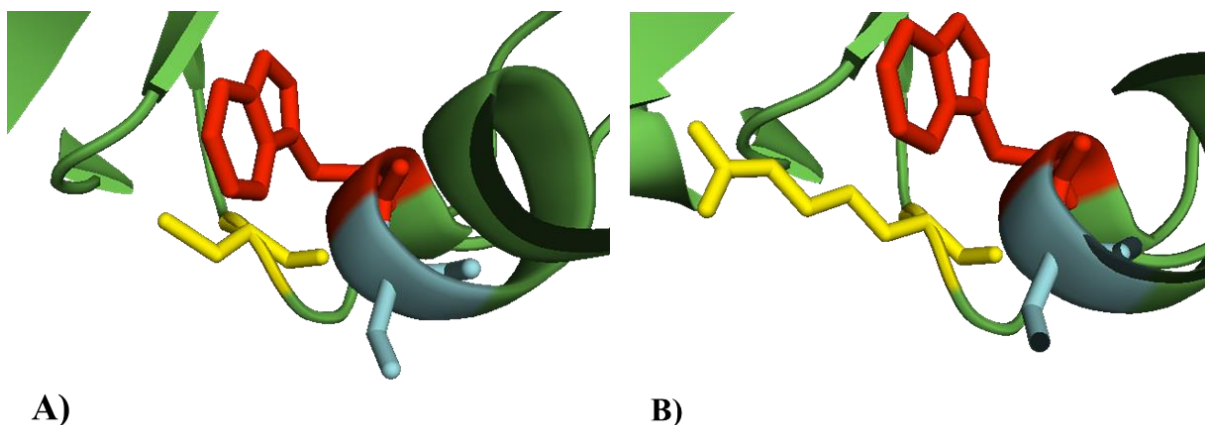


Figure 3.36. *In silico* introduction of a C251R mutation to the Ly49A receptor. **A)** Ly49A with wild type residues at positions equivalent to Ly49B 166 (tryptophan), 167 (serine) and 251 (cysteine). **B)** Ly49A with residue 251 substituted with the equivalent C57 Ly49B residue, arginine. Colour coding as in Figure 3.31.

It is worth noting that the simulations shown in **Figures 3.31-3.36** do not necessarily reflect the tertiary structure of Ly49B, as the models were based on Ly49A. Ly49B shares only ~50 % homology with other Ly49s and contains an additional 20 amino acids at its C-terminus (**Appendix I**). It is therefore possible that three residues of interest occupy slightly different positions in Ly49B. Furthermore, the crystals of Ly49A were generated using recombinant protein, which was expressed in *E. coli* and may therefore not have undergone the post-translational modifications that would have occurred endogenously. Ly49 receptors are indeed predicted to be glycosylated and the presence of glycans could well affect the manner in which they fold. As such, the interaction sites identified in the crystal structures presented here may be slightly different under native conditions.

3.10. Summary

The study presented here has shown that residues 166 and 167 are critical for the selective binding of the 1A1 antibody to C57 Ly49B and, together with residue 251, play a crucial role in the binding of MHC class I tetramers to BALB/c Ly49B. The residues corresponding to Ly49B 166 and 167 residues are also critical for the structure and function of Ly49A. It seems that, in general, Ly49 receptor residues, which do not come into direct contact with the ligand, can significantly but indirectly influence the strength of binding. The H-2D^b MHC molecule seems to be the primary ligand for Ly49B due to the fact that binding is robustly retained upon introduction of alternative residues or manipulation of the glycosylation sites, in comparison to H-2K^b and H-2D^d. C-terminal HA-tag may slightly affect the strength of ligand binding by Ly49 receptors but it does not have an ability to completely abolish it. Finally, Ly49B ligand binding appears to undergo fine tuning by receptor glycosylation.

Chapter 4. Molecular nature of Ly49B

4.1. Introduction

This chapter outlines Western blotting and immunoprecipitation experiments that were carried out to investigate the molecular nature of Ly49B and other related receptors. The majority of experiments were performed on whole cell lysates of transfectants expressing a specific receptor. The cell extracts were subjected to SDS-PAGE analysis, transferred to nitrocellulose membrane and blotted with a monoclonal antibody directed against either the receptor of interest or a tag co-expressed with the receptor. The membranes were then blotted with a horseradish peroxidase (HRPO)-conjugated secondary antibody directed against the primary antibody. The proteins of interest were visualised using enhanced chemiluminescence (ECL) reagent, which contains luminol - a compound that is converted to 3-aminophthalate upon interaction with HRPO, causing emission of light at 428nm. This emission can then be captured on photographic film.

In some of the experiments, the receptor of interest was immunoprecipitated from whole cell lysates using appropriate antibodies prior to Western blotting. This approach, combined with surface labeling of the receptor, is a traditional staple for investigating the molecular nature of other Ly49 receptors. In such experiments the surface label is used to detect the receptor of interest. One drawback of this approach is that *only* the surface-associated proteins are subjected to analysis. Here, an alternative method was used, which enables visualization of both the intracellular and surface-associated receptor populations. This approach has provided new insights into the biochemistry of Ly49 receptors.

4.2. Ly49B exists in multiple molecular forms in cells transfected with Ly49B constructs.

C57 Ly49B-FLAG transfected RNK cells were lysed in buffer containing a non-ionic surfactant; Triton X-100. The reduced (R) lysate samples containing β -mercaptoethanol (2ME), which reduces disulphide bonds and untreated non-reduced (NR) samples were analysed by 15 % SDS-PAGE, then blotted to nitrocellulose membranes. The membranes were incubated with N1027 rabbit anti-FLAG followed by N1197 HRPO bovine anti-rabbit immunoglobulin (Ig) and imaged with ECL reagent. Two bands running at ~110 kDa and 150 kDa were revealed in the NR lysate and a single band running at ~47 kDa in the R material (**Figure 4.1A**). The bands were not detected in lysates of RNK cells transfected with Ly49H or in lysates of YB2 cells transfected with Ly49B bearing a C-terminal HA tag, suggesting that the bands detected in RNK-C57 Ly49B-FLAG lysates represented Ly49B. Comparison of reduced and non-reduced RNK-C57 Ly49B-FLAG samples suggests that Ly49B may form dimers or multimers or that it may associate with other proteins through the formation of disulphide bonds. The 47 kDa band is likely to represent the Ly49B monomer.

Prolonged film exposure revealed a faint band of ~47 kDa in the NR material, suggesting that free monomeric Ly49B may be present at low concentrations in living cells (**Figure 4.1B**). Alternatively, the appearance of the 47 kDa band in the non-reduced samples may have resulted from 2ME spillover from the reduced samples. Prolonged film exposure revealed an additional faint band of ~55 kDa in the reduced material, as well as faint bands in the upper part of the gel, which may represent residual non-reduced material.

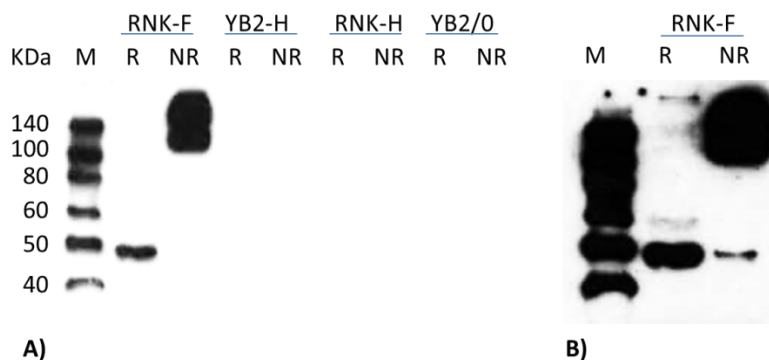


Figure 4.1. N1027 anti-FLAG blot of NR and R lysates of RNK-Ly49B-FLAG, YB2-Ly49B-HA, RNK-Ly49H and YB2/0 cells. Cell lysates at 1.5×10^4 cells/ μ l were run for 1 h at 200 V on a 15 % SDS-PAGE gel and transferred for 1 h at 200 V onto nitrocellulose membrane using wet transfer method. The membranes were incubated for 1 h at 4 °C with N1027 anti-FLAG antibody at 1/ 5000 dilution and then for 1 h at room temperature with N1197 HRPO bovine anti-rabbit Ig at 1/2500 dilution. Images were developed using Pierce ECL reagent for 1 min (A) and 2 min (B). M= molecular weight marker, NR= non-reduced, R=reduced, RNK-F=RNK-C57 Ly49B-FLAG, YB2-H=YB2-Ly49H, RNK-H=RNK-Ly49H.

To further investigate the specificity of the Ly49B detection in Western blots, membranes with the same cell lysates were incubated with N1028 rabbit anti-HA followed by N1197 HRPO bovine anti-rabbit Ig. As shown in **Figure 4.2**, untreated NR lysate from YB2-C57 Ly49B-HA cells revealed 2 bands running at ~110 kDa and ~150 kDa, which were at equivalent positions to the bands detected with anti-FLAG antibody. Moreover, in the NR samples another band was detected at ~47 kDa, which suggested again, that free monomeric Ly49B may be present in the living cells. R material contained a strong band at ~47 kDa with much fainter bands running at ~110 kDa and ~150 kDa, representing most likely residual non reduced Ly49B material. Lysates of RNK-Ly49B-FLAG cells or other control cells did not contain band at ~110 kDa or ~47 kDa, although some weak non-specific bands were present at ~80 kDa and ~150 kDa.

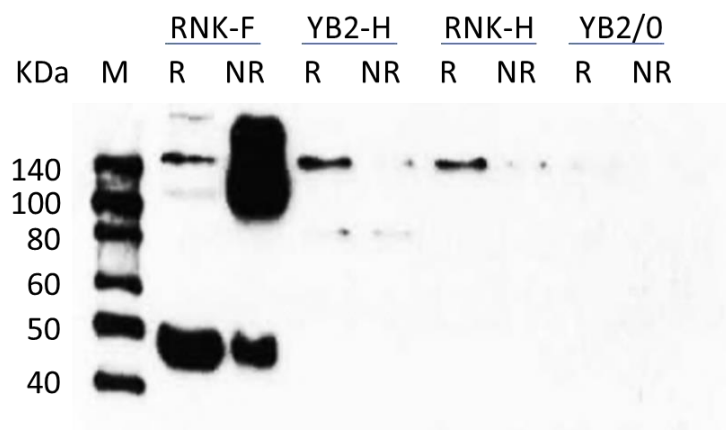


Figure 4.2. N1028 anti-HA blot of NR and R lysates of YB2-Ly49B-HA, RNK-Ly49B-FLAG, RNK-Ly49H and YB2/0 cells. Cell lysates at 1.5×10^4 cells/ μ l were run for 1 h at 200 V on a 15 % SDS-PAGE gel and transferred for 1 h at 200 V onto nitrocellulose membrane using wet transfer method. The membranes were incubated for 1 h at 4 °C with N1028 anti-HA antibody at 1/5000 dilution and then for 1h at room temperature with N1197 HRPO bovine anti-rabbit Ig at 1/2500 dilution. Image was developed using Pierce ECL reagent for 2 min. M= molecular weight marker, NR=non-reduced, R=reduced, RNK-F=RNK-C57 Ly49B-FLAG, YB2-H=YB2-Ly49H, RNK-H=RNK-Ly49H.

Interestingly, monoclonal antibody (mAb) 2G4 anti-Ly49B, turned out to be effective in detection of bands on the membranes containing lysates of Ly49B-transfected YB2 cells that were not observed in lysates of control cells (**Figure 4.3**). This was slightly surprising because mAbs such as 2G4, which have been raised by using live cells for immunisation, are thought to be poor reagents for Western blotting. Such mAbs usually recognize discontinuous, conformational epitopes on properly folded proteins, which can be disrupted following denaturation in SDS. One possible explanation is that following protein transfer to the nitrocellulose membrane, SDS was washed off and Ly49B spontaneously refolded to the

extent that enabled reconstitution of the 2G4 epitope. Another possibility is that the 2G4 epitope is, in fact, continuous epitope and its conformation was not drastically affected following Ly49B denaturation.

The banding pattern detected by 2G4 was clearly specific for Ly49B-transfected cell lysates but it was also strikingly different from that revealed with the N1027 rabbit anti-FLAG and N1028 rabbit anti-HA polyclonal Abs. The NR lysates contained bands at positions equivalent to previously detected bands at ~110 kDa, ~150 kDa, but also additionally contained a band at ~200 kDa, whereas the R lysates contained not only previously detected band at ~47 kDa but also a clear band at ~55 kDa. Importantly, HA-tagged BALB/c Ly49B or untagged BALB/c Ly49B extracts samples contained virtually identical multiple banding pattern, indicating that the observed heterogeneity of Ly49B is not an artefact caused by the presence of a C-terminal tag. It is worth noting that the bands observed in lysates of cells transfected with HA-tagged Ly49B ran at a slightly higher position than bands from cells transfected with untagged Ly49B. This further confirms that the multiple bands detected in this experiment undeniably represented multiple molecular forms of Ly49B and no other protein. Some non-specific bands were revealed in all of the tested samples at ~75 kDa. YB2/0 samples contained an additional non-specific band at ~80 kDa.

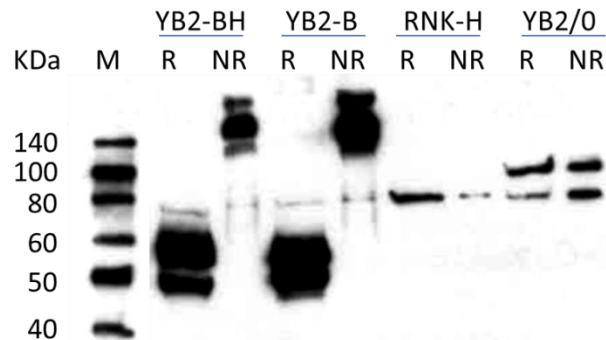


Figure 4.3. N1184 2G4 anti-Ly49B blot of NR and R lysates of YB2-Ly49B, YB2-Ly49B-HA, RNK-Ly49H and YB2/0 cells. Cell lysates at 1.5×10^4 cells/ μ l were run for 1 h at 200 V on a 15 % SDS-PAGE gel and transferred for 1 h at 200 V onto nitrocellulose membrane using wet transfer method. Membranes were incubated overnight at 4 °C with N1184 rat 2G4 anti-Ly49B antibody at 1/2500 dilution and then 1 h at room temperature with N1196 HRPO goat anti-mouse IgG and N1194 HRPO anti-biotin antibody both at 1/5000 dilution. Image was developed using Pierce ECL reagent for 1 min. M=molecular weight marker, NR=non-reduced, R=reduced, YB2-BH = C57 YB2-Ly49B-HA, YB2-B =YB2-BALB/c Ly49B, RNK-H=RNK-Ly49H.

Further investigation revealed that another monoclonal anti-Ly49B antibody, referred to as 1A1, which is specific for C57 Ly49B, was also able to detect Ly49B multiple banding

pattern in Western blot experiments (**Figure 4.4**). The pattern was essentially identical to that detected by 2G4, but as expected from the specificity of 1A1, the bands were only observed in extracts of cells transfected with the C57 Ly49B and not the BALB/c Ly49B. Blotting with 2G4 on the other hand, revealed bands in lysates of YB2 cells that have been transfected with the Ly49B BALB/c or Ly49B BALB/c-HA. The specificity of 1A1 for C57 Ly49B samples *only*, further confirmed that the multiple bands detected in Western blot experiments with various antibodies described above represented Ly49B. Notably, the relative intensity of the multiple bands in BALB/c samples was different to the relative intensity of bands in C57 sample. In particular, in the non-reduced Ly49B BALB/c samples a band at ~150 kDa was much stronger than the bands at ~110 and ~200 kDa. However, longer exposure to ECL revealed that those bands undoubtedly were present in the lysate. Moreover, the mobility of C57-HA bands was slightly retarded in comparison to BALB/c-HA bands and untagged Ly49B ran faster than the HA-tagged version.

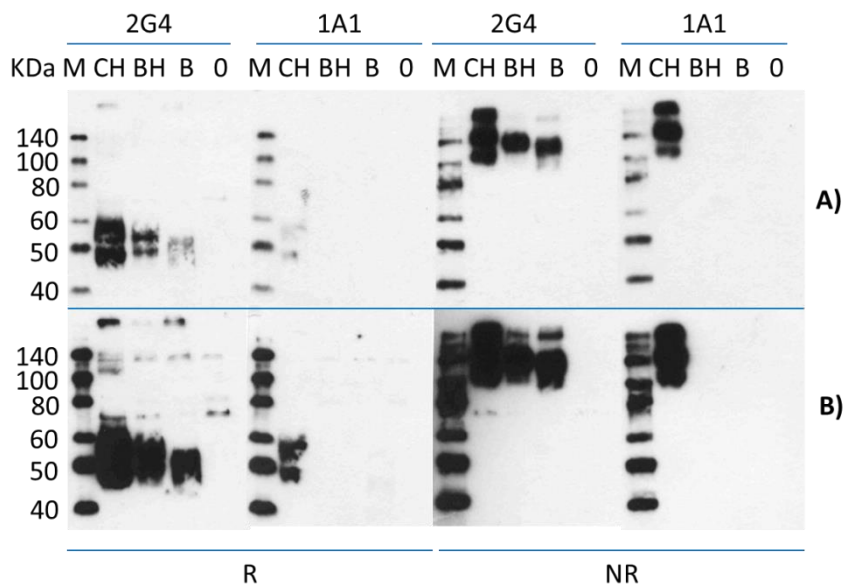


Figure 4.4. N1176 biotin 2G4 anti-Ly49B and N869 biotin 1A1 anti-Ly49B blot of R and NR YB2-C57 Ly49B-HA cell lysates. YB2-C57 Ly49B-HA, YB2-BALB/c Ly49B-HA, YB2-BALB/c Ly49B and YB2/0 lysates at 2000 cells/ μ l were run for 1.5 h at 200 V on 15 % SDS-PAGE gels and transferred for 1.5 h at 200 V onto a nitrocellulose membranes by wet transfer method. Membranes were incubated overnight at 4 °C with N1176 biotin 2G4 anti-Ly49B antibody at 1/2500 dilution or N869 biotin 1A1 anti-Ly49B antibody at 1/1000 dilution, followed by incubation at room temperature for 1 h with N1194 HRPO anti-biotin antibody at 1/2500 dilution. Images were developed using Thermo ECL reagent for 20 sec (A) and 5 min (B). M= molecular weight marker, NR=non-reduced, R=reduced, CH=YB2-C57 Ly49B-HA, BH=YB2-BALB/c Ly49B-HA, B=YB2-BALB/c Ly49B, O=YB2/0, 2G4=N1176 biotin 2G4, 1A1=N869 biotin 1A1.

To extend investigation of the specificity of antibodies for Ly49B in Western blot experiments, a blot was performed on YB2-C57 Ly49B-HA lysates with 2G4, 1A1 and three different anti-HA antibodies in parallel to one another (**Figure 4.5**). In the case of reduced

samples, N1028 anti-HA antibody recognised only one band at ~47 kDa. 2G4 recognised two bands at ~47 kDa and ~55 kDa. Results with the 1A1 antibody were comparable to those obtained for 2G4 antibody. The N1229 biotin anti-HA antibody bound preferentially to a band of ~47 kDa and N1222 biotin anti-HA to a band of ~55 kDa but they also associated to a lesser extent with bands at ~55 kDa and ~47 kDa, respectively. In the case of non-reduced samples, a band of ~200 kDa was revealed by all of the antibodies. N1028 anti-HA additionally recognised a band at ~110 kDa. A weak band at a similar position was also present in samples incubated with 2G4, N1222 anti-HA and N1229 anti-HA antibodies. All of the antibodies, with the exception of N1028 anti-HA, bound to a protein of ~150 kDa. These results indicate that different antibodies can bind different molecular weight forms of Ly49B with varying strength.

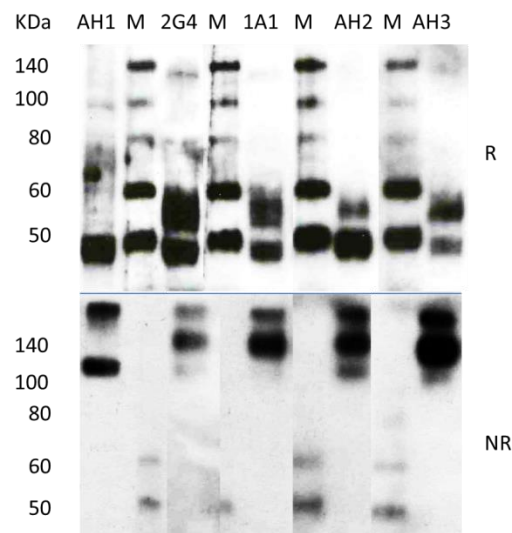


Figure 4.5. N1028 anti-HA, N1176 biotin 2G4 anti-Ly49B, N869 biotin 1A1 anti-Ly49B, N1229 biotin rabbit anti-HA and N1222 biotin 16.43 anti-HA blot of R and NR YB2-C57 Ly49B-HA lysates. Cell lysates at 2000 cells/ μ l were run for 1.5 h at 200 V on 15 % SDS-PAGE gels and transferred for 1.5 h at 200 V onto nitrocellulose membranes using wet transfer method. Membranes were incubated overnight at 4 °C with N1028 anti-HA antibody at 1/100,000 dilution, N1176 biotin 2G4 rat anti-Ly49B antibody at 1/5000 dilution, N869 biotin rat 1A1 anti-Ly49B at 1/1000 diltion, N1229 biotin anti-HA antibody at 1/100,000 and N1222 biotin 16.43 anti-HA antibody at 1/100,000 dilution. Membranes treated with biotinylated antibodies were incubated for 1 h at room temperature with N1192 HRPO SA at 1/5000 dilution and N1028 treated membrane with N1197 HRPO bovine anti-rabbit IgG at and N1194 HRPO anti-biotin antibody at 1/5000 dilution. Images were developed using Pierce ECL reagent for 20 sec. M=molecular weight marker, R=reduced, NR=non-reduced, AH1=N1028 anti-HA, 2G4=N1176 biotin 2G4, 1A1=N869 biotin 1A1, AH2=N1229 biotin rabbit anti-HA, AH3=N1222 biotin 16.43 anti-HA.

To further explore this notion, YB2-C57 Ly49B-HA cells were lysed and subjected to immunoprecipitation with sepharose protein G beads coated with N1028 anti-HA, N1109 16.43 anti-HA or N1184 2G4 anti-Ly49B antibodies. **Figure 4.6** shows an N1176 biotin 2G4

anti-Ly49B blot of protein samples immunoprecipitated from the lysates using sepharose protein G beads. The samples on the left side of the panel contain proteins that did not associate with the beads and remained in the supernatant (SN) following immunoprecipitation. The samples on the right hand side of the panel contain proteins eluted from the beads (labelled BEADS).

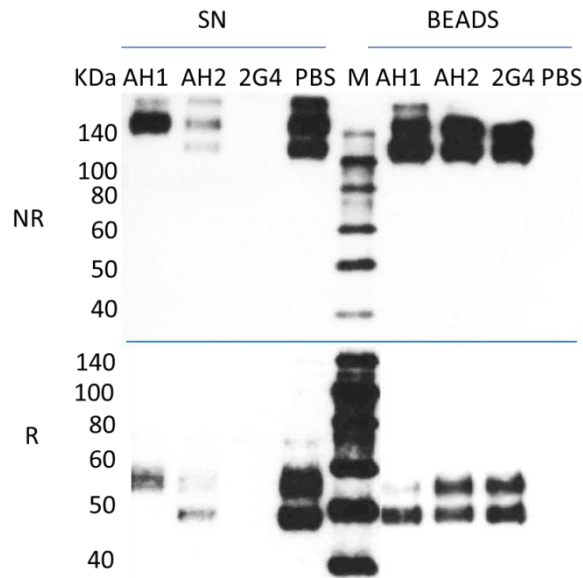


Figure 4.6. N1176 biotin 2G4 anti-Ly49B blot of NR and R C57 Ly49B-HA immunoprecipitated from YB2-C57 Ly49B-HA lysates using sepharose protein G beads coated with a range of antibodies. Samples of immunoprecipitated material prepared from YB2-C57 Ly49B-HA lysates at 2000 cells/ μ l using sepharose protein G beads coated with N1028 anti-HA, N1109 16.43 anti-HA, N1184 2G4 rat anti-Ly49B or PBS were run for 1.5 h at 200 V on 15 % SDS-PAGE gels and transferred for 1.5 h at 200 V onto nitrocellulose membranes by wet transfer. Membranes were incubated overnight at 4 °C with N1176 biotin 2G4 rat anti-Ly49B antibody at 1/2500 dilution followed by N1194 HRPO anti-biotin antibody at 1/2500 dilution for 1h at room temperature. Images were developed using Pierce ECL reagent for 1 min. M= molecular weight marker, NR=non-reduced, R=reduced, AH1=N1028 anti-HA, AH2=N1129 16.43 anti-HA 2G4=N1184 2G4 rat anti-Ly49B, SN=supernatant collected following incubation of the antibody covered protein G beads with YB2- C57 Ly49B-HA lysates, prior to elution. BEADS =material eluted from the antibody covered protein G beads.

SN samples collected following incubation with PBS control beads contained three non-reduced (~110 kDa, ~150 kDa and ~200 kDa) and two reduced (~47 kDa and ~55 kDa) bands similar to those previously observed in blots with the 2G4 antibody, suggesting that all of the molecular weight forms of Ly49B were present in the lysate. The corresponding BEADS samples indicated that there was no non-specific Ly49B binding. N1028 anti-HA antibody-coated beads associated with proteins, which appeared on the blot as a predominant band of ~47 kDa in the reduced samples or three bands at ~110 kDa, ~150 kDa and ~200 kDa in the non-reduced samples. The corresponding SN samples contained a reduced band at ~55

kDa and a predominant, non-reduced band at 150 kDa, as well as a weaker non-reduced band at ~200 kDa. These results suggest that the N1028 antibody preferentially binds the lowest molecular weight form of Ly49B.

Beads coated with the second anti-HA antibody, N1109 16.43 anti-HA or with the 2G4 antibody, were able to associate with all molecular forms of Ly49B since virtually all bands were absent in the SN samples. The corresponding eluted samples contained all of the expected putative Ly49B bands, except the band at 200 kDa. The observation that this band was not retained in the SN samples and the fact that it did not appear in the eluted samples suggests that the highest molecular form of Ly49B observed in Western blot experiments may not be stable.

These extensive analyses provide evidence to support the theory that Ly49B exists in transfected cells in multiple molecular weight forms, which are capable of associating with each other or other proteins through the formation of disulphide bonds. Various antibodies specific for C-terminal tags, as well as monoclonal anti-Ly49B antibodies are able to recognise different molecular weight forms of Ly49B on Western blots with varying strength.

4.3. Multiple molecular weight forms of Ly49B represent differentially glycosylated Ly49B

Ly49B contains four predicted N-glycosylation motifs (**Appendix I**), with asparagines that could potentially serve as glycan attachment points at positions 94, 105, 114 and 177. YB2/0 cells were transfected with C57 Ly49B-HA, BALB/c Ly49B and BALB/c Ly49B-HA mutants, in which all four of the N-glycosylation motifs were disrupted by mutating the critical asparagine residues (N) to glutamines (Q). **Figure 4.7** shows an N1176 biotin 2G4 blot of lysed NR and R Ly49B glycosylation mutants and wild type controls. YB2-BALBc Ly49B-HA and YB2-C57 Ly49B-HA lysate samples contained bands at positions analogous to those previously identified as Ly49B. YB2-C57 Ly49B lysate sample contained bands at positions marginally smaller than those identified for the YB2-C57 Ly49B-HA counterpart. As with BALB/c constructs (**Figures 4.3 and 4.4**), the presence of the C-terminal HA tag appeared to slightly reduce the speed of migration of C57 Ly49B on SDS-PAGE gels.

Interestingly, all of the glycosylation mutant variants of Ly49B appeared as one predominant band of ~80 kDa for the non-reduced samples and ~34 kDa for the reduced samples. Both HA-tagged forms ran marginally higher than the untagged variants. A weak

200 kDa band could be observed in all of the non-reduced glycosylation mutant samples and in reduced YB2-Ly49B C57 and YB2-C57 Ly49B-HA glycosylation mutant samples.

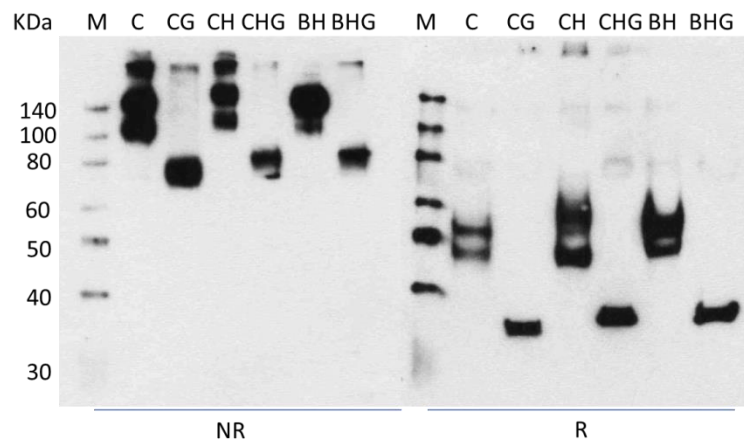


Figure 4.7. N1176 biotin 2G4 anti-Ly49B blot of NR and R Ly49B glycosylation mutants. YB2- C57 Ly49B, YB2-C57 Ly49B-N94Q-N105Q-N114Q-N177Q, YB2- C57 Ly49B-HA, YB2-C57 Ly49B-N94Q-N105Q-N114Q-N177Q-HA, YB2- BALB/c Ly49B-HA, YB2-BALB/c Ly49B-N94Q-N105Q-N114Q-N177Q-HA lysates at 5000 cells/ul were run for 1.5 h at 200 V on 15 % SDS-PAGE gels and transferred for 17 min at 1.3 A and 25 V to nitrocellulose membranes using the Trans-Blot Turbo system. Membranes were incubated overnight at 4 °C with N1176 biotin 2G4 rat anti-Ly49B antibody at 1/2000 dilution and then N1243 HRPO anti-biotin antibody at 1/1000 dilution for 1 h at room temperature. Image was developed using Thermo ECL reagent for 20 sec. M= molecular weight marker, NR=non-reduced, R=reduced, C=YB2- C57 Ly49B, CG=YB2-C57 Ly49B-N94Q-N105Q-N114Q-N177Q, CH=YB2- C57 Ly49B-HA, CHG=YB2-C57 Ly49B-N94Q-N105Q-N114Q-N177Q-HA, BH=YB2- BALB/c Ly49B-HA, BHG=YB2-BALB/c Ly49B-N94Q-N105Q-N114Q-N177Q-HA.

The predicted molecular weight of Ly49B is ~34 kDa but the smallest molecular form observed for wild type Ly49B in Western blot experiments was ~47 kDa. The results presented here demonstrate that the difference between the predicted and the observed molecular weight of Ly49B is most likely due to the presence of glycans at the N-glycosylation motifs. In light of the observation that only one predominant band was observed for the reduced and non-reduced Ly49B glycosylation mutants, as opposed to two bands observed for reduced samples and three bands observed for non-reduced samples in lysates containing wild type protein, it is reasonable to conclude that the multiple molecular weight forms of Ly49B represent differentially glycosylated Ly49B. Notably, the C57 and BALB/c HA-tagged glycosylation mutants ran at virtually identical positions, unlike their wild type counterparts, suggesting that the differences observed for the wild type proteins might be due to different kinds of glycans being attached to C57 and BALB/c forms of Ly49B.

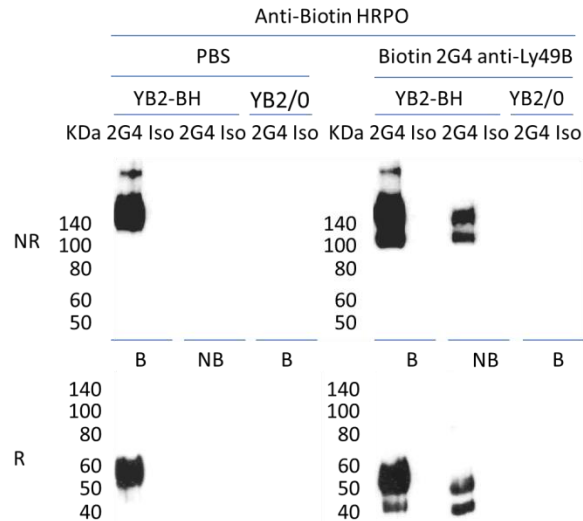


Figure 4.8. Western blot of biotinylated NR and R C57 Ly49B-HA immunoprecipitated from YB2-C57 Ly49B-HA lysates using protein G beads coated with 2G4 anti-Ly49B. Samples of immunoprecipitated material prepared from biotinylated and non-biotinylated YB2-C57 Ly49B-HA lysates at 5000 cells/ μ l using sepharose protein G beads coated with N1184 2G4 rat anti-Ly49B or isotype control were run in duplicates for 40 min at 200 V on 15 % SDS-PAGE gels and transferred for 17 min, at 1.3 A and 25 V to nitrocellulose membranes using the Trans-Blot Turbo system. The membranes were incubated overnight at 4 °C with N1176 biotin 2G4 rat anti-Ly49B antibody at 1/2000 dilution or PBS, followed by N1194 HRPO anti-biotin antibody at 1/2000 dilution for 1 h at room temperature. Images were developed using Thermo ECL reagent for 1 min. M=molecular weight marker, NR=non-reduced, R=reduced, 2G4=N1184 2G4 rat anti-Ly49B, Iso=N1089 MR3 rat IgG2c, Anti-Biotin HRPO=N1194 HRPO anti-biotin antibody, B=biotinylated, NB=non-biotinylated, YB2-BH=YB2-C57 Ly49B-HA.

To further address the question of what the multiple molecular forms of Ly49B observed in Western blot experiments are likely to be, YB2/0 and YB2-C57 Ly49B-HA cells were surface biotinylated, lysed and subjected to immunoprecipitation using sepharose protein G beads coated with 2G4 antibody or isotype control. **Figure 4.8** shows a blot with the biotinylated samples and non-biotinylated control samples incubated with N1194 HRPO anti-biotin antibody in conjunction with either PBS or N1176 biotin 2G4 rat anti-Ly49B as the primary layers. The right hand side of the panel, which contains samples incubated with biotinylated 2G4 antibody followed by anti-biotin HRPO antibody, shows two strong bands at ~47 kDa and ~55 kDa in the reduced samples and two strong bands at ~110 kDa and ~150 kDa in non-reduced samples, following immunoprecipitation from biotinylated and non-biotinylated YB2-C57 Ly49B-HA lysates. The biotinylated, non-reduced YB2-C57 Ly49B-HA sample contained an additional faint band at ~200 kDa. The bands were at positions analogous to those previously identified as multiple molecular weight forms of Ly49B. No bands were present in lanes that contained samples, which had been immunoprecipitated with isotype coated beads from YB2-C57 Ly49B-HA or YB2/0 lysates. Moreover, 2G4 coated beads were unable to immunoprecipitate any proteins from YB2/0 lysates, suggesting that the

proteins immunoprecipitated from YB2-C57 Ly49B-HA lysates were indeed Ly49B. The left hand side panel of **Figure 4.8** contains samples incubated with PBS control, followed by N1194 HRPO anti-biotin antibody. No bands were detected in the case of non-biotinylated cell lysate samples, suggesting that the N1194 antibody is specific for biotin.

Strikingly, the biotinylated, reduced samples that were immunoprecipitated from YB2-C57 Ly49B-HA cell lysates contained a band at ~55 kDa, but lacked the ~47 kDa Ly49B band. The non-reduced samples also contained ~150 kDa and ~200 kDa bands but lacked the band at 110 kDa, suggesting that the “missing” molecular forms were not biotinylated. Since the experimental design allowed biotinylation of *only* the surface proteins, it is reasonable to conclude that the reduced ~55 kDa and non-reduced ~110 kDa molecular forms of Ly49B are not expressed on the cell surface and were only released following cell lysis.

To extend the analysis of the different molecular forms of Ly49B, YB2-C57 Ly49B-HA cells were lysed and treated for 1 h at 37 °C either with the endoglycosidase enzyme, PNGase F, which removes all glycans attached to asparagines residue within N-glycosylation motifs, or with Endo H enzyme, which specifically cleaves high mannose from N-linked glycoproteins. An N1176 biotin 2G4 blot of NR and R C57 Ly49B-HA treated with either PNGase F or Endo H is shown on **Figure 4.9**. Development with the N1243 anti-biotin antibody revealed the same range of Ly49B bands as previously identified (**Figures 4.3-4.6 and 4.7**) in the untreated samples, although the 200 kDa band was barely visible, suggesting that the highest molecular form of Ly49B may not be stable. PNGase F-treated samples contained only one band in the reduced and non-reduced samples; at ~34 kDa and ~80 kDa respectively. The position of these bands was analogous to the position of bands found with the Ly49B N-glycosylation mutants, providing further evidence that the multiple molecular forms of Ly49B are indeed differentially glycosylated Ly49B. The reduced samples treated with Endo H enzyme contained two bands at ~34 kDa and ~55 kDa and the non-reduced samples contained two bands at ~80 kDa and 150 kDa. It appears that only the lowest reduced and non-reduced molecular weight forms of Ly49B observed on Western blots were sensitive to Endo H.

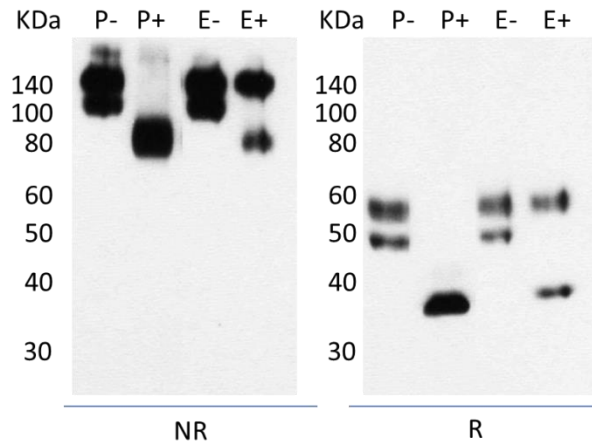


Figure 4.9. N1176 biotin 2G4 anti-Ly49B blot of NR and R C57 Ly49B-HA treated with PNGase F and Endo H enzymes. YB2-C57 Ly49B-HA lysates at 5000 cells/ μ l were treated with PNGase F and Endo H at 25,000 U/ml, at 37 °C for 1 h, were run for 1.5 h at 200 V on 15 % SDS-PAGE gels and transferred for 17 min at 1.3 A and 25 V to nitrocellulose membranes using the Trans-Blot Turbo system. Membranes were incubated overnight at 4 °C with N1176 biotin 2G4 rat anti-Ly49B antibody at 1/2000 dilution and then for 1 h at room temperature with N1243 HRPO anti-biotin antibody at 1/1000 dilution. Image was developed using Thermo ECL reagent for 5 sec. M=molecular weight marker, NR=non-reduced, R=reduced, P=PNGase F, E= Endo H.

As explained in detail in the Introduction (**Section 1.3**), the process of N-glycosylation is a multi-stage event; as the glycoprotein travels through different intracellular compartments to the cell surface various glycans are attached, cleaved and replaced by other glycans at the same glycosylation motif. Immature glycoproteins, localised in the ER are often associated with mannose polymers and for that reason are referred to as high mannose glycoproteins. Taking into account results presented in **Figures 4.8** and **4.9**, it is possible to conclude that the lowest reduced and non-reduced molecular weight forms of Ly49B detected on Western blots could represent immature, intracellular, high mannose forms of Ly49B and that the larger species are surface-associated mature receptors.

To establish which of the predicted Ly49B N-glycosylation motifs undergo glycosylation, BALB/c Ly49B mutants, which contained glutamine rather than asparagine at each of the individual motifs, were transfected into YB2/0 cells and examined by Western blotting. **Figure 4.10** shows an N1176 biotin 2G4 blot of NR and R BALB/c Ly49B single glycosylation mutants. All of the reduced samples ran at a lower position than wild type BALB/c Ly49B, suggesting that glycans are attached at each of the individual glycosylation motifs. Interestingly, the lane with reduced YB2-BALB/c Ly49B-N114Q lysate sample contained 3 bands, rather than 2, as was the case with the wild type sample and all of the other mutants. The lowest band in this sample ran at ~42 kDa and was not observed in any

other sample. This suggests that glycosylation of asparagine 114 may have a positive effect on the glycosylation of other motifs. In the absence of a glycan at asparagine 114, glycosylation of the remaining motif(s) may be impaired. Alternatively, the presence of a glycan at position 114 may dictate what kinds of glycans are attached to the remaining motifs. In the absence of a glycan at position 114, glycans of varying size may be attached at the remaining glycosylation motifs, which resulted in a greater heterogeneity of band sizes in the YB2-BALB/c Ly49B-N114Q lysate samples.

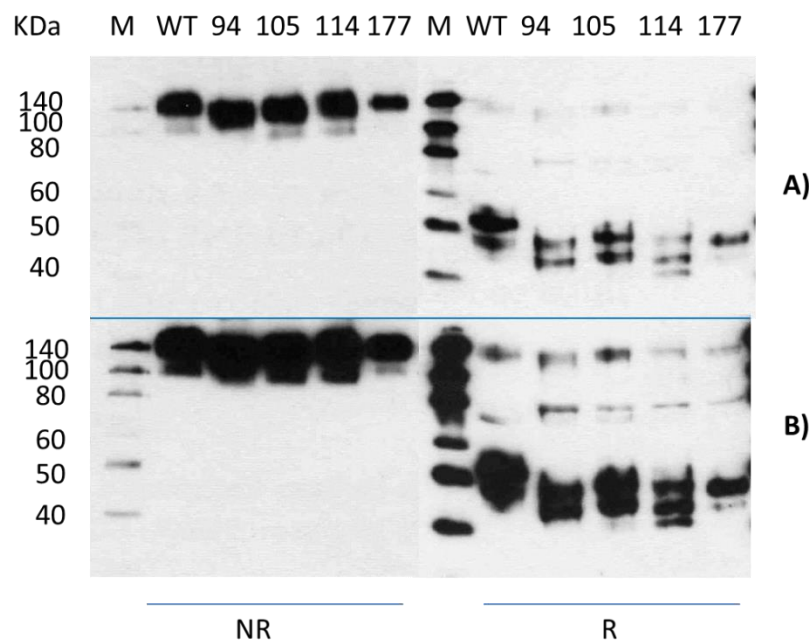


Figure 4.10. N1176 biotin 2G4 anti-Ly49B blot of NR and R BALB/c Ly49B single glycosylation mutants. YB2-BALB/c Ly49B, YB2-BALB/c Ly49B-N94Q, YB2-YB2-BALB/c Ly49B-N105Q, YB2-BALB/c Ly49B-N114Q and YB2-BALB/c Ly49B-N177Q lysates at 1.5×10^4 cells/ μ l were run for 1.5 h at 200 V on 15 % SDS-PAGE gels and transferred for 17 min at 1.3 A and 25 V to nitrocellulose membranes using the Trans-Blot Turbo system. Membranes were incubated overnight at 4 °C with N1176 biotin 2G4 rat anti-Ly49B antibody at 1/2000 dilution and then for 1 h at room temperature with N1242 HRPO anti-biotin antibody at 1/2000 dilution. Images were developed using Thermo ECL reagent for 10 min (A) and 15 min (B). M=molecular weight marker, NR=non-reduced, R=reduced, WT =YB2- BALB/c Ly49B, 94 =YB2-BALB/c Ly49B-N94Q, 105=YB2-YB2-BALB/c Ly49B-N105Q, 114 =YB2-BALB/c Ly49B-N114Q, 177 =YB2-BALB/c Ly49B-N177Q.

The results obtained for the non-reduced samples are somewhat contradictory to those obtained for the reduced samples. The bands detected in YB2-BALB/c Ly49B-N94Q and YB2-BALB/c Ly49B-N105Q lysates ran at a slightly lower position than the wild type BALB/c Ly49B, but the bands detected in YB2-BALB/c Ly49B-N114Q and YB2-BALB/c Ly49B-N177Q lysates appeared to run at a very similar position to the wild type. This discrepancy might simply be due to the lower resolving capacity of high molecular weight species on 15 % acrylamide SDS-PAGE gels.

4.4. Differentially glycosylated Ly49B forms exist in native cells expressing Ly49B.

Unlike other Ly49s, which are expressed on NK cells, Ly49B was found to be expressed predominantly on myeloid cells including monocytes and macrophages (Gays *et al.* 2006). However, Ly49B expression may be induced on the surface of mature NK cells cultured with IL-12 and IL-18 and on immature NK cells (Gays *et al.* 2006). To check whether or not Ly49B expressed in native cells can be detected by Western blotting using anti-Ly49B mAbs and, if so, whether or not the banding pattern is similar to that detected in transfected cell lysates, C57 spleen (S) and bone marrow (BM) cells were cultured for 10 days with macrophage colony stimulating factor (MCSF) to obtain cultures rich in macrophages (MQ). One third of the MQ culture was then incubated for 2 days with either interferon alpha (IFN- α) or lipopolysaccharide (LPS), both of which have previously been shown to stimulate expression of Ly49B (Gays *et al.* 2006). Next, Ly49B expression levels were assessed by flow cytometry, as shown in **Figure 4.11**. The panels on the left hand side show scatter plots with gates surrounding the cells of interest and indicate that the cells exhibited high side light scattering, which is characteristic for myeloid cells. The right hand panels show that the cells of interest expressed the F4/80 membrane protein on their surface; F4/80 being one of the best characterised murine macrophage and monocyte markers (McKnight *et al.* 1996). The panels in the centre show that all of the MQ cells expressed low levels of Ly49B on their surfaces.

Following flow cytometric analysis, the cells were lysed and examined by Western blotting. **Figure 4.12** shows N1176 biotin 2G4 blots of NR YB2/0 and YB2-C57 Ly49B-HA cell lysates, as well as samples containing lysates of IFN- α and LPS-treated C57 spleen and bone marrow cells. Unexpectedly, a large band at ~80 kDa was detected in all of the non-reduced and reduced native cells samples, which was not present in the YB2/0 or YB2-C57 Ly49B-HA samples. All of the non-reduced samples contained a non-specific band at ~75 kDa. The bands at ~110 kDa and ~150 kDa observed in the non-reduced samples, which were similar to Ly49B bands detected in transfected cell lysates, were revealed in native cell lysates after prolonged exposure (**Figure 4.12 B**). The ~110 kDa band was stronger than that at ~150 kDa in all of the native cell lysate samples. As well as the strong band at ~80 kDa, the reduced native cell samples also contained a very weak band at ~47 kDa (**Figure 4.12 B**). Collectively, these results suggest that Ly49B might exist in native cells predominantly as a

molecular form of ~80 kDa; this form does not exist in transfected cells and is not amendable to reduction. The 110 kDa and 150 kDa non-reduced forms and the 47 kDa reduced form of Ly49B are also likely to exist in native cells but in much smaller proportions.

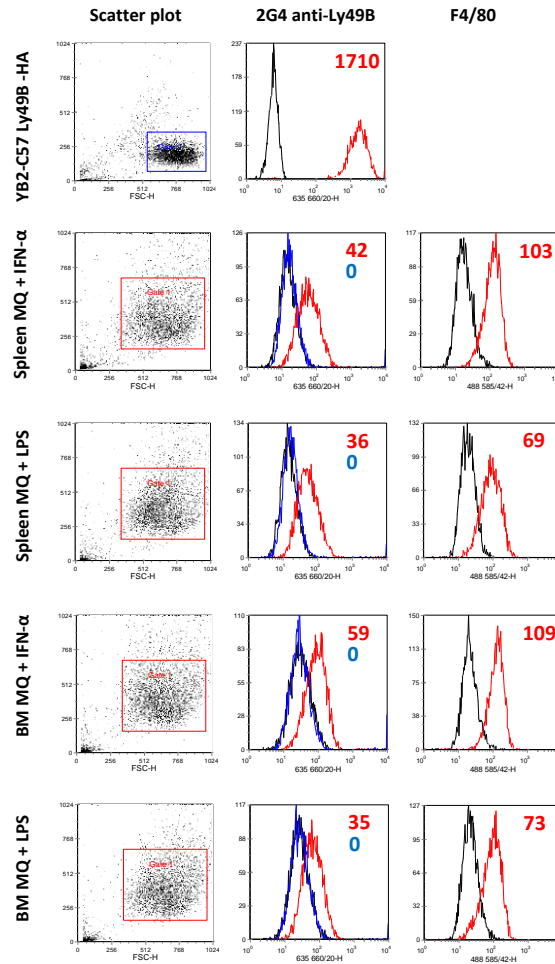


Figure 4.11. Staining of C57 spleen and bone marrow (BM) macrophages with 2G4 anti-Ly49B antibody. C57 spleen and bone marrow cells were harvested and cultured with 5 % macrophage colony stimulating factor (MCSF) for 10 days. The cells were then divided into three cultures, two of which were cultured for 2 days with either 10^4 U/ml IFN- α or 2 mg/ml LPS. Cells were then harvested and incubated with a saturating concentration of N415 2.4G2 anti-CD16/32 at a final dilution of 1/100 to block FcR, followed by N382 Biotin F4/80 at a final dilution of 1/500. The cultures were then divided into four samples, which were stained with the following: A) medium, B) medium, C) N1059 AF647 MR3 IgG2c isotype control at final 1/500 dilution, D) N1058 AF647 2G4 anti-Ly49B at final 1/500 dilution. Samples B-D were additionally stained with N883 PE streptavidin at a final dilution of 1/1000. In parallel with this, staining of two samples of YB2-C57 Ly49B-HA cells was performed with medium and N1058 AF647 2G4 anti-Ly49B a at final dilution of 1/500. The black peaks in the “2G4 anti-Ly49B” histograms in the centre of the panel represent the medium control. The red peaks represent cells stained with 2G4 anti-Ly49B and the blue peaks cells stained with isotype control. The black peaks in the “F4/80” histograms on the right hand side of the panel represent cells stained with F4/80 followed by medium control and the red peaks cells stained with Biotin F4/80 followed by PE streptavidin. Red numbers in the right hand corner of the histograms represent net median fluorescence values of the cells stained with the reagent indicated as red peaks and the blue numbers represent net median fluorescence values of the cells stained with the reagents indicated as blue peaks.

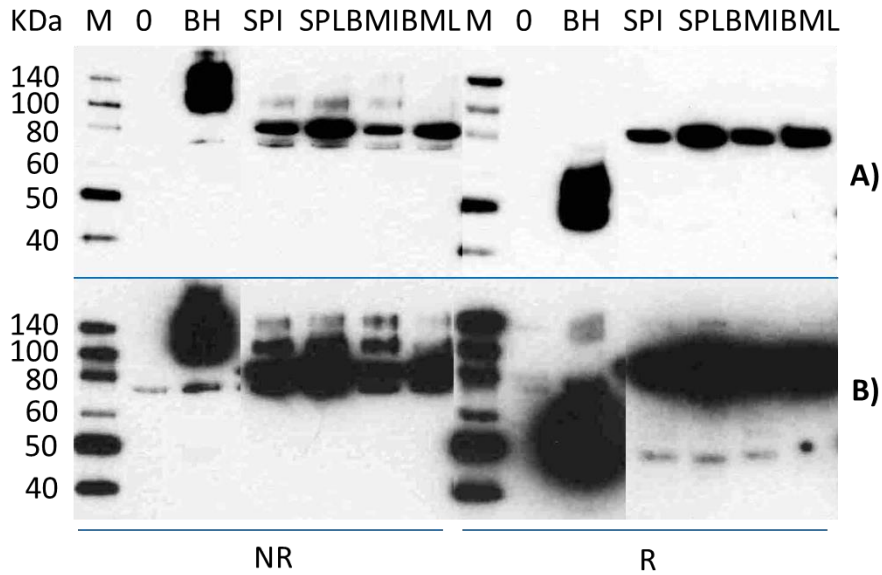


Figure 4.12. N1176 biotin 2G4 anti-Ly49B blot of NR and R cell lysates prepared from YB2/0, YB2-C57 Ly49B-HA transfectants and C57 spleen and bone marrow cells cultured with MCSF followed by either INF- α or LPS. YB2/0 and YB2-C57 Ly49B-HA cell lysates at 2000 cells/ μ l and C57 spleen and bone marrow cells cultured with MCSF followed by INF- α or LPS at 5000 cells/ μ l were run for 1.5 h at 200 V on 15 % SDS-PAGE gels and transferred for 15 min at 1.3 A and 25 V to nitrocellulose membranes using the Trans-Blot Turbo system. Membranes were incubated overnight at 4 °C with N1176 biotin 2G4 anti-Ly49B antibody at 1/2000 dilution followed incubation for 1 h at room temperature with N1194 HRPO anti-biotin antibody at 1/2000 dilution. Images were developed using Thermo ECL reagent for 5 min (A) and 20 min (B). M=molecular weight marker, NR=non-reduced, R=reduced, 0=YB2/0, BH=YB2-C57 Ly49B-HA, SP=spleen cells, BM=bone marrow cells, I=INF- α , L=LPS.

Figure 4.13 shows repeat flow cytometric staining of C57 spleen MQs with 2G4 anti-Ly49B mAb (**Figure 4.13 A**) and staining of the BALB/c fetal liver NK cell line, LNK, using a variety of anti-Ly49 mAbs (**Figure 4.13 B**). The LNK cell line has previously been shown to contain Ly49B transcripts (Gays *et al.* 2006).

The presence of Ly49B was detected in all of the tested samples of C57 spleen MQs (**Figure 4.13 A**). The net median fluorescence value for IFN- α -treated C57 spleen MQs stained with 2G4 mAb was approximately twice that of LPS-treated and untreated counterparts, suggesting that Ly49B was up-regulated in the presence of IFN- α but not LPS. Only Ly49B and not any of the other tested Ly49s was shown to be expressed on LNK cells (**Figure 4.13 B**).

Western blot on NR YB2/0, YB2-Ly49B-HA, LNK cell lysates and cell lysates prepared from C57 spleen MQs, which were untreated or treated with either IFN- α or LPS was developed with N1176 biotin 2G4 anti-Ly49B or N869 biotin 1A1 anti-Ly49B, followed by N1194 HRPO anti-biotin antibody (**Figure 4.14**). The YB2-C57 Ly49B-HA pattern with

three bands at ~110 kDa, ~150 kDa and ~200 kDa was observed for blots developed with the 2G4 and 1A1 mAbs.

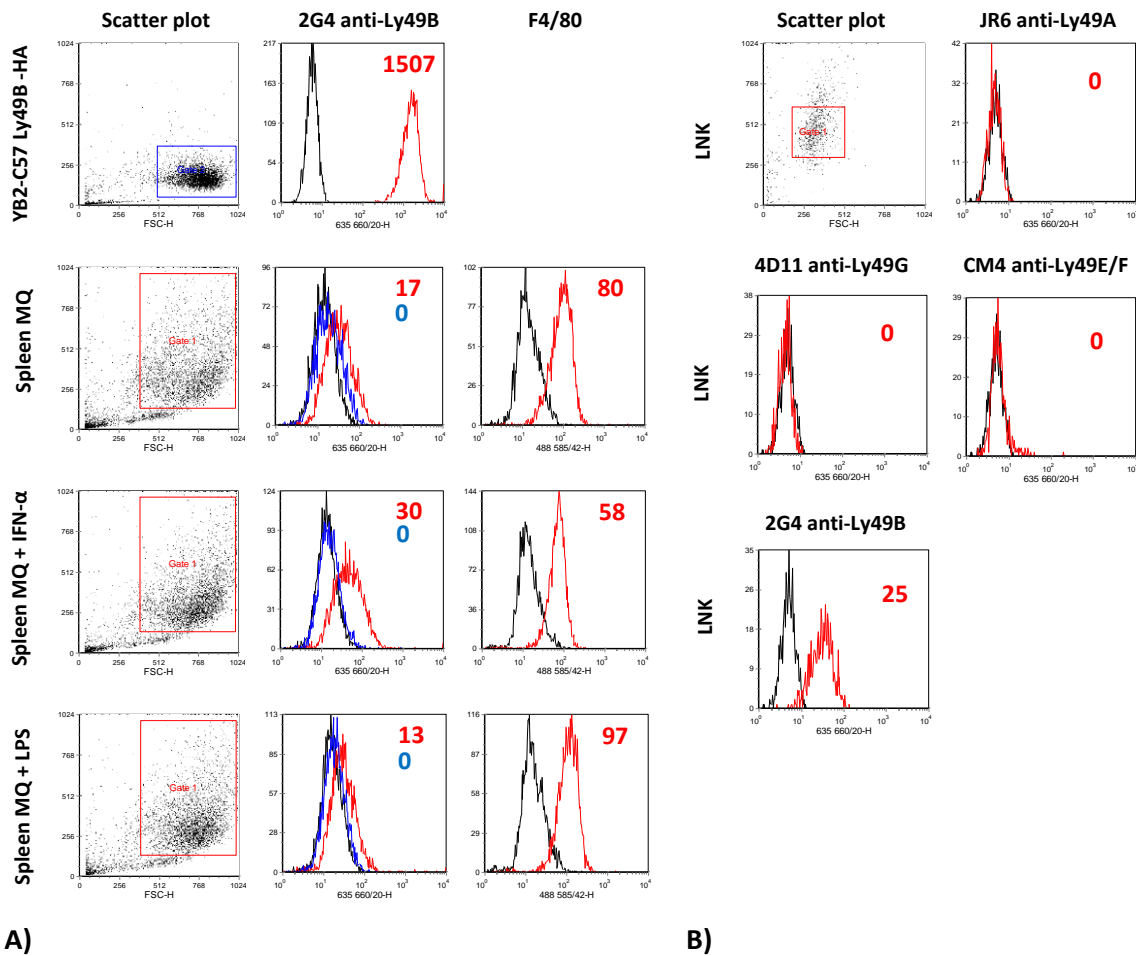


Figure 4.13. Staining of C57 spleen macrophages with 2G4 anti-Ly49B antibody (A) and LNK cells with a variety of monoclonal anti-Ly49 antibodies (B). A) C57 spleen cells were harvested and cultured with 5 % macrophage colony stimulating factor (MCSF) for 10 days. The cells were split into three cultures, two of which were cultured for 2 days in the presence of 10^4 U/ml IFN- α or 2 mg/ml LPS. Cells were then harvested and incubated with a saturating concentration of N415 2.4G2 anti-CD16/32 at a final dilution of 1/100 to block FcR followed by incubation with N382 Biotin F4/80 at a final dilution of 1/500. Cultures were further divided into four samples and stained with one of the following: A) medium, B) medium, C) N1059 AF647 MR3 IgG2c isotype control at final 1/500 dilution, D) N1058 AF647 2G4 anti-Ly49B at final 1/500 dilution. Samples B-D were then stained with N883 PE streptavidin at a final dilution 1/1000. In parallel, staining of two samples of YB2-C57 Ly49B-HA cells was performed with medium or N1058 AF647 2G4 anti-Ly49B at final dilution of 1/500. Black peaks in the “2G4 anti-Ly49B” histograms in the centre of the panel represent medium control, red peaks represent cells stained with 2G4 anti-Ly49B and blue peaks represent cells stained with isotype control. The black peaks in the “F4/80” histograms on the right hand side of the panel represent cells stained with F4/80 followed by medium control and the red peaks cells stained with Biotin F4/80 followed by PE streptavidin. Red numbers in the right hand corner of the histograms represent net median fluorescence values of the cells stained with the reagent indicated as red peaks and the blue numbers represent net median fluorescence values of the cells stained with the reagents indicated as blue peaks **B)** LNK cells were harvested and stained with a) medium, b) N538 JR9 anti-Ly49A at a final dilution of 1/1000, c) N156 4D11 anti-Ly49G at a final dilution of 1/10,000, d) N865 CM4 anti-Ly49E/F at a final dilution of 1/10, e) N837 2G4 anti-Ly49B at a final dilution of 1/30. The cells were then stained with N1217 AF647 chicken anti-rat at a final dilution of 1/1,000. Black peaks in the histograms represent medium control and red peaks represent cells stained with the monoclonal anti-Ly49 antibodies. Red numbers in the right hand corner of the histograms represent net median fluorescence values of cells stained with monoclonal antibodies.

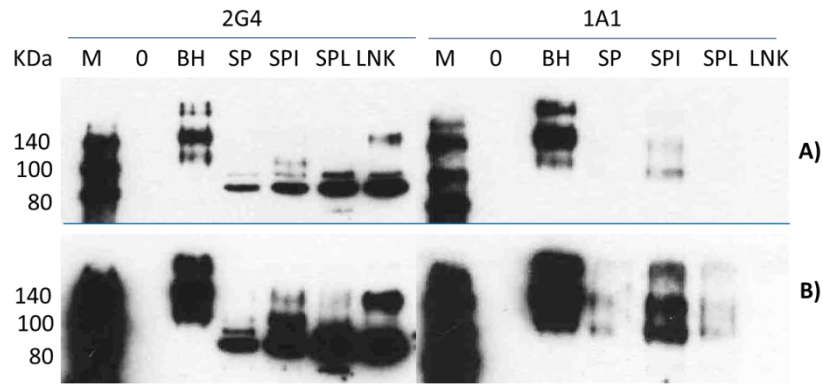


Figure 4.14. N1176 biotin 2G4 anti-Ly49B and N869 biotin 1A1 anti-Ly49B blots of NR cell lysates prepared from YB2/0, YB2-C57 Ly49B-HA transfectants, LNK cells and C57 spleen cells cultured with MCSF followed by INF- α or LPS. YB2/0 and YB2-C57 Ly49B-HA cell lysates at 2000 cells/ μ l and LNK cells and C57 spleen cells cultured with MCSF followed by either IFN- α or LPS at 5000 cells/ μ l were run for 40 min at 200 V on 15 % SDS-PAGE gels and transferred for 1.5 h at 200 V onto nitrocellulose membranes using wet transfer method. Membranes were incubated overnight at 4 °C with N1176 biotin 2G4 anti-Ly49B antibody at 1/1000 dilution or N869 biotin 1A1 anti-Ly49B at 1/250 dilution followed by N1194 HRPO anti-biotin antibody at 1/2000 dilution for 1 h at room temperature. Images were developed using Thermo ECL reagent for 1 min (A) and 15 min (B). M=molecular weight marker, 0=YB2/0, BH=YB2-C57 Ly49B-HA, SP=spleen cells, I=IFN- α , L=LPS.

The 2G4 blot of three MQ samples revealed a strong band at ~80 kDa and a weaker, slightly larger in size band, surprisingly neither of which was detected by 1A1 mAb, suggesting that these bands may not in fact have been Ly49B. Longer exposure of the 2G4 blot revealed two bands at ~110 kDa and ~150 kDa in the SPI sample. Both bands are likely to represent Ly49B as they were also detected by 1A1. The 1A1 mAb additionally detected a high molecular weight band at ~200 kDa (**Figure 4.14 B**).

The longer exposure of the 1A1 blot revealed that Ly49B bands may be present in SP and SPL samples (**Figure 4.14 B**). The fact that the SPI sample contains stronger bands than SP and SPL samples correlates with stronger 2G4 staining of this sample detected by flow cytometry (**Figure 4.13 A**). All of the Ly49B bands detected in SP samples ran slightly faster than YB2-C57 Ly49B-HA sample, which was most likely due to the presence of the HA tag. The results obtained for spleen MQ samples suggest that Ly49B may be present in the same multiple molecular forms on native myeloid cells as observed in transfected cells.

Consistent with the specificity of the 1A1 antibody for C57 Ly49B, no bands were detected in the BALB/c LNK sample on the blot developed with 1A1 (**Figure 4.14**). The 2G4 blot contained strong bands at ~80 kDa and one just above it. These are unlikely to have been specific due to the fact they ran at similar positions to the non-specific bands that were detected in MQ samples. In addition to these bands, a strong band was detected at ~145 kDa;

this position corresponds to the main NR band detected previously for BALB/c Ly49B in transfected YB2 cells (**Figures 4.3 and 4.4**). It seems that, as with C57 spleen MQ cells, BALB/c Ly49B can be detected on Western blots in samples prepared from the fetal LNK cell line in a similar form to that found in transfected cells.

4.5. NK cell receptors tend to exist in multiple molecular forms in YB2/0 transfectants.

The results obtained for Ly49B suggest that other Ly49 and NK cell receptors could exist in multiple molecular weight forms. To address this question, as well as to validate results obtained for Ly49B, four additional HA-tagged C57 Ly49s (A, E, G and Q) were transfected onto YB2/0 cells, as well as a HA-tagged Clrg receptor, which is encoded in the NK gene complex and, like the Ly49 receptors belongs to C-type lectin superfamily. Cell lysate samples were prepared in parallel to Ly49B-HA lysate and examined by Western blot using N1229 biotin anti-HA antibody (**Figure 4.15**).

4.5.1. Assessment of Ly49B molecular forms

The results for YB2-C57 Ly49B-HA lysates were similar to those observed in previous experiments. The non-reduced sample contained three strong bands at ~110 kDa, ~150 kDa and ~200 kDa. The reduced sample contained two bands at ~47 kDa and ~55 kDa and very weak bands at ~110 kDa, ~150 kDa and ~ 200 kDa, which was most likely residual non-reduced material.

4.5.2. Assessment of Ly49A molecular forms

The samples containing non-reduced YB2-Ly49A-HA lysate contained a relatively weak band at ~80 kDa, and a particularly strong band between 100-140 kDa. The reduced sample contained a very weak band of ~80 kDa, a prominent band between 50 and 60 kDa, a weak band at ~49 kDa and a moderate intensity band slightly greater than 40 kDa. The band at ~80 kDa could be residual non-reduced material or simply a non-specific band, since a band of a similar size was detected in YB2/0 lysates.

As described in the introduction, there was some discrepancy between the Ly49A monomer and dimer sizes identified by previous studies using Western blotting, but generally, there was only one band observed for the Ly49A monomer and one for the Ly49A dimer (Takei 1983, Chan *et al.* 1986, Chan *et al.* 1988, Nagasawa *et al.* 1987, Mason *et al.* 1996,

Ortaldo *et al.* 1999, Roland *et al.* 1992, Yokoyama *et al.* 1989, Chang *et al.* 1996). The monomer size was in the range of 42-55 kDa and the dimer in the range of 82-95 kDa.

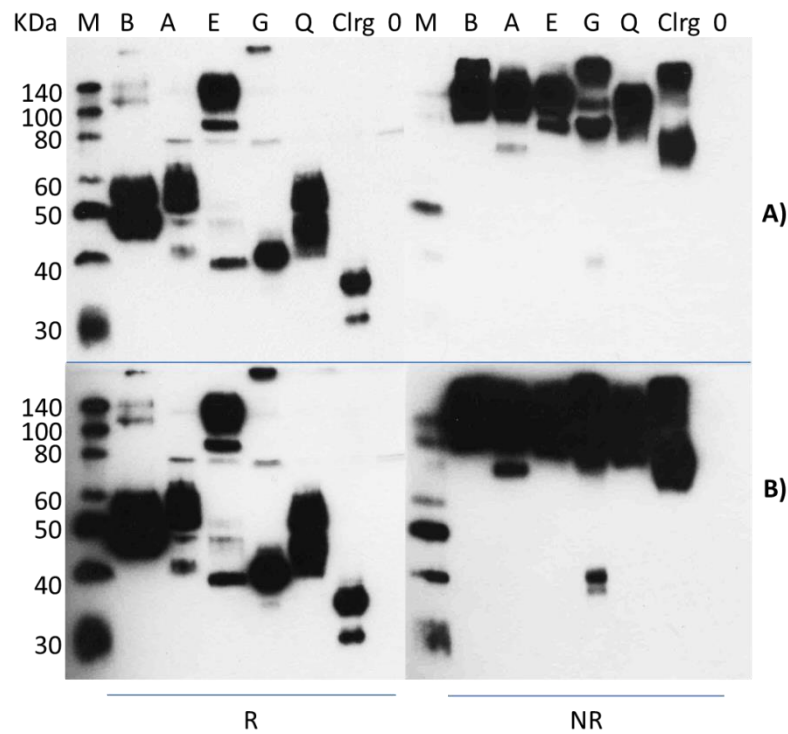


Figure 4.15. N1229 biotin anti-HA blot of NR and R YB2-C57 Ly49B-HA, YB2-Ly49A-HA, YB2-Ly49E-HA, YB2-Ly49G-HA, YB2-Ly49Q-HA and YB2-Clrg-HA cell lysates. YB2-C57 Ly49B-HA, YB2-Ly49A-HA, YB2-Ly49E-HA, YB2-Ly49G-HA, YB2-Ly49Q-HA and YB2-Clrg-HA lysates (all at 2000 cells/ μ l, except for YB2-Ly49G-HA and YB2-Clrg-HA, which were both at 8000 cells/ μ l) were run for 1.5 h at 200 V on 15 % SDS-PAGE gels and transferred for 1.5 h at 200 V to nitrocellulose membranes by wet transfer. Membranes were incubated overnight at 4 °C with N1229 biotin anti-HA antibody at 1/25,000 dilution and then for 1 h at room temperature with N1194 HRPO anti-biotin antibody at 1/2500 dilution. Images were developed using Pierce ECL reagent for 1 min (A) and 15 min (B). M=molecular weight marker, NR=non-reduced, R=reduced, B=YB2-C57 Ly49B-HA, A=YB2-Ly49A-HA, E=YB2-Ly49E-HA, G=YB2-Ly49G-HA, Q=YB2-Ly49Q-HA, Clrg=YB2-Clrg-HA, 0=YB2/0.

4.5.3. Assessment of Ly49G molecular forms

The non-reduced sample of YB2-Ly49G-HA lysate contained a clear high molecular weight band of ~200 kDa and two bands at ~100 kDa and ~92 kDa. Longer exposure revealed two bands of ~40 kDa in close proximity to one another, suggesting that Ly49G might exist as a monomer in living cells. The reduced sample contained prominent bands at ~40 kDa and ~200 kDa, as well as a very weak band at ~ 80 kDa, which may simply be non-specific since a band of similar size was also detected in YB2/0 cells. Previous studies have found bands of 40 kDa or 43 kDa in reduced samples of Ly49G and bands of 86 kDa or 97-110 kDa in non-reduced samples (Mason *et al.* 1996, Ortaldo *et al.* 1999, Mason *et al.* 1988, Chang *et al.* 1999).

4.5.4. Assessment of Ly49Q molecular forms

The non-reduced sample of YB2-Ly49Q-HA lysate contained a prominent band of ~100 kDa, which upon longer exposure stretched between ~80-140 kDa. The reduced sample of Ly49Q-HA contained two dispersed bands between at ~45 kDa and 55 kDa. A previous study identified a reduced band at ~45-60 kDa and non-reduced bands of ~130 kDa and ~200 kDa (Toyama-Sorimachi *et al.* 2004). Interestingly, a different study identified a relatively well defined band of ~82 kDa in non-reduced samples (Scarpellino *et al.* 2007).

4.5.5. Assessment of Clrg molecular forms

Two bands were observed for the reduced sample of YB2-Clrg-HA lysate at ~35 kDa and ~38 kDa. The non-reduced sample contained two bands at ~77 kDa and ~200 kDa.

4.5.6. Assessment of Ly49E molecular forms

The non-reduced YB2-Ly49E-HA lysate sample contained one clearly defined band at ~90 kDa, which agrees well with previously published data (Van Beneden *et al.* 2001). An additional a strong band of between 100 kDa and 140 kDa was also clearly visible. Unexpectedly, the reduced sample contained prominent bands at similar positions to those found in the non-reduced sample, suggesting that Ly49E may be more resistant to 2ME treatment than other Ly49s. An additional band of moderate intensity was observed at ~39 kDa, as well as a very weak band at ~49 kDa. A band was previously observed in reduced samples of Ly49E at ~46 kDa (Van Beneden *et al.* 2001).

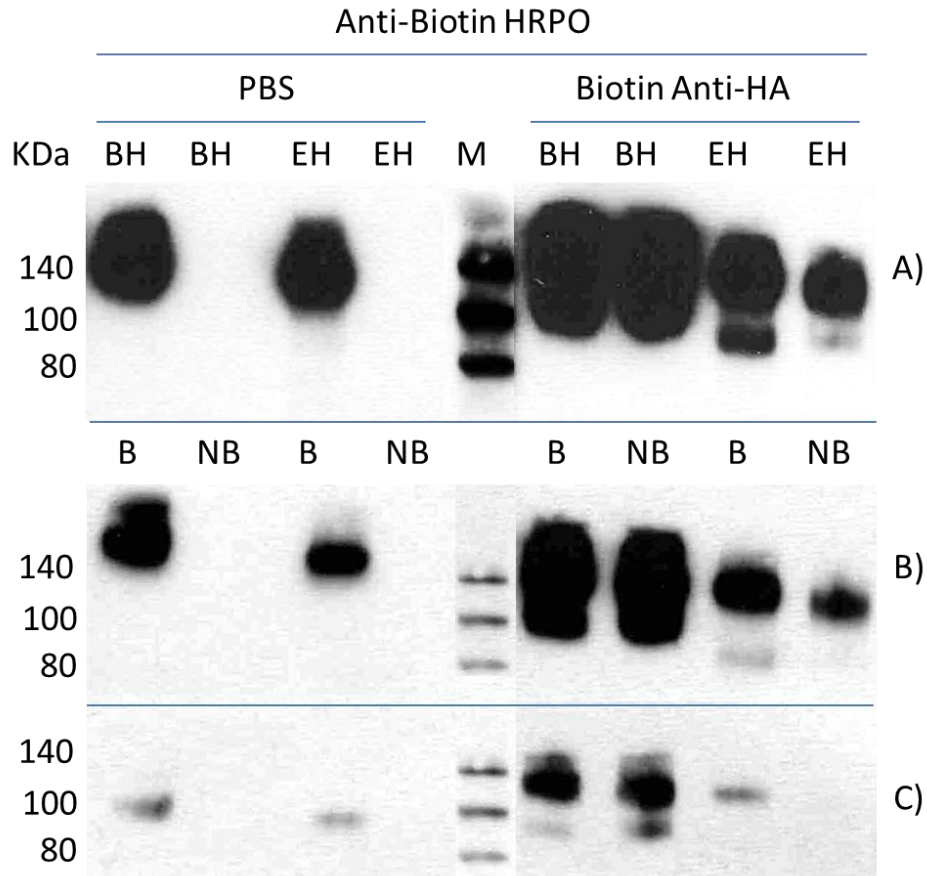


Figure 4.16. Western blot of biotinylated NR C57 Ly49B-HA and Ly49E-HA immunoprecipitated from YB2-C57 Ly49B-HA lysates or YB2-Ly49E-HA lysates respectively, using protein G beads coated with anti-HA antibody. Samples of immunoprecipitated material prepared from biotinylated and non-biotinylated YB2-C57 Ly49B-HA or YB2-Ly49E-HA lysates at 2000 cells/ μ l using sepharose protein G beads coated with N1184 2G4 rat anti-Ly49B or N1141 CM4 anti-Ly49E/F were run in duplicates for 1.5 h at 200 V on 15 % SDS-PAGE gels and transferred for 17 min at 1.3 A and 25 V to nitrocellulose membranes using the Trans-Blot Turbo system. Membranes were incubated overnight at 4 °C with N1229 biotin anti-HA antibody at 1/10.000 dilution or PBS and then for 1 h at room temperature with N1243 HRPO anti-biotin antibody at 1/1000 dilution. Images were developed using Thermo ECL reagent for A) 5 min B) 2min C) 20sec. M=molecular weight marker, NR=non-reduced, Biotin Anti-HA=N1229 biotin anti-HA, Anti-Biotin HRPO=N1243 HRPO anti-biotin, B=biotinylated, NB=non-biotinylated, BH=C57 Ly49B-HA, EH=Ly49E-HA.

To extend the analysis of multiple molecular forms of NK cell receptors, surface biotinylated and non-biotinylated YB2-Ly49E-HA and YB2-C57 Ly49B-HA cells were lysed and examined by Western blotting. Membranes containing NR lysate samples were incubated with anti-HA HRPO in conjunction with biotin anti-HA or PBS control (**Figure 4.16**). Results obtained for Ly49B-HA samples were similar to those shown in **Figure 4.8**. No bands were observed in the non-biotinylated YB2-Ly49E-HA sample tested with anti-biotin antibody alone. The equivalent biotinylated YB2-Ly49E-HA sample contained one band at ~140 kDa. Both biotinylated and non-biotinylated YB2-Ly49E-HA samples tested

with anti-biotin antibody in conjunction with anti-HA antibody contained two bands at ~140 kDa and ~90 kDa. These results suggest that, as with Ly49B, the smallest non-reduced molecular form of Ly49E observed on Western blots is likely to be intracellular, whereas the larger one appears to be surface-associated. A more comprehensive analysis of the individual NK cell receptors is required to formally establish whether or not the multiple molecular weight forms detected by Western blotting in **Figure 4.15** represent the receptors at different stages of glycosylation.

4.6. Summary

The results presented here suggest that Ly49B monomers have a tendency to form homodimers or associations with other proteins through the formation of disulphide bonds. The large molecular weight band observed in some of the experiments indicates that Ly49B may also form multimers under certain circumstances. The visualisation of a monomeric form of Ly49B in some of the non-reduced samples represents an important observation and suggests that Ly49B may exist as a monomer in endogenous cells.

Ly49B monomers and dimers appeared in Western blots as multiple bands. Analyses of Ly49B glycosylation mutants and of wild type protein digested with PNGase revealed that the multiple molecular forms of Ly49B represent the receptor at different stages of N-glycosylation. Digestion with high-mannose-specific Endo-H enzyme and surface biotinylation experiments revealed that the smallest molecular weight form in the reduced and non-reduced samples represent immature, intracellular forms of the receptor, while the larger species represent mature, surface-associated proteins. Both forms were identified in transfected and native cells.

Preliminary results indicate that immature, intracellular and mature, extracellular forms of other Ly49s and also perhaps other NK cell receptors may be detectable in Western blot experiments. Detailed analysis of individual receptors using immunoprecipitation, surface labelling and Endo-H digestion is required to unambiguously establish whether or not this is the case.

Chapter 5. Purification and refolding of Ly49B.

5.1. Introduction

Protein crystallisation is an inherently challenging process, requiring milligram quantities of pure, homogeneous, correctly folded protein. Certain features make some proteins harder to crystallise than others, including flexible, dynamic domains, post-translational modifications, a tendency to multimerise and existing natively in a transmembrane state; features which all apply to Ly49 receptors. In spite of this, crystal structures of Ly49A, Ly49C, Ly49G, Ly49I, and Ly49L have been solved to date (Tormo, *et al.* 1999; Deng *et al.* 2008; Dimasi *et al.* 2002; Back *et al.* 2009).

As outlined in **Section 1.8.** structure of Ly49B may differ significantly from other Ly49s and it would be advantageous to obtain its crystal structure in order to understand its biochemistry. In this chapter a method is described for obtaining pure, correctly folded Ly49B with the potential for use in crystallisation. The method involves cloning of the extracellular portion of Ly49B, followed by optimisation and implementation of an *E. coli* expression system. Procedures for isolation, solubilisation and refolding of Ly49B from bacterial inclusion bodies are outlined. Next, the purification using gel filtration, anion exchange and/or affinity chromatography is described. Finally, an immunoassay and circular dichroism were employed to assess the integrity of the re-folded protein.

5.2. Construct design and cloning

The Ly49B constructs used in this study were designed based on strategies applied to other Ly49s that have been crystallised to date. In the majority of previous studies the full length extracellular (EC) portion of the protein has been used, but the stalk region was problematic for crystallization, most likely due to its inherent flexibility. The first Ly49 crystal structure to be solved, Ly49A, contained only the natural killer domain (NKD), which was obtained by limited proteolysis of the refolded full length EC portion (Tormo *et al.* 1999). Since then, subsequent attempts to crystallise Ly49s have all included both the full length EC portion and the truncated NKD homologous to that of Ly49A. It has proven possible to crystallise the full length EC portion of some Ly49s (Deng *et al.* 2008). However, the diffraction pattern of the stalk region was obtained only for Ly49L and, even then, it contained only a fraction of the stalk (Back *et al.* 2009). Therefore, two sets of constructs were prepared for crystallisation of Ly49B; one containing the full length EC portion and one containing just the NKD sequence and cloned to pET24a vector.

Table 5.1. Ly49B constructs designed for this study. Full sequences of primers are listed in the materials and methods.

Construct number	Construct name	Primers used for amplification	Construct size (bp)	Approximate protein size (kDa)
1A	Ly49B EC C57	KP1, KP5	675	28
1B	Ly49B ECFX C57	KP2, KP5	687	29
1C	Ly49B NKD C57	KP3, KP5	462	18
1D	Ly49B NKDFX C57	KP4, KP5	474	19
2A	Ly49B EC BALB/c	KP1, KP5	675	28
2B	Ly49B ECFX BALB/c	KP2, KP5	687	29
2C	Ly49B NKD BALB/c	KP3, KP5	462	18
2D	Ly49B NKDFX BALB/c	KP4, KP5	474	19

To simplify the purification process, an additional set of homologous constructs was designed to incorporate the N-terminal polyhistidine (His) tag encoded by pET28b. The primers used for amplification of these constructs contained sequences corresponding to the Factor Xa cleavage site directly upstream from the start of the EC and NKD sequences, to facilitate removal of the His-tag and any extra residues encoded by pET28b between the tag and the NdeI cloning site.

Since comparison of the Ly49Bs from C57 and BALB/c strains is one of the key aims of this project, it was also necessary to prepare constructs using DNA from both of these strains. The primers designed for amplification of the EC and NKD regions of C57 Ly49B

were aligned against the BALB/c sequence and showed 100 % homology, so it was possible to use the same primers for amplification of both constructs. The 8 constructs required for this study are summarised in **Table 5.1**.

The constructs above were successfully amplified from the plasmids containing full length C57 and BALB/c Ly49B, then visualised by agarose gel electrophoresis (**Figure 5.1**). After setting up cloning reactions, the plasmids were amplified, purified and subjected to double restriction digests to produce unique restriction patterns characteristic for plasmids containing the cloned sequences or not (**Figure 5.2**). Positive clones were sent for sequencing to confirm the presence and integrity of the cloned regions. All of the constructs cloned into pET24a were found to possess the correct sequences. However, of the constructs that were cloned into pET28b only Ly49B ECFX C57 was correct. All of the remaining pET28b constructs had additional bases incorporated between the His-tag sequence and that of the construct, resulting in frame shift mutations which rendered the constructs unusable for protein expression. Several attempts were made to produce the correct pET28b constructs but all were unsuccessful. Since the extra bases seemed to originate from the primer sequences upstream of the NdeI restriction site, it was speculated that the NdeI enzyme may have been cleaving the construct at the incorrect site. Unfortunately, even after using a new stock of NdeI the extra bases were still present. Due to time constraints, expression experiments were therefore carried out using the pET24a constructs and the one intact pET28b construct.

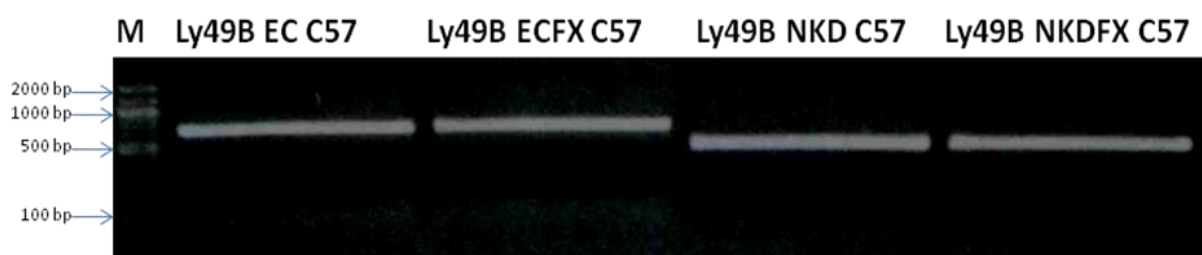


Figure 5.1. Verification of PCR amplification of C57 constructs by agarose gel electrophoresis. *M* indicates the lane containing the DNA ladder with some of the main band sizes highlighted on the left. Analogous verification was also performed for BALB/c constructs. Ly49B EC C57 construct contains full length extracellular portion of Ly49B (675 bp), Ly49B ECFX C57 contains full length extracellular portion of Ly49B and Factor Xa cleavage site (687 bp), Ly49B NKD C57 contains only NK domain (642 bp) and Ly49B NKDFX C57 construct contains NK domain and Factor Xa cleavage site (474 bp).

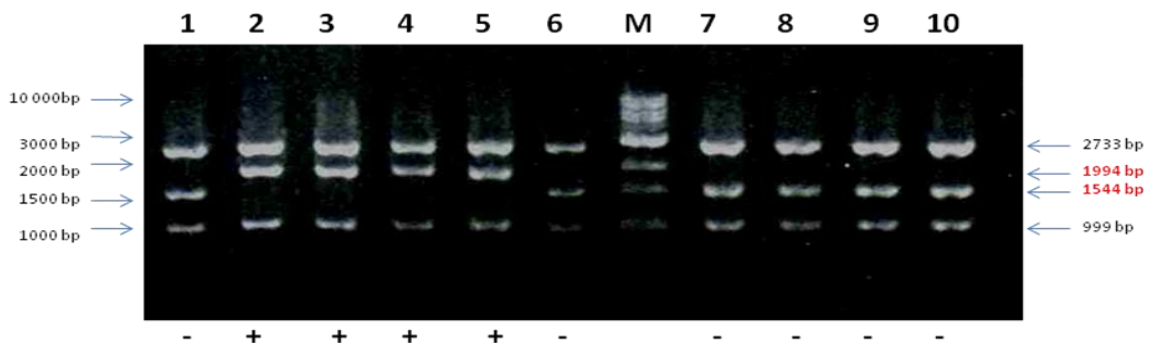


Figure 5.2. Restriction patterns of *Pvu II/Sal I* - digested *pET28b* plasmids with and without the *NKDFx C57* insert. Plasmids containing the construct are recognisable due to the 450 bp shift in the middle band. Plasmid preps of clones 2, 3, 4 and 5 were all found to contain the desired constructs. Clone numbers are indicated along the top from 1-10. M indicates the DNA ladder with some of the main increments shown on the left. The sizes of the bands of the digested plasmids are shown on the right with critical bands highlighted in red.

5.3. Ly49B expression

Expression of heterologous recombinant proteins can be an extremely challenging process, the success of which is often dependent upon the selection of an appropriate expression system. The most commonly exploited and best understood involves utilising *E. coli* strains, such as those listed in the Materials and Methods. The main advantages of such systems include high yields of recombinant protein, the ease and speed of cultivation and the tight control over protein expression (Zerbs *et al.* 2009).

However, using *E. coli* for expression of complex eukaryotic proteins such as Ly49s can be problematic, as bacteria do not support a number of processes specific to higher organisms, including the formation of disulphide bonds and post-translational modifications such as glycosylation. Basic bacterial expression systems also lack chaperones that may be needed for correct folding of some proteins. Consequently, the expression of eukaryotic proteins in *E. coli* often leads to the formation of insoluble inclusion bodies (IBs) in the cytoplasm or periplasm of the bacterium (Pain 1996; Burgess 2009; Arie *et al.* 2006). In such cases, the expressed protein is packed into high density structures, which are held together by non-covalent interactions, and are clearly visible under a light microscope. Although the conformation of proteins contained within IBs is not completely random, it is usually far from the native form. To obtain the protein in the native conformation, it is necessary to denature and refold the protein, which can be extremely problematic. For instance, IBs can be difficult to disrupt and establishing the correct conditions under which the protein readily refolds into its native state is both time-consuming and labour-intensive. Furthermore, the yields obtained on recovery from inclusion bodies are typically very low, so downstream

applications, like crystallisation, which require large amounts of protein are compromised. One advantage of extracting proteins from IBs is the relative ease of isolation from endogenous bacterial proteins, which can be achieved quite simply by multiple rounds of centrifugation, because IBs are denser than the other components of the cell.

Alternative expression systems to *E. coli* include yeast, insect or mammalian cell lines, or even cell-free expression systems (Cregg *et al.* 2009; Geisse and Fux 2009; Goren *et al.* 2009; Jarvis 2009). The main advantages of these systems are the production of soluble protein, rather than inclusion bodies, and the ability to carry out post-translational modifications. However, such systems are not without their drawbacks; yields are typically very low and the processes are time consuming. Moreover, eukaryotic cell cultures can be difficult to maintain, often requiring specialist equipment.

Taking into account the above considerations, and the fact that all Ly49s crystallised to date have been expressed recombinantly in *E. coli*, a bacterial system was also chosen for Ly49B. The candidate strains that were screened for suitability included the standard expression strain *E. coli* BL21 and a number of its derivatives. All were compatible with the pET vector expression system.

Several strains were tested on a small scale to establish which one gave the highest protein yield and whether or not Ly49B was expressed in *E. coli* in the soluble fraction, rather than as inclusion bodies. *E. coli* BL21 CodonPlus (RIL) was chosen for initial tests as it contains extra copies of the genes that encode rare tRNAs that most frequently limit translation of eukaryotic proteins in *E. coli*. In addition, the BL21 Tuner strain, which contains a mutation in the permease gene resulting in homogenous IPTG uptake by all bacteria in the population, and the Origami 2 strain, which facilitates formation of disulphide bonds in the bacterial cytoplasm, were chosen for expression trials. Unfortunately, none of the strains were able to produce soluble Ly49B. Phase contrast microscopy image shown in **Figure 5.3** illustrated that Ly49B accumulated in the cytoplasm of the bacteria in the form of inclusion bodies. Comparison of the micrographs of induced and uninduced cells revealed low levels of Ly49B expression even without induction by IPTG, probably because of the inherently leaky T7 promoter. These results suggest that Ly49B has no observable toxic effect on the bacterium.

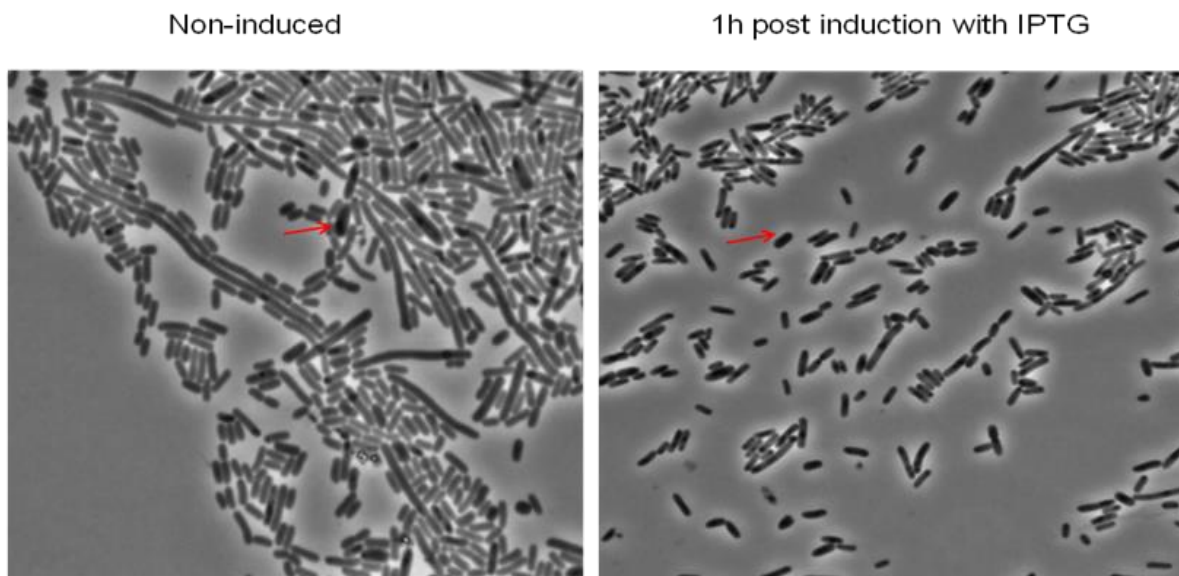


Figure 5.3. Phase contrast image of induced and non-induced *E.coli* BL21(DE3)Tuner cells transfected with an expression plasmid encoding Ly49B. The inclusion bodies marked with red arrow are visible as dark clusters inside the cells. Some of the non-induced bacteria contain inclusion bodies due to inherently leaky T7 promoter.

Since the expression of recombinant proteins is known to be greatly affected by growth conditions, the strains were tested using different IPTG levels, variable lengths of induction and a range of temperatures. Induction of Ly49B expression with different levels of IPTG (0.1 mM to 1 mM) had no observable effect on the amount of protein produced in any of the strains tested (**Figure 5.4**). There was also little observable difference between expression levels at different time points post-expression at 30°C (1-6 hours and overnight). Dropping the temperature to 16 °C did not improve expression levels; it simply increased the time required for the culture to reach a suitable density for harvesting (~16 hours). The expression levels were similar for all of the constructs in all of the strains tested, but the *E. coli* Tuner strain gave the most consistent results and was therefore chosen for large scale experiments.

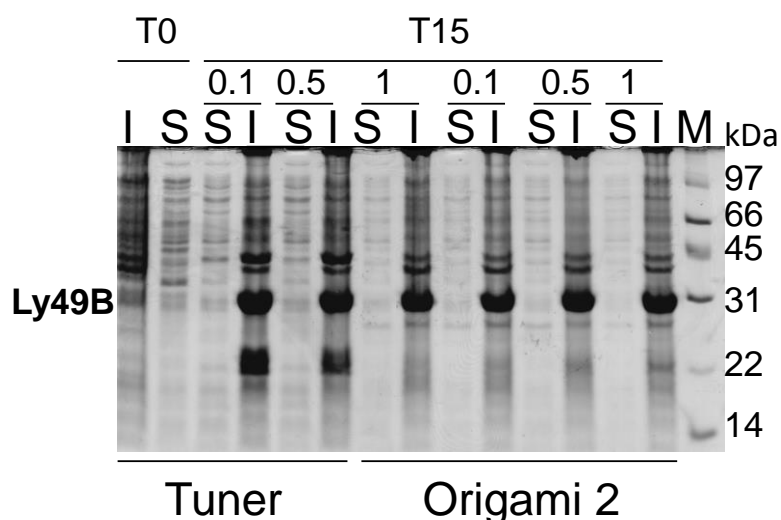


Figure 5.4. Ly49B expression test in BL21 Tuner and Origami 2 E.coli stains with varying amounts of IPTG. 10 ml cultures of E.coli BL21 Tuner and E.coli Origami 2 strains transformed with pET28 Ly49B ECFx C57 plasmid were grown at 37 °C, 200 rpm, until OD reached 0.6. The cultures were then inoculated with 0.1, 0.5 or 1 mM IPTG and incubated for 15 h at 16 °C, 200 rpm. 1 ml samples were harvested, disrupted by sonication and analysed on 15 % SDS-PAGE. S=soluble fraction, I=insoluble fraction, M= molecular weight marker, T0=before induction with IPTG, T15=15h post-induction with IPTG, 1, 0.5, 0.1=concentration of IPTG in mM.

5.4. Crude purification and solubilisation of Ly49B from inclusion bodies

The first construct to be expressed on a large scale was Ly49B EC C57 (**Figure 5.5**) following the small-scale expression procedure. Transformed BL21 Tuner cells were grown under selective conditions in 2 l of LB broth at 37 °C until the A_{600} reached 0.6. The temperature was then dropped to 30°C and the cells induced with 1 mM IPTG for 3 hours. Cells were harvested by centrifugation, resuspended in 1xPBS buffer and the culture was disrupted by sonication.

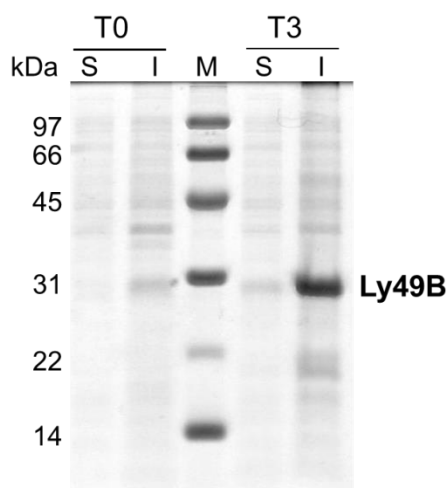


Figure 5.5. Expression of Ly49B EC C57 in E. coli BL21 Tuner strain. S=soluble fraction, I=insoluble fraction, T0=before induction with IPTG, T3= 3 h post-induction with IPTG, M= molecular weight marker

The cell membranes and soluble proteins were removed by performing multiple rounds of washing in Triton X-100 buffer (0.5 % Triton X-100, 50 mM Tris (pH8.0), 100 mM NaCl) followed by homogenisation and centrifugation. To avoid any possibility that Triton X-100 could interfere with protein folding, an extra wash was performed using detergent free buffer. The bacterial proteins were progressively removed from the Ly49B preparation at each wash step (**Figure 5.6**). After the last wash step Ly49B was solubilised and the disulphide bonds were reduced. Measurement of the optical density at 280 nm at this point indicated that roughly 150 mg of total protein was recovered from 2 l of culture.

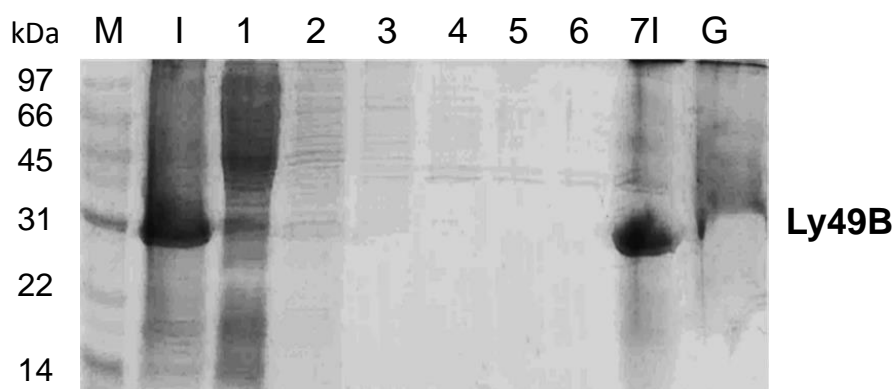


Figure 5.6. Preparation of Ly49B inclusion bodies. *M- molecular weight marker, I- insoluble fraction before washing, 1-6 subsequent washing steps (soluble material in the supernatant), 7I-insoluble fraction in wash 7, G- Ly49B solubilised in guanidine*

5.5. Development of refolding strategy.

Appropriate conditions for protein refolding need to be determined empirically. For instance, the methods used in the respective publications for Ly49 proteins are summarised in **Table 5.2**. In general, the refolding steps for Ly49 receptors listed in **Table 5.2** involved reoxidation of intrachain disulphide bonds in the presence of glutathione (5 mM oxidised and 0.5 mM reduced or 0.8 mM oxidised and 3 mM reduced) and dilution into 400-600 mM L-arginine to help prevent protein aggregation. In the case of Ly49I this process was carried out over 48 hours at 4 °C. The Ly49I refolding buffer also contained 2 mM EDTA to chelate any divalent cations that could promote proteolysis by contaminant proteases and the Ly49L refolding buffer contained 30 % (v/v) glycerol to prevent aggregation.

In the next step Ly49 refolding solutions were dialyzed at 4 °C into 25 mM Tris-HCl (pH8.0) and 150 mM NaCl or 25 mM MES (pH 5.5) and 150 mM NaCl. The presence of NaCl provided ionic strength to the solution, inhibited ionic interactions and suppressed

aggregation. In all cases, the Ly49 receptors were purified using size exclusion columns and/or by ion exchange affinity chromatography.

Table 5.2. Methods used to solubilise, refold and purify Ly49 receptors.

Receptor	Solubilisation and denaturation	Refolding	Purification	Reference
Ly49A	6 M guanidine hydrochloride (GuHCL), 0.1 mM DTT	Reoxidation in the presence of glutathione (5 mM oxidised and 0.5 mM reduced) and dilution into 0.4 M L-arginine, Dialysis to TBS (25 mM Tris HCL pH8 and 150 mM NaCl)	Affinity chromatography, Anion exchange chromatography, Size exclusion chromatography	Tormo <i>et al.</i> 1999
Ly49C	6 M guanidine hydrochloride (GuHCL), 0.1 mM DTT	Reoxidation in the presence of glutathione (5 mM oxidised and 0.5 mM reduced) and dilution into 0.4 M L-arginine, Dialysis to TBS (25 mM Tris HCL pH8 and 150 mM NaCl)	Anion-exchange chromatography, Size exclusion chromatography	Deng <i>et al.</i> 2008
Ly49G	6 M guanidine hydrochloride (GuHCL), 0.1 mM DTT	Reoxidation in the presence of glutathione (5 mM oxidised and 0.5 mM reduced) and dilution into 0.4 M L-arginine, Dialysis to TBS (25 mM Tris HCL pH8 and 150 mM NaCl)	Anion-exchange chromatography, Size exclusion chromatography	Deng <i>et al.</i> 2008
Ly49I	4 washes with 50 mM Tris HCl (pH 8), 0.5 % Triton-X-100, 100 mM NaCl, 1 mM EDTA, 1 mM DTT, one wash with the same buffer + 2 M urea. Solubilisation into 100 mM Tris, 6 M guanidine, 10 mM EDTA and 0.1 mM DTT	Folding in vitro at 4 C by slow dilution into 1 l of 0.6 M arginine, 100 mM Tris – HCl (pH 8), 2 mM EDTA, 5 mM reduced glutathione and 0.5 mM oxidised glutathione. After 48 h, the folding mixture was concentrated to a volume of 30 ml and dialyzed at 4 C against 25 mM Mes (pH 5.5), 150 mM NaCl	Size-exclusion chromatography, Anion-exchange chromatography	Dimasi <i>et al.</i> 2002
Ly49L	6 M guanidine	Dilution into 30 % glycerol, 0.4 M arginine, 3 mM reduced glutathione and 0.8 mM oxidised glutathione	Ion exchange chromatography, Size exclusion chromatography	Back <i>et al.</i> 2009

The difference in sequence and function of Ly49B compared to other Ly49s indicates the conditions required for its refolding will also differ. Nevertheless, the protocols used to refold other Ly49s provided guidance for developing a protocol for Ly49B, which will be outlined below.

Attempt #1

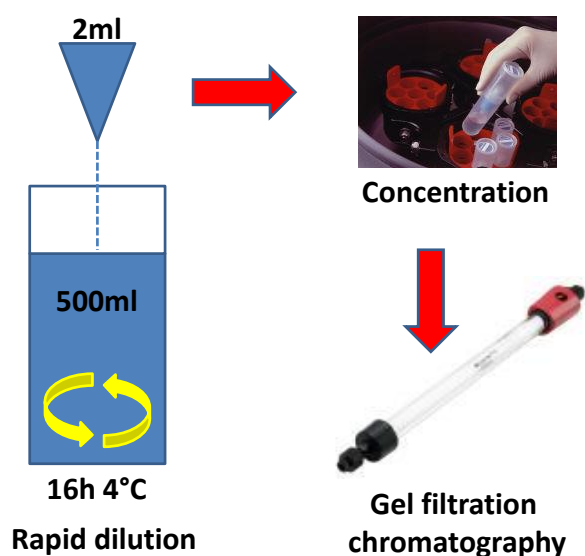


Figure 5.7. Refolding and purification of Ly49B using rapid dilution and gel filtration. 2 ml of Ly49B EC C57 solubilised in denaturing buffer (6 M guanidine hydrochloride, 50 mM Tris (pH 8.0), 100 mM NaCl, 10 mM EDTA) at a concentration of 20 mg/ml was added drop wise to 500 ml of refolding buffer 1 (Materials and Methods, **Table 2.7**) with continuous stirring, and incubated for 16 h at 4 °C. The protein was then concentrated to 2 ml volume using 50 ml Centricon concentrator (Vivacel) with a 10 kDa MW cut off. The concentrated Ly49B was applied to a pre-equilibrated Superdex-75 10/300 gel filtration column (GE Healthcare) attached to an ÄKTA chromatographic system (GE Healthcare) with buffer containing 200 mM NaCl and 50 mM Tris (pH8.0) at 0.5 ml/min. 3 ml eluted fractions were collected and analysed for UV absorbance. Centricon image adapted from <http://www.labplus.co.kr>, Superdex-75 10/300 column image adapted from <http://chromatography-online.co.uk>.

The first attempt to refold and purify Ly49B is described in detail in **Figure 5.7**. A 2 ml aliquot of Ly49B EC C57, solubilised in denaturing buffer, was refolded by rapid dilution into 500 ml of refolding buffer 1 (see Materials and Methods) and incubated for 16 hours at 4°C with continuous stirring. The sample was then concentrated to 2 ml volume using a Centricon concentrator to enable purification by gel filtration. Unfortunately, the concentration step was extremely time-consuming due to the filter becoming increasingly blocked. Furthermore, based on the A_{280} reading, approximately 50 % of the protein was lost during this step; presumably due to precipitation on the Centricon membrane. The remaining sample was purified by size exclusion using a Superdex-75 gel filtration column. The correctly folded Ly49B monomer was expected to elute in the time predicted for a protein of roughly 30 kDa, indicated by a clear, sharp peak on the UV absorbance (A_{280}) trace. The aggregated protein was predicted to elute in the void volume. Unfortunately, as shown on **Figure 5.8**, virtually all of the protein was lost during purification.

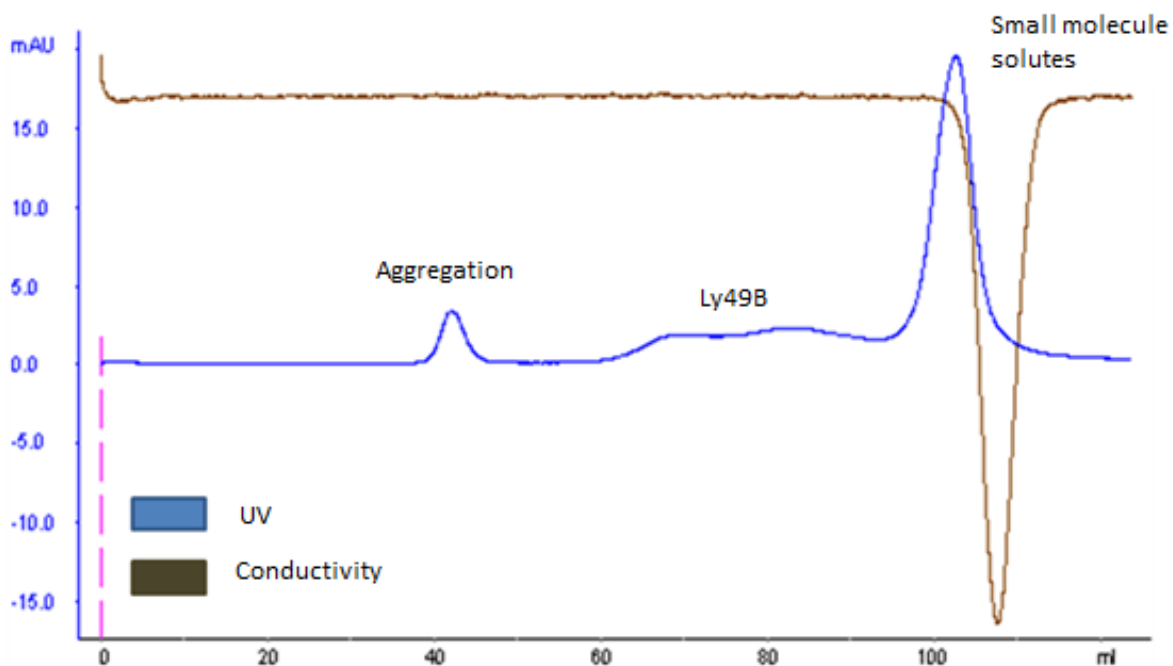


Figure 5.8. Size exclusion chromatographic purification of refolded Ly49B EC C57. Aggregated protein was eluted in the void volume. Ly49B produced two negligible peaks. The fractions with greatest UV absorbance comprised nucleotides, which were not removed during the wash step and eluted due to the change in conductivity

Attempt #2

Figure 5.9 describes details of the second attempt to refold and purify Ly49B. Ly49B ECFX C57, expressed with an N-terminal His-tag, was solubilised in denaturing buffer. To avoid the problems previously encountered when concentrating a large volume of protein solution, refolding was performed by dialysis rather than rapid dilution. Based on the A_{280} reading, approximately 20 % of the protein precipitated during dialysis. Use was made of the construct's poly-histidine tag, by incorporating an additional purification step. Affinity chromatography was performed using a nickel-charged HiTrap chelating column and the samples were analysed by SDS-PAGE (**Figure 10**).

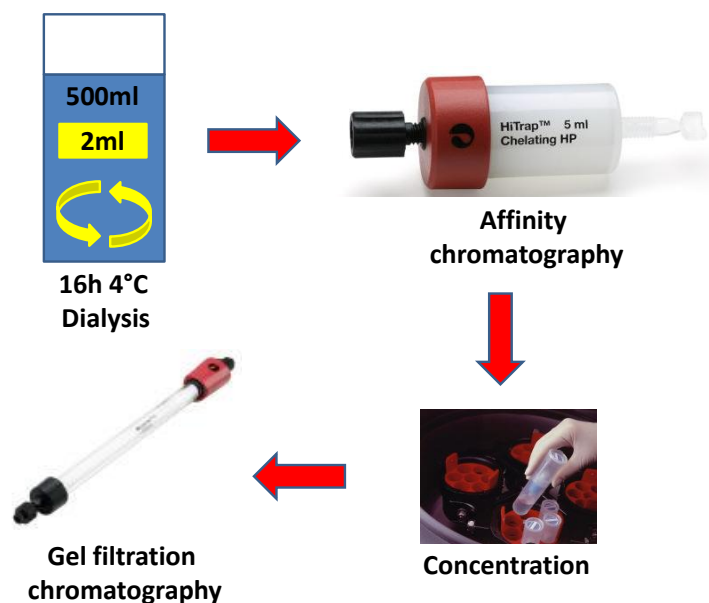


Figure 5.9. Refolding and purification of Ly49B by dialysis, affinity chromatography and gel filtration chromatography. 2 ml of Ly49B ECFX C57, solubilised in denaturing buffer (6 M guanidine hydrochloride, 50 mM Tris (pH 8.0), 100 mM NaCl), was dialysed with continuous stirring for 16 h at 4 °C into 500 ml of refolding buffer 1 (Materials and Methods, **Table 2.7**). The protein solution was applied at 1 ml/min to a pre-equilibrated nickel-charged 5 ml HiTrap Chelating HP column (GE Healthcare) attached to an ÄKTA chromatographic system and eluted over a linear 30 ml gradient of 0-500 mM imidazole in 25 mM Tris-HCl (pH 8.0), 500 mM NaCl at 1 ml/min. 3 ml fractions were collected, analysed by SDS-PAGE and the peak fractions were pooled together and concentrated to 2 ml volume using a 50 ml Centricon concentrator (Vivacel) with a 10 kDa MW cut off insert. Ly49B was purified using a pre-equilibrated Superdex-75 10/300 gel filtration column (GE Healthcare) attached to an ÄKTA chromatographic system (GE Healthcare) with buffer containing 200 mM NaCl and 50 mM Tris (pH 8.0) at 0.5 ml/min. 3 ml fractions were collected following purification. Centricon image adapted from <http://www.labplus.co.kr> , Superdex-75 10/300 column image adapted from <http://chromatography-online.co.uk>, Hi-Trap Chelating HP column image adapted from <http://www.gelifesciences.com>

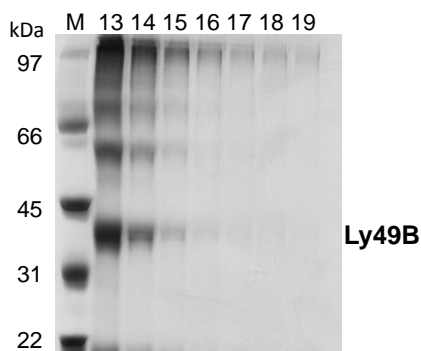


Figure 5.10. 10 % SDS analysis of Ly49B ECFX C57 purified by affinity chromatography. M=molecular weight marker, 13-19=numbers of fractions containing Ly49

Following purification on the chelating column, 3x3 ml eluted protein fractions were pooled together and Ly49B was purified by gel filtration as described in the Materials and Methods. Unfortunately, the purified Ly49B appeared to be incorrectly folded as the UV

absorbance spectrum showed broad, irregular peaks. Moreover, the amount of protein recovered was negligible.

Attempt #3

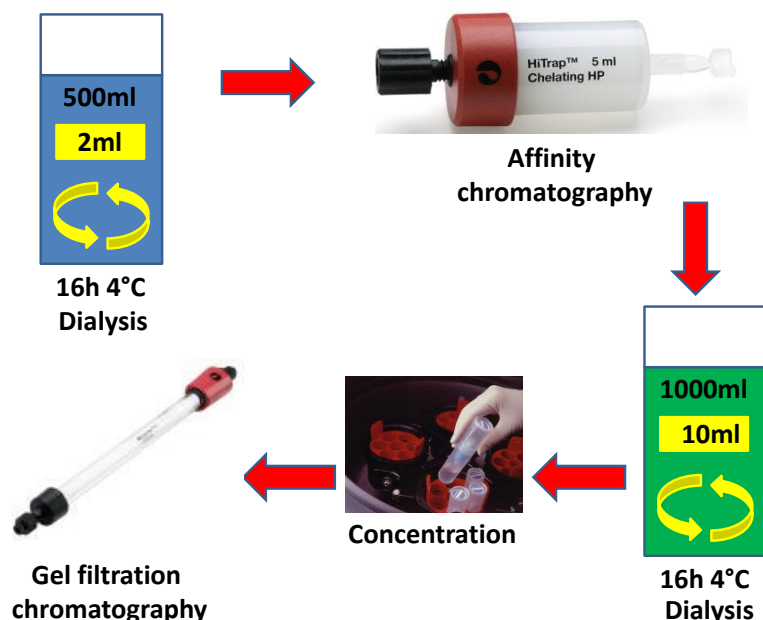


Figure 5.11. Refolding of Ly49B by dialysis, affinity chromatography and gel filtration chromatography. 2 ml of Ly49B ECFX C57, solubilised in denaturing buffer (6 M guanidine hydrochloride, 50 mM Tris (pH 8.0), 100 mM NaCl), was dialysed with stirring for 16 h at 4 °C into 500 ml of refolding buffer 1 (Materials and Methods, **Table 2.7**). The protein solution was applied at 1 ml/min to a pre-equilibrated nickel-charged 5 ml HiTrap Chelating HP column (GE Healthcare) attached to an ÄKTA chromatographic system and eluted over a linear 30 ml gradient of 0-500 mM imidazole in 25 mM Tris-HCl (pH 8.0), 500 mM NaCl at 1 ml/min. 3 ml fractions were collected; the peak fractions were pooled together and dialysed with continuous stirring for 16 h at 4 °C into 1 l of gel filtration buffer containing 200 mM NaCl and 50 mM Tris (pH 8.0). Ly49B was then concentrated to 2 ml volume using a 50 ml Centricon concentrator (Vivacel) with a 10 kDa MW cut off insert and purified using a pre-equilibrated Superdex-75 10/300 gel filtration column (GE Healthcare) attached to an ÄKTA chromatographic system (GE Healthcare) at 0.5 ml/min. 3 ml fractions were collected following purification and the peak fractions were analysed by 15 % SDS-PAGE. Centricon image adapted from <http://www.labplus.co.kr> , Superdex-75 10/300 column image adapted from <http://chromatography-online.co.uk>, Hi-Trap Chelating HP column image adapted from <http://www.gelifesciences.com>.

It is possible that the second attempt failed because the protein aggregated under gel filtration conditions. In the next attempt (described in **Figure 5.11**) the His tag-purified preparation of Ly49B ECFX C57 was first dialysed into gel filtration buffer over 16 hours, which was gentler method to mix the protein with gel filtration buffer. However, ~90 % of the protein still precipitated. The remaining protein was purified by gel filtration using the S75 column, as previously described. **Figure 5.12** shows that Ly49B ECFX C57 eluted over 7x3 ml fractions 65-85 minutes post-injection.

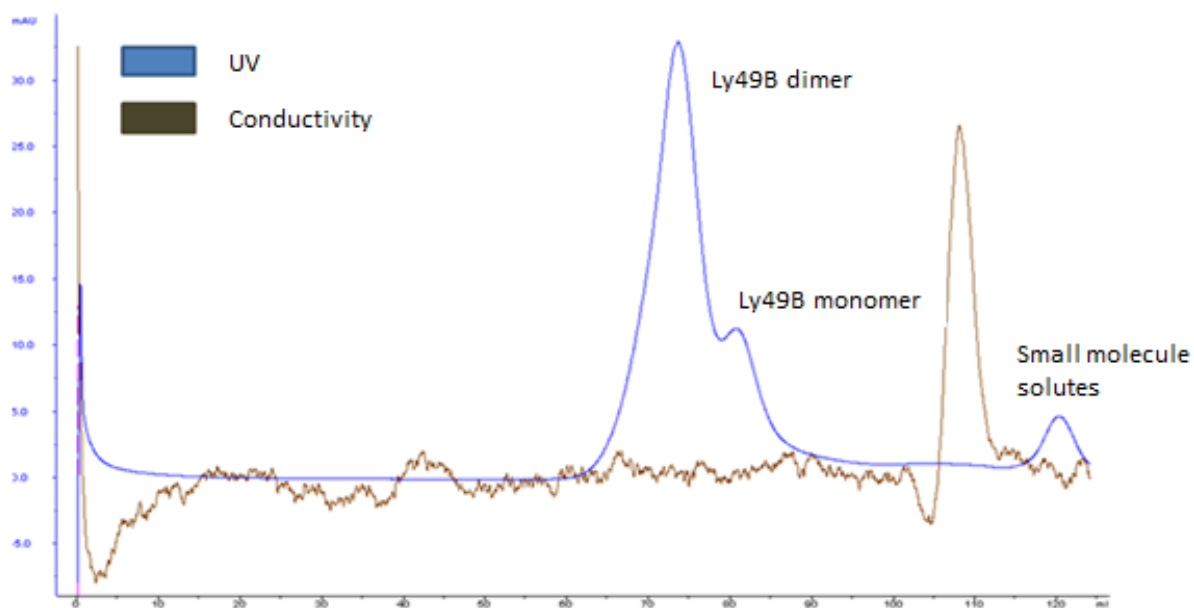


Figure 5.12. Gel filtration of Ly49B ECFX C57

Two predominant peaks were present on the trace at 75 and 85 minutes, most likely representing Ly49B dimer and monomer populations respectively. The fractions were analysed by 15 % SDS-PAGE (**Figure 5.13**) and pooled giving a total of 400 μ g of Ly49B, which was insufficient for crystallisation. However, the apparent purity and integrity of the protein meant that it was suitable for the developing of an assay to assess whether or not the Ly49B preparation was folded correctly.

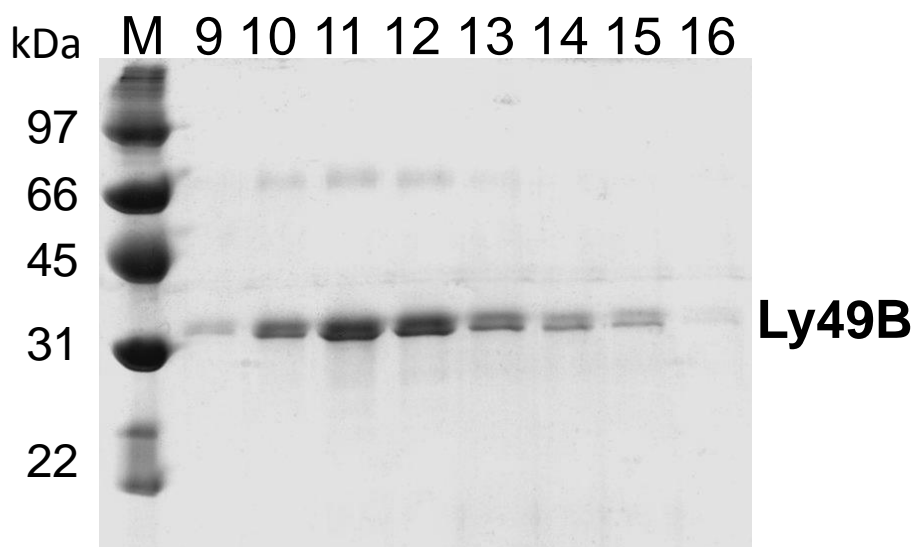


Figure 5.13. 15 % SDS-PAGE analysis of Ly49B ECFX C57 purified by gel filtration. M=molecular weight marker, 9-16=numbers of fractions containing Ly49B.

Subsequent attempts

Numerous other refolding attempts were made using a range of buffers (described in Materials and Methods **Table 4**), varying the starting amount of protein (from 7 mg to 100 mg), refolding by dialysis or rapid dilution and concentrating using a large scale concentrator, rather than a Centricon. Different constructs were tested and ion exchange columns used with untagged constructs. However, all of these strategies gave low yields due to protein aggregation and the production of partially-folded or incorrectly folded Ly49B. Nevertheless, it was possible to set up preliminary crystallisation screens in 96 well formats. Ly49B NKD C57 protein concentrated to 4 mg/ml and 5.6 mg/ml was screened for crystallisation using JCSG, PACT and STRUCTURE pre-made grid screens (Molecular Dimensions), set up in sitting drops using the Mosquito Crystallisation robot (TTPLabtech). Ly49B EC C57 protein was also subjected to crystallisation screening at 4.5 mg/ml in the same way as for Ly49B NKD C57. Unfortunately, no crystals were obtained.

5.6. Assessment of the refolded Ly49B

5.6.1. Assessment of the refolded Ly49B using pull-down assay

The proteins folding patterns in the native conditions are precisely defined but the potential folding patterns for a given protein outside of its natural environment are numerous. It is therefore necessary to assess whether or not *in vitro* refolding faithfully reproduces the *in vivo* conformation. As discussed previously, the gel filtration trace provides an indication of a protein's integrity; a tendency not to aggregate is an indicator of stable folding, though the conformation may not represent the most stable thermodynamic form. A functional assay therefore ought to be applied whenever possible, for instance, by comparing the catalytic activities of refolded and native enzymes. Unfortunately, the assessment of the activity of extracellular portion of Ly49B would be difficult, as it is not an enzyme, lacks a signalling domain and is not attached to the cells whose action it regulates. Instead, the tendency of monoclonal antibodies to bind to properly-folded proteins (e.g. Bogdanov et al. 1996; Middelberg 2002)-was used in this study.

To address the question whether or not Ly49B ECFX C57 was folded correctly an assay was developed using nickel charged agarose beads. Since Ly49B ECFX C57 was His-tagged, mixing equimolar amounts of the protein and the monoclonal 2G4 anti-Ly49B antibody with an excess of the Ni agarose beads was expected to lead to crosslinking of the

three components. As shown in **Figure 5.14** the antibody on its own did not bind the beads, whereas Ly49B alone and Ly49B mixed with the antibody did bind to the beads. Since virtually all the antibody was occupied by the refolded Ly49B, these results suggested that the majority of the protein refolded correctly. Unfortunately, this assay is only applicable to the tagged protein.

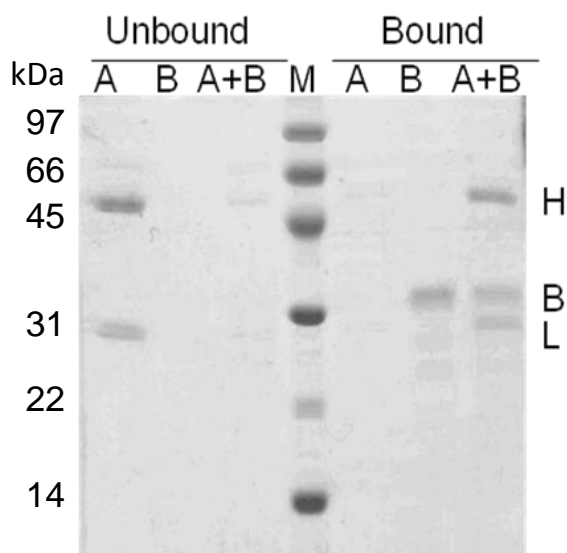


Figure 5.14. Ly49B binding assay. NiNTA beads were incubated with refolded Ly49B ECFX C57 (B), 2G4 anti-Ly49B antibody (A) or with both of those components together (A+B). Supernatant samples were collected following the incubation period. The beads were then washed and the bound protein was eluted with 200 mM Imidazole. Eluted protein samples (right hand side of the molecular weight marker) and the samples collected prior to elution (left hand side of the molecular weight marker) were analysed by 15 % SDS-PAGE A= 2G4 anti-Ly49B antibody, B=Ly49B ECFX, M=molecular weight marker. H=heavy chain of the antibody, L=light chain of the antibody.

5.6.2. Assessment of the refolded Ly49B using circular dichroism (CD)

The immunoassay described in **Section 5.6.1.** is suitable only for His-tagged proteins. The presence of a polyhistidine tag can interfere with the crystallisation process and/or affect protein structure. It is thus preferable to use untagged proteins for structural studies. In those cases where a tag *is* necessary for purification, it is often best to remove it prior to crystallisation and it is imperative to check that the protein's integrity has not been affected during the process. Circular dichroism (CD) is often used as a means of assessing folding of proteins and does not rely on the presence of a tag. In CD, protein samples are subjected to left and right circularly polarised light and the difference between the absorption of the two is measured. Differences arise due to structural asymmetry (Berg *et al.* 2002). Peptide bonds act as chromophores and the secondary structure of proteins is determined by analysis in the far UV spectrum (190-250nm) (Berg *et al.* 2002). Each protein structure generates characteristic CD spectrum; the unfolded proteins generate pattern characteristic for a simple peptide bond (Gokce *et al.* 2005). **Figure 5.15** shows typical spectra for a correctly folded alpha helix, a beta sheet and a random coil structure.

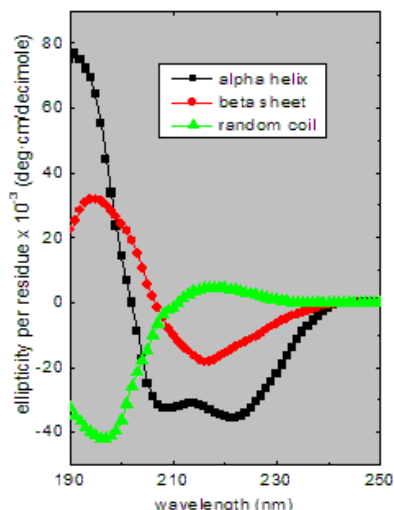


Figure 5.15. Typical CD spectra for an alpha helix, a beta sheet and a random coil structure. Figure adapted from http://www.ap-lab.com/circular_dichroism.htm

Figure 5.16 shows CD spectra of unfolded and re-folded Ly49B EC C57. Following solubilisation of Ly49B EC C57 from inclusion bodies, an aliquot of sample was retained for CD analysis, while the remainder of the protein was used for refolding and purification. Solubilised and refolded samples of Ly49B EC C57 were then compared by CD analysis at 1 mg/ml. The solubilised sample gave a spectrum typical for a protein dissolved in the presence of guanidine hydrochloride (Smith *et al.* 1997). The refolded sample produced a spectrum typical of an ordered protein, containing elements of beta sheets, alpha helices and random coils, which is consistent with the content of secondary structures for Ly49B EC C57 construct predicted by GOR IV secondary structure prediction server (30 % alpha helix, 20 % beta sheet and 52 % random coil) and previously determined structures of other Ly49s.

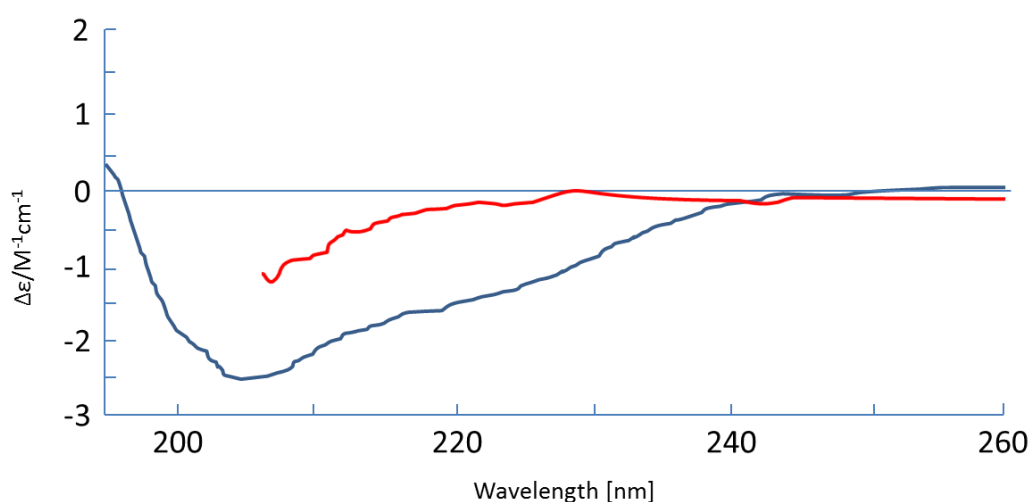


Figure 5.16. Circular dichroism spectra of unfolded and re-folded Ly49B EC C57 at 1 mg/ml. Blue trace = folded protein, red trace = unfolded protein.

5.7. Summary

In this chapter a method is presented for recombinant expression of the extracellular portion of Ly49B in *E. coli*, followed by refolding and purification. Unfortunately, none of the tested *E. coli* strains were able to support expression of soluble protein, most likely due to the lack of appropriate chaperones required for eukaryotic protein folding, as well as the bacteria's inability to support eukaryotic-specific post-translational modifications, such as glycosylation. Ly49B was deposited in the cytoplasm of the bacteria in the form of inclusion bodies. Following induction tests, it was established that the *E. coli* Tuner (DE3) strain was most efficient at Ly49B expression and was therefore used for subsequent large scale preparations.

Extracting and reconstituting Ly49B from inclusion bodies was the most problematic part of the procedure due to the large quantities of protein that were lost during this process. For the untagged version of Ly49B refolding was performed by rapid dilution into a large volume of refolding buffer. The protein was then concentrated and purified by gel filtration. For the tagged version of the protein it was possible to refold by dialysis, thereby avoiding the lengthy concentration process. Purification was therefore performed using affinity chromatography, followed by dialysis into gel filtration buffer and a second round of purification by gel filtration chromatography. Both procedures gave low yields. However, enough protein was obtained to set up several crystallisation trials. The remaining protein was used to develop a method for confirming the integrity of the refolded protein using an immunoassay and circular dichroism. Further optimisation is needed to increase yields of the refolded Ly49B. However, the method described here represents a good starting point for auxiliary optimisation.

6. Discussion

A monoclonal anti-Ly49B antibody named 1A1 was previously found to bind only the C57 form of Ly49B but not the BALB/c form (Gays *et al.* 2006). The study presented here shows that MHC class I tetramers selectively associate with BALB/c but not C57 Ly49B isoform. These observed differences suggest that the two forms of Ly49B may possess different three dimensional structures and perhaps fulfil different roles. Since the two forms differ by 12 amino acids, it follows that one or more of these variable residues are responsible for the selective mode of binding of MHC class I ligands and the 1A1 antibody. The existence of these two naturally occurring variants presented a unique system for studying interactions between Ly49 molecules and their ligands.

Until now the majority of studies that have aimed to identify interaction sites between Ly49s and their ligands were based on available crystal structures of either Ly49s or related C-type lectin-like molecules (Kielczewska *et al.* 2007, Deng *et al.* 2008, Sundback *et al.* 2002, Lian *et al.* 1999, Dam *et al.* 2003). Sequence alignments in combination with crystal structures have been used to identify putative residues involved in ligand binding, which were then mutated to assess their effect on ligand binding.

Crystallography has also been directly used to identify residues responsible for Ly49 ligand binding. Co-crystal structures of Ly49A-H-2D^d and Ly49C-H-2K^b complexes have been solved, which have enabled identification of Ly49 residues that form hydrogen bonds or salt bridges with residues in MHC class I ligands (Tormo *et al.* 1999, Dam *et al.* 2003).

The benefits of crystallography in identifying interaction sites are manifest; three dimensional models enable visualisation of proteins and modelling of the manner in which they sterically fit with other molecules. However, crystallographic approaches are not without limitations and it is worth bearing these in mind when considering such data. For example, growing protein crystals requires milligram quantities of pure, soluble, homogenous protein. Ly49s and MHC class I molecules are heavy glycosylated and exist endogenously as transmembrane molecules; features which can significantly interfere with crystallisation. The Ly49s and their ligands, whose crystal structures were solved, were expressed without their transmembrane and intracellular domains. The proteins in these studies were recombinant and expressed in *E. coli*, which does not support glycosylation. It is therefore possible that under native conditions, where full-length proteins are expressed and undergo glycosylation,

interactions sites differ from those identified by crystallography. Neighbouring proteins, located within the membrane, may also affect receptor-ligand interactions. It is important to consider that under native conditions proteins might exhibit greater mobility due to dynamic interactions with the local environment so residues responsible for ligand binding may vary depending on the adopted conformation. In a crystal, on the other hand, proteins are immobilized and, as such, the structure represents only a “snapshot” of the interaction. For these reasons the putative interaction sites, which have been identified to date using crystal structures, must be treated with caution and verified by a combination of other approaches. The best such example of this is Ly49A, whose co-crystal structure with H-2D^d ligand revealed two interaction sites (Tormo *et al.* 1999). Subsequent studies using different methods have since demonstrated that only one of these sites is functional (Doucey *et al.* 2004, Back *et al.* 2011).

One of the key advantages of this study is that the residues responsible for ligand and monoclonal antibody binding by Ly49B have been narrowed down to 12 variable amino acids between C57 and BALB/c forms. Systematic replacement by side directed mutagenesis of C57-specific residues with BALB/c-specific residues, followed by assessment of the mutated proteins for binding of both MHC class I ligands and the monoclonal 1A1 antibody, allowed precise identification of residues responsible for forming interactions.

The work presented here indicated that two variable amino-acids at positions 166 and 167 are able to affect binding of the monoclonal 1A1 antibody. Together with residue 251, these same two residues appeared to determine binding of MHC class I tetramers. The C57 residue at position 166 was shown to be necessary and sufficient for binding of the 1A1 antibody to chimeric Ly49B molecules, unless the remaining 11 variable residues were all of BALB/c origin. In order to maintain the integrity of the 1A1 epitope in the BALB/c background, introduction of the C57 residue at position 167, as well as 166, was required. This finding suggests that even though variable residues other than 166 and 167 do not directly influence 1A1 binding, they may indirectly affect the conformation of the 1A1 epitope. Since the presence of C57 residues at positions 166 and 167 can induce 1A1 binding in the BALB/c Ly49B background, one can conclude that these residues may play a critical role in the overall folding and function of Ly49B. Indeed, it was found that the combination of BALB/c residues at positions 166, 167 and 251 was optimal for binding of all three of the tested MHC class I tetramers. Interestingly, binding was strongest for mutants with BALB/c

residues at positions 166, 167 and 251 and C57 residues at all of the remaining variable positions.

Staining of cells expressing chimeric Ly49B mutants with MHC class I tetramers have shown that H-2D^b binding was less restricted by the sequence of the variable Ly49B residues than H-2K^b and H-2D^d binding. These results explain to some extent the hierarchy of tetramer binding to wild type BALB/c Ly49B; H-2D^b was found to bind most strongly out of all tested ligands, while the H-2K^b and H-2D^d were binding at a similar level to each other, roughly 40 % weaker than H-2D^b.

Taking into consideration the results obtained for Ly49A mutants (**Section 3.7**), it seems that residues equivalent to Ly49B residues 166 and 167 are also critical for the structure and function of Ly49A. This finding was somewhat surprising since these residues were not identified as important for forming ligand interactions in a published co-crystal structure of Ly49A and H-2D^d (Tormo *et al.* 1999). However, as shown in **Appendix I**, these residues form part of the α -1 helix and are positioned right next to the β 1-sheet, creating a “hinge” in Ly49A. Furthermore, both α -1 and β -1 contain residues that were shown in the crystal structure to come into contact with the MHC class I ligand. It is possible that introducing changes at the “hinge” of Ly49A and in proximity to residues critical for ligand binding may have a dramatic effect on the overall folding of the protein and, through this, on ligand and antibody binding. Moreover, as previously mentioned, it is probable that the contact residues identified in the crystal structure are slightly different to those found in native conditions. Ly49C K225 and I226 residues were identified by a mutagenesis study to be important for ligand binding even though they were shown not to be directly involved at the ligand binding site in a co-crystal structure of Ly49C/H-2K^b (Sundback *et al.* 2002). Kielczewska *et al.* have shown that residues, which lie on the interface of the Ly49H dimer, also affect ligand binding (Kielczewska *et al.* 2007). Considering targeted mutagenesis of receptors from a broader context, point mutations introduced to a glucocorticoid receptor at distant positions from the co-activator binding surface and ligand binding pocket have been shown to improve transcriptional activity and affinity for aldosterone, respectively (Carlson *et al.* 2005).

The C57 and BALB/c forms of Ly49B contain an additional 20 amino acids at the molecules' C-terminus in comparison to other Ly49s. Curiously, binding of the control 2G4 anti-Ly49B antibody to mutants, which were deprived of this region, was completely

abolished, suggesting that the 2G4 epitope lies within this 20 residue region or that its correct folding is dependent on the C-terminus. Binding of MHC class I tetramers was not affected, suggesting that this region is not important for ligand binding.

However, the role of the C-terminus in ligand binding was apparent when staining of transfectants expressing HA-tagged and untagged molecules was compared. HA-tagged Ly49B stained weaker with all three MHC class I tetramers than its untagged counterpart. As with previous results, the effect was least noticeable for the H-2D^b tetramer. In the case of Ly49A staining, the presence of the HA-tag had a positive effect on binding. These results suggest that either the presence of the HA-tag at the C-terminus affects folding of Ly49 receptors or it directly interferes with ligand binding. Interestingly, one study suggested that the presence of HA-tag was able to completely abolish ligand binding by Ly49B (Scarpellino *et al.* 2007). This study shows that HA-tag may influence ligand binding but is unlikely to prevent it.

Several Ly49s and other NK cell receptors have been shown to exist as disulphide-linked dimers on the cell surface (**Appendix II**). This study reveals that Ly49B also has a tendency to multimerise, both in transfected and in native cells. SDS-PAGE analyses of material containing Ly49B glycosylation mutants and de-glycosylated wild type Ly49B show that, in the presence of 2ME, Ly49B migrates at the predicted molecular weight of ~34 kDa, while non-reduced material migrates at ~80 kDa, which is slightly larger than the combined weight of two monomers. This observation suggests that Ly49B monomers may associate with a different, slightly larger protein through the formation of disulphide bridges, or that Ly49B forms homodimers whose migration by SDS-PAGE is slightly retarded due to the presence of disulphide bridges in between two monomers and within the globular domains. The second explanation would seem more likely due to the tendency of the protein to dimerise during purification of the extracellular portion of Ly49B, as observed by SDS-PAGE analysis of the purified fractions and from gel filtration traces. The fact that other members of the Ly49 family have been shown to dimerise by immunoprecipitation, Western blotting, and X-ray crystallography adds further weight to the possibility that Ly49B forms dimers. Migration of protein complexes on SDS-PAGE is known to be affected by the presence of disulphide bonds (Dunker and Kenyon 1976). SDS denaturation is often referred to as “reconstructive denaturation”, because it does not result in complete unfolding of the protein, but rather in aggregation of the detergent particles on its hydrophobic surfaces, which

forces proteins into stretched conformation (Imamura 2006). Rath *et al.* showed that differential solvation by SDS may result from replacing detergent-protein contacts with protein-protein contacts (Rath *et al.* 2009), such as those provided by disulphide bonds.

Interestingly, some of the Western blot experiments presented here show that Ly49B may engage in complexes larger than dimers, which appear as a large molecular weight band of ~200 kDa in SDS-PAGE analyses. The same tendency has been observed for Ly49A and Ly49Q by other groups (Takei 1983; Toyama-Sorimachi *et al.* 2004). In the experiments presented here the 200 kDa Ly49B band was not present in all experiments and was diminished following immunoprecipitation and incubation at 37 °C for 1 h, suggesting that the complex may not be stable. It is also possible that the 200 kDa band represents protein aggregation, which developed following cell lysis, rather than true Ly49B multimers.

The Ly49B monomer was observed in non-reduced samples in some, but not all, experiments, suggesting that the monomeric Ly49B may exist in living cells under certain conditions. However, it is possible that this observation may have resulted from 2ME spill-over from neighbouring, reduced samples. Interestingly, the Ly49G monomer was also observed in a non-reduced sample, and in this case the gel did not contain any reduced samples, which excluded the possibility that the obtained result was caused by 2ME spill-over. The non-reduced sample of Ly49G was analysed in parallel with four other Ly49 receptors and the Clrg NK cell receptor on the same gel; monomeric forms could not be observed in any of the other samples, even after prolonged exposure. Furthermore, monomeric Ly49G has also been observed in non-reduced samples by another group (Mason *et al.* 1988).

The observation that Ly49B and/or other Ly49 receptors could potentially exist in living cells in the form of monomers, dimers and oligomers raises the possibility that each of these molecular forms fulfils a different role. KIR receptors, human functional orthologues of Ly49s, exist as monomers and tend to cluster in a doughnut shape configuration around central LFA-1/ICAM-1 receptor clusters at NK cell immune synapses (Davis *et al.* 1999). This clustering is thought to be necessary for effective signal transduction. Dendritic cell SIGN receptors, which like Ly49s are C-type lectin-like molecules, have been found in different states of organisation (monomers to oligomers), depending on the developmental stage of the cells that they are expressed on (Cambi 2003). Moreover, the adhesion molecule, P-selectin, exists in platelets and epithelial cells as monomers and dimers; the P-selectin

monomers have been shown to exhibit distinct biochemical properties to individual subunits in P-selectin homodimers and are therefore thought to fulfil different roles (Barkalow *et al.* 2000).

Glycosylation plays an important role in both the folding and the function of many eukaryotic proteins (Taylor *et al.* 2006). Surface expression of C57 and BALB/c Ly49B mutants, in which all of the glycosylation motifs were disrupted, was shown here, by flow cytometric analysis, to be compromised in comparison to wild type counterparts. This result suggests that glycosylation is not absolutely required for Ly49B expression, but may be important, for correct folding and stability of Ly49B. Eukaryotic chaperones called calnexin and calreticulin act as quality control checkers for the majority of glycosylated proteins and prevent egress of misfolded proteins from the ER to the Golgi apparatus (Taylor *et al.* 2006). Aberrant glycosylation of proteins has been shown to affect protein interactions with the aforementioned chaperones (Molinari and Helenius 2000, Deprez *et al.* 2005, Daniels *et al.* 2003). It is possible that the refolding experiments performed here, using Ly49B expressed as inclusion bodies, gave low yields partially due to the fact that the refolded protein did not contain glycans facilitating its folding and stability.

The Ly49B monomers and dimers were shown here by Western blotting to exist in transfected and native cells in multiple molecular weight forms, which represent the receptor at different stages of N-glycosylation. The smallest molecular weight forms identified in the reduced and non-reduced samples in Western blot experiments represent immature, intracellular, high-mannose forms of the receptor, while the larger forms represent surface-associated, mature forms. The intracellular form has never been shown before for any other Ly49 receptor, mainly because of the methodologies used for investigating the molecular nature of Ly49s. Traditionally, the majority of experiments have been performed on surface-labelled Ly49s, enabling visualisation of the surface associated forms *only*. Another example, where a multiple banding pattern was overlooked, concerns YE1/48 anti-Ly49A affinity purification of Ly49A from MBL-2 cells (Chan and Takei 1988). Purified material was analysed by non-reducing SDS-PAGE and visualised by silver staining. The sample contained a predominant band at ~95 kDa, a clear band at 200 kDa and a weak band at ~85 kDa. The band at ~95 kDa was thought to be Ly49A and the 200 kDa band was thought to be non-specific aggregation or Ly49A multimer. The weak band was thought to represent an impurity, rather than a differentially glycosylated form of Ly49A. An example of an

experiment that did allow visualisation of intra- and extracellular Ly49 receptors was performed by Ortaldo *et al.*, who used anti-phosphotyrosine antibody for blots of non-reduced Ly49A, Ly49C, Ly49D and Ly49G2, which had been immunoprecipitated using monoclonal antibodies from NK cells of different mouse strains (C57, BALB/c, CB6F1, C3H/HeJ, DBA2 and AKR) (Ortaldo *et al.* 1999). Phosphorylated Ly49A, Ly49C and G2 appeared as multiple bands, which varied slightly in size between different strains. This variation was thought to be due to different glycosylation patterns in each of the strains. However, the authors did not comment on the multiple banding pattern seen in the individual samples of the detected Ly49s from each mouse strain.

The existence of a relatively abundant pool of intracellular, immature NK receptors, as well as surface-associated mature forms, may be important for the function that NK cells fulfil. It may not be favourable for the cell to constitutively display all available receptors on the surface, but the existence of an intracellular reservoir would enable a rapid increase in the number of surface-associated receptors when required, for example in a pathological situation. Rather than investing energy in *de novo* synthesis of receptors, glycan modification of existing, intracellular proteins would allow instantaneous export of the protein to the surface. It is worth noting that the high mannose form of Ly49B is more abundant in the C57 strain than in BALB/c, suggesting that the receptor may fulfil different roles in the two strains.

The co-existence of immature and mature versions of a protein in similar quantities has been reported for other eukaryotic proteins. One example of a protein that exhibits a multiple banding pattern in Western blot experiments is the MHC-DM molecule, which facilitates peptide loading of classical MHC class II molecules in the endosomal compartments of antigen presenting cells. MHC-DM is a heterodimer composed of two chains: DM α and DM β . DM α appears as a doublet in Western blot experiments, but only when co-expressed with DM β (Denzin *et al.* 1996, Van Ham *et al.* 1996, Sanderson *et al.* 1996). A recent publication revealed that the smaller band represents a high mannose, immature form of the protein, while the larger band represents a mature form of DM α , which arises from a glycan modification at N15 (Lith and Benham 2006). This example shows that molecular forms of proteins at different stages of glycosylation can co-exist in similar proportions within the same cell.

Another intriguing example is that of the D² dopamine receptor, which is expressed in two differentially spliced forms: long and short (Fishburn *et al.* 1995). Pulse chase experiments have shown that the short form of the protein is processed from the ER to the cell surface much faster than the long form. Moreover, the short form exists predominantly as a mature surface-associated protein, while a proportion of the long form of the protein remains intracellularly as an immature, high mannose form. Mature and immature variants of the long form of the D² receptor co-exist natively in similar proportions, as observed here for Ly49B. It is not clear why the long form of the D² receptor is retained in the ER more efficiently than the short form, but it is likely to be related to their differing biochemical properties and the respective functions that they fulfil.

The role of Ly49 glycosylation in ligand binding has previously been assessed for Ly49D and Ly49G2 (Mason *et al.* 2003). It was shown that unglycosylated Ly49D and Ly49G2 bind H-2D^d MHC class I ligand more strongly than controls. The presence of carbohydrates at a glycosylation motif, which is specific to Ly49D and Ly49G2 (NTT221-23) and adjacent to the MHC binding site identified in a Ly49A-H-2D^d co-crystal, was shown to lower the affinity of these receptors for H-2D^d. A recent study has shown that differential glycosylation of the human activating NK cell receptor, NKp30, may allow the receptor to recognise a series of different ligands (Hartman *et al.* 2011).

Ly49B contains four predicted N-glycosylation motifs, three of which reside in the predicted stalk region of the protein and the fourth in the CRD (**Appendix I**). Mutants with the four sites disrupted, individually and together, were created and analysed using Western blotting and flow cytometry. BALB/c Ly49B mutants with all glycosylation sites disrupted associated with all of the tested MHC class I tetramers to a similar extent as the wild type protein, suggesting that Ly49B glycosylation is not a prerequisite for ligand binding. Small variations in binding levels can be attributed to much lower expression levels of the mutant receptors, compared to the wild type.

Western blot analysis has shown that all of the individual Ly49B motifs are glycosylated. Mutation of N94 did not have a significant effect on binding of any of the tetramers, suggesting that the presence of carbohydrates at this position does not affect ligand binding. Single glycosylation mutants, N105Q and N114Q, bound all three tetramers more strongly than the wild type protein, confirming that glycans are present at these positions and, furthermore, that even though they are not required for ligand binding, they appear to fine

tune the process of association. Interestingly, the two glycosylation motifs reside in the stalk region of Ly49B, which suggests that either the ligands come into direct contact with the stalk or that the glycans at these positions can affect the overall folding of Ly49B. The majority of Ly49s contain two conserved glycosylation motifs in the stalk region, but in Ly49B one of these motifs is shifted by four residues in relation to the conserved position (**Appendix II**). The same motif contains a conserved cysteine in Ly49s other than Ly49B, which may be involved in disulphide bond formation and therefore is unlikely to be glycosylated. This motif was shown experimentally not to be glycosylated in Ly49D (Mason *et al.* 2003). Moreover, Ly49B contains one more, non-conserved glycosylation motif in the stalk region. Ly49B was shown to be incapable of associating with its ligand in *cis* (Scarpellino *et al.* 2007). It would be interesting to investigate whether the stalk glycosylation at these positions may prevent Ly49B ligand binding in *cis*.

The glycosylation motif containing asparagine at position 177 is specific to Ly49B and resides in the CRD. As such, as with Ly49D and Ly49H, it was predicted that the motif may play a role in Ly49B's association with ligands. Binding of the H-2K^b and H-2D^d tetramers to the single N177Q glycosylation mutant was unaffected, but weaker for the H-2D^b tetramer. It seems that glycosylation of asparagine at position 177 is yet another factor which promotes preferential binding of the H-2D^b MHC class I molecule over H-2K^b and H-2D^d. As with the Ly49D and Ly49H receptors, carbohydrates attached to Ly49B at specific positions may play a role in fine tuning of ligand binding.

In summary, this study has shown that BALB/c Ly49B binds to a variety of tested MHC class I tetramers, whereas C57 Ly49B does not bind any of the tetramers. Variable Ly49B residues 166 and 167 influence binding of a monoclonal 1A1 anti-Ly49B antibody and together with the variable residue 251 also ligand binding. C-terminal HA-tag can marginally affect ligand binding by Ly49 receptors, but has not got the ability to completely abolish ligand binding.

Moreover, this study revealed that Ly49B has the ability to dimerise, or even multimerise, on the cell surface. Differentially glycosylated forms of Ly49B co-exist in similar proportions in the intra- and extracellular compartments of cells that express this receptor. Ly49B glycosylation is not essential for surface expression of Ly49B but is beneficial and most likely promotes correct folding and stability. The presence of glycans is not required for ligand binding, but may play a role in the fine tuning of ligand binding.

The data presented here reveal new insights regarding the structure and function of Ly49B and other Ly49 receptors. In depth knowledge of NK cell regulation is necessary for the development of new therapies in our fight against pathogens and cancer; this study brings us one step closer to achieving this end.

6.1. Future work

Ly49B residues 166, 167 and 251 were shown here to be important for ligand binding. Modelling of these residues onto known crystal structures of other Ly49s, has shown that the equivalent residues lay on the surface of the proteins and that all three are brought into close proximity with one another upon folding. Residues equivalent to Ly49B 166 and 167 were shown to be important for Ly49A ligand binding, despite the fact that they were not identified as contact residues in a Ly49A-H-2D^d co-crystal structure. Moreover, the residue equivalent to Ly49B 167 was shown to facilitate Van der Waals interactions with the ligand in a co-crystal structure of Ly49C and H-2K^b (Deng *et al.* 2008). Taking into consideration these findings, it would be interesting to create a series of Ly49 mutants, similar to the Ly49A mutants used here, which would enable investigation of residues equivalent to Ly49B 166, 167 and 251 in terms of whether or not they also play a role in ligand binding of other Ly49s.

Solving a crystal structure of Ly49B would be pivotal in terms of understanding its biochemistry. Since receptor glycosylation seems to be important for surface expression of Ly49B, it is possible that glycosylation may also be needed for optimal folding and stability. Using an expression system that supports glycosylation, for example HEK293 cell line or insects, could enable the production and purification of large quantities of correctly folded Ly49B. Since protein glycosylation can interfere with the crystallisation process, it would be advisable to run crystal trials with de-glycosylated protein following purification, as well as with fully glycosylated protein. As well as crystallisation, pure, glycosylated, soluble Ly49B could be used in other biochemical experiments, for example in assessing the exact kinetics of ligand binding using surface plasmon resonance.

Ly49B was shown here to exist in transfected and native cells in differentially glycosylated, intra- and extracellular forms, which were present in roughly equal abundance. Preliminary experiments have shown that this may also be the case for other Ly49 and NK cell receptors. To unambiguously establish that this is in fact the case, detailed analysis, using the same methods applied here for Ly49B, would be necessary for each of the receptors. It would be interesting to see whether or not monoclonal antibodies previously developed against other Ly49s can be used in Western blotting experiments in the same manner as anti-Ly49B 2G4 and 1A1 mAbs and if they are able to bind differentially glycosylated forms of the same receptor, assuming such forms exist. An intriguing question

to address would be whether or not the proportions of intra- and extracellular Ly49 receptors change in different circumstances. One way of doing this would be to compare lysates prepared from activated and non-activated NK cells in Western blot experiments using antibodies that are capable of recognising differentially glycosylated Ly49 receptors.

As mentioned in the discussion, assessing the ability of Ly49B glycosylation mutants to bind ligands that are expressed by the same cell would enable determination of whether or not glycosylation of the stalk region of Ly49B prevents the wild type receptor from binding *in cis*. To resolve this question, tetramer binding assays could be performed using Ly49B glycosylation mutant-transfected cells deficient or proficient for MHC class I receptor expression. Comparison of the tetramer binding pattern between the two groups would provide an indication as to the importance of stalk glycosylation in preventing Ly49B interactions with its ligand *in cis*.

Finally, it is important to explicitly establish whether Ly49B is able to form homodimers or if it associates with an alternative protein. In order to achieve this, one could employ cells that have been transfected with Ly49B constructs expressed from two different plasmids; with each construct carrying a different molecular tag. Transfectant cell lysates could then be subjected to sequential immunoprecipitation with antibodies against the two tags. If immunoprecipitated lysates contain material which can be detected by Western blotting using the second antibody, it would indicate that Ly49B is indeed capable of forming homodimers. Results could be further confirmed by mass spectrometric analysis of purified, non-reduced Ly49B receptor.

7. References

- Ajit Varki, R. C., Jeffrey Esko, Hudson Freeze, Gerald Hart, and Jamey Marth (2009) Essentials of glycobiology.
- Alvarez-Errico, D., Aguilar, H., Kitzig, F., Brckalo, T., Sayos, J. & Lopez-Botet, M. (2004) Irem-1 is a novel inhibitory receptor expressed by myeloid cells. *Eur J Immunol*, 34(12), 3690-701.
- Anderson, S. K., Ortaldo, J. R. & Mcvicar, D. W. (2001) The ever-expanding ly49 gene family: Repertoire and signaling. *Immunol Rev*, (181), 79-89.
- Aoki, N., Kimura, Y., Kimura, S., Nagato, T., Azumi, M., Kobayashi, H., Sato, K. & Tateno, M. (2009) Expression and functional role of mdl-1 (clec5a) in mouse myeloid lineage cells. *J Leukoc Biol*, 85(3), 508-17.
- Arie, J. P., Miot, M., Sassoon, N. & Betton, J. M. (2006) Formation of active inclusion bodies in the periplasm of escherichia coli. *Mol Microbiol*, 62(2), 427-37.
- Back, J., Angelov, G. S., Mariuzza, R. A. & Held, W. (2011) The interaction with h-2d(d) in cis is associated with a conformational change in the ly49a nk cell receptor. *Front Immunol*, (2) 2-55.
- Back, J., Chalifour, A., Scarpellino, L. & Held, W. (2007) Stable masking by h-2dd cis ligand limits ly49a relocalization to the site of nk cell/target cell contact. *Proc Natl Acad Sci U S A*, 104(10), 3978-83.
- Back, J., Malchiodi, E. L., Cho, S., Scarpellino, L., Schneider, P., Kerzic, M. C., Mariuzza, R. A. & Held, W. (2009) Distinct conformations of ly49 natural killer cell receptors mediate mhc class i recognition in trans and cis. *Immunity*, 31(4), 598-608.
- Barkalow, F. J., Barkalow, K. L. & Mayadas, T. N. (2000) Dimerization of p-selectin in platelets and endothelial cells. *Blood*, 96(9), 3070-7.
- Berg, J. M., Tomyczko J. L., Stryer, L. (2002) *Biochemistry*, (5 edn) (New York, W H Freeman).
- Blery, M., Delon, J., Trautmann, A., Cambiaggi, A., Olcese, L., Biassoni, R., Moretta, L., Chavrier, P., Moretta, A., Daeron, M. & Vivier, E. (1997) Reconstituted killer cell inhibitory receptors for major histocompatibility complex class i molecules control mast cell activation induced via immunoreceptor tyrosine-based activation motifs. *J Biol Chem*, 272(14), 8989-96.

- Bogdanov, M., Sun, J., Kaback, H. R. & Dowhan, W. (1996) A phospholipid acts as a chaperone in assembly of a membrane transport protein. *J Biol Chem*, 271(20), 11615-8.
- Boles, K. S., Barten, R., Kumaresan, P. R., Trowsdale, J. & Mathew, P. A. (1999) Cloning of a new lectin-like receptor expressed on human nk cells. *Immunogenetics*, 50(1-2), 1-7.
- Brennan, J., Lemieux, S., Freeman, J. D., Mager, D. L. & Takei, F. (1996) Heterogeneity among ly-49c natural killer (nk) cells: Characterization of highly related receptors with differing functions and expression patterns. *J Exp Med*, 184(6), 2085-90.
- Brennan, J., Mahon, G., Mager, D. L., Jefferies, W. A. & Takei, F. (1996) Recognition of class i major histocompatibility complex molecules by ly-49: Specificities and domain interactions. *J Exp Med*, 183(4), 1553-9.
- Brennan, J., Takei, F., Wong, S. & Mager, D. L. (1995) Carbohydrate recognition by a natural killer cell receptor, ly-49c. *J Biol Chem*, 270(17), 9691-4.
- Browning Michael, A. M. E. (1999) *Hla and mhc: Genes, molecules and function*, (Elsevier Science & Technology Books).
- Bryceson, Y. T., March, M. E., Ljunggren, H. G. & Long, E. O. (2006) Activation, coactivation, and costimulation of resting human natural killer cells. *Immunol Rev*, (214), 73-91.
- Burgess, R. R. (2009) Refolding solubilized inclusion body proteins. *Methods Enzymol*, (463), 259-82.
- Burshtyn, D. N., Scharenberg, A. M., Wagtmann, N., Rajagopalan, S., Berrada, K., Yi, T., Kinet, J. P. & Long, E. O. (1996) Recruitment of tyrosine phosphatase hcp by the killer cell inhibitor receptor. *Immunity*, 4(1), 77-85.
- Cambi, A. & Figdor, C. G. (2003) Dual function of c-type lectin-like receptors in the immune system. *Curr Opin Cell Biol*, 15(5), 539-46.
- Campbell, R. D. & Trowsdale, J. (1993) Map of the human mhc. *Immunol Today*, 14(7), 349-52.
- Carlsson, P., Koehler, K. F. & Nilsson, L. (2005) Glucocorticoid receptor point mutation v571m facilitates coactivator and ligand binding by structural rearrangement and stabilization. *Mol Endocrinol*, 19(8), 1960-77.
- Cassatella, M. A., Anegon, I., Cuturi, M. C., Griskey, P., Trinchieri, G. & Perussia, B. (1989) Fc gamma r(cd16) interaction with ligand induces ca²⁺ mobilization and

- phosphoinositide turnover in human natural killer cells. Role of ca^{2+} in $fc\ \gamma$ (cd16)-induced transcription and expression of lymphokine genes. *J Exp Med*, 169(2), 549-67.
- Chaffey, B. T., Mitchell, E., Birch, M. A. & Lakey, J. H. (2008) A generic expression system to produce proteins that co-assemble with alkane thiol sam. *Int J Nanomedicine*, 3(3), 287-93.
- Chan, P. Y. & Takei, F. (1986) Expression of a t cell receptor-like molecule on normal and malignant murine t cells detected by rat monoclonal antibodies to nonclonotypic determinants. *J Immunol*, 136(4), 1346-53.
- Chan, P. Y. & Takei, F. (1988) Characterization of a murine t cell surface disulfide-linked dimer of 45-kda glycopeptides (ye1/48 antigen). Comparison with t cell receptor, purification, and partial amino acid sequences. *J Immunol*, 140(1), 161-9.
- Chan, P. Y. & Takei, F. (1989) Molecular cloning and characterization of a novel murine t cell surface antigen, ye1/48. *J Immunol*, 142(5), 1727-36.
- Chang, C. S. & Kane, K. P. (1998) Evidence for sulfate modification of h-2dd on n-linked carbohydrate(s): Possible involvement in ly-49a interaction. *J Immunol*, 160(9), 4367-74.
- Chang, C. S., Shen, L., Gong, D. E. & Kane, K. P. (1996) Major histocompatibility complex class i-dependent cell binding to isolated ly-49a: Evidence for high-avidity interaction. *Eur J Immunol*, 26(12), 3219-23.
- Chang, C. S., Silver, E. T. & Kane, K. P. (1999) Generation of a monoclonal antibody that recognizes a polymorphic epitope of c57bl/6 ly-49g2. *Hybridoma*, 18(5), 423-9.
- Chung, D. H., Dorfman, J., Plaksin, D., Natarajan, K., Belyakov, I. M., Hunziker, R., Berzofsky, J. A., Yokoyama, W. M., Mage, M. G. & Margulies, D. H. (1999) Nk and ctl recognition of a single chain h-2dd molecule: Distinct sites of h-2dd interact with nk and tcr. *J Immunol*, 163(7), 3699-708.
- Chung, D. H., Natarajan, K., Boyd, L. F., Tormo, J., Mariuzza, R. A., Yokoyama, W. M. & Margulies, D. H. (2000) Mapping the ligand of the nk inhibitory receptor ly49a on living cells. *J Immunol*, 165(12), 6922-32.
- Correa, I. & Raulet, D. H. (1995) Binding of diverse peptides to mhc class i molecules inhibits target cell lysis by activated natural killer cells. *Immunity*, 2(1), 61-71.
- Cregg, J. M., Tolstorukov, I., Kusari, A., Sunga, J., Madden, K. & Chappell, T. (2009) Expression in the yeast *pichia pastoris*. *Methods Enzymol*, (463) 169-89.

- Dam, J., Baber, J., Grishaev, A., Malchiodi, E. L., Schuck, P., Bax, A. & Mariuzza, R. A. (2006) Variable dimerization of the ly49a natural killer cell receptor results in differential engagement of its mhc class i ligand. *J Mol Biol*, 362(1), 102-13.
- Dam, J., Guan, R., Natarajan, K., Dimasi, N., Chlewicki, L. K., Kranz, D. M., Schuck, P., Margulies, D. H. & Mariuzza, R. A. (2003) Variable mhc class i engagement by ly49 natural killer cell receptors demonstrated by the crystal structure of ly49c bound to h-2k(b). *Nat Immunol*, 4(12), 1213-22.
- Daniels, B. F., Karlhofer, F. M., Seaman, W. E. & Yokoyama, W. M. (1994) A natural killer cell receptor specific for a major histocompatibility complex class i molecule. *J Exp Med*, 180(2), 687-92.
- Daniels, B. F., Nakamura, M. C., Rosen, S. D., Yokoyama, W. M. & Seaman, W. E. (1994) Ly-49a, a receptor for h-2dd, has a functional carbohydrate recognition domain. *Immunity*, 1(9), 785-92.
- Daniels, R., Kurowski, B., Johnson, A. E. & Hebert, D. N. (2003) N-linked glycans direct the cotranslational folding pathway of influenza hemagglutinin. *Mol Cell*, 11(1), 79-90.
- Davis, D. M., Chiu, I., Fassett, M., Cohen, G. B., Mandelboim, O. & Strominger, J. L. (1999) The human natural killer cell immune synapse. *Proc Natl Acad Sci U S A*, 96(26), 15062-7.
- Deng, L., Cho, S., Malchiodi, E. L., Kerzic, M. C., Dam, J. & Mariuzza, R. A. (2008) Molecular architecture of the major histocompatibility complex class i-binding site of ly49 natural killer cell receptors. *J Biol Chem*, 283(24), 16840-9.
- Denzin, L. K., Hammond, C. & Cresswell, P. (1996) Hla-dm interactions with intermediates in hla-dr maturation and a role for hla-dm in stabilizing empty hla-dr molecules. *J Exp Med*, 184(6), 2153-65.
- Deprez, P., Gautschi, M. & Helenius, A. (2005) More than one glycan is needed for er glucosidase ii to allow entry of glycoproteins into the calnexin/calreticulin cycle. *Mol Cell*, 19(2), 183-95.
- Dimasi, N. & Biassoni, R. (2005) Structural and functional aspects of the ly49 natural killer cell receptors. *Immunol Cell Biol*, 83(1), 1-8.
- Dimasi, N., Sawicki, M. W., Reineck, L. A., Li, Y., Natarajan, K., Margulies, D. H. & Mariuzza, R. A. (2002) Crystal structure of the ly49i natural killer cell receptor reveals variability in dimerization mode within the ly49 family. *J Mol Biol*, 320(3), 573-85.

- Doucey, M. A., Scarpellino, L., Zimmer, J., Guillaume, P., Luescher, I. F., Bron, C. & Held, W. (2004) Cis association of ly49a with mhc class i restricts natural killer cell inhibition. *Nat Immunol*, 5(3), 328-36.
- Dunker, A. K. & Kenyon, A. J. (1976) Mobility of sodium dodecyl sulphate - protein complexes. *Biochem J*, 153(2), 191-7.
- Fazi, B., Melino, S., Di Sano, F., Cicero, D. O., Piacentini, M. & Paci, M. (2006) Cloning, expression, and preliminary structural characterization of rtn-1c. *Biochem Biophys Res Commun*, 342(3), 881-6.
- Fishburn, C. S., Elazar, Z. & Fuchs, S. (1995) Differential glycosylation and intracellular trafficking for the long and short isoforms of the d2 dopamine receptor. *J Biol Chem*, 270(50), 29819-24.
- French, A. R., Yokoyama, W. M. (2003) Natural killer cells and autoimmunity. *Arthritis Res Ther*, 6(1), 8–14.
- Gao, G. F., Tormo, J., Gerth, U. C., Wyer, J. R., Mcmichael, A. J., Stuart, D. I., Bell, J. I., Jones, E. Y. & Jakobsen, B. K. (1997) Crystal structure of the complex between human cd8alpha(alpha) and hla-a2. *Nature*, 387(6633), 630-4.
- Gays, F., Aust, J. G., Reid, D. M., Falconer, J., Toyama-Sorimachi, N., Taylor, P. R. & Brooks, C. G. (2006) Ly49b is expressed on multiple subpopulations of myeloid cells. *J Immunol*, 177(9), 5840-51.
- Gays, F., Koh, A. S., Mickiewicz, K. M., Aust, J. G. & Brooks, C. G. (2011) Comprehensive analysis of transcript start sites in ly49 genes reveals an unexpected relationship with gene function and a lack of upstream promoters. *PLoS One*, 6(3), e18475.
- Geisse, S. & Fux, C. (2009) Recombinant protein production by transient gene transfer into mammalian cells. *Methods Enzymol*, (463), 223-38.
- Givan, A. L. (2004) Flow cytometry: An introduction. *Methods Mol Biol*, (263), 1-32.
- Gokce, I., Woody, R. W., Anderluh, G. & Lakey, J. H. (2005) Single peptide bonds exhibit poly(pro)ii ("random coil") circular dichroism spectra. *J Am Chem Soc*, 127(27), 9700-1.
- Goren, M. A., Nozawa, A., Makino, S., Wrobel, R. L. & Fox, B. G. (2009) Cell-free translation of integral membrane proteins into unilamellar liposomes. *Methods Enzymol*, (463), 647-73.
- Grzonka, Z., Jankowska, E., Kasprzykowski, F., Kasprzykowska, R., Lankiewicz, L., Wicz, W., Wieczerek, E., Ciarkowski, J., Drabik, P., Janowski, R., Kozak, M., Jaskolski,

- M. & Grubb, A. (2001) Structural studies of cysteine proteases and their inhibitors. *Acta Biochim Pol*, 48(1), 1-20.
- Guseva, N. V., Fullenkamp, C. A., Naumann, P. W., Shey, M. R., Ballas, Z. K., Houtman, J. C., Forbes, C. A., Scalzo, A. A. & Heusel, J. W. Glycosylation contributes to variability in expression of murine cytomegalovirus m157 and enhances stability of interaction with the nk-cell receptor ly49h. *Eur J Immunol*, 40(9), 2618-31.
- Hanke, T., Takizawa, H., McMahon, C. W., Busch, D. H., Pamer, E. G., Miller, J. D., Altman, J. D., Liu, Y., Cado, D., Lemonnier, F. A., Bjorkman, P. J. & Raulet, D. H. (1999) Direct assessment of mhc class i binding by seven ly49 inhibitory nk cell receptors. *Immunity*, 11(1), 67-77.
- Hartmann, J., Tran, T. V., Kaudeer, J., Oberle, K., Herrmann, J., Quagliano, I., Abel, T., Cohnen, A., Gatterdam, V., Jacobs, A., Wollscheid, B., Tampe, R., Watzl, C., Diefenbach, A. & Koch, J. (2012) The stalk domain and the glycosylation status of the activating natural killer cell receptor nkp30 are important for ligand binding. *J Biol Chem*, 287(37), 31527-39.
- Held, W. & Kunz, B. (1998) An allele-specific, stochastic gene expression process controls the expression of multiple ly49 family genes and generates a diverse, mhc-specific nk cell receptor repertoire. *Eur J Immunol*, 28(8), 2407-16.
- Hoglund, P. & Brodin, P. (2010) Current perspectives of natural killer cell education by mhc class i molecules. *Nat Rev Immunol*, 10(10), 724-34.
- I, S. (1990) Molecules related to class-i major histocompatibility complex antigens. *Annual Review of Immunology*, (8), 501-530
- Ibrahim, S. F. & Van Den Engh, G. (2007) Flow cytometry and cell sorting. *Adv Biochem Eng Biotechnol*, (106), 19-39.
- Iizuka, K., Naidenko, O. V., Plougastel, B. F., Fremont, D. H. & Yokoyama, W. M. (2003) Genetically linked c-type lectin-related ligands for the nkrp1 family of natural killer cell receptors. *Nat Immunol*, 4(8), 801-7.
- Imamura, T. (2006) *Encyclopedia of surface and colloid science*, (New York, Taylor & Francis).
- Ito, D., Iizuka, Y. M., Katepalli, M. P. & Iizuka, K. (2009) Essential role of the ly49a stalk region for immunological synapse formation and signaling. *Proc Natl Acad Sci U S A*, 106(27), 11264-9.

- Janeway Charles A, T. P. J., Walport Mark, Shlomchik Mark J (2001) Immunobiology, the immune system in health and disease, (5 edn) (New York, Garland Science).
- Jarvis, D. L. (2009) Baculovirus-insect cell expression systems. *Methods Enzymol*, (463), 191-222.
- Kane, K. P. (1994) Ly-49 mediates e14 lymphoma adhesion to isolated class i major histocompatibility complex molecules. *J Exp Med*, 179(3), 1011-5.
- Kane, K. P., Lavender, K. J. & Ma, B. J. (2004) Ly-49 receptors and their functions. *Crit Rev Immunol*, 24(5), 321-48.
- Karlhofer, F. M., Hunziker, R., Reichlin, A., Margulies, D. H. & Yokoyama, W. M. (1994) Host mhc class i molecules modulate in vivo expression of a nk cell receptor. *J Immunol*, 153(6), 2407-16.
- Karlhofer, F. M., Ribaldo, R. K. & Yokoyama, W. M. (1992) Mhc class i alloantigen specificity of ly-49+ il-2-activated natural killer cells. *Nature*, 358(6381), 66-70.
- Karre, K. (1981) On the immunobiology of natural killer cells. Phd thesis
- Kielczewska, A., Kim, H. S., Lanier, L. L., Dimasi, N. & Vidal, S. M. (2007) Critical residues at the ly49 natural killer receptor's homodimer interface determine functional recognition of m157, a mouse cytomegalovirus mhc class i-like protein. *J Immunol*, 178(1), 369-77.
- Kim, H. S., Das, A., Gross, C. C., Bryceson, Y. T. & Long, E. O. (2010) Synergistic signals for natural cytotoxicity are required to overcome inhibition by c-cbl ubiquitin ligase. *Immunity*, 32(2), 175-86.
- Kim, S. & Yokoyama, W. M. (1998) Nk cell granule exocytosis and cytokine production inhibited by ly-49a engagement. *Cell Immunol*, 183(2), 106-12.
- Kveberg, L., Back, C. J., Dai, K. Z., Inngjerdingen, M., Rolstad, B., Ryan, J. C., Vaage, J. T. & Naper, C. (2006) The novel inhibitory nkr-p1c receptor and ly49s3 identify two complementary, functionally distinct nk cell subsets in rats. *J Immunol*, 176(7), 4133-40.
- Kveberg, L., Dai, K. Z., Dissen, E., Ryan, J. C., Rolstad, B., Vaage, J. T. & Naper, C. (2006) Strain-dependent expression of four structurally related rat ly49 receptors; correlation with nk gene complex haplotype and nk alloreactivity. *Immunogenetics*, 58(11), 905-16.

- Kveberg, L., Ryan, J. C., Rolstad, B. & Inngjerdigen, M. (2005) Expression of regulator of g protein signalling proteins in natural killer cells, and their modulation by ly49a and ly49d. *Immunology*, 115(3), 358-65.
- Laemmli, U. K. (1970) Cleavage of structural proteins during the assembly of the head of bacteriophage t4. *Nature*, 227(5259), 680-5.
- Lanier, L. L. (1998) Nk cell receptors. *Annu Rev Immunol*, (16), 359-93.
- Lanier, L. L. (2003) Natural killer cell receptor signaling. *Curr Opin Immunol*, 15(3), 308-14.
- Lazetic, S., Chang, C., Houchins, J. P., Lanier, L. L. & Phillips, J. H. (1996) Human natural killer cell receptors involved in mhc class i recognition are disulfide-linked heterodimers of cd94 and nkg2 subunits. *J Immunol*, 157(11), 4741-5.
- Lian, R. H., Freeman, J. D., Mager, D. L. & Takei, F. (1998) Role of conserved glycosylation site unique to murine class i mhc in recognition by ly-49 nk cell receptor. *J Immunol*, 161(5), 2301-6.
- Lian, R. H., Li, Y., Kubota, S., Mager, D. L. & Takei, F. (1999) Recognition of class i mhc by nk receptor ly-49c: Identification of critical residues. *J Immunol*, 162(12), 7271-6.
- Long, E. O., Burshtyn, D. N., Clark, W. P., Peruzzi, M., Rajagopalan, S., Rojo, S., Wagtmann, N. & Winter, C. C. (1997) Killer cell inhibitory receptors: Diversity, specificity, and function. *Immunol Rev*, (155), 135-44.
- Lopez-Botet, M., Angulo, A. & Guma, M. (2004) Natural killer cell receptors for major histocompatibility complex class i and related molecules in cytomegalovirus infection. *Tissue Antigens*, 63(3), 195-203.
- Makrigiannis, A. P., Etzler, J., Winkler-Pickett, R., Mason, A., Ortaldo, J. R. & Anderson, S. K. (2000) Identification of the ly49l protein: Evidence for activating counterparts to inhibitory ly49 proteins. *J Leukoc Biol*, 68(5), 765-71.
- Makrigiannis, A. P., Gosselin, P., Mason, L. H., Taylor, L. S., Mcvicar, D. W., Ortaldo, J. R. & Anderson, S. K. (1999) Cloning and characterization of a novel activating ly49 closely related to ly49a. *J Immunol*, 163(9), 4931-8.
- Maniatis T, F. E., Sambrook J (1989) *Molecular cloning: A laboratory manual*, (New York).
- Mason, L., Giardina, S. L., Hecht, T., Ortaldo, J. & Mathieson, B. J. (1988) Lgl-1: A non-polymorphic antigen expressed on a major population of mouse natural killer cells. *J Immunol*, 140(12), 4403-12.

- Mason, L. H., Anderson, S. K., Yokoyama, W. M., Smith, H. R., Winkler-Pickett, R. & Ortaldo, J. R. (1996) The ly-49d receptor activates murine natural killer cells. *J Exp Med*, 184(6), 2119-28.
- Mason, L. H., Gosselin, P., Anderson, S. K., Fogler, W. E., Ortaldo, J. R. & Mcvicar, D. W. (1997) Differential tyrosine phosphorylation of inhibitory versus activating ly-49 receptor proteins and their recruitment of shp-1 phosphatase. *J Immunol*, 159(9), 4187-96.
- Mason, L. H., Ortaldo, J. R., Young, H. A., Kumar, V., Bennett, M. & Anderson, S. K. (1995) Cloning and functional characteristics of murine large granular lymphocyte-1: A member of the ly-49 gene family (ly-49g2). *J Exp Med*, 182(2), 293-303.
- Mason, L. H., Willette-Brown, J., Anderson, S. K., Alvord, W. G., Klabansky, R. L., Young, H. A. & Ortaldo, J. R. (2003) Receptor glycosylation regulates ly-49 binding to mhc class i. *J Immunol*, 171(8), 4235-42.
- Mason, L. H., Yagita, H. & Ortaldo, J. R. (1994) Lgl-1: A potential triggering molecule on murine nk cells. *J Leukoc Biol*, 55(3), 362-70.
- Matsumoto, N., Mitsuki, M., Tajima, K., Yokoyama, W. M. & Yamamoto, K. (2001) The functional binding site for the c-type lectin-like natural killer cell receptor ly49a spans three domains of its major histocompatibility complex class i ligand. *J Exp Med*, 193(2), 147-58.
- Matsumoto, N., Ribaud, R. K., Abastado, J. P., Margulies, D. H. & Yokoyama, W. M. (1998) The lectin-like nk cell receptor ly-49a recognizes a carbohydrate-independent epitope on its mhc class i ligand. *Immunity*, 8(2), 245-54.
- Matsumoto, N., Yokoyama, W. M., Kojima, S. & Yamamoto, K. (2001) The nk cell mhc class i receptor ly49a detects mutations on h-2dd inside and outside of the peptide binding groove. *J Immunol*, 166(7), 4422-8.
- Maureen E. Taylor, K. D. (2003) *Introduction to glycobiology*, (New York, Oxford University Press).
- Mcknight, A. J., Macfarlane, A. J., Dri, P., Turley, L., Willis, A. C. & Gordon, S. (1996) Molecular cloning of f4/80, a murine macrophage-restricted cell surface glycoprotein with homology to the g-protein-linked transmembrane 7 hormone receptor family. *J Biol Chem*, 271(1), 486-9.
- Mcmahon, C. W. & Raulet, D. H. (2001) Expression and function of nk cell receptors in cd8+ t cells. *Curr Opin Immunol*, 13(4), 465-70.

- Mcvicar, D. W. & Burshtyn, D. N. (2001) Intracellular signaling by the killer immunoglobulin-like receptors and ly49. *Sci STKE*, 2001(75), re1.
- Mcvicar, D. W., Taylor, L. S., Gosselin, P., Willette-Brown, J., Mikhael, A. I., Geahlen, R. L., Nakamura, M. C., Linnemeyer, P., Seaman, W. E., Anderson, S. K., Ortaldo, J. R. & Mason, L. H. (1998) Dap12-mediated signal transduction in natural killer cells. A dominant role for the syk protein-tyrosine kinase. *J Biol Chem*, 273(49), 32934-42.
- Mesecke, S., Urlaub, D., Busch, H., Eils, R. & Watzl, C. (2011) Integration of activating and inhibitory receptor signaling by regulated phosphorylation of vav1 in immune cells. *Sci Signal*, 4(175), ra36.
- Michaelsson, J., Achour, A., Rolle, A. & Karre, K. (2001) Mhc class i recognition by nk receptors in the ly49 family is strongly influenced by the beta 2-microglobulin subunit. *J Immunol*, 166(12), 7327-34.
- Michaelsson, J., Achour, A., Salcedo, M., Kase-Sjostrom, A., Sundback, J., Harris, R. A. & Karre, K. (2000) Visualization of inhibitory ly49 receptor specificity with soluble major histocompatibility complex class i tetramers. *Eur J Immunol*, 30(1), 300-7.
- Middelberg, A. P. (2002) Preparative protein refolding. *Trends Biotechnol*, 20(10), 437-43.
- Molinari, M. & Helenius, A. (2000) Chaperone selection during glycoprotein translocation into the endoplasmic reticulum. *Science*, 288(5464), 331-3.
- Moremen, K. W., Tiemeyer, M. & Nairn, A. V. (2012) Vertebrate protein glycosylation: Diversity, synthesis and function. *Nat Rev Mol Cell Biol*, 13(7), 448-62.
- Nagasawa, R., Gross, J., Kanagawa, O., Townsend, K., Lanier, L. L., Chiller, J. & Allison, J. P. (1987) Identification of a novel t cell surface disulfide-bonded dimer distinct from the alpha/beta antigen receptor. *J Immunol*, 138(3), 815-24.
- Nakamura, M. C., Naper, C., Niemi, E. C., Spusta, S. C., Rolstad, B., Butcher, G. W., Seaman, W. E. & Ryan, J. C. (1999) Natural killing of xenogeneic cells mediated by the mouse ly-49d receptor. *J Immunol*, 163(9), 4694-700.
- Nakamura, M. C., Niemi, E. C., Fisher, M. J., Shultz, L. D., Seaman, W. E. & Ryan, J. C. (1997) Mouse ly-49a interrupts early signaling events in natural killer cell cytotoxicity and functionally associates with the shp-1 tyrosine phosphatase. *J Exp Med*, 185(4), 673-84.

- Naper, C., Hayashi, S., Joly, E., Butcher, G. W., Rolstad, B., Vaage, J. T. & Ryan, J. C. (2002) Ly49i2 is an inhibitory rat natural killer cell receptor for an mhc class ia molecule (rt1-a1c). *Eur J Immunol*, 32(7), 2031-6.
- Naper, C., Hayashi, S., Lovik, G., Kveberg, L., Niemi, E. C., Rolstad, B., Dissen, E., Ryan, J. C. & Vaage, J. T. (2002) Characterization of a novel killer cell lectin-like receptor (klrh1) expressed by alloreactive rat nk cells. *J Immunol*, 168(10), 5147-54.
- Naper, C., Ryan, J. C., Nakamura, M. C., Lambracht, D., Rolstad, B. & Vaage, J. T. (1998) Identification of an inhibitory mhc receptor on alloreactive rat natural killer cells. *J Immunol*, 160(1), 219-24.
- Natarajan, K., Boyd, L. F., Schuck, P., Yokoyama, W. M., Eliat, D. & Margulies, D. H. (1999) Interaction of the nk cell inhibitory receptor ly49a with h-2dd: Identification of a site distinct from the tcr site. *Immunity*, 11(5), 591-601.
- Ohnishi, T., Muroi, M. & Tanamoto, K. (2001) N-linked glycosylations at asn(26) and asn(114) of human md-2 are required for toll-like receptor 4-mediated activation of nf-kappab by lipopolysaccharide. *J Immunol*, 167(6), 3354-9.
- Olcese, L., Lang, P., Vely, F., Cambiaggi, A., Marguet, D., Blery, M., Hippen, K. L., Biassoni, R., Moretta, A., Moretta, L., Cambier, J. C. & Vivier, E. (1996) Human and mouse killer-cell inhibitory receptors recruit ptp1c and ptp1d protein tyrosine phosphatases. *J Immunol*, 156(12), 4531-4.
- Orihuela, M., Margulies, D. H. & Yokoyama, W. M. (1996) The natural killer cell receptor ly-49a recognizes a peptide-induced conformational determinant on its major histocompatibility complex class i ligand. *Proc Natl Acad Sci U S A*, 93(21), 11792-7.
- Ortaldo, J. R., Mason, A. T., Winkler-Pickett, R., Raziuddin, A., Murphy, W. J. & Mason, L. H. (1999) Ly-49 receptor expression and functional analysis in multiple mouse strains. *J Leukoc Biol*, 66(3), 512-20.
- Pain, R. H. (1996) *Mechanisms of protein folding*, (Oxford, Oxford University Press).
- Pan, T., Colucci, M., Wong, B. S., Li, R., Liu, T., Petersen, R. B., Chen, S., Gambetti, P. & Sy, M. S. (2001) Novel differences between two human prion strains revealed by two-dimensional gel electrophoresis. *J Biol Chem*, 276(40), 37284-8.
- Pause, A., Belsham, G. J., Gingras, A. C., Donze, O., Lin, T. A., Lawrence, J. C., Jr. & Sonenberg, N. (1994) Insulin-dependent stimulation of protein synthesis by phosphorylation of a regulator of 5'-cap function. *Nature*, 371(6500), 762-7.

- Perez-Villar, J. J., Carretero, M., Navarro, F., Melero, I., Rodriguez, A., Bottino, C., Moretta, A. & Lopez-Botet, M. (1996) Biochemical and serologic evidence for the existence of functionally distinct forms of the cd94 nk cell receptor. *J Immunol*, 157(12), 5367-74.
- Perfetto, S. P., Chattopadhyay, P. K. & Roederer, M. (2004) Seventeen-colour flow cytometry: Unravelling the immune system. *Nat Rev Immunol*, 4(8), 648-55.
- Peterson, M. E. & Long, E. O. (2008) Inhibitory receptor signaling via tyrosine phosphorylation of the adaptor crk. *Immunity*, 29(4), 578-88.
- Plougastel, B., Dubbelde, C. & Yokoyama, W. M. (2001) Cloning of clr, a new family of lectin-like genes localized between mouse nkrp1a and cd69. *Immunogenetics*, 53(3), 209-14.
- Radaev, S. & Sun, P. D. (2003) Structure and function of natural killer cell surface receptors. *Annu Rev Biophys Biomol Struct*, (32), 93-114.
- Rath, A., Glibowicka, M., Nadeau, V. G., Chen, G. & Deber, C. M. (2009) Detergent binding explains anomalous sds-page migration of membrane proteins. *Proc Natl Acad Sci U S A*, 106(6), 1760-5.
- Raziuddin, A., Longo, D. L., Mason, L., Ortaldo, J. R. & Murphy, W. J. (1996) Ly-49 g2+ nk cells are responsible for mediating the rejection of h-2b bone marrow allografts in mice. *Int Immunol*, 8(12), 1833-9.
- Rieseberg, M., Kasper, C., Reardon, K. F. & Scheper, T. (2001) Flow cytometry in biotechnology. *Appl Microbiol Biotechnol*, 56(3-4), 350-60.
- Roland, J. & Cazenave, P. A. (1992) Ly-49 antigen defines an alpha beta tcr population in i-iel with an extrathymic maturation. *Int Immunol*, 4(6), 699-706.
- Rolstad, B. & Seaman, W. E. (1998) Natural killer cells and recognition of mhc class i molecules: New perspectives and challenges in immunology. *Scand J Immunol*, 47(5), 412-25.
- Sanderson, F., Thomas, C., Neefjes, J. & Trowsdale, J. (1996) Association between hla-dm and hla-dr in vivo. *Immunity*, 4(1), 87-96.
- Sawicki, M. W., Dimasi, N., Natarajan, K., Wang, J., Margulies, D. H. & Mariuzza, R. A. (2001) Structural basis of mhc class i recognition by natural killer cell receptors. *Immunol Rev*, (181), 52-65.
- Scarpellino, L., Oeschger, F., Guillaume, P., Coudert, J. D., Levy, F., Leclercq, G. & Held, W. (2007) Interactions of ly49 family receptors with mhc class i ligands in trans and cis. *J Immunol*, 178(3), 1277-84.

- Sentman, C. L., Hackett, J., Jr., Kumar, V. & Bennett, M. (1989) Identification of a subset of murine natural killer cells that mediates rejection of hh-1d but not hh-1b bone marrow grafts. *J Exp Med*, 170(1), 191-202.
- Shimazu, R., Akashi, S., Ogata, H., Nagai, Y., Fukudome, K., Miyake, K. & Kimoto, M. (1999) Md-2, a molecule that confers lipopolysaccharide responsiveness on toll-like receptor 4. *J Exp Med*, 189(11), 1777-82.
- Sjostrom, H., Noren, O. & Danielsen, E. M. (1985) Enzymatic activity of "high-mannose" glycosylated forms of intestinal microvillar hydrolases. *J Pediatr Gastroenterol Nutr*, 4(6), 980-3.
- Smith, C. J., Drake, A. F., Banfield, B. A., Bloomberg, G. B., Palmer, M. S., Clarke, A. R. & Collinge, J. (1997) Conformational properties of the prion octa-repeat and hydrophobic sequences. *FEBS Lett*, 405(3), 378-84.
- Smith, H. R., Chuang, H. H., Wang, L. L., Salcedo, M., Heusel, J. W. & Yokoyama, W. M. (2000) Nonstochastic coexpression of activation receptors on murine natural killer cells. *J Exp Med*, 191(8), 1341-54.
- Smith, H. R., Heusel, J. W., Mehta, I. K., Kim, S., Dorner, B. G., Naidenko, O. V., Iizuka, K., Furukawa, H., Beckman, D. L., Pingel, J. T., Scalzo, A. A., Fremont, D. H. & Yokoyama, W. M. (2002) Recognition of a virus-encoded ligand by a natural killer cell activation receptor. *Proc Natl Acad Sci U S A*, 99(13), 8826-31.
- Sundback, J., Achour, A., Michaelsson, J., Lindstrom, H. & Karre, K. (2002) Nk cell inhibitory receptor ly-49c residues involved in mhc class i binding. *J Immunol*, 168(2), 793-800.
- Sundback, J., Nakamura, M. C., Waldenstrom, M., Niemi, E. C., Seaman, W. E., Ryan, J. C. & Karre, K. (1998) The alpha2 domain of h-2dd restricts the allelic specificity of the murine nk cell inhibitory receptor ly-49a. *J Immunol*, 160(12), 5971-8.
- Takei, F. (1983) Two surface antigens expressed on proliferating mouse t lymphocytes defined by rat monoclonal antibodies. *J Immunol*, 130(6), 2794-7.
- Takei, F., Brennan, J. & Mager, D. L. (1997) The ly-49 family: Genes, proteins and recognition of class i mhc. *Immunol Rev*, (155), 67-77.
- Taylor, M. E., Drickamer, K. (2006) *Introduction to glycobiology*, (2 edn) (Oxford, Oxford University Press).

- Tormo, J., Natarajan, K., Margulies, D. H. & Mariuzza, R. A. (1999) Crystal structure of a lectin-like natural killer cell receptor bound to its mhc class i ligand. *Nature*, 402(6762), 623-31.
- Toyama-Sorimachi, N., Tsujimura, Y., Maruya, M., Onoda, A., Kubota, T., Koyasu, S., Inaba, K. & Karasuyama, H. (2004) Ly49q, a member of the ly49 family that is selectively expressed on myeloid lineage cells and involved in regulation of cytoskeletal architecture. *Proc Natl Acad Sci U S A*, 101(4), 1016-21.
- Trowsdale, J. (1993) Genomic structure and function in the mhc. *Trends Genet*, 9(4), 117-22.
- Tung, J. W., Parks, D. R., Moore, W. A., Herzenberg, L. A. & Herzenberg, L. A. (2004) New approaches to fluorescence compensation and visualization of facs data. *Clin Immunol*, 110(3), 277-83.
- Van Beneden, K., Stevenaert, F., De Creus, A., Debacker, V., De Boever, J., Plum, J. & Leclercq, G. (2001) Expression of ly49e and cd94/nkg2 on fetal and adult nk cells. *J Immunol*, 166(7), 4302-11.
- Van Den Broeck, T., Stevenaert, F., Taveirne, S., Debacker, V., Vangestel, C., Vandekerckhove, B., Taghon, T., Matthys, P., Plum, J., Held, W., Dewerchin, M., Yokoyama, W. M. & Leclercq, G. (2008) Ly49e-dependent inhibition of natural killer cells by urokinase plasminogen activator. *Blood*, 112(13), 5046-51.
- Van Ham, S. M., Gruneberg, U., Malcherek, G., Broker, I., Melms, A. & Trowsdale, J. (1996) Human histocompatibility leukocyte antigen (hla)-dm edits peptides presented by hla-dr according to their ligand binding motifs. *J Exp Med*, 184(5), 2019-24.
- Vyas, J. M., Van Der Veen, A. G. & Ploegh, H. L. (2008) The known unknowns of antigen processing and presentation. *Nat Rev Immunol*, 8(8), 607-18.
- Wahle, J. A., Paraiso, K. H., Costello, A. L., Goll, E. L., Sentman, C. L. & Kerr, W. G. (2006) Cutting edge: Dominance by an mhc-independent inhibitory receptor compromises nk killing of complex targets. *J Immunol*, 176(12), 7165-9.
- Wang, J., Whitman, M. C., Natarajan, K., Tormo, J., Mariuzza, R. A. & Margulies, D. H. (2002) Binding of the natural killer cell inhibitory receptor ly49a to its major histocompatibility complex class i ligand. Crucial contacts include both h-2dd and beta 2-microglobulin. *J Biol Chem*, 277(2), 1433-42.
- Wang, J. W., Howson, J. M., Ghansah, T., Desponts, C., Ninos, J. M., May, S. L., Nguyen, K. H., Toyama-Sorimachi, N. & Kerr, W. G. (2002) Influence of ship on the nk repertoire and allogeneic bone marrow transplantation. *Science*, 295(5562), 2094-7.

- Weis, W. I., Taylor, M. E. & Drickamer, K. (1998) The c-type lectin superfamily in the immune system. *Immunol Rev*, (163), 19-34.
- Westgaard, I. H., Berg, S. F., Orstavik, S., Fossum, S. & Dissen, E. (1998) Identification of a human member of the ly-49 multigene family. *Eur J Immunol*, 28(6), 1839-46.
- Wong, S., Freeman, J. D., Kelleher, C., Mager, D. & Takei, F. (1991) Ly-49 multigene family. New members of a superfamily of type ii membrane proteins with lectin-like domains. *J Immunol*, 147(4), 1417-23.
- Yeo, M. G., Partridge, M. A., Ezratty, E. J., Shen, Q., Gundersen, G. G. & Marcantonio, E. E. (2006) Src sh2 arginine 175 is required for cell motility: Specific focal adhesion kinase targeting and focal adhesion assembly function. *Mol Cell Biol*, 26(12), 4399-409.
- Yokoyama, W. M., Jacobs, L. B., Kanagawa, O., Shevach, E. M. & Cohen, D. I. (1989) A murine t lymphocyte antigen belongs to a supergene family of type ii integral membrane proteins. *J Immunol*, 143(4), 1379-86.
- Yokoyama, W. M., Koning, F., Kehn, P. J., Pereira, G. M., Stingl, G., Coligan, J. E. & Shevach, E. M. (1988) Characterization of a cell surface-expressed disulfide-linked dimer involved in murine t cell activation. *J Immunol*, 141(2), 369-76.
- Yokoyama, W. M. & Plougastel, B. F. (2003) Immune functions encoded by the natural killer gene complex. *Nat Rev Immunol*, 3(4), 304-16.
- Yu, Y. Y., George, T., Dorfman, J. R., Roland, J., Kumar, V. & Bennett, M. (1996) The role of ly49a and 5e6(ly49c) molecules in hybrid resistance mediated by murine natural killer cells against normal t cell blasts. *Immunity*, 4(1), 67-76.
- Zelensky, A. N. & Gready, J. E. (2005) The c-type lectin-like domain superfamily. *FEBS J*, 272(24), 6179-217.
- Zerbs, S., Frank, A. M. & Collart, F. R. (2009) Bacterial systems for production of heterologous proteins. *Methods Enzymol*, (463), 149-68.
- Zimmer, J. E. (2010) *Natural killer cells, at the forefront of modern immunology* (1 edn) (Springer).

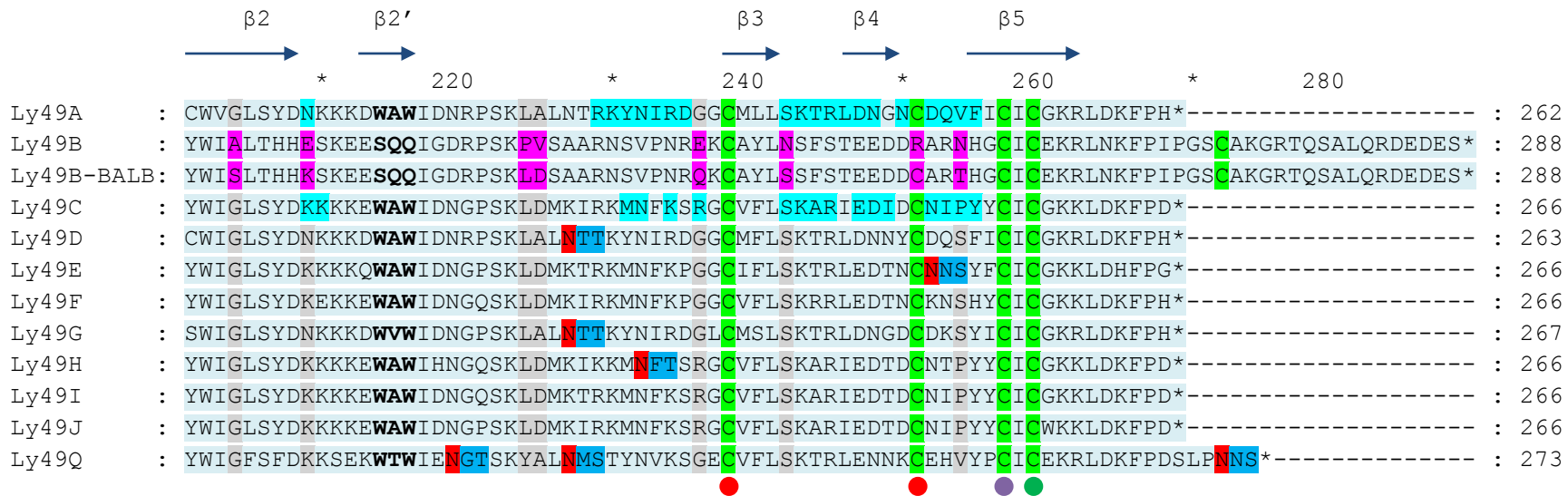
Appendix I) Alignment of all known C57 Ly49 receptor amino acid sequences, as well as that of BALB/c Ly49B.

Light green = intracellular region. Yellow = transmembrane region. White = stalk region. Light blue = NK domain (NKD). Purple = residues showing variation between the C57 and BALB/c isoforms of Ly49B. Red and blue = glycosylation motifs, with critical asparagine residues highlighted in red. Dark green = cysteine residues contained within the Ly49B sequence and conserved cysteines, Blue, purple and green dots indicate cysteine pairs that form disulphide bonds, Bold = WAW motif, highly conserved amongst other Ly49s, and equivalent Ly49B residues, Underline = ITIM motif in Ly49Bs, Grey = residues present in other Ly49s corresponding to highlighted Ly49B residues, Turquoise = residues that were identified to form direct contacts with ligands in co-crystal structures of Ly49C-H-2K^b and Ly49A-H-2D^d, as stated in table 1.1. Blue arrows = β sheets in Ly49A, identified by X-ray crystallography. Regions annotated with blue α symbols = α helices in Ly49A, identified by X-ray crystallography.

		*	20	*	40	*	60	*	80	*	100		
Ly49A	:	MSEQEVTYSMVR	FKHSAGLQKQVR	PEETKGP	REAGYRR	CSFHWK	FIVIALGIF	CFLLLV	AVSVLAI	KIFQYDQK	-KLQEF	LNHHNCS	-NMQSDINLKD : 98
Ly49B	:	MSEQEVTYTTLR	FKHSSGLQNPVR	PEETQR	PRDVGHRE	CSVPWK	FIVIVLGIL	CFLLLV	TVAVLVI	HIRFDGQEK	HEQEKTLN	NLRQEQVMK	NDSS SLME : 100
Ly49BBALB	:	MSEQEVTYTTLR	FKHSSGLQNPVR	PEETQR	PRDVGHRE	CSVPWK	FIVIVLGIL	CFLLLV	TVAVLVI	HIRFDGQEK	HEQEKTLN	NLRQEQVMK	NDSS SLME : 100
Ly49C	:	MSEPEVTYSTVRL	LHKSSGLQKLR	RHEETQGP	PREVGNRKC	SAPWQL	LIVKALGIL	CFLLLV	TVAVLAV	KIFQYNQHKQEI	NET LNHHNCS	-NMQRAFNLKE : 99	
Ly49D	:	MTEQEDTFSAVR	FKHSSGLQEMRL	KETRK	PEKARLRV	CSVPWL	LIVIALGIL	ISLRLV	TVAVLMT	NIFQYGGQK	HELKEFLK	HHNCS	-IMQSDINLKD : 99
Ly49E	:	MSEPEVTYSTVRL	LHKSSGLQRLV	SHEEI	QGPGEAGYRK	CSVPWL	TVRSLGIF	CFLLLV	TVAVLAV	KIFQYSQHKQEI	HETLNHHNCS	-NMQSDIKLKE : 99	
Ly49F	:	MSEPEVTYSTVRL	LHKSSRLQKLR	RHEETQGP	REAGYRK	CSVCWL	LIVKALGIL	CFLLLV	TVAVLAV	KIFQYGGQHNQEI	HETLNHHNCS	-NMQSDFNLKE : 99	
Ly49G	:	MSEQEVTYSTVRF	HSSRLQKLR	TTEPQR	PREACYREYS	VPWKL	LIVIAACGIL	CFLLLV	TVALLAI	TIFQHSQQK	HELQETLN	CHDNCS	-PTQSDVNLKD : 99
Ly49H	:	MSEQEVTFTPTMR	FKHSSGLNSQVR	LEGTQ	RSRAGLRV	CSVPWL	LIVIALGIL	CSLRLV	IVAVFVT	KFFQYSQHKQEI	NET LNHRHCS	-NMQRDFNLKE : 99	
Ly49I	:	MNEPEVTYSTVRL	LHKSSGLQKLR	RHEETQGP	REAGNRKC	CSVSWL	LIVKALGIL	CFLLLV	IVAVLTI	KIFQYSQHKQEI	NET LNHYHCS	-NMQSDFNLKE : 99	
Ly49J	:	MSELEVTYSTVNL	LHKSSGLQKLR	RHEETQGP	REAGNRKC	CSIYWL	LIVKALGIL	CFLLLV	IVAVLAV	KIFQYSQHKQEI	NET LNHHNCS	-NMQRDFNLKE : 99	
Ly49Q	:	MSEQEVTYSTVRF	FKHSSGLQNP	QVRPED	NQGSREAGHKE	CSIPWHL	LIVIAFGIL	CVLLLV	IVAVLVT	NILQYKQEK	HELQETLN	CHHCS	-TMQNDINAKE : 99

						β 0	β 1	α 1	α 2												
		*	120	*	140	*	160	*	180	*	200										
Ly49A	:	EMLK NKSIE C---	DLLESLNRDQNR	LY NKT KTIVLDS	SLQHTGRGDKVYWF	CYGMK	CYFVMDR	RKTWSG	CKQT	CSSSL	SLLKIDDE	DELKFLQLVVP	SDS : 194								
Ly49B	:	EMLRN KSS ECAL ND SLH	YLNRQNR	CLRKT	KIVLDS	CSQNK	GKQVEGYWF	CCGMK	CYFIMDDK	KLK	CKQI	COAY NT LLKT	NDEDELKFLKSQ	LQRNT : 200							
Ly49B-BALB	:	EMLRN KSS ECAL ND SLH	YLNRQNR	CLRKT	KIVLDS	CSQNK	GKQVEGYWF	CCGMK	CYFIMDDK	KLK	CKQI	COAY NT LLKT	NDEDELKFLKSQ	LQRNT : 200							
Ly49C	:	EMLT NKSID CRPS NET	LEYIKREQDR	WDSKT	KTIVLDS	SSRDT	GRGVK-YWF	CYSTK	CYFIM	NKT WSG	CKAN	CQHSV	PILKIEDEDELKFLQR	HVIPEN : 198							
Ly49D	:	ELLK NKSIE C---	NLLESLNRDQNIL	CDKTR	TVLDYL	QHTGRG	VKQVYWF	CYGMK	CYFVMDR	PKPWSR	CKQS	CQ SS L	TLLKIDDEDELKFLQ	LVVPSDS : 195							
Ly49E	:	EMLRN KSID CSPG	EELLESLNREQNR	WYSET	KTDLDS	SSQDT	GTGVK-HWF	CYGTK	CFYFIM	SKNTWSG	CKQT	CQHYS	LPLVKIEDEDELKFLQ	FQVISDS : 198							
Ly49F	:	EMLT NRSID SRPG	NELLESLNREQNR	GYSET	KTDLDS	SSQDT	GTGVK-YWF	CYRTK	CYFIMN	KNNTWSG	CKQN	CQHYS	LPLVKIDDEDELKFLQ	FQVIPDS : 198							
Ly49G	:	ELLRN KSIE CRPG	NDLLESLSRDQNR	WYSET	KTFS	SSQHT	GRGFEKYWF	CYGIK	CYFNMDR	KTWSG	CKQT	QISS	L	SLLKIDNEDELKFLQ	NLAPSDI : 199						
Ly49H	:	EMLT NKSID CRPS	YELLEYIKREQER	WDS	ETKSVSDS	SSRDT	GRGVK-YWF	CYGTK	CYFIM	NKT WSG	CKAN	CQHSV	P	IVKIEDEDELKFLQR	HVILE : 198						
Ly49I	:	EMLT NKSID CRPS	NELLDYIKREQDR	WNSET	KTIVLDS	SSRDT	GRGVK-HWF	CYGTK	CYFIM	NKT WSG	CKAN	CQHSV	P	IVKIEDEDELKFLQR	HVIPES : 198						
Ly49J	:	EMLT NKSID CRPS	NELLEYIKREQDR	WNSET	NTILD	SSRDT	G	GGVK-YWF	CYSTK	CYFIM	NKT WSG	CKAN	CQHSV	P	IVKIEDEDELKFLQR	HVIPES : 198					
Ly49Q	:	EMLRN	MPLE	CSTG	DDLKSLNREQ	KRWYSET	KS	SVL	NSS KHP	GG	SLEI	HWF	CYGIK	CYFIMN	KKGWRK	CKQI	CEHYS	L	SLLKIDA	EDELKFLQ	LQVTPDS : 199





Appendix II) Characterisation of Ly49s and other NK cell receptors from murine strains by immunoprecipitation and Western blotting.

Predicted MW of monomer (kDa)	Monomer size (kDa)	Dimer size(kDa)	Cell type	Surface labelling	Tags	% of the gel	IP antibodies	Detecting antibodies	References
Ly49A (mouse)									
30.7	44-54 (+ over 200 band)	90-95 (+over 200 band)	EL-4	125 I or s35 met	-	7.5	YE1/48	-	Takei 1983
30.7	45-55 (+ over 200 band)	90-95 (+ over 200 band)	Normal thymocytes and splenocytes, MBL-2, EL-4	125I	-	10 12.5	YE1/48, YE1/32	-	Chan and Takei 1986
30.7	42-45 (Reduced to 30 with EndoF)	85 (+ over 200 band)	C6VLB, normal splenocytes and thymocytes	125I	-	10, 12.5	A1	-	Nagasawa <i>et al.</i> 1987
30.7	45-55 (reduced to 32 with EndoF)	90-95 (+ over 200 band)	EL-4, MBL-2	125I	-	10	YE1/48	-	Chan and Takei 1988
30.7	44	85	EL-4, COS	125I	-	10	A1	-	Yokoyama <i>et al.</i> 1989
30.7	47	97	IL-2 activated NK cells	125I	-	10	A1	-	Mason <i>et al.</i> 1996
30.7	-	82-90	C1498	-	VSV	8	Anti-VSV	Anti-VSV, rabbit anti-pan-class I Abs	Scarpellino <i>et al.</i> 2007
30.7	-	95 and 110	IL-2 activated NK cells	-	-	10	YE1/48	Biotin Anti-phosphotyrosine, HRPO SA	Ortaldo <i>et al.</i> 1999
30.7	44 (reduced to 32 with PNGase F)	88	EL-4	125I		10	1A	-	Chang <i>et al.</i> 1996
30.7	45-50	85-90 (+ over 200 band)	EL-4, M14T cells	125I	-	10	JR9-318	-	Roland and Cazenave 1992

Ly49B (mouse)									
33.5	-	100	C1498	-	VSV	8	Anti-VSV	Anti-VSV, rabbit anti-pan-class I Abs	Scarpellino <i>et al.</i> 2007
Ly49C/I (mouse)									
31.3 (Ly49C) 31.2 (Ly49I)	50-54	108-110	IL-2 activated NK cells	125I	-	-	SW5E6	-	Sentman <i>et al.</i> 1989
31.3 (Ly49C) 31.2 (Ly49I)	50-54	110	IL-2 activated NK cells	125I	-	10	SW5E6	-	Mason <i>et al.</i> 1996
31.3 (Ly49C)	-	129	C1498	-	VSV	8	Anti-VSV	Anti-VSV, rabbit anti-pan-class I Abs	Scarpellino <i>et al.</i> 2007
31.3 (Ly49C) 31.2 (Ly49I)		110	IL-2 activated NK cells	-	-	10	SW5E6	Biotin Anti-phosphotyrosine, HRPO SA	Ortaldo <i>et al.</i> 1999
Ly49D (mouse)									
27.8	48-52	97-100	IL-2 activated NK cells	125I	-	10	12A8	-	Mason <i>et al.</i> 1996
27.8	-	97-100	IL-2 activated NK cells	-	-	10	12A8	Biotin Anti-phosphotyrosine, HRPO SA	Ortaldo <i>et al.</i> 1999
Ly49E (mouse)									
30.8	46 (reduced to 31 with N-glyco-F)	~90	IL-2 activated FD17 thymocytes, HEK-T cells	Biotin	-	-	4D12	HRPO-SA	Van Beneden <i>et al.</i> 2001
Ly49G2 (mouse)									
31.1	-	85-89	Liver and spleen NK cells	125I	-	7.5	4D11	-	Mason <i>et al.</i> 1988
31.1	40	97	IL-2 activated NK cells	125I	-	10	4D11	-	Mason <i>et al.</i> 1996
31.1	-	97-110	IL-2 activated NK cells	-	-	10	4D11	Biotin Anti-phosphotyrosine, HRPO SA	Ortaldo <i>et al.</i> 1999
31.1	43 (+ over 200)	86	A-LAK	Biotin	-	10	Cwy-3	-	Chang <i>et al.</i> 1999

	band)									
Ly49I (mouse)										
31.2	-	110	C1498	-	VSV	8	Anti-VSV	Anti-VSV, rabbit anti-pan-class I Abs	Scarpellino <i>et al.</i> 2007	
Ly49P (mouse)										
30.5	-	97-110	IL-2 activated NK cells	-	-	10	YE1/48, YE1/32, 4E5	Biotin Anti-phosphotyrosine, HRPO SA	Makrigiannis <i>et al.</i> 1999	
Ly49Q (mouse)										
31.8	45-60	130 and 200	COS7	Biotin	FLAG	-	Anti-FLAG	HRPO-SA, anti-FLAG	Toyama-Sorimachi <i>et al.</i> 2004	
31.8	-	82	C1498	-	VSV	8	Anti-VSV	Anti-VSV, rabbit anti-pan-class I Abs	Scarpellino <i>et al.</i> 2007	
NKR-P1C (Rat)										
24.9	45 (reduced to 28 with PNGase F)	90	IL-2 activated NK cells	Biotin	-	10	STOK27	HRPO-SA	Keveberg <i>et al.</i> 2006	
KRH1 (Rat)										
26.6	37 (reduced to 26.6 with PNGase F)	75	IL-2 activated NK cells	Biotin	-	10	STOK9	HRPO-SA	Naper <i>et al.</i> 2002	
Ly49i2 (Rat)										
32.6	47-49 (reduced to 35 with EndoF)	100-110 (reduced to 50-55 with Endo F)	IL-2 activated NK cells	Biotin	-	10	STOK1/2	HRPO-SA	Naper <i>et al.</i> 1998	

Appendix III. Staining of Ly49B mutants. The numbers represent intensity of staining expressed in fluorescence intensity units. The bold numbers represent average values and the underlined numbers represent standard deviation (SD).

Name	AA code name	Kb	Db	Dd	N837 2G4	N1176 2G4	N838 1A1	N1222 anti-HA
C57	VLKAAEPVENRN	0	0	0				
		0	0	0	415	492	580	
		0	0	0	262	330	397	
		0	0	0	308	476	366	0
		0	0	0	314	423	325	
		0	0	0	386	312	408	
		0	0	0	224	248	252	
		0	0	0	363	317	288	
		0	0	0	371	395	511	
		0	0	0	635	547	818	
		0	0	0	364	393	438	0
		<u>0</u>	<u>0</u>	<u>0</u>	<u>118</u>	<u>99</u>	<u>176</u>	

C57-HA	VLKAAEPVENRN-HA	0	0	0				
		0	0	0	353	382	502	241
		0	0	0	493	462	560	
					308	266	386	237
					172		393	328
					273			222
						305		328
		0	0	0	200			407
						292	283	317
					447		971	
						318	294	
					575		824	915
		0	0	0	353	338	527	374
		<u>0</u>	<u>0</u>	<u>0</u>	<u>143</u>	<u>72</u>	<u>250</u>	<u>227</u>

BALB	LWNDSKLDQSCT	63	128	81		
		45	59	35		
		104	97	65	595	
		19	22	98	263	
		130	220	138	501	
		115	222	87	559	
		86	156	92	606	0
		311	479	358	591	
		53	332	215	449	
		139	375	188	459	454 0
		144	426	165	493	288 0
		111	529	221	539	549 0
		91	305	153	147	375 0
		106	396	139	334	273 0
		66	180	75	219	311 0
		135	303	182	412	383 0

	172	278	196	535	419	0
	87	228	107	319	412	0
	114	264	150	566	580	0
	68	184	116	494	356	0
	113	259	159	439	412	0
	138	317	207		516	
	157	325	220		472	
				211		0
	54	122	69		297	0
	60	137	81		353	0
	105	209	132		408	
	99	227	146		580	
	84	166	103		334	0
	134	223	163		418	
	185	328	241		455	
	196	333	265		658	0

		112	253	150	437	423	0	0
		<u>56</u>	<u>118</u>	<u>70</u>	<u>141</u>	<u>103</u>	<u>0</u>	<u>0</u>
BALB-HA	LWNSKLDQSCT-HA	33	102	80				
		22	145	28				510
		30	131	53				
		27	79	31	605			
		3	17	6	327			
		14	47	12	396			
		14	77	14	862			
		6	89	19	472			439
		9	101	10	366	382		467
		46	184	51	628	595	0	
		52	211	61	521	525	0	467
		54	174	71		426		366
		42	129	53		353		419

		16	74	23		340		412
		19	80	22		390		427
		11	59	19		296		376
		25	106	35	522	413	0	431
		<u>16</u>	<u>53</u>	<u>23</u>	<u>175</u>	<u>100</u>	<u>0</u>	<u>46</u>
C57-V59L	LLKAAEPVENRN	0	0	0	317	365		392
		0	0	0	279	228		241
					162			214
		0	0	0	253	297		282
		<u>0</u>	<u>0</u>	<u>0</u>	<u>81</u>	<u>97</u>		<u>96</u>
BALB-N167K	LWKDSKLDQSCT	0	2	0	198			
		0	0	0	390	356	0	
		0	1	0	294	356	0	
		<u>0</u>	<u>1</u>	<u>0</u>	<u>136</u>			

BALB-N167S	LWSDSKLDQ SCT	13	70	23	149		
		20	94	26	364	292	
		12	82	24		349	
		9	57	12		400	
		13	67	16		480	
		13	74	20	257	380	
		<u>4</u>	<u>14</u>	<u>6</u>	<u>152</u>	<u>80</u>	
1	LWNDSKLD ENRN	0	0	0	201	217	0
		0	0	0	151	150	0
		0	0	0	176	184	0
		<u>0</u>	<u>0</u>	<u>0</u>	<u>35</u>	<u>47</u>	<u>0</u>
2	VLKAAEPV Q SCT	0	0	0	476	403	463
					201		235

		0	0	0	339	403	349
					<u>194</u>		<u>161</u>
2.1	LLKAAEPVQ SCT	0	0	0	862		979
		0	2	0	359	472	390
					305		350
		0	1	0	509	472	573
		<u>0</u>	<u>1</u>	<u>0</u>	<u>307</u>		<u>352</u>
2.2	VW KAAEPVQ SCT	0	14	0	693		0
		0	11	0	340	407	0
		0	23	0	390	379	0
		0	10	0		346	
		0	9	0		343	
		0	13	0	474	369	0
		<u>0</u>	<u>6</u>	<u>0</u>	<u>191</u>	<u>30</u>	<u>0</u>

2.3	VLN AAEPVQSCT	40	125	3	1024		767
		29	147	3	467	235	498
		23	105	2		446	
							308
		16	88	0		389	
		26	58	0	989	336	463
		27	105	2	827	352	509
		<u>9</u>	<u>34</u>	<u>2</u>	<u>312</u>	<u>90</u>	<u>191</u>
3	LWN AAEPVENRN	0	0	0			
		0	0	0	90	111	0
		0	0	0	90	111	0
		<u>0</u>	<u>0</u>	<u>0</u>			
3.1	VWN AAEPVENRN	0	0	0			

		0	0	0	208	259	0
		0	0	0	208	259	0
		<u>0</u>	<u>0</u>	<u>0</u>			
3.2	LLN AAEPVENRN	0	0	0			
		0	0	0	423	308	284
					300		264
		0	0	0	362	308	274
		<u>0</u>	<u>0</u>	<u>0</u>	<u>87</u>		<u>14</u>
3.3	LW KAAEPVENRN	0	0	0			0
		0	0	0	190	212	
		0	0	0	190	212	0
		<u>0</u>	<u>0</u>	<u>0</u>			
3.4	VLN AAEPVENRN	0	0	0			

		0	0	0	252	314	
					202		211
		0	0	0	227	314	211
		<u>0</u>	<u>0</u>	<u>0</u>	<u>35</u>		
3.5	VW KAA EPVENRN	0	0	0			
		0	0	0	80	91	0
		0	0	0	80	91	0
		<u>0</u>	<u>0</u>	<u>0</u>			
4	VLK DSKLD QSCT	0	0	0			
		0	2	0	397	297	281
		0	0	0	401	356	230
					259		87
		0	1	0	352	327	199
		<u>0</u>	<u>1</u>	<u>0</u>	<u>81</u>	<u>42</u>	<u>101</u>

4.1	LLKDSKLDQSCT	0	0	0			
		0	0	0	289	369	163
		0	0	0	467	383	292
					180		131
		0	0	0	312	376	195
		<u>0</u>	<u>0</u>	<u>0</u>	<u>145</u>	<u>10</u>	<u>85</u>
4.2	VWKDSKLDQSCT	0	9	0			
		0	24	0	243	412	0
		0	2	0	586		0
		0	12	0	415	412	0
		<u>0</u>	<u>11</u>	<u>0</u>	<u>243</u>		<u>0</u>
4.3	VLNDSKLDQSCT	7	33	0			
		13	99	0	319	419	0

		0	20	0	521		0
		7	51	0	420	419	0
		<u>7</u>	<u>42</u>	<u>0</u>	<u>143</u>		<u>0</u>
4.4	LWKDSKLDQSCT	0	4	0			0
		0	0	0	195	220	0
		0	0	0	404		
		0	1	0	300	220	0
		<u>0</u>	<u>2</u>	<u>0</u>	<u>148</u>		<u>0</u>
4.5	LLNSKLDQSCT	8	31	0			
		10	104	0	348	427	0
		0	27	0	545		0
		6	54	0	447	427	0
		<u>5</u>	<u>43</u>	<u>0</u>	<u>139</u>		<u>0</u>

5	VLK DSKLD ENRN	0	0	0	516	407	274
		0	0	0	260	290	251
		0	0	0	388	349	263
		<u>0</u>	<u>0</u>	<u>0</u>	<u>181</u>	<u>83</u>	<u>16</u>
6	LWNAAEPV QSCT	321	623	378	647	579	0
		174	313	207	455	489	0
		222	393	308		459	
		239	443	298	551	509	0
		<u>75</u>	<u>161</u>	<u>86</u>	<u>136</u>	<u>62</u>	<u>0</u>
6.1	VWNAAEPV QSCT	289	386	303	1024		0
		317	747	498	641	591	0
		342	629	471	624	379	0
		307	515	327		520	
		314	569	400	763	497	0

		<u>22</u>	<u>155</u>	<u>99</u>	<u>226</u>	<u>108</u>	<u>0</u>
7	LWNAAEPVENCN	334	311	379	733		0
		285	356	369	379	507	0
		145	170	187		234	
		196	219	286		288	
		240	264	305	556	343	0
		<u>85</u>	<u>85</u>	<u>89</u>	<u>250</u>	<u>145</u>	<u>0</u>
7.1	VWNAEPVENCN	463	401	511	1015		0
		575	613	689	575	530	0
		359	407	135		414	
		430	426	515		375	
		457	462	463	795	440	0
		<u>90</u>	<u>101</u>	<u>234</u>	<u>311</u>	<u>81</u>	<u>0</u>

7.2	VLNAAEPVENCN	16	27	0	862		927	
		7	27	0	412	414	369	
		9	32	0		324		
		6	21	0		307		
		10	27	0	637	348	648	
		<u>5</u>	<u>5</u>	<u>0</u>	<u>318</u>	<u>58</u>	<u>395</u>	
7.3	VWKAAEPVENCN	22	146	96	1121		0	
		70	196	103	489	467	0	
		34	121	43		385		
		45	126	61		442		
		43	147	76	805	431	0	
		<u>20</u>	<u>34</u>	<u>29</u>	<u>447</u>	<u>42</u>	<u>0</u>	
7-HA	LWNAAEPVENCN -HA	281	427	364	545	507	0	463
		112	145	140	248	271	0	91

		175	194	196		322		250
		189	255	233	397	367	0	268
		<u>85</u>	<u>151</u>	<u>117</u>	<u>210</u>	<u>124</u>	<u>0</u>	<u>187</u>
7.1-HA	VWNAEPVENCN -HA	266	303	287	870		0	
		313	450	392	442	446	0	414
		223	359	308	343	259	0	259
		248	284	284		252		235
		263	349	318	552	319	0	303
		<u>38</u>	<u>74</u>	<u>51</u>	<u>280</u>	<u>110</u>	<u>0</u>	<u>97</u>
7.2-HA	VLNAEPVENCN -HA	5	17	0	832		935	
		2	21	0	390	355	443	347
		5	20	0	303	319	350	233
		2	9	0		271		252
		4	17	0	508	315	576	277

		<u>2</u>	<u>5</u>	<u>0</u>	<u>284</u>	<u>42</u>	<u>314</u>	<u>61</u>
7.3-HA	VWKAAEPVENCN -HA	48	145	65	944		0	
		36	263	77	607	640	0	560
		30	141	75	177	471	0	386
		32	125	61		150		472
		37	169	70	576	420	0	473
		<u>8</u>	<u>64</u>	<u>8</u>	<u>384</u>	<u>249</u>	<u>0</u>	<u>87</u>
BALB-A		111	256	161	390			
		58	168	116		325		
		34	100	49		252		
		68	175	109	390	289		
		<u>39</u>	<u>78</u>	<u>56</u>		<u>52</u>		
BALB-B		150	210	164	402			

	149	259	201	340
	75	122	98	207
	125	197	154	402
	<u>43</u>	<u>69</u>	<u>52</u>	<u>94</u>
BALB-C	270	446	223	496
	173	363	243	427
	139	236	174	339
	194	348	213	496
	<u>68</u>	<u>106</u>	<u>36</u>	<u>62</u>
BALB-D	77	159	98	322
	43	98	82	314
	33	66	49	205
	51	108	76	322
	<u>23</u>	<u>47</u>	<u>25</u>	<u>77</u>

BALB-BC	99	130	80	293			
	48	89	49		226		
	29	42	27		161		
	59	87	52	293	194		
	<u>36</u>	<u>44</u>	<u>27</u>		<u>46</u>		
BALB-ABCD-HA	2	12	5	69		0	
	2	8	5		46		37
	0	9	4		56		48
	2	9	6		56		45
	2	10	5	69	53	0	43
	<u>1</u>	<u>2</u>	<u>1</u>		<u>6</u>		<u>6</u>
C57-ABCD	0	0	0	21		10	0
	0	0	0		10		0

	0	0	0		10	8	2
					10	7	0
	0	0	0	21	10	8	1
	<u>0</u>	<u>0</u>	<u>0</u>		<u>0</u>	<u>2</u>	<u>1</u>
C57-ABCD-HA	0	0	0	16		8	
	0	0	0		12		12
					8	6	8
					10	11	10
	0	0	0	16	10	8	10
	<u>0</u>	<u>0</u>	<u>0</u>		<u>2</u>	<u>3</u>	<u>2</u>
BALB-20-H	11	49	23		0		
	10	30	23		0		
	31	73	44	0			
	17	51	30	0	0		

	<u>12</u>	<u>22</u>	<u>12</u>		<u>0</u>	
BALB-20-H-HA	20	93	34		0	151
	14	57	17		0	125
	18	56	21	0		232
	17	69	24	0	0	169
	<u>3</u>	<u>21</u>	<u>9</u>		<u>0</u>	<u>56</u>

Appendix IV. Staining of Ly49A mutants. The numbers represent intensity of staining expressed in fluorescence intensity units. The bold numbers represent average values and the underlined numbers represent standard deviation (SD).

Name	Kb	Db	Dd	N538 JR9	N509 A1	N358 YE1/48	N1222 anti-HA
Ly49A	0	0	214	43	30	38	
	0	0	162	27	22	37	
	0	0	164	28	16	42	
	0	0	180	33	23	39	
	<u>0</u>	<u>0</u>	<u>29</u>	<u>9</u>	<u>7</u>	<u>3</u>	
Ly49A HA	3	3	328	27	45	47	359
	3	6	317	23	36	36	359
	4	6	325	26	35	34	340
	3	5	323	25	39	39	353
	<u>1</u>	<u>2</u>	<u>6</u>	<u>2</u>	<u>6</u>	<u>7</u>	<u>11</u>
Ly49A-W166L-HA	0	0	0	0	0	0	
	0	0	0	0	0	0	61

	0	0	0	0	0	0	24
	0	0	0	0	0	0	48
	0	0	0	0	0	0	44
	<u>0</u>	<u>0</u>	<u>0</u>	<u>0</u>	<u>0</u>	<u>0</u>	<u>19</u>
Ly49A-S167K-HA							
	19	24	570				
	12	21	455	47	47	51	324
	7	13	343	27	29	32	248
	10	15	439	25	28	33	307
	12	18	452	33	35	39	293
	<u>5</u>	<u>5</u>	<u>93</u>	<u>12</u>	<u>11</u>	<u>11</u>	<u>40</u>

